A MULTI-LEVEL MULTI-DESIGN POINT APPROACH FOR GAS TURBINE CYCLE AND TURBINE CONCEPTUAL DESIGN

A Thesis
Presented to
The Academic Faculty

by

Eric S. Hendricks

In Partial Fulfillment
of the Requirements for the Degree
Doctor of Philosophy in the
School of Aerospace Engineering

Georgia Institute of Technology
May 2017

A MULTI-LEVEL MULTI-DESIGN POINT APPROACH FOR GAS TURBINE CYCLE AND TURBINE CONCEPTUAL DESIGN

Approved by:

Dr. Dimitri Mavris, Advisor
School of Aerospace Engineering
Georgia Institute of Technology

Dr. Jechiel Jagoda
School of Aerospace Engineering
Georgia Institute of Technology

Dr. Jimmy C. M. Tai
School of Aerospace Engineering
Georgia Institute of Technology

Dr. Daniel P. Schrage
School of Aerospace Engineering
Georgia Institute of Technology

Dr. Gerard E. Welch
Aeronautics Mission Office
NASA Glenn Research Center

Date Approved: 4 November 2016

ACKNOWLEDGEMENTS

There are a number of people that I would like to acknowledge for their support, guidance and encouragement throughout my work on this thesis. First and foremost, I would first like to thank my advisor Dr. Mavris. Dr. Mavris took me under his wing as an undergraduate student and encouraged me to participate in a variety of research efforts within his Aerospace Systems Design Laboratory (ASDL). His mentoring pushed me to pursue graduate studies at ASDL and apply for the NASA Graduate Student Research Program, ultimately leading to my current position at NASA Glenn Research Center. The completion of this thesis as a distance learning student while working at NASA was only possible as a result of his continued support and encouragement over the years.

Next, I would like to thank the members of my thesis committee: Dr. Jagoda, Dr. Tai, Dr. Schrage and Dr. Welch. Your thoughtful review of my research was extremely valuable and helped me focus on the important aspects of my research. In particular, I would like to acknowledge Dr. Tai and his colleague Russell Denney for their extensive support and guidance throughout my graduate studies. Our weekly phone conversations discussing my ideas, results and next steps were invaluable for the completion of this research.

In addition, I would like to thank my colleauges at NASA Glenn Research Center in the Propulsion Systems Analysis Branch. I would first like to acknowledge my supervisors during this process, Robert Plencner and Mary Reveley, for their support of my continuing education. I also would like to thank Justin Gray, Scott Jones, Jon Seidel, Tristan Hearn, Jeff Berton, Bill Haller and Chris Snyder for their technical guidance and review of my work. Beyond these individuals, there are two NASA teams and projects I wish to acknowledge. First, I would like to thank the members of the VSPT research team within the Revolutionary Vertical Lift Technologies Project for their technical feedback on my ideas and results. Second, I would like to thank the OpenMDAO development team within the Transformative Tools and Technologies Project for their support in setting up and running

many of my computationally intensive experiments.

I would also like to thank my many family and friends for their continued support of my educational goals. Specifically, I would like to thank my parents Scott and Joni as well as my sister Rebecca for their ever present support throughout this journey. My educational and career achievements would not have been possible without your encouragement and sacrifices. Finally, I would express my deepest thanks to Maddie for her everpresent support, understanding and love throughout this journey. It meant the world to me and I hope to give you the same support and love as you begin your own graduate education journey.

TABLE OF CONTENTS

LIST OF TABLES

LIST OF FIGURES

LIST OF SYMBOLS AND ABBREVIATIONS

A	Area (in^2)
A/C	Aircraft
ADP	Aerodynamic Design Point
ARP	Aerospace Recommended Practice
BPR	Bypass Ratio
CFD	Computational Fluid Dynamics
CMDP	Cycle MDP
CPT	Conventional Power Turbine
CRP	Contingency Rated Power
DCMDP	Decoupled MDP
DoE	Design of Experiments
DPMM	Design Point Mapping Matrix
EDS	Environmental Design Space
EEE	Energy Efficient Engine
E^3	Energy Efficient Engine
EPSFC	Effective Power Specific Fuel Consumption
f	Fuel-to-Air Ratio
FAA	Federal Aviation Administration
F	Thrust
FPR	Fan Pressure Ratio
g	Gravitational Constant
h	Specific Enthalpy
HOGE	Hover Out of Ground Effect
HP	Horsepower
HPC	High Pressure Compressor
HPT	High Pressure Turbine

IRP	Intermediate Rated Power
ISA	International Standard Atmosphere
LABC	Large Advancing Blade Concept
LCTC	Large Civil Tandem Compound
LCTR	Large Civil Tiltrotor
LCTR2	Large Civil Tiltrotor - Generation 2
LHV	Lower Heating Value
LPC	Low Pressure Compressor
LPT	Low Pressure Turbine
m	Meanline Slope
$\dot{m}$	Mass Flow Rate (lbm/sec)
MCP	Maximum Continuous Power
MDP	Multi-Design Point
MLMDP	Multi-Level, Multi-Design Point
MRP	Maximum Rated Power
N	Rotation Speed (RPM)
NASA	National Aeronautics and Space Administration
NextGen	Next Generation Air Transportation System
NPR	Nozzle Pressure Ratio
NPSS	Numerical Propulsion System Simulation
OEI	One Engine Inoperative
OGE	Out of Ground Effect
OPR	Overall Pressure Ratio
OTAC	Object-Oriented Turbomachinery Analysis Code
P	Pressure (psi)
PIMDP	Partially Integrated MDP
PR	Pressure Ratio
PSFC	Power Specific Fuel Consumption (lbm/hr/hp)
$\dot{Q}$	Heat Input

r	Radius
Re	Reynolds Number
RFP	Request for Proposal
s	Specific Entropy
S	Wing Area (ft^2)
S	Scalar Value
SAE	Society of Automotive Engineers
SLS	Sea-Level Static
SPD	Single Point Design
T	Temperature (°R)
T	Thrust (lbf)
TFF	Turbine Flow Function
TM	Turbomachinery
TMDP	Turbine MDP
TOC	Top of Climb
TSFC	Thrust Specific Fuel Consumption (lbm/hr/lbf)
U	Wheel Speed (ft/s)
UEET	Ultra-Efficient Engine Technology
V	Velocity (ft/s)
V/STOL	Vertical or Short Takeoff and Landing
VSPT	Variable-Speed Power-Turbine
VTOL	Vertical Takeoff and Landing
WATE++	Weight Analysis of Turbine Engines
$\dot{W}$	Power
W	Mass Flow Rate (lbm/s)
x	Axial Location
Y	Loss Coefficient
z	Axial Direction
$^\circ R$	Degree of Reaction

α	Angle Between Absolute Flow and Axial Direction
β	Angle Between Relative Flow and Axial Direction
δ	Ratio of Pressure to Reference Pressure
γ	Ratio of Specific Heats
η	Adiabatic Efficiency
θ	Ratio of Temperature to Reference Temperature
ϕ	Flow Coefficient
ψ	Loading Coefficient
ω	Rotation Speed (rad/s)
μ	Axial Velocity Ratio
ν	Radius Ratio

Subscripts

br	Best Range
c	Corrected Property
C	Compressor
in	Input
out	Output
Prop	Propeller
PT	Power Turbine
R	Rotor
ref	Reference Value
rel	Relative Property
S	Stator
SL	Sea-Level
t	Total or Stagnation Property
t	Thermal
T	Turbine
TO	Takeoff

z	Axial Component
θ	Tangential Component

SUMMARY

The focus of NASA's Advanced Air Vehicle Program (AAVP) is to develop new aviation technologies that can be integrated in to existing and future aircraft to address key challenges facing the aviation industry such as limiting environmental impacts, reducing air traffic congestion and improving safety. Within the Advanced Air Vehicle Program, there is a dedicated focus on the development of rotorcraft concepts in support of these objectives under the Revolutionary Vertical Lift Technology Project. While this project explores a number of different vertical lift vehicle concepts, one concept of particular interest is a civil tiltrotor as it can reduce congestion at major airports while expediently moving passengers throughout the air transportation system. Research on these tiltrotor aircraft concepts has identified the design of the propulsion systems as a critical area requiring further concept and technology development. Examining the design of the propulsion system reveals that there are numerous performance requirements and constraints for the design that arise from operation at a variety of points in the flight profile. Developing designs for the engine thermodynamic cycle and its individual components, particularly the power turbine, with this myriad of requirements and constraints therefore presents a challenging problem for the designer.

The traditional engine conceptual design process applies an iterative design process to the development of the engine cycle as well as the turbine component to ensure that each of these requirements and constraints are satisfied. This process involves first developing the cycle design at a single operating point with assumed component performance characteristics in what is referred to as the on-design phase of the analysis. Following this on-design phase, the performance of the determined cycle design is evaluated over the entire operating envelope in an off-design phase to assess the design relative to the requirements and constraints. If the design developed is not acceptable, the designer must manually alter the parameters defining the design and re-execute both phases of the cycle design process until

a viable design is identified. A similar design process is employed for the turbine component with both the on-design and off-design phases executed in an iterative process. Developing designs for the cycle and turbine with this process can be difficult, especially when numerous requirements and constraints must be considered at a variety of operating conditions. Furthermore, the cycle and turbine designs must eventually be converged adding additional complexity to the problem.

To address the limitations of the cycle design portion of the overall engine design process, previous research developed a simultaneous multi-design point (MDP) method which enabled the integration of the requirements and constraints at the various operating conditions into the on-design cycle analysis. This simultaneous MDP procedure creates additional design points within the cycle on-design phase and coupled them through the formation of a set of design rules. As a result, the challenging step of evaluating the off-design results and making changes to the design inputs is eliminated. While this previously developed MDP method addressed the challenge of designing the engine cycle to satisfy all performance requirements and constraints, the method did not address the challenges associate with designing the individual engine components and converging final cycle and component designs.

This thesis develops two new design methods to address the limitations of the traditional turbine design process and coupled engine-turbine design process when applied to challenging problems such as the design of the propulsion system for a tiltrotor aircraft. The first method developed in this thesis aims to improve the design process for the turbine components of the propulsion system. Similar to the engine cycle, these components have stringent performance requirements and constraints which must be satisfied at a number of different operating conditions. This design problem therefore also falls into the category of a multi-design point problem which can be addressed with a simultaneous MDP method along the lines of the previously described cycle MDP procedure. Development of the simultaneous MDP method for the turbine therefore started with examining the fundamental characteristics of the cycle MDP procedure and generalizing them for broader application. The key features identified included the parameterization of the turbine design along with

classifying the parameters and equations which should be considered by the design rules. Identification of these key features lead to the definition of a formal turbine MDP methodology which was then implemented on the design of three different turbines including two for the tiltrotor turboshaft engine. Evaluation of the method with these turbine design problems showed the method creates fully feasible design spaces with all requirements and constraints satisfied.

The second method developed in this thesis focused on improving the coupled design of the engine cycle and turbine with a particular focus on problems where MDP methods are applied within each analysis level. This simultaneous multi-level, multi-design point (MLMDP) method aims to ensure that the requirements and constraints at each level are satisfied while also having consistent turbine operating and performance characteristics across the analysis levels. To develop this MLMDP method, existing methods for coupling analysis levels for gas turbine engines were explored leading to the formulation of an additional set of design rules consisting of cross-level coupling equations. Combining these cross-level coupling equations with the design rules from the cycle and turbine MDP methods allows for a simultaneous solution of both levels to satisfy the requirements and constraints. With these critical cross-level coupling equations identified, the MLMDP methodology could be formally defined and applied to three engine and turbine design problems. Experimental results generated to evaluate the MLMDP method showed that for a high percentage of cases (greater than 90%) throughout the combined cycle and turbine design space the method was able to find a viable engine cycle and turbine design. Additional experiments examined the differences in the cycle and turbine designs produced by the individual cycle MDP and turbine MDP methods and those produced by the MLMDP method. The results of this experiment showed that coupling the analysis levels in the MLMDP method altered the cycle and turbine design spaces as well as the optimum designs for each level.

CHAPTER I

INTRODUCTION AND MOTIVATION

The ability for an aircraft to takeoff and land vertically without the need of a runway while also being able to maintain a high forward flight speed during cruise has been a goal for many aeronautical engineers since the successful development of the helicopter. These vertical or short takeoff and landing (V/STOL) aircraft provide many unique capabilities with application to both military and civil missions. However, designing successful V/STOL aircraft is extremely difficult as evidenced by the limited number of production vehicles resulting from V/STOL research efforts.[11] While historically the development of V/STOL aircraft has been limited, the continual advancement of aerospace technology by industry, academia, and the government will likely enable more successful V/STOL concepts in the future. The National Aeronautics and Space Administration (NASA) is investigating the potential for new V/STOL designs that could provide regional commercial transportation without the need for long runways. Designing for this mission is challenging, particularly for the propulsion system. This chapter examines these propulsion challenges and identifies the need for a propulsion system conceptual design approach capable of developing tiltrotor engine concepts to meet these requirements.

1.1 Civil Tiltrotor Benefits and Concepts

The 2014-2034 Federal Aviation Administration (FAA) Aerospace Forecast projects that the number of revenue passenger miles per year will grow at an average rate of 2.8% per year over the next 20 years with the number of enplaned passengers growing by 2.2% per year over the same timeframe.[36] However, this growth in demand for air travel has historically not been matched by increases in airport capacity leading to several airports reaching capacity limits.[62] Capacity for an airport is defined as the throughput (number of takeoffs and landings) per hour that an airport's runways are able to sustain during periods of high demand.[40] Since some of the nation's busiest airports are reaching their capacity limits,

one of the stated goals of the FAA in recent years has been to "work with local governments and airspace users to provide increased capacity and better operational performance in the United States airspace system that reduces congestion and meets projected demand in an environmentally sound manner."[35]

To address this goal, the FAA has traditionally turned to building additional runways or extending current runways. For example, a total of 12 major improvement projects have been completed at U.S. core airports over the past decade.[40] However, other non-infrastructure based options exist for increasing airport capacity. Over the past two decades, NASA has been studying the use of vertical takeoff and landing (VTOL) aircraft to help reduce congestion at airports and possibly open up air transportation to rural and unimproved areas.[62] The potential for VTOL aircraft to enable high capacity regional air travel was cited at the start of NASA's Subsonic Rotary Wing Project in 2006.[44]

The feasibility and benefits of increasing the use of VTOL aircraft for regional air travel have been assessed in several studies.[2, 3, 105, 116, 19, 115, 20] Johnson et. al.[62] estimated that about 10% of flights nationally could be replaced by a small VTOL aircraft concept. The flights considered eligible for replacement by a VTOL aircraft were those which were flown by small turbojets and turboprops (less than 50 passengers) and covered less than 500 nautical miles. As a result of replacing these flights with VTOL aircraft, it was estimated that delays at the major airports considered would decrease by about 80%. Replacing these regional flights by conventional aircraft with flights by VTOL aircraft would also open up runway capacity for longer haul flights potentially enabling an additional 85 billion revenue passenger miles to be flown each year. A later study by Chung et al.[19, 115] published in 2011 showed that civil tiltrotor aircraft can provide significant benefits in the Next Generation Air Transportation System (NextGen). The study examined future flights in three regional networks: the northeast corridor, Atlanta and Las Vegas. By replacing conventional regional flights of less than 500nm with tiltrotor capable of carrying 90 and 120 passengers, the average system-wide delay was reduced by over 60%. Furthermore, the study assessed the environmental impact of the new tiltrotor operations. The results indicate that airport noise would be similar to conventional operations while the overall fuel

burn would be higher than conventional operations. The report states that an improved design which incorporates new technology could close the fuel burn gap between tiltrotor and conventional operations.

While these studies on the potential benefit of VTOL aircraft assumed generic vehicle designs, additional research efforts at NASA focused on developing specific vehicle designs that satisfied the mission requirements used in these studies. The Heavy Lift Rotorcraft Systems Investigation examined three different concepts that could carry 120 passengers over 1200 nm at a cruise speed of 350 knots.[63] These concepts included the Large Civil Tandem Compound (LCTC), Large Advancing Blade Concept (LABC) and Large Civil Tiltrotor (LCTR) vehicles. The conclusion from the study was that the LCTR concept was the most promising for meeting performance and technology goals. Therefore, the LCTR design was examined in ensuing studies and a refined design known as the LCTR2 was developed. The LCTR2 design is smaller with the capability to transport 90 passengers over 1000 nautical miles with cruise at 300 knots at an altitude of 28,000 feet.[8] This reduction in size was made to account for improved design methods, changing marketplace trends and additional operational constraints that were not available in the initial study. Details of the LCTR2 design are provided in Table 1 with a notional drawing shown in Figure 1. Of note, the propulsion system is envisioned to consist of four turboshaft engines that each produce approximately 7000 horsepower during takeoff. The four engine configuration is deemed necessary due to hover requirements for VTOL aircraft in emergency situations where one engine is inoperable (OEI). In addition, the design flight profile for the LCTR2 is depicted in Figure 2. The proposed design characteristics and mission profile for the LCTR concept place challenging requirements, especially on the propulsion system design, requiring further research and technology development to achieve.

1.2 Challenging Tiltrotor Engine and Turbine Requirements

The mission profile for tiltrotors, such as the one shown in Figure 2 for the LCTR2 concept, places challenging requirements on the propulsion system design. Specifically, a high power level must be provided for takeoff to vertically lift the fully loaded vehicle off the ground.

Table 1: Design Characteristics of the LCTR2.[100]

Design Characteristic	Value
Cruise Speed (90 percent MCP), knots	300
Rotor Radius, ft	31.4
Engine Power (MCP, SLS, ISA), hp	4x6,476
Gross Weight, lbm	96,500
Payload (90 passengers), lbm	19,800
Length, ft	108.9
Wingspan, ft	107.0

Figure 1: NASA's LCTR2 Concept Vehicle.[45]

Even higher power operations are also required for emergency situations where one of the engines may become inoperable. During these emergency situations, normal operating limits such as maximum temperatures and speeds are relaxed to achieve the power with the tradeoff of reduced engine life. These limits are established by the engine manufactures and are specified in accordance with the FAA's regulations on engine ratings and operating limits for turbine engines.[34] While these ratings are important for certification, they also impact the engine and aircraft matching. As stated by Jenkinson et al., "the interplay between the engine ratings and the aircraft requirements is quite important in optimizing

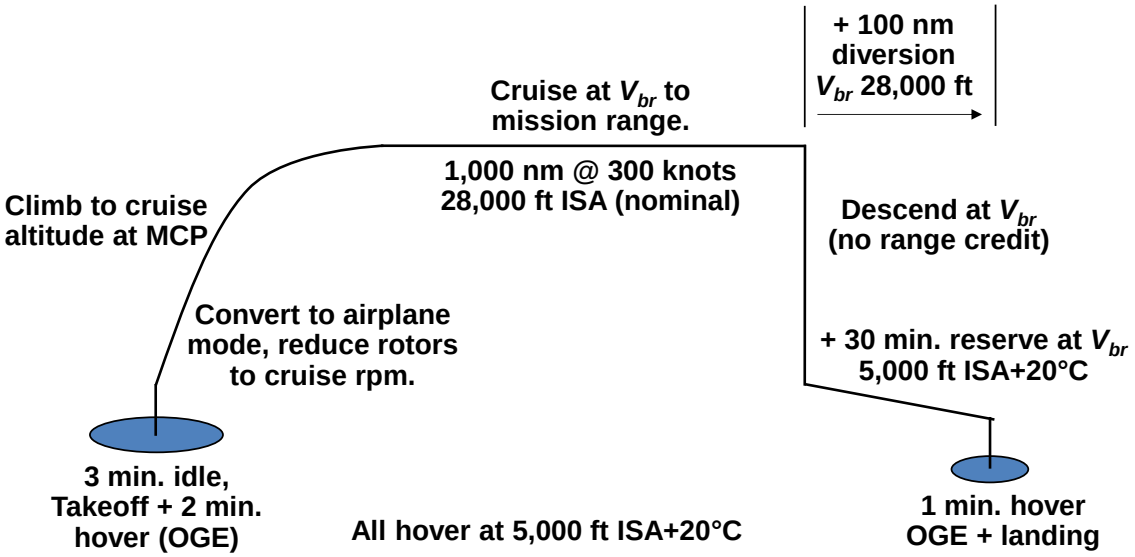

Figure 2: NASA's LCTR2 Flight Profile.[7]

the engine size and hence the powerplant weight and costs."[61] For NASA's studies on tiltrotor aircraft, turboshaft engine ratings have been assumed as specified in Table 2.

Table 2: NASA's Assumed Turboshaft Power Ratings for Tiltrotor Aircraft.[100]

Power Rating	Time Limit	Power/MCP
Maximum Continuous (MCP)	none	1.000
Intermediate Rated (IRP)	30 min	1.185
Maximum Rated (MRP)	10 min	1.269
Contingency Rated (CRP)	2.5 min	1.330

In this assumed rating structure, the maximum continuous power (MCP) is used to describe the highest power that can be produced over an extended time period without impacting the engine life. The intermediate and maximum rated power levels (IRP and MRP) increase the available power and thus degrade the engine performance at a faster rate. Operation at these ratings is limited to short periods during the flight, typically during takeoff and landing when additional power is needed for hover. Contingency rated power (CRP) is reserved for emergency operations, usually in a situation where one engine is inoperative (OEI) and extreme power levels are required to safely land. Operating at CRP power levels typically necessitates engine maintenance be performed as damage may

have occurred requiring engine overhaul or replacement.

In addition to these power rating requirements, the propulsion system design for tiltrotor aircraft is also challenged by the integration of the turboshaft and rotor/propeller. During hover operations, the rotor needs to operate at high rotation speeds as the rotor lift is proportional to the square of the tip velocity.[29] While high tip speed is desired for hover, maintaining this speed during forward flight will typically result in transonic or supersonic flow at the rotor tips. Operating in these regimes produces high losses leading to low propeller efficiency. Therefore during forward flight it is beneficial to reduce the propeller speed to as little as 50% of hover speed as shown in Figure 3. While slowing the propeller speed improves the propeller efficiency, the figure shows the opposite trend for the power turbine that would drive the propeller. Reducing the power turbine speed during cruise results in lower turbine efficiency. As the overall propulsion system performance depends on both the propeller and power turbine operation, selecting an intermediate cruise rotation speed will produce the best overall efficiency.

The cruise performance of the LCTR2 propulsion system is critical as 75% of the mission fuel is consumed during this phase and any improvement in the performance will have an impact on the vehicle sizing and mission capabilities.[92] Hence, NASA is studying ways to improve overall cruise propulsive system efficiency. Two general options are currently being considered with many other options having been suggested.[29] These two options are a conventional engine and power turbine connected through a multi-speed gearbox and an engine with a variable-speed power-turbine (VSPT) connected through a single-speed gearbox.

The first option proposed for improving propulsion system performance at cruise for tiltrotor aircraft is a gas generator and conventional free power turbine connected to the propeller through a multi-speed gearbox. In this solution, both the turbine and propeller operate at high speeds during hover and transition to forward flight. After transition a speed shifting procedure is undertaken using the multi-speed gearbox to reduce the propeller speed while maintaining high turbine speed. The exact shifting procedure is still undefined but an initial process was suggested by Snyder.[100] The procedure begins by reducing

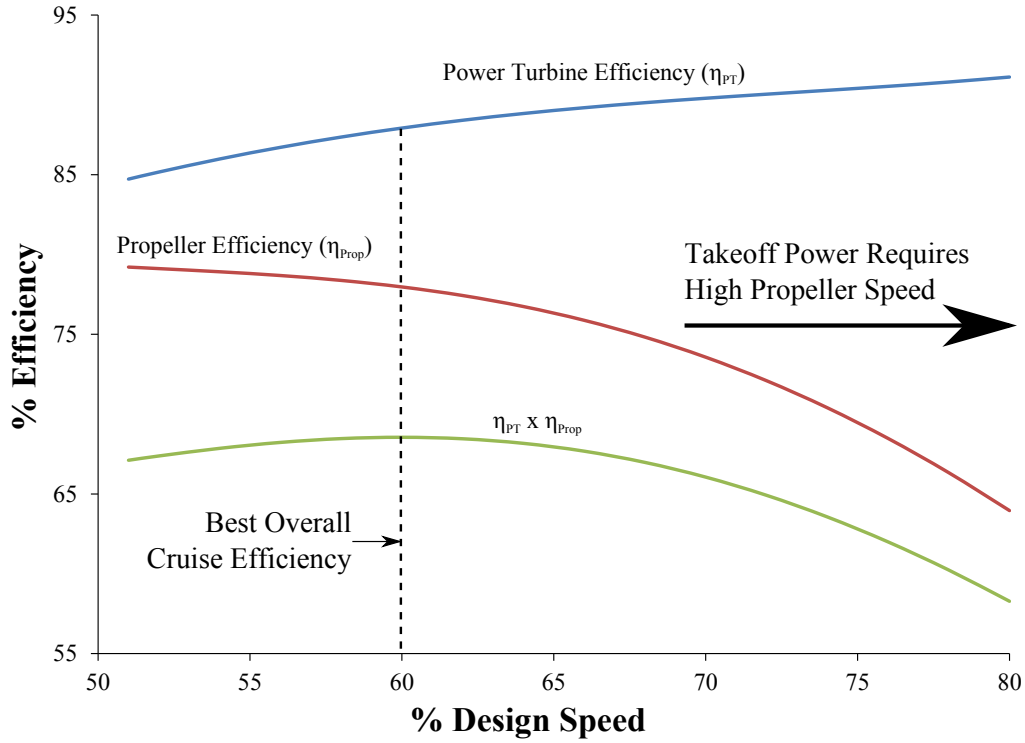

Figure 3: Cruise Efficiency of the Propeller, Turbine and Overall Propulsion System as a Function of Percent Design Speed.[29]

the propeller speeds to cruise levels by reducing the speed of all the engines. One engine is then taken off-line with the cross-shafting through the wing distributing the remaining power to the two rotors. The speed for that engine is then increased back to the preferred speed turbine. The engine is then brought back online at a new gear ratio. This process is repeated for each of the other engines. This process would then have to be repeated in the opposite direction before the vehicle could transition back to a hover configuration for landing. Overall, this procedure is complex with many steps and would require a heavy gearbox due to the multiple gear ratios and shifting mechanism. The higher gearbox weight increases the overall vehicle weight and will increase the overall mission fuel burn.

The second option for improving propulsion system efficiency at cruise is to use a gas generator and VSPT connected to the propeller through a single-speed gearbox. The VSPT is a turbine that is designed to have performance which is robust to changes in speed thereby flattening the power turbine efficiency curve shown in Figure 3. Both variable and fixed

geometry VSPT designs have been considered. The variable geometry VSPT has higher efficiency than the fixed geometry design, but that benefit is offset by the heavier, more complex design. Overall, the variable geometry design results in a higher vehicle gross weight than the fixed geometry resulting in the fixed geometry option being the focus of ongoing studies.[92] Designing the fixed geometry VSPT to be robust over the large anticipated speed range is challenging as the blades will experience large incidence variations. A comparison of the typical incidence ranges experienced by a conventional turbine and the VSPT is shown in Figure 4. While designing the turbine to operate efficiently over the wide speed range is challenging, the benefits of this option are a simpler, lighter gearbox and the elimination of the complex shifting procedure.

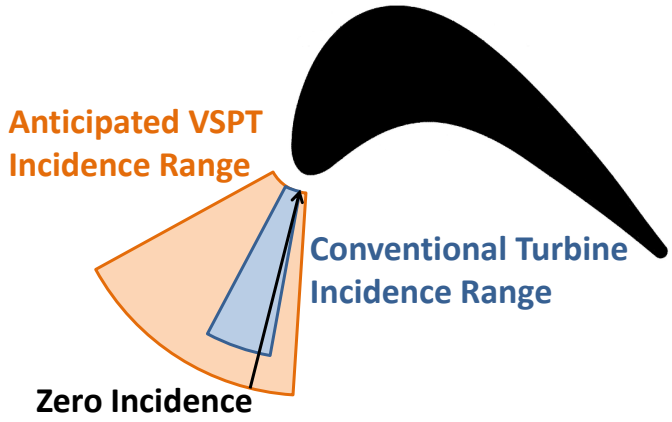

Figure 4: Incidence Ranges for Conventional Turbines and the Variable-Speed Power-Turbine.

To understand the strengths and weaknesses of these two tiltrotor propulsion system architectures, several studies have been conducted by industry and NASA. In the study by Robeck et al.[92], the concepts evaluated had different entry into service dates and therefore different technology levels making a comparison of the concepts difficult. However, the study by Acree and Snyder[7] assumed consistent technology levels making direct comparison possible. The results from this study show that the VSPT concept has lower vehicle empty weight and mission fuel at all altitudes for all but the lowest cruise tip speeds. Selecting the best tip speed for each option resulted in nearly identical vehicles with many of the design characteristics falling within 1% of each other.

The performance similarities between these architectures indicates that further research and development is required as the results are based on initial performance assumptions, especially for the VSPT. To enhance the knowledge base relating to the VSPT design and operating characteristics, detailed research on the concept is ongoing at NASA and in industry. This research includes both experimental and computational investigations of blade geometries that are incident tolerant.[37, 10, 113] The results from this research effort will be used to improve component level models and the assumptions used in future propulsion system design studies.

These two engine architecture options have been proposed as a means to provide cruise power at a reduced propeller tip speed. The cruise power and speed requirements couple with the power ratings outlined in Table 2 to form a challenging propulsion system design problem. In this problem, the critical challenge is to develop engine designs that satisfy requirements and constraints at a wide variety of operating points. This challenge is further complicated by the dependence of the engine designs on the individual component performance characteristics. Furthermore, these characteristics depend on the design of the individual component which typically has not yet been determined in the conceptual design phase. Developing a component design to generate the performance characteristics will also require considering requirements and constraints at multiple operating conditions, especially in the case of the VSPT. The dependency of the engine and turbine designs on each other indicates there is a need to consider both engine and components in a coupled engine/turbine conceptual design capability. Additionally, that design capability needs to consider requirements and constraints at multiple operating points in each analysis. The ultimate goal is to produce engine and turbine designs that combine to balance performance across the operating range while meeting all requirements and constraints. As stated by Robuck, "the best engine for the aircraft is the one that best fits the rotorcraft's particular hover and cruise requirements, while providing low fuel consumption. Features that provide excess cruise power that add to engine weight, which cannot effectively be used in flight, may not pay their way into the aircraft design."[92]

1.3 Thesis Organization

The previous sections of this chapter have served to motivate the need for commercial tiltrotor aircraft and describe the challenging propulsion system design problem. This challenging design problem primarily stems from the need to simultaneously design both the engine cycle and turbine to meet requirements and constraints at multiple operating points. The resulting question is: Does the current engine conceptual design process enable this analysis? The next chapter provides a review of the current engine conceptual design process along with a description of each of the steps. This review includes an examination of the turbine design process and modeling techniques. Following this discussion, Chapter 3 describes some recent developments and key enablers that will help address the limitations of the current engine design process. With this information, Chapter 4 summarizes the formulation of two new design methods leading to four research questions which will be answered in this thesis. Development, implementation and experimental results for the first design method which facilitates the design of turbines to satisfy performance requirements and constraints at multiple operating conditions is presented in Chapter 5. Chapter 6 then presents the development, implementation and experimental results for the second design method, a Multi-Level, Multi-Design Point (MLMDP) approach to facilitate the simultaneous design of both the engine cycle and turbine. Finally, Chapter 7 summarizes the findings, contributions and potential future directions of this research.

CHAPTER II

THE CURRENT ENGINE CONCEPTUAL DESIGN PROCESS

As described in the previous chapter, completing the conceptual design and assessment of tiltrotor propulsion systems requires certain characteristics in the design process. First, the process must effectively consider the unique requirements and constraints that occur throughout the operating regime and determine the feasibility of the design. Second, the process must include the component (turbine) conceptual design as a critical element since the requirements are likely to require a design outside of the historical database and designer's experience. These requirements raise the question: does the current engine design process meet the need to simultaneous design the engine and turbine to meet requirements and constraints at multiple operating points? This chapter explores the answer to this question by first summarizing the current engine design process. Following this discussion, elements of the design process including cycle analysis/design, engine flowpath and weight analysis, and turbine analysis/design are reviewed. The chapter concludes by assessing the applicability of the current engine design process for designing tiltrotor propulsion systems.

2.1 The Current Engine Conceptual Design Process

The engine design process generally consists of three phases with an increasing level of detail added to the engine definition in each phase. The three phases, conceptual, preliminary and detailed design, are described in Figure 5. The complete engine design process is only fully executed by the engine manufacturers. The manufactures hold their individual views of this overall process as closely guarded industry secrets to gain a competitive advantage over rival companies. Therefore, it is difficult to precisely state the engine design process as practiced by industry. However, several authors with extensive industry experience have presented several different views of the overall engine design process.

Saravanamuttoo, Cohen and Rogers[94] document the complete gas turbine engine development process covering all three phases. Their description of the process is shown in

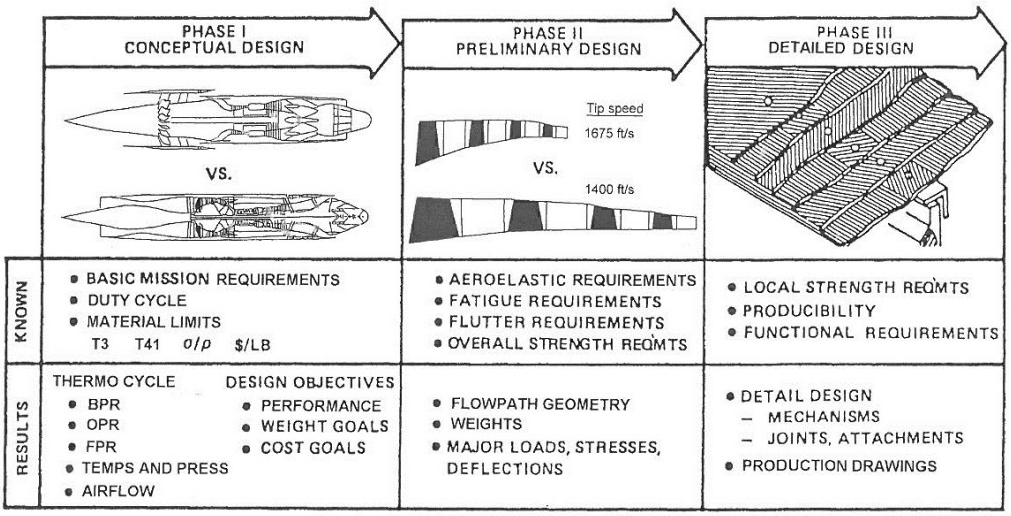

Figure 5: Engine Design Phases.[76]

Figure 6 and extends from the specification of requirements to the final production and field service. The layout of the steps in this version of the engine design process identifies a critical path down the center of the diagram. The critical path starts with thermodynamic design point studies leading to the aerodynamic assessments of the components. Following the aerodynamic assessment, the mechanical and detailed design of the components is completed before testing and production. All along this critical path, there are modification feedback loops (labeled mods) that allow for a previous step to be reexamined if unsatisfactory designs are produced. Of particular interest in this representation of the design process is the exclusion of the off-design performance from the critical path. The authors state this step can be carried out separately from the critical path steps, thereby limiting the ability to effectively satisfy performance requirements at off-design operating conditions.

A different perspective on the propulsion system design process was presented by Mattingly and is shown in Figure 7.[74] This process places the engine design in the context of the larger aircraft design process. Therefore, the process begins with determining the aircraft specifications and drag polar then completing the constraint and mission analyses. At the end of the process, the engine design is used to predict the aircraft performance, possibly resulting in a return to the mission analysis to complete another iteration of the

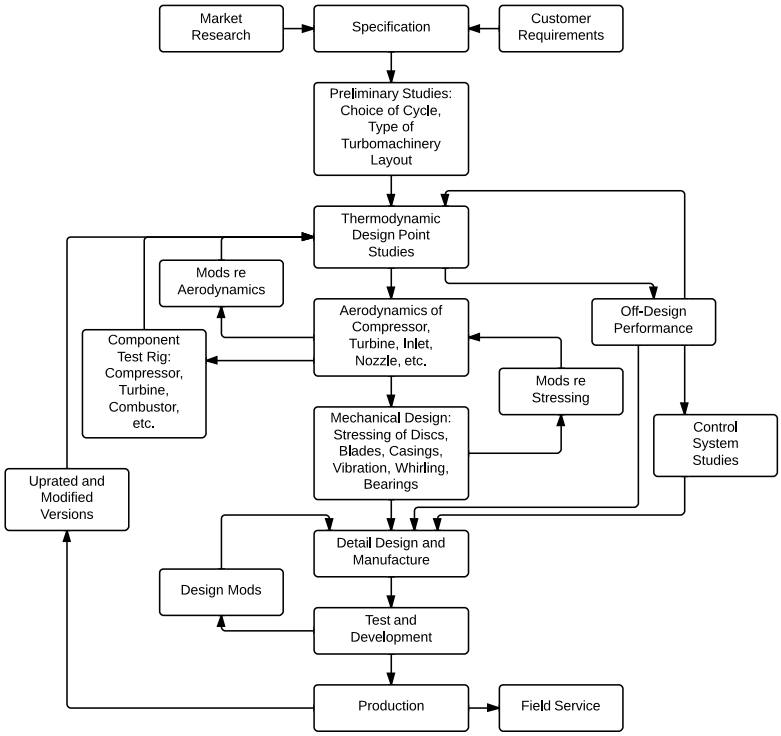

Figure 6: Aircraft Engine Design Process according to Saravanamutto, Cohen and Rogers.[94]

engine design. The actual engine design steps lie in the middle of the process and start with design point and off-design analyses. Following engine cycle selection and evaluation of the complete off-design performance envelope, the engine size and component design is finally completed. The component design is therefore addressed near the very end of the process and will require iteration when the performance does not match assumptions made in previous steps.

The third perspective on the gas turbine design process was proposed by Walsh and Fletcher and is shown in Figure 8. This process focuses only on the engine design steps during the conceptual design phase. These steps are generally similar to those proposed by Mattingly, however they are presented in a different order. The on-design cycle analysis and component design are the first steps in Walsh and Fletcher's process. Off-design evaluation of both the cycle and component performance occur later in the process. An additional step to assess engine operability is included in the process but the authors mention this step is

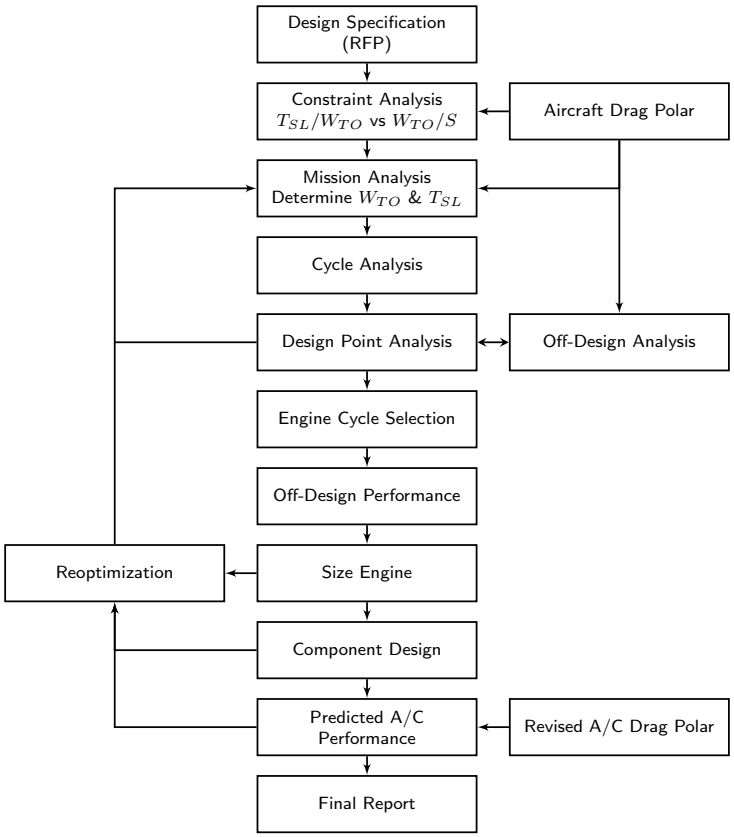

Figure 7: Aircraft Engine Design Process according to Mattingly.[74]

often skipped. Similar to the previous two engine design descriptions, several iteration loops are identified that must be executed when cycle and component performance do not match or the overall engine performance does not meet requirements and constraints.

Finally, a conceptual design focused process was published by Glassman as shown in Figure 9. This process essentially includes the same steps as Walsh and Fletcher, but does not specifically distinguish on-design and off-design steps and organizes the process as a cycle. Additionally, the diagram provides a general description of the information passed between each of the analyses.

Through the review of these four descriptions of the engine design process, several observations can be made. First, there is no single agreed upon gas turbine engine design process as the steps depend on the experience of the author and the scope of the engine

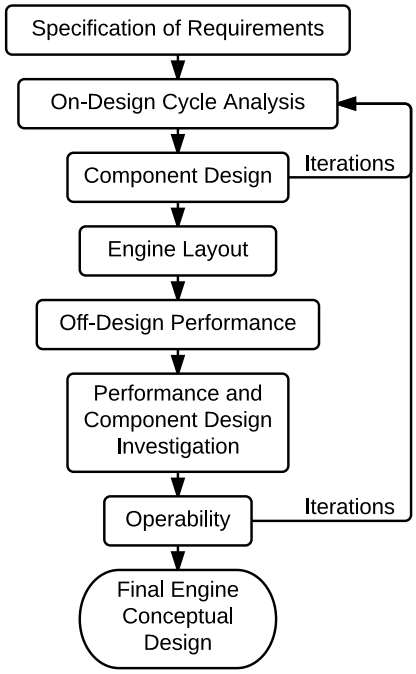

Figure 8: Aircraft Engine Design Process according to Walsh and Fletcher.[110]

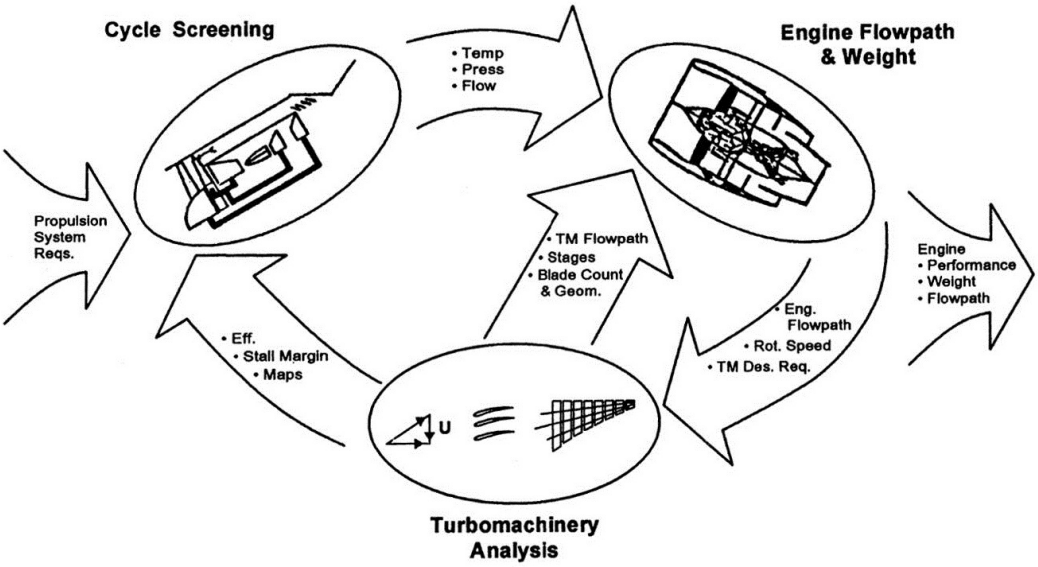

Figure 9: Aircraft Engine Design Process according to Glassman.[43]

design problem they are addressing (conceptual, preliminary or detailed). However, the processes generally contain similar steps of thermodynamic cycle analysis, component design (both aerodynamic and mechanical) and engine layout (flowpath and weight analysis). The

breakdown of the process into these steps is also representative of the way most companies conduct engine design with separate engineering groups completing each step.[24] Second, the processes all exhibit several iteration loops that require convergence. These iterations fall into three categories: iterations to match off-design thermodynamic cycle requirements, iterations to match off-design component performance requirements and iterations to converge the cycle and component designs. As Mattingly states, "the process is inherently iterative, often requiring the return to an earlier step when prior assumptions are found to be invalid."[74] Making assumptions about certain design characteristics then updating them later in the process is necessary because the true performance of the components is not known early in the design process. However, the assumptions made are typically reasonable as many engines are derivatives or evolutionary improvements of previous designs. General Electric states that two of the key elements of its gas turbine design philosophy are the evolutionary design and geometric scaling based on known designs.[14]

The observations made in the previous paragraph highlight many of the key features of current engine conceptual design practices. Based on these observations, a generic engine design process capturing the relevant features is defined in Figure 10 and will serve as the starting point for the method developed in this thesis. This generic process is representative of the steps historically followed by NASA researchers for systems analysis.[98]

2.2 Cycle Analysis and Design

The first step after the specification of requirements in all the engine design process presented in Section 2.1 is cycle analysis. As described by Oates:

> The object of cycle analysis is to obtain estimates of the performance parameters (primarily thrust and specific fuel consumption) in terms of the design limitations (such as the maximum allowable turbine temperature), the flight conditions (the ambient pressure and temperature and the Mach number) and design choices (such as the compressor pressure ratio, fan pressure ratio, by-pass ratio, etc.).[80]

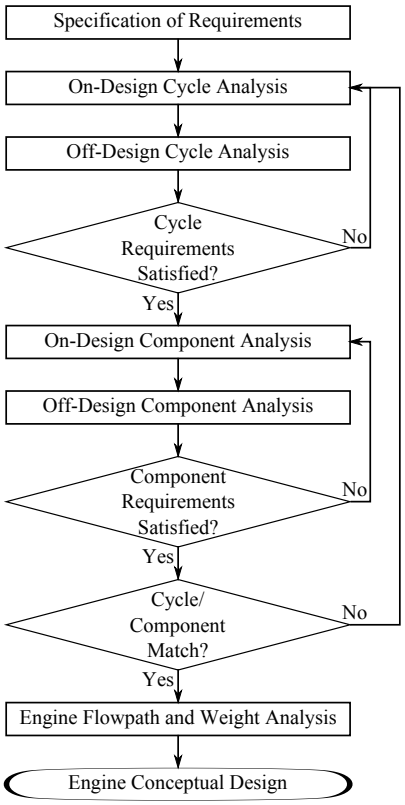

Figure 10: Generic Aircraft Engine Design Process.

Completing this objective is achieved by determining the thermodynamic state of the gas (air, fuel and combustion products) as it moves through each of the engine components. A detailed description of cycle analysis is covered in numerous aerospace engineering text books.[28, 33, 56, 75, 74] This section will provide a brief summary of the cycle analysis process and calculations relevant to this thesis.

2.2.1 The Brayton Cycle

The air flowing through a gas turbine engine passes through a number of different engine components. The components for a typical separate flow turbofan are shown in Figure 11. In addition, the figure also describes the numbering scheme used to identify locations throughout the engine. This numbering convention is based on a standard, Aerospace Recommended Practice (ARP) 755B, developed by the Society of Automotive Engineers (SAE).[4] Cycle analysis focuses on determining the thermodynamic changes to the air as

it passes through each of the engine components. While thermodynamic changes take place internal to each component, the gas's thermodynamic states of interest are those between each of the components identified by the numbered stations in the figure.

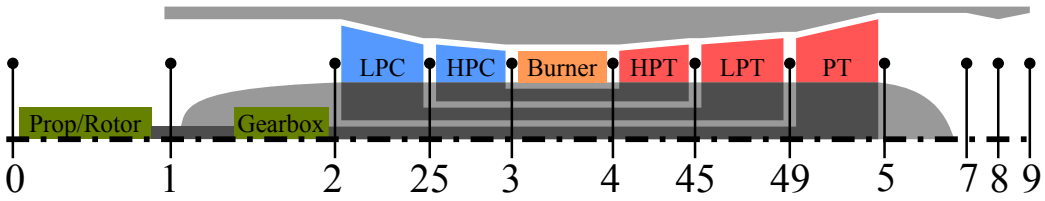

Figure 11: Turboshaft Engine Station Numbering Convention.[4]

The thermodynamic changes to the air moving through a gas turbine engine follow a process referred to as the Brayton cycle. The ideal Brayton cycle which assumes no losses in the components is typically described using an enthalpy-entropy diagram as shown in Figure 12. For the ideal Brayton cycle of a gas turbine for aerospace application, the cycle consists of the following processes:

- Isentropic compression through the inlet and compressor(s) (from station 0 to 3)
- Isobaric heat addition through the burner or combustor (from station 3 to 4)
- Isentropic expansion through the turbine(s) and nozzle (from station 4 to 9)
- Isobaric heat rejection external to the engine (from station 9 to 0)

In reality, gas turbine engines cannot achieve the ideal Brayton cycle as losses are present in each of the components. The losses through each component result in increased entropy that moves all the points to the right on the enthalpy-entropy diagram. In the turbomachinery components, the effect of these losses is that more enthalpy is required to produce the same pressure change in the compressor while in the turbine a larger pressure drop is required to produce the same power output (change in enthalpy). These changes can be seen graphically by comparing the ideal and real Brayton cycles shown in Figure 13.

By comparing the ideal and real changes through each turbomachinery component, component efficiencies can be defined. The adiabatic compressor efficiency is defined in

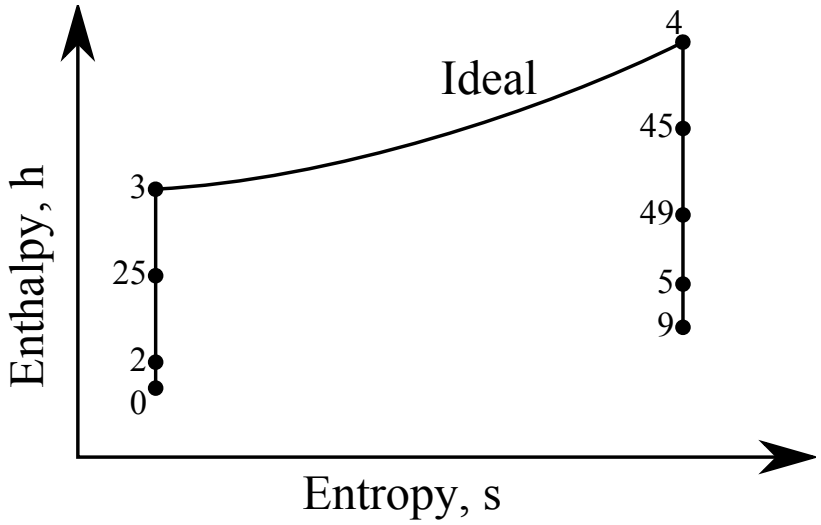

Figure 12: Ideal Brayton Cycle for the Turboshaft.

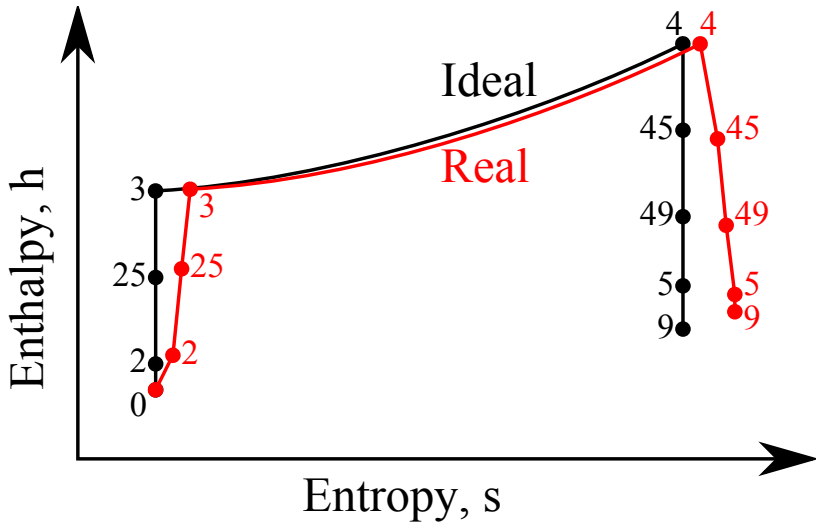

Figure 13: Ideal and Real Brayton Cycles for the Turboshaft.

Equation 1 and the adiabatic turbine efficiency is defined in Equation 2.

$$\eta_C = \frac{\Delta h_{t,ideal}}{\Delta h_{t,actual}} \tag{1}$$

$$\eta_T = \frac{\Delta h_{t,actual}}{\Delta h_{t,ideal}} \tag{2}$$

For the non-turbomachinery engine components, similar efficiencies or a component pressure loss term may be used to capture the performance of the individual component. Details regarding performance metrics for other components are not presented here for

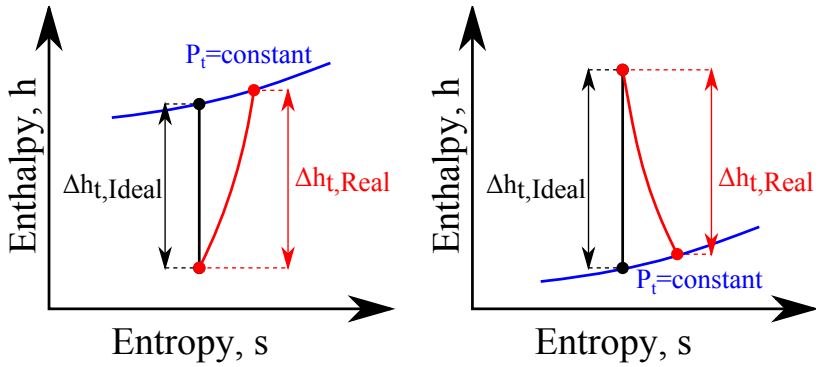

Figure 14: Enthalpy-entropy diagrams for compressors (left) and turbines (right) showing actual verses ideal enthalpy changes.

brevity, but can be found in the numerous texts that describe gas turbine cycle analysis.[75, 56] The definition of these component performance parameters allows for the real cycle to be defined leading to the calculation of overall cycle performance metrics.

2.2.2 Cycle Performance Calculations

Calculating the changes to the flow properties through the engine enables the calculation of overall engine performance metrics. These metrics capture the propelling potential and efficiency of the engine. The metrics presented in this section are focused on the turboshaft engine architecture. Therefore, some metrics more suited to turbojet and turbofan engines are not discussed here. Readers are again referred to the numerous texts on gas turbine cycle analysis for the definition of these metrics.

The purpose of changing the thermodynamic properties via the core (gas generator) components is to generate a high energy flow. This flow can then be used to create useful shaft power, $\dot{W}$, by a power turbine or thrust via a nozzle to propel the aircraft. For a turboshaft engine, most of the available energy is used to create shaft power to drive the rotor/propeller. This shaft power results from the change in enthalpy across the power turbine and the airflow through the power turbine as shown in Equation 3.

$$\dot{W}_{out,shaft} = \dot{m}_{45} \left(h_{t,45} - h_{t,5} \right) \tag{3}$$

In addition to the output shaft power, some of the flow energy may be converted to kinetic energy to create thrust from the engine nozzle. The output power from thrust is

defined as the change in kinetic energy from the engine entrance to exit as given in Equation 4. The mass flow exiting the engine is higher than the flow entering the engine as a result of adding fuel in the combustor. The flow at the exit can be described relative to the entrance flow by defining the fuel to air ratio as $f = \dot{m}_f/\dot{m}_0$ giving the right hand side of the equation. The total work out (W_{out}) can then be determined by summing Equations 3 and 4. For a turboshaft engine, the power in the nozzle thrust is often small relative to the shaft power and therefore is not included.

$$\dot{W}_{out,thrust} = \frac{1}{2g}\left(\dot{m}_9 V_9^2 - \dot{m}_0 V_0^2\right) = \frac{\dot{m}_0}{2g}\left((1+f)\,V_9^2 - V_0^2\right) \tag{4}$$

Additionally, the net thrust force can be calculated from the flow velocities with Equation 5. The last term in the equation accounts for potential differences between the entrance and exit static pressures. This difference is often close to zero at design and therefore has a limited contribution to the net thrust.

$$F_{net} = \frac{1}{g}\left(\dot{m}_9 V_9 - \dot{m}_0 V_0\right) + A_9\left(P_9 - P_0\right) = \frac{\dot{m}_0}{g}\left((1+f)\,V_9 - V_0\right) + A_9\left(P_9 - P_0\right) \tag{5}$$

Calculation of the output power and thrust is important for determining the feasibility of an engine for a specific aircraft and mission. To compare the propelling abilities of engines with different powers or thrusts, these values are often divided by the inlet airflow as shown in Equations 6 through 8. These metrics, the specific power and specific thrust, describe how much power or thrust is produced per unit airflow. Hence, higher specific power and thrust values are indicative of engines that more efficiently create power or thrust from the same airflow. Higher values also indicate less airflow is needed for the same power or thrust resulting in a smaller, lower weight engine which is of importance for aviation applications.[75, 110]

$$\frac{\dot{W}_{out,shaft}}{\dot{m}_0} = h_{t,45} - h_{t,5} \tag{6}$$

$$\frac{\dot{W}_{out,thrust}}{\dot{m}_0} = \frac{1}{2g}\left((1+f)\,V_9^2 - V_0^2\right) \tag{7}$$

$$\frac{F_{net}}{\dot{m}_0} = \frac{1}{g}\left((1+f)\,V_9 - V_0\right) + \frac{A_9}{\dot{m}_0} * \left(P_9 - P_0\right) \tag{8}$$

Specific power and thrust describe how well power and thrust are produced based on the inlet airflow. Other important metrics describe how well power and thrust are produced for

the amount of fuel consumed. These metrics are the power specific fuel consumption (PSFC) defined in Equation 9 and thrust specific fuel consumption (TSFC) defined in Equation 10. The thrust produced by the rotor/propeller could be included in the TSFC equation, but is not here as a model capturing the propeller performance is not considered. For both PSFC and TSFC, lower values are preferred as this indicates less fuel is needed of each unit of power or thrust.

$$PSFC = \frac{\dot{m}_f}{\dot{W}_{out}} = \frac{f}{\dot{W}_{out}/\dot{m}_0} \tag{9}$$

$$TSFC = \frac{\dot{m}_f}{F_{net}} = \frac{f}{F_{net}/\dot{m}_0} \tag{10}$$

Finally, another performance metric measuring the efficiency of converting the energy in the fuel to power can be defined. This metric is referred to as the thermal efficiency and is calculated using Equation 11. The numerator is the power output described by Equations 3 and 4 with the denominator defined by Equation 12. Here, LHV is the lower heating value of the fuel which describes the amount of energy released during combustion.

$$\eta_t = \frac{\dot{W}_{out}}{\dot{Q}_{in}} \tag{11}$$

$$\frac{\dot{Q}_{in}}{\dot{m}_0} = fLHV \tag{12}$$

The determination of the performance metrics described in this section allow for the assessment and comparison of engine cycles. The assessment and comparison may occur both when developing the engine design and then evaluating its performance throughout the flight envelope. The next section describes these two phases of cycle analysis.

2.2.3 On-Design and Off-Design Cycle Analysis

The descriptions of the engine design processes in Section 2.1 identified two phases of cycle analysis: on-design and off-design. In both these phases, the objective remains the same: calculate the thermodynamic changes to determine the overall engine performance metrics. Despite this similarity, the phases differ in their purpose, required inputs, and required solution method, making the phases distinct and worthy of further description.

The first phase of cycle analysis is the on-design phase which alternatively is referred to as design point analysis or parametric cycle analysis.[75] In the on-design phase, a design

operating condition is specified by the atmospheric conditions (pressure and temperature) and flight speed or Mach number. In addition, the engine power or thrust required to propel the aircraft is specified. The objective of this phase then is to develop cycle designs that provide the required power or thrust through the specification (input) of design variables. These design variables may include the compressor pressure ratio(s), component efficiencies or pressure losses and maximum component temperatures. Developing the design based on these design parameters can be completed by calculating the thermodynamic changes to the flow, working from the front to back of the engine. This sequential solution process is enabled by the dependence of component calculations only on the upstream flow conditions and shaft power. As a result of the on-design phase, an engine design is developed that meets the required power or thrust at that operating condition. Typically, numerous designs will be developed in this phase to determine the combination of design inputs that give the best overall performance. This process identifies a cycle design space that contains the feasible designs for the specified required performance.

The second cycle analysis phase is off-design, also commonly referred to as the engine performance analysis phase. In this phase, the engine designed in the on-design phase is evaluated at other atmospheric, flight and throttle conditions. The overall engine layout, geometry and size are fixed in this phase to the values determined during the on-design phase. The off-design phase therefore requires the engine definition from on-design as input. Additionally, the atmospheric conditions, flight speed or Mach number and throttle setting are required. The throttle setting is typically specified by the fuel flow or fuel-to-air ratio with a constraint that maximum turbine entrance temperature not be exceeded. The final input needs for off-design are component performance characteristics. In the off-design phase, component performance correlations (maps) are required to achieve an accurate representation of the engine. These correlations often relate the component performance to parameters such as shaft speed and mass flow. The off-design performance characteristics of the turbomachinery components are of particular interest in this thesis and are discussed in more detail in the following section. As a result of using component maps, a different solution process is required for the off-design phase. In this phase, an iterative solution is

required to ensure both mass flow and energy on the shaft are conserved as the values for each component must be determined from the maps. Most modern cycle analysis tools use matrix based methods, such as the Newton method, to complete this iteration. Newton-like methods are preferred over solving the equations with serial nested loops as nested loops become computationally inefficient for even moderately complex engines.[110] Completing the off-design analysis for an engine at many different atmospheric, flight and throttle setting is required to ensure the engine meets performance requirements throughout the flight envelope. Additionally, this data may be accumulated into an engine performance deck that can be provided to the aircraft mission analyst.[51, 76]

2.2.4 Turbomachinery Component Operating Characteristics

Producing accurate performance predictions in the off-design cycle analysis phase requires the use of component performance correlations. These correlations are commonly referred to by cycle analysts as 'maps.' For turbomachinery components, maps describe the relationship between mass flow, pressure ratio, speed and efficiency for a range of conditions. The map correlations between these parameters are dependent on the geometry and design characteristics of each component. However, the maps for all compressors and turbines generally have the same features.

Before presenting and describing example compressor and turbine maps, several corrected parameters need to be defined. Corrected parameters are obtained through dimensional analysis and allow for data taken at one set of atmospheric conditions to be valid at other conditions.[75] Using the corrected parameters therefore simplifies the map representation of the component performance. The corrected parameters typically use non-dimensional temperatures and pressures where the values are divided by standard values at sea-level as shown in Equations 13 and 14.

$$\theta = \frac{T_t}{T_{t,ref}} \text{ where } T_{t,ref} = 518.69^{\circ}\text{R} \tag{13}$$

$$\delta = \frac{P_t}{P_{t,ref}} \text{ where } P_{t,ref} = 14.696 \text{ psia} \tag{14}$$

Using these dimensionless quantities for temperature and pressure, a corrected flow and

corrected speed can be defined in Equations 15 and 16, respectively.

$$\dot{m}_c = \frac{\dot{m}\sqrt{\theta}}{\delta} \tag{15}$$

$$N_c = \frac{N}{\sqrt{\theta}} \tag{16}$$

In addition to these parameters, the non-dimensional pressure ratio across the component and adiabatic efficiency (defined in Section 2.2.1) are typically used to describe the component performance.

An example compressor map is shown in Figure 15. By convention, the abscissa is the corrected mass flow while the ordinate is the pressure ratio. The blue lines on the map represent lines of constant corrected speed and are labeled with the percentage on the left. The color contours show the adiabatic efficiency and are defined by the scale on the right. One additional set of lines is also drawn on the map in green. These lines are commonly referred to as R-lines and are non-physical lines needed for computational modeling. The R-lines are used to define locations on the maps in conjunction with the corrected speed. The upper bound of the map contours indicates conditions that result in the onset of compressor stall. Operation near this bound is discouraged resulting in a stall margin that is to be maintained between an operating point on the map and the stall/surge line.

The turbine map generally contains the same information as the compressor map and is shown in Figure 16. The corrected flow and pressure ratio are again used for the axes with blue lines indicating corrected speed and the color contours depicting adiabatic efficiency. The turbine map does not contain R-lines as they are not needed for the computational solution. Typically the range of corrected flows covered by the turbine map is much smaller than the range covered by the compressor maps. In addition, significant portions of the speed lines are usually horizontal indicating choked flow through the blade passages. The separation between the speed lines in Figure 16 results from choking occurring at different locations within a multi-stage turbine. Many texts provide example maps for a single stage turbine maps where choking occurs at only one location resulting in the choked sections of the speed lines stacking on top of each other. As a result, these texts often propose alternate coordinate systems to better present the map.[75, 114]

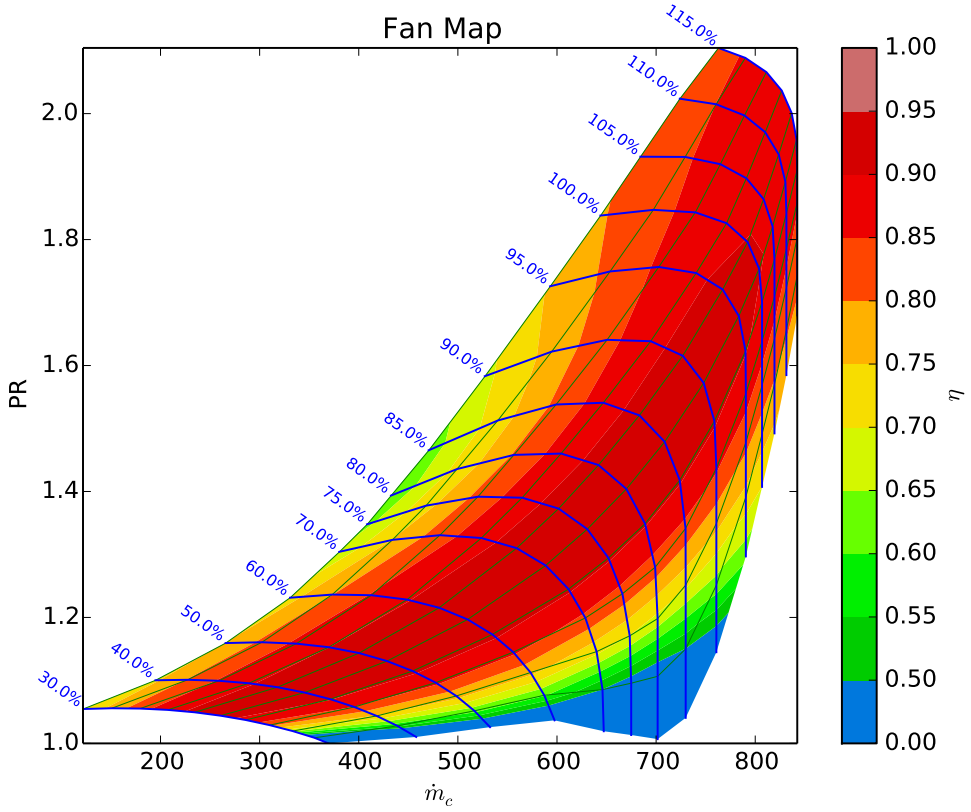

Figure 15: Sample Fan Map

These example compressor and turbine maps depict the general features observed in the maps for these components. In addition to the map correlations, a map design point must be specified. This point identifies the location on the map where the turbine was designed to operate. During conceptual design of engine cycles, the turbomachinery components have not yet been designed and therefore maps are not available. In these situations, it is common for cycle analysts to use a map from a database of previously developed designs. In this case, the map design conditions will not match those specified during the on-design case. Therefore, map scaling equations are used to adjust the correlations such that the map design point and assumed on-design cycle performance agree. The scaling equations for both compressors and turbines generally used in cycle analysis are given by Equations 17 to 20.[64] The scalar values are calculated from the on-design cycle analysis phases and then applied to the values read from the map during off-design analysis. Some cycle analysis

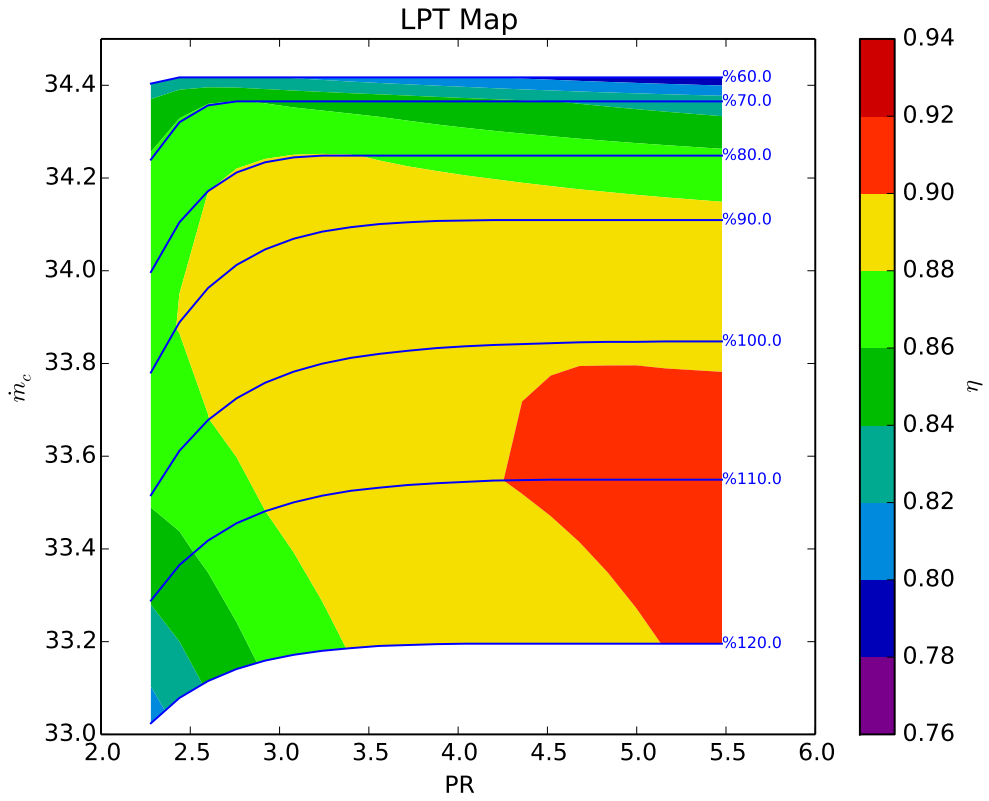

Figure 16: Sample Low Pressure Turbine Map

models may include additional terms in these equations for Reynolds number affects.[78]

$$S_{N_{c,design}} = \frac{N_{c,design}}{N_{c,mapdesign}} \tag{17}$$

$$S_{\eta_{design}} = \frac{\eta_{design}}{\eta_{mapdesign}} \tag{18}$$

$$S_{PR_{design}} = \frac{PR_{design} - 1}{PR_{mapdesign} - 1} \tag{19}$$

$$S_{\dot{m}_{c,design}} = \frac{\dot{m}_{c,design}}{\dot{m}_{c,mapdesign}} \tag{20}$$

Scaling maps during the conceptual design phase is a reasonable approach in conceptual design when the turbomachinery component is expected to be similar to the assumed map. For unconventional concepts however, the available empirical database may not contain maps representative of the unique design features making this approach problematic.[51] Applying an empirical map may therefore reduce the quality of the analysis and have a

significant impact on the predicted cycle performance during off-design operation. The engine conceptual design processes described in Section 2.1 generally allow for reassessment of the engine cycle using preliminary maps from the component design. Before proceeding to a review of the component design process, the step of estimating the engine flowpath and weight is described in the next section.

2.3 Engine Flowpath and Weight Analysis

The cycle analysis and design process described in the previous section defines the changes to the airflow's thermodynamic properties through each of the engine components in order to estimate overall engine performance characteristics. The inputs to the cycle analysis process are typically the design point component performance parameters and correlations (maps) for off-design component performance. None of these parameters specifically relate to the actual geometry of the engine or its components (although assumed maps do represent a specific geometry). Engine flowpath and weight analysis builds off of the cycle analysis results to provide an initial estimate of the overall engine geometry and total weight. Estimating these two characteristics is important for several reasons. First, engine mass and geometry are two of the main engine characteristics of interest to aircraft designers.[61] Second, estimating these characteristics helps identify potential difficulties in meeting geometry constraints set by airframe and engine matching.[110] Third, it provides valuable information to the ensuing turbomachinery design and analysis as evidenced by the design process in Figure 9.

The flowpath portion of this analysis estimates the major engine geometry characteristics. These estimates includes the dimensions of the external engine geometry such as the inlet, nacelle and nozzle as well as the internal flow channels through the components (a.k.a. the flowpath). The important parameters required from the cycle analysis to determine the flowpath are the flow rate, pressure, and temperature at each of the numbered stations between components. This information can be then used to determine the flow areas between the components. An initial estimate of the flowpath internal to the components is developed using high level design assumptions to connect the inlet and exit annulus geometries.

The initial flowpath design also uses inputs and assumptions to estimate the number of stages (blade rows) required to achieve the changes in thermodynamic properties for each component. The result from this analysis is typically an initial drawing of the engine cross section. An example flowpath output for a turboshaft engine is provided in Figure 17.

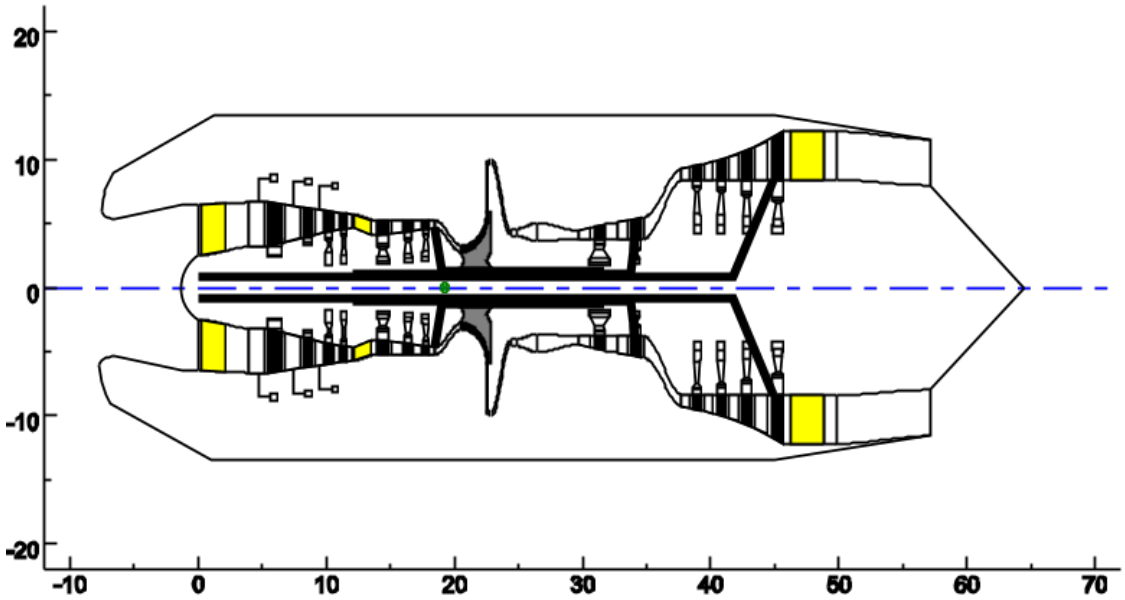

Figure 17: Sample Turboshaft Geometry from Flowpath Analysis.[101]

The weight portion of this analysis is used to estimate the mass of the engine. The overall engine mass is built up by estimating the mass of the individual components using empirical correlations. These correlations generally require inputs such as material properties, basic blade geometry characteristics, stage loading and shaft speed.[81] Using this input information, preliminary design of the blades, disks, casing and other connecting hardware is completed to accurately predict the component weights.[81] The design includes calculation of basic stress parameters for the disks and blades to ensure they fall within acceptable limits. The blade centrifugal stresses are proportional to the annulus area and maximum rotation speed, AN^2.[75] The acceptable value for this parameter is set by the material properties and operating temperatures[110] that will be experienced with typical values on

the order of $45 \times 10^9 in^2 rpm^2$[51]. The disk design and stress depend on the blade stress and selected disk geometry.[98] The total engine weight is estimated by summing the individual component weights. The goal is to develop a mass estimate with an accuracy of 2% for the total engine weight.[51]

2.4 The Current Turbine Design Process

The last major element to be examined from the current engine conceptual design process is the component analysis and design. Based on the motivating problem of the tiltrotor engine design, the turbine is the component of interest for this thesis. In many ways, the current turbine design process is similar to the current engine design process described in Section 2.1. The turbine design process can be broken down into similar phases as the cycle design process: conceptual, preliminary and detailed. While the turbine design process used by engine companies is similarly held as proprietary, several authors have published their perspective on the process. As expected, there are some significant variations in these suggested design processes. However, the processes all contain the characteristics described by Dring and Heiser:

> The designer has before him the task of satisfying certain requirements and remaining within certain constraints while meeting or exceeding his performance goal. The *requirements are generally specified by the cycle* and they include, for example, producing a given power at given values of inlet pressure, temperature and mass flow. The *constraints stem from many different sources including structural, mechanical and aerodynamic considerations.* They could include limits on rotor blade pull stress, disk rim speed, airfoil maximum thickness and trailing edge thickness, flow turning and Mach number. The performance goal that must be met is efficiency.[31]

Three proposed turbine design processes that fit this description will be presented and reviewed in this section. The first proposed process to be reviewed comes from Wilson and Korakianitis and shown in Figure 18. The process begins with the specification of the design requirements. As described by Wilson:

> These specifications will (presumably) be for the so-called 'design point.' The specifications should also contain some information on the conditions, and to what extent the machine will operate at other conditions. The specifications must also give 'trade-offs', or an objective function. This will enable the designer to aim for maximum efficiency, or minimum first cost, or minimum weight, or minimum rotating inertia, or maximum life, or some other combination of these and other measures. (The designer is often left to guess at the trade-offs.)[114]

Using these requirements, the next two steps focus on selecting the stage count and determining the velocity diagrams at the meanline and other radial locations. The velocity diagrams are important as they define the energy transfer between the flow and turbine. A description of the velocity diagrams is presented in Section 2.5.1. Based on the velocity diagrams and the airfoil shapes, the design and off-design performance can be calculated. The remaining steps in the process examine the detailed blade shape, mechanical stresses, heat transfer and vibrations.

A second perspective on the turbine design process is presented by Mattingly and is shown in Figure 19. While this process starts with a slightly different step (selecting rotation speed and annulus dimensions) the next three steps are the same as steps 2 and 3 described by Wilson and Korakianitis. The process differs after these steps however, as the focus shifts to the blade material and heat transfer analysis. Mattingly's process also emphasizes using experimental data from cascades and rotating rigs. As a result, the design and off-design efficiency characteristics of the turbine are not predicted until the end of his suggested process.

Finally, a third description of the turbine design process is presented by Halliwell and is shown in Figure 20. Halliwell's process begins with considering the turbine configuration and the design point or points that impact the design. The inclusion of multiple design points is unique among the reviewed design processes. An additional description of this step suggests that both an aerodynamic and mechanical design point need to be considered.[76] The ensuing steps follow a similar pattern as the previous processes with the number of stages, velocity diagrams and performance metrics being calculated. The last two steps

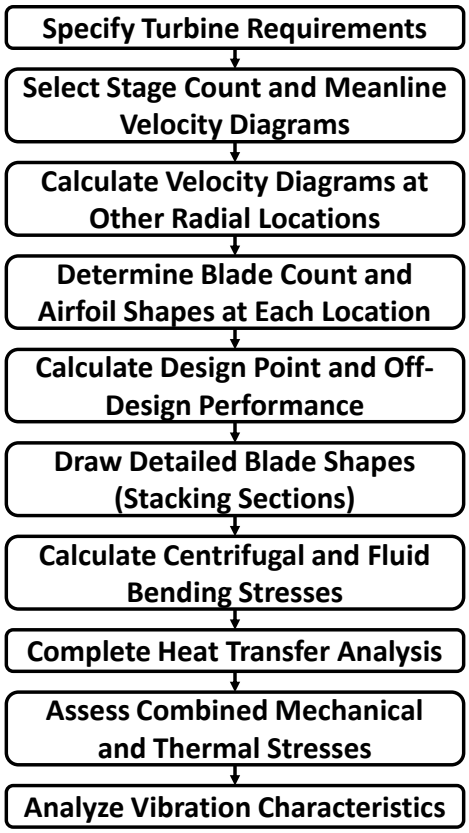

Figure 18: Turbine Design Process according to Wilson and Korakianitis.[114]

of this process are also unique. Here, Halliwell suggests that the turbine design must be assessed in terms of its compatibility with other components with iterations resulting if the design is not acceptable. This process appears to be most consistent with the level of detail required for conceptual design. However, a preliminary assessment of the stresses and heat transfer needs to be added to capture those constraints on the design.

From the three descriptions of the turbine design process reviewed in this section, several observations can be made. First, the processes generally start with a statement of the engine requirements. These requirements are typically for a single aerodynamic design point but may be supplemented by the requirements from a mechanical design point. This step is followed by the selection of stage count and annulus geometry. The processes all then move on to determining the velocity diagrams at the mean radius (meanline) before considering radial variations. Higher fidelity aerodynamic analyses and experiments may be considered later in the process but are preceded by the lower fidelity meanline and

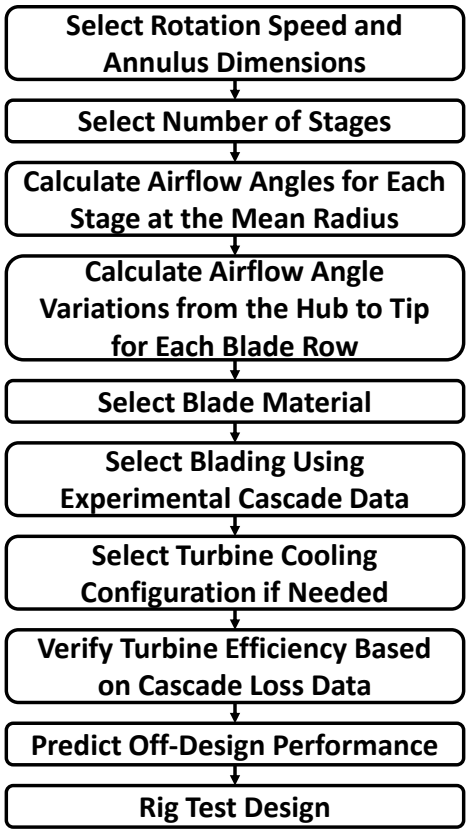

Figure 19: Turbine Design Process according to Mattingly.[75]

streamline calculations. The necessity to proceed in this order is provided by Japikse:

> It is occasionally suggested that the design process can begin with the two- or three-dimensional flow field calculations; however, this is not practical. As indicated, most designs today require optimization to ensure good performance over diverse operating conditions. Therefore, to carry out an optimization requires repeated analysis under many different conditions, and the cost of the two- and three-dimensional flow field calculations is excessive for this approach. Thus, with the exception of the rarest of conditions, two- and three-dimensional tools are used for detailed refinement of a basic concept that has been optimized previously with effective mean line calculations.[60]

The reviewed turbine design processes all use the flow angles found through meanline and streamline analyses with the addition of basic airfoil geometry definition to predict both

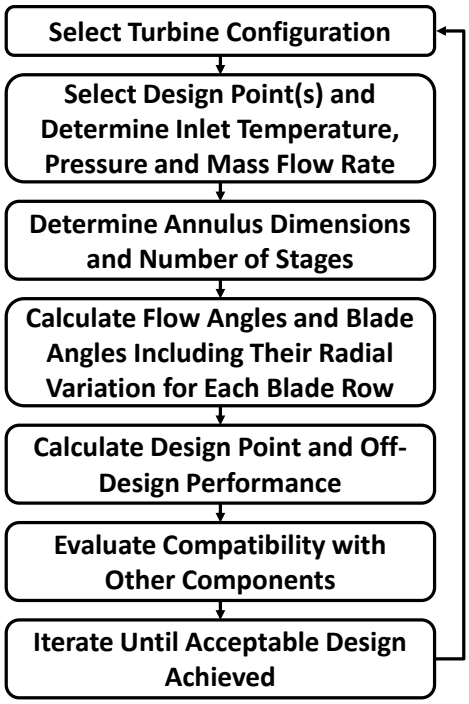

Figure 20: Turbine Design Process according to Halliwell.[51]

the on-design and off-design turbine performance. The processes generally consider the mechanical and thermal stresses only after the aerodynamic design is completed. When considering only the conceptual design (as in the case of Halliwell), a low-fidelity assessment of the mechanical and thermal stresses may be completed.

These observations highlight that several modeling and analysis tools appear consistently in the turbine conceptual design process, specifically in regards to the aerodynamic and mechanical design. The next section provides a brief description of these modeling and analysis tools.

2.5 Turbine Modeling for Conceptual Design

The design processes described in the previous section identify several analysis and design steps for conceptual design. The first analysis step in the design process is to determine the velocity diagram at the meanline or midspan. Following the meanline analysis, radial variations are considered through a process referred to as streamline analysis. For phases

beyond conceptual design, other higher order modeling analysis may be conducted to further refine the design. As a result of these analyses, the turbine performance and map correlations can be determined. Meanline and streamline analyses will be reviewed in the following sections along with two complementary low fidelity approaches that facilitate generating performance maps. For the conceptual design phase, only a limited assessment of the mechanical constraints is considered. This assessment generally consists of the AN^2 and disk stress calculations presented in Section 2.3 and therefore will not be described again in this section.

2.5.1 Meanline Analysis

Meanline analysis is the first step in the turbine design process and considers the flow only along the meanline or midspan of the turbine. A cross-section of a two stage turbine with the meanline identified is shown in Figure 21. Similar to cycle analysis, the objective of this analysis is to compute the changes in flow properties across each blade row. Therefore, the flow properties of interest are those between the blade rows identified by red lines and numbers in the figure. Changes to the flow internal to the blade passages are not computed. As a result, the detailed blade geometry is not required for the analysis

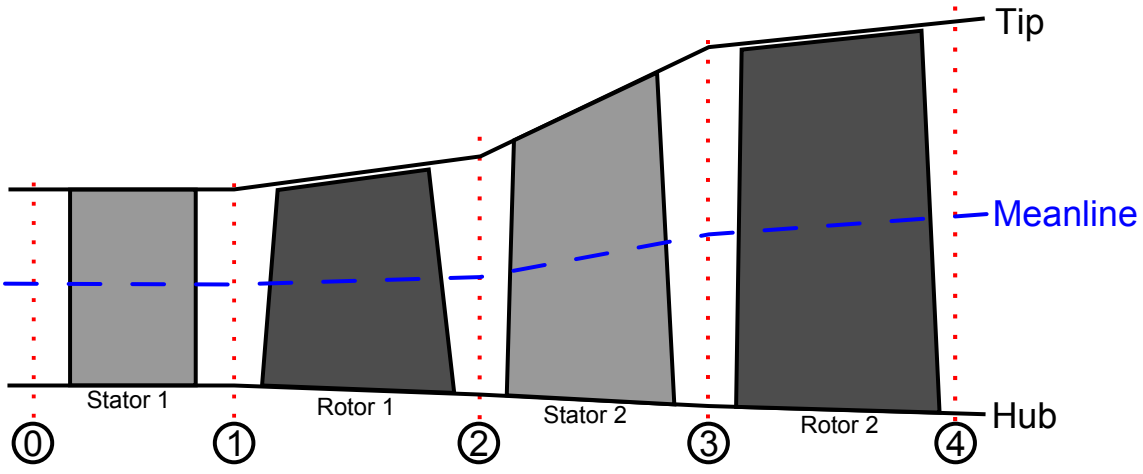

Figure 21: Flowpath for a Two Stage Turbine with Meanline.

Again similar to cycle analysis, meanline analysis can be executed in both an on-design

and off-design mode. The design mode determines the required general blade row characteristics, the initial flowpath size and design point performance.[104] Using the established design characteristics, the off-design mode predicts performance at other operating conditions defined by inlet flow conditions and shaft speed. In both of these modes, two coupled but distinctly different sets of equations are used to analyze the design. The first set of equations required are based upon physical relations and define the changes to the flow velocity and power produced by the turbine. These equations are valid for both ideal and real turbines. The second set of equations are non-physics based correlations that predict the losses for real turbines. These loss models vary significantly as they are typically based on empirical data sources. The following two sections describe these different elements of meanline analysis.

2.5.1.1 Velocity Diagrams and Energy Transfer

The foundation of meanline analysis is a set of physics equations that relate changes in velocity through the turbine blade rows to the power output. The flow velocities of interest are shown in Figure 22 which depicts the axial-tangential plane. Therefore, this plane shows the turbine geometry that would be observed at the meanline location shown in Figure 21. Figure 22 shows the stator and rotor blade rows for the first two stages along with vectors indicating the flow velocity at the numbered stations.

In this figure, thick black arrows represent actual flow in the absolute reference frame which is fixed to the stator blade row. Examining station 0, the actual velocity vector can be decomposed down into both axial and tangential velocity components as shown by the thinner arrows. The axial and tangential components can be calculated using the simple trigonometric relationships given in Equations 21 and 22 assuming a flow angle, α, that measures the actual velocity vector angle relative to the axial direction.

$$V_\theta = V \sin \alpha \tag{21}$$

$$V_z = V \cos \alpha \tag{22}$$

At stations 1 and 2, the velocity diagrams get more complicated as an additional set of vectors is shown. These vectors are added to describe the flow velocities relative to the

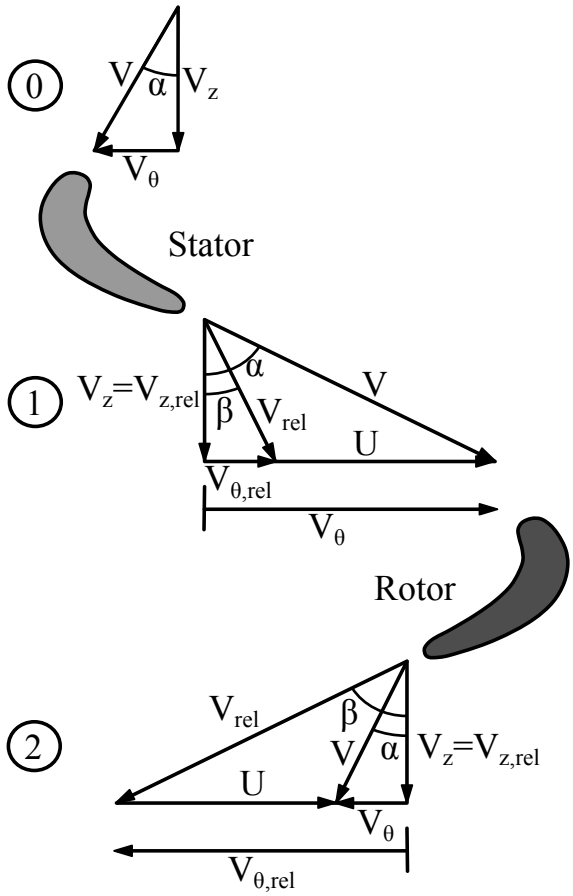

Figure 22: Meanline Velocity Diagram for the First Turbine Stage.

rotor as it is moving to the right with a velocity $U = \omega r$. The relative velocity of the flow entering the rotor can then be determined by vector summation using Equation 23. Because the blade velocity U is only in tangential direction, the vector summation can be simplified to only consider this direction as given in Equation 24.

$$\overrightarrow{V} = \overrightarrow{V_{rel}} + \overrightarrow{U} \tag{23}$$

$$V_\theta = V_{\theta,rel} + U \tag{24}$$

Finally, the relative components in the axial and tangential components can again be computed with simple trigonometry using Equations 25 and 26 with β defining the angle between the relative velocity and the axial direction.

$$V_{\theta,rel} = V_{rel} \sin \beta \tag{25}$$

$$V_{z,rel} = V_{rel} \cos \beta \tag{26}$$

The definition of these velocity vectors, also commonly referred to as velocity triangles, enables the calculation of the power produced by each turbine blade row. From the conservation of angular momentum, the turbine power can be calculated using Equation 27. In this equation, r is the meanline radius, ω is the angular rotation speed and the subscript numbers refer to the station locations in Figure 22. The power output from the rotor blade row is also defined by the first law of thermodynamics as given in Equation 28. Combining these two definitions gives the Euler turbomachinery equation (Equation 29) which relates the change in flow velocity to the change in the flow enthalpy.

$$\dot{W}_T = \dot{m}\omega \left(r_1 V_{\theta,1} - r_2 V_{\theta,2}\right) \tag{27}$$

$$\dot{W}_T = \dot{m} \left(h_{t,1} - h_{t,2}\right) \tag{28}$$

$$\Delta h_t = h_{t,1} - h_{t,2} = \omega(r_1 V_{\theta,1} - r_2 V_{\theta,2}) \tag{29}$$

Before moving on to discuss loss modeling, three non-dimensional turbine parameters need to be defined. These parameters relate to the velocity triangle shapes and act as similarity parameters for comparing turbine designs. The first parameter is the flow coefficient (ϕ) which is defined as the ratio of the axial flow velocity entering a rotor to the meanline rotor speed (Equation 30). Second, the loading coefficient (ψ) is defined as the ratio of the change in total enthalpy across a stage to the rotor speed squared as given in Equation 31. Finally, the degree of reaction ($^\circ R$) of a turbomachinery stage describes the amount of expansion that occurs in the rotor relative to the expansion in the entire stage. Several different definitions for degree of reaction are available in the literature based on changes in pressure[104] and changes in enthalpy[60, 114]. The pressure based definition is appropriate for incompressible, isentropic flow[51] and is less precise[114] for general turbines. Therefore, the enthalpy based definition given in Equation 32 is used in most references.

$$\phi = \frac{V_z}{\omega r} = \frac{V_z}{U} \tag{30}$$

$$\psi = \frac{\Delta h_t}{(\omega r)^2} = \frac{\Delta h_t}{U^2} \tag{31}$$

$$^\circ R = \frac{\Delta h_{rotor}}{\Delta h_{t,stage}} \tag{32}$$

2.5.1.2 Loss Prediction

The velocity diagram calculations presented in the previous section provide a physics based approach to determine the turbine power from only the meanline velocity vectors. In order to calculate the complete change in thermodynamic properties across each blade row for a real (non-ideal) turbine, additional equations describing the losses must be added. These equations differ from those in the previous section as they cannot be derived from physics and are instead developed from empirical data. Hence, there is no single agreed upon set of standard equations for this part of meanline analysis. Each researcher and company will use and prefer a different model of the losses. While the loss models used by engine companies are proprietary, numerous models are available in the open literature including those by Ainley-Mathieson[9], Dunham-Came[32], Kacker-Okapuu[67] and Craig-Cox[27]. Readers are directed to the Ph.D. work of Wei[111] for a full review and comparison of meanline turbine loss models.

While each of these loss models contains different correlations based on the data used during their creation, the models do have some similar features. First, the loss models typically compute a pressure loss coefficient defined by Equation 33 for the stator and Equation 34 for the rotor.[60]

$$Y_S = \frac{P_{t0} - P_{t1}}{P_{t1} - P_1} \tag{33}$$

$$Y_R = \frac{P_{t1,rel} - P_{t2,rel}}{P_{t2,rel} - P_2} \tag{34}$$

To compute these loss coefficients, the various loss models generally attempt to correlate the loss values with the characteristics of each blade row. Some of these values come from the velocity triangles such as the entrance and exit flow angles, flow Mach numbers, Reynolds number and annulus geometry (blade height). Additional parameters defining the blade row must also be input such as the pitch-to-chord ratio, blade thickness-to-chord ratio, blade aspect ratio, tip clearance and trailing edge thickness. Figure 23 provides the definition for many of these blade row geometric parameters.

Correlating this wide variety of flow and geometric parameters to the total blade row loss coefficient is a challenging task. To simplify the correlations, many authors attempt

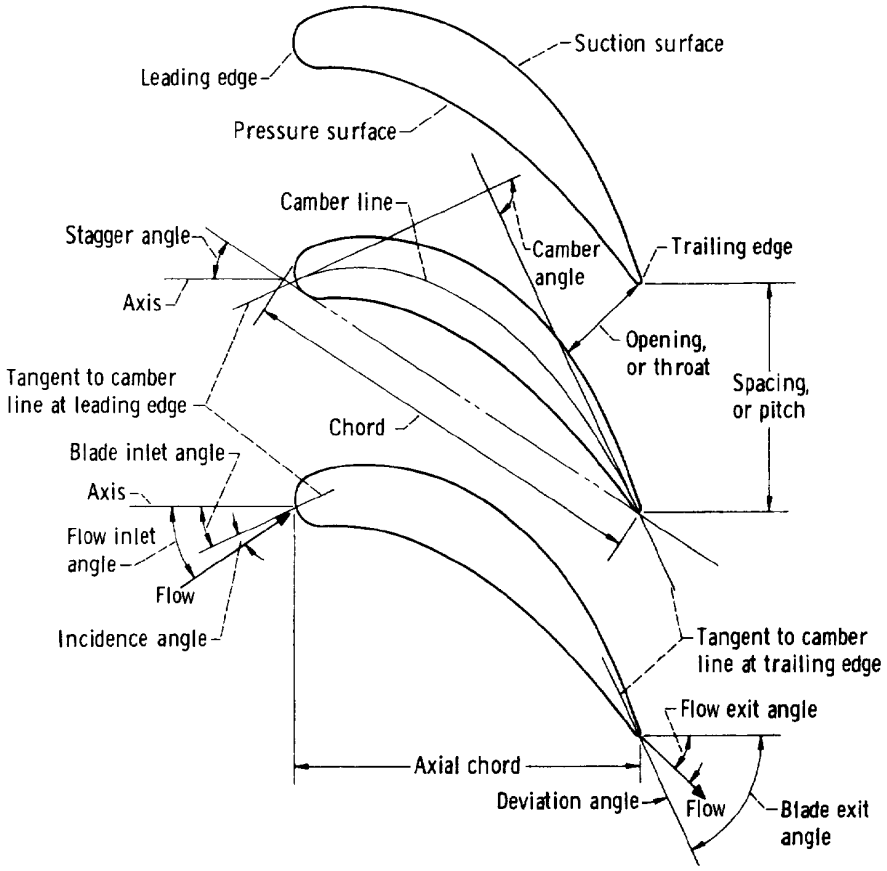

Figure 23: Turbine Blade Parameter Definitions.[42]

to decompose the losses and attribute them to different sources. For example, the Ainley-Mathieson, Dunham-Came and Kacker-Okapuu loss models contain correlations which relate the flow and geometric parameters to losses from the blade profile, secondary flows, tip leakage, trailing edge thickness, shocks, incidence and deviation. These individual loss sources are then combined (through summation, multiplication or a combination of both) to estimate the total blade row loss coefficient. After computing the loss coefficients for each blade row, the real pressures at each inter-blade row station can be determined. Combining the turbine exit pressure and enthalpy allows the turbine adiabatic efficiency to be calculated as given in Equation 2.

2.5.2 Streamline Analysis

After completion of meanline analysis, the next step in turbine design processes review is typically to consider radial variation of the velocity diagrams. The radial variations occur as the value of U changes with radius. As a result of these radial differences, the blade airfoil geometry must vary to match the flow and provide high overall efficiency.

Streamline analysis is similar to meanline analysis but accounts for radial variations in the flow properties at each turbine station. Instead of assuming a single streamline at the midspan approximates the flow, multiple streamlines are defined. Each of these streamlines essentially serve as the meanline for its individual stream segment and assumes no transfer of mass, momentum or energy between the segments. A three streamline example is shown in Figure 24. The dashed lines identify the three streamlines along which the same velocity diagram and loss model calculations as meanline analysis are completed. The dotted blue lines indicate boundaries defining the individual stream segments.

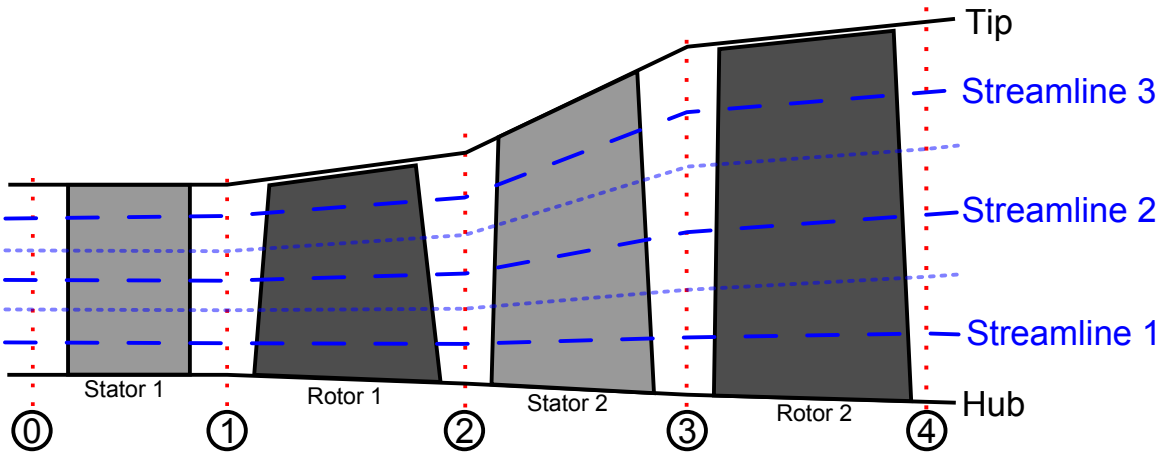

Figure 24: Flowpath for a Two Stage Turbine with Streamlines.

One of the major differences between meanline and streamline analyses relates to the position of the streamlines. While in meanline analysis the meanline location is fixed by the annulus geometry, in streamline analysis the radial location at each streamline must be determined. The streamline locations and stream segment boundaries are specified at the turbine inlet (station 0) along with radial distributions of the flow properties such as

temperature and pressure. As the flow moves through each blade row, the properties in each stream segment change in accordance with the local velocity diagrams. Because the changes may be different in each stream segment, the location of the streamlines must be adjusted such that the flow fills the entire annulus.

Determining the locations of the streamlines is achieved through satisfying the radial equilibrium equation. This equation balances the centrifugal force acting on the flow with radial pressure variations.[42, 60] The radial equilibrium equation is formed by combining the Euler-n equation and a form of the Gibbs equation (Equations 35 and 36 respectively).[60, 114] This combination leads to the radial equilibrium equation in terms of static parameters given in Equation 37. Substituting in the relationship between static and total enthalpy allows for the radial equilibrium equation to be defined in terms of total properties as given in Equation 38.[57, 60, 114] The terms in the equation (from left to right) account for the work distribution, entropy or loss distribution, streamline curvature, axial velocity distribution and tangential velocity distribution (last two terms).

$$V_r \frac{dV_r}{dr} + V_z \frac{dV_r}{dz} - \frac{dV_\theta^2}{r} = -\frac{1}{\rho}\frac{dP}{dr} \tag{35}$$

$$\frac{1}{\rho}\frac{dP}{dr} = \frac{dh}{dr} - T\frac{dS}{dr} \tag{36}$$

$$\frac{dh}{dr} = T\frac{dS}{dr} - V_r \frac{dV_r}{dr} - V_z \frac{dV_r}{dz} + \frac{dV_\theta^2}{r} \tag{37}$$

$$\frac{dh_t}{dr} = T\frac{dS}{dr} - V_z \frac{dV_r}{dz} + V_z \frac{dV_z}{dr} + V_\theta \frac{dV_\theta}{dr} + \frac{V_\theta^2}{r} \tag{38}$$

The complete radial equilibrium equation is often simplified by removing several terms that have negligible impact. For axial machines, the stream line curvature term ($V_z \frac{dV_r}{dz}$) is removed as there is little change in the radial velocity with the change in axial location. Another common assumption is that the entropy distribution ($\frac{dS}{dr}$) is negligible compared to the other terms. Removing these terms results in Equation 39 which is commonly referred to as simple radial equilibrium.[60] Streamline analysis codes will solve one form of the radial equilibrium equation (Equation 35, 37, 38, or 39) to determine the streamline locations that produce physically valid solutions.

$$\frac{dh_t}{dr} = V_z \frac{dV_z}{dr} + V_\theta \frac{dV_\theta}{dr} + \frac{V_\theta^2}{r} \tag{39}$$

Similar to meanline analysis, streamline analysis also requires loss calculations to determine the change in properties across the blade rows for each stream segment. Streamline loss models for turbines do not seem to be available in the open literature. Of the available streamline codes that describe their loss models, they typically describe adapting the meanline loss models previously discussed.[52, 107] In these adaptations, the loss calculations for each streamline may only include certain loss source correlations. For example, streamlines near the midspan may include the profile and secondary loss correlations while excluding the losses calculations for tip clearance. Calculating losses in this manner may result in high losses in some flow segments (generally near the hub and tip) producing low energy flow and a poor overall solution. Therefore, some mixing of the losses across the streamlines is desired to produce a realistic result.[52]

Historically several basic solutions were used to determine the radial changes to the velocity diagrams such that radial equilibrium was satisfied. The most common solution for turbines was referred to as the free vortex solution.[42] In this solution, the simple radial equilibrium equation is used with the following assumptions: $dh_t/dr = 0$ and $dV_z/dr = 0$. The result from these assumptions is that $rV_\theta = constant$. While this solution is common, the free vortex approach to designing blades presents several challenges however. Primarily, applying free vortex design to long blades results in significant variations in the velocity diagrams across the span. The blades required to match these velocity diagrams are highly twisted and may be difficult to manufacture.[42, 60] These large changes can result in degree of reaction values that are small at the hub (close to zero or negative) and large at the tip (close to or greater than one).[42, 60, 114] Therefore, other solutions to the radial equilibrium equations are often considered and referred to as non-free-vortex[42] or controlled vortex[104] solutions. These solutions allow for control of the reaction and losses over the span resulting in increased turbine efficiency.[104]

2.6 Assessment of the Current Engine Conceptual Design Process

The previous sections of this chapter have described the engine design process and its constituent steps. The discussion provided a brief overview of cycle analysis, flowpath and

weight analysis, and several modeling approaches used for the conceptual design of turbines. Through this examination, an assessment of the applicability of the current process for designing tiltrotor engines can be made. The key features for the conceptual tiltrotor engine design process are that it must:

- Effectively and efficiently produce engine cycle designs that meet the performance requirements and design constraints at the various critical engine operating conditions
- Include the turbine conceptual design process to determine the component design features and actual map characteristics as the turbine design (specifically for the VSPT) will be outside the empirical map database
- Effectively and efficiently produce turbine designs that meet the performance requirements and design constraints at a number of operating conditions
- Effectively and efficiently converge the engine cycle, turbine and flowpath/weight conceptual designs to produce the overall design

For the first required feature, the current engine cycle design process does consider the requirements and constraints at the various operating conditions. However, this consideration occurs in a separate off-design phase after the cycle design has been determined. Failure to satisfy all requirements and constraint at the various operating conditions analyzed in this off-design phase requires a return to the on-design analysis to modify the design. This iterative approach may be feasible when requirements and constraints are present at two operating points as changes to a limited number of design inputs are likely to be required to find a viable solution.[103] As requirements and constraints are included at additional operating conditions however, the process for identifying designs that satisfy all requirements and constraints becomes more complex. First, identifying acceptable cycle designs when requirements are present at more than two operating conditions through a series of nested iterations quickly becomes computationally inefficient.[97] Second, there is often a limited understanding of how the design created in the on-design phase must be modified to satisfy the various, often conflicting, requirements and constraints.[97] As a result of these

two limitations, the current cycle design process will not effectively and efficiently produce tiltrotor engine cycle designs.

The second and third required features for the engine conceptual design process relate to the turbine. For the second feature, the processes described in Section 2.1 clearly show that the turbine (or component) design is part of the overall process. In practice however, this step is often omitted in conceptual design in favor of using assumed empirical maps that are deemed to reasonably represent the turbine performance. In regards to the third required feature, the current turbine conceptual design process uses a single design point approach with the computation and assessment off-design performance being completed later in the process. Similar to cycle analysis, developing the turbine design with this single point design method does not effectively and efficiently produce turbine designs. Several recent studies of the VSPT concept have used the single design point approach.[106, 112] In these studies, the designs created met requirements (although not precisely in some cases) at two operating conditions, cruise and takeoff. The design approach applied in these studies will struggle to develop designs when additional requirements at other operating points are added (again similar to cycle analysis). Therefore, the current turbine conceptual design process is also not suitable for addressing the tiltrotor engine design problem.

Finally, the last requirement from the tiltrotor engine design problem is that the various analyses converge to produce the overall design. The importance of this convergence is emphasized by Hall:

> "During the engine development period, component efficiencies often fall short of desired goals by significant margins. The engine cycle rebalance which results causes other components to operate at non-optimal (off-design) flow conditions, further reducing efficiency and complicating the identification of the original source of inefficiency."

While the various engine conceptual design processes show iteration to converge the entire design, the actual amount of iteration may be limited. The steps of the design process are typically conducted by different teams or individuals and the limited communication

between these groups may prevent accounting for all interactions.[23] As a result, issues with the integration of the individual components are often identified late in the design process resulting in designs that are over budget and behind schedule.[25] Based on these considerations, the manual iteration process typically used to converge the different elements of the conceptual design process will not effectively and efficiently produce tiltrotor engine cycle designs.

The assessment of the current engine conceptual design process presented in this section has identified limitations of the current process when applied to tiltrotor engine design. As a result, the following research objective was developed to guide this research effort.

Research Objective: Develop a combined engine/turbine design method that simultaneously considers the requirements and constraints at multiple operating points for both the turbine and engine cycle

CHAPTER III

RECENT DEVELOPMENTS AND KEY ENABLERS RELATED TO ENGINE DESIGN AND ANALYSIS

The research objective stated at the end of the previous chapter identifies the need to develop a new aircraft engine conceptual design approach. Given this need, a literature review was conducted to identify new ideas that could help address the specific deficiencies identified. In this review, two relatively recent developments were identified that address several of the concerns with the current process. The first development of interest is multi-design point (MDP) methods for cycle analysis. Second is the investigation of multi-fidelity level analyses for analyzing engine components. In addition to these topics, a well establish third topic of interest, methods for solving systems of non-linear equations, is considered in this chapter. A discussion of each of these topics is presented in the following sections.

3.1 Simultaneous Multi-Design Point Approach for On-Design Cycle Analysis

The first recent development related to engine conceptual design of interest for this thesis is the formulation of a simultaneous multi-design point (MDP) approach for on-design cycle analysis. As discussed in Chapter 1, aircraft engines, especially for tiltrotor aircraft, must operate over a wide range of flight conditions. The engine design must therefore consider the requirements and constraints present at these operating conditions. The simultaneous MDP procedure developed for on-design cycle analysis ensures the designs developed during the on-design phase will meet the identified requirements and constraints at other specified operating points. This section describes the development, implementation procedure and capabilities of the simultaneous MDP methodology for cycle analysis.

3.1.1 MDP Methodology Development

The traditional approach to cycle analysis, as described in Section 2.2, uses a single operating point during the on-design phase. While this approach is typically presented in undergraduate level texts[33, 55, 56, 74, 75], engine manufactures have developed proprietary methods for considering multiple operating conditions as part of the on design phase.[97] In 2004, researchers began development of the Environmental Design Space (EDS) for the FAA to support the environmental assessment of aircraft engines.[5] During development of this tool, it was recognized that a multi-design point approach was required to accurately model the engines.[70] One of the major accomplishments of the EDS development was the formulation of the simultaneous MDP method in the thesis of Schutte.[97] In this thesis, a step-by-step process was established for completing the MDP design of gas turbine cycles.

3.1.2 The Simultaneous MDP Process

The simultaneous MDP process focuses on identifying engine cycle designs that satisfy the requirements and constraints, thereby falling within the feasible cycle design space. The objective of this process is not to identify the single best engine in the design space as selecting the best engine depends on other factors outside of cycle analysis (e.g. engine weight, emissions, noise). This section summarizes the simultaneous MDP method established by Schutte in his thesis.[97]

The simultaneous MDP method incorporates five different types of parameters in the analysis. These parameter types are defined below:

- **Cycle design variables**: parameters that can be varied to form the cycle design space
- **Operating conditions**: parameters that define the freestream flow
- **Cycle independent parameters**: parameters controlled by a solver to match performance targets
- **Cycle dependent functions**: functions defined by the designer or as part of cycle analysis that ensure a converged, valid solution is reached

- **Constraints**: technology and performance limits place on the cycle that cannot be exceeded

The distinction between these parameter types is important as they are each handled differently in the method. Parameters in each of these categories must be supplied or determined in order to complete the simultaneous MDP process.

In formulating the simultaneous MDP method, Schutte decomposed the process into three phases: the requirements and technology definition phase, MDP setup phase and MDP execution phase. Figure 25 shows these three phases and the key pieces of information that must be determined in each phase. The arrows indicate the flow of this information both within and between the phases.

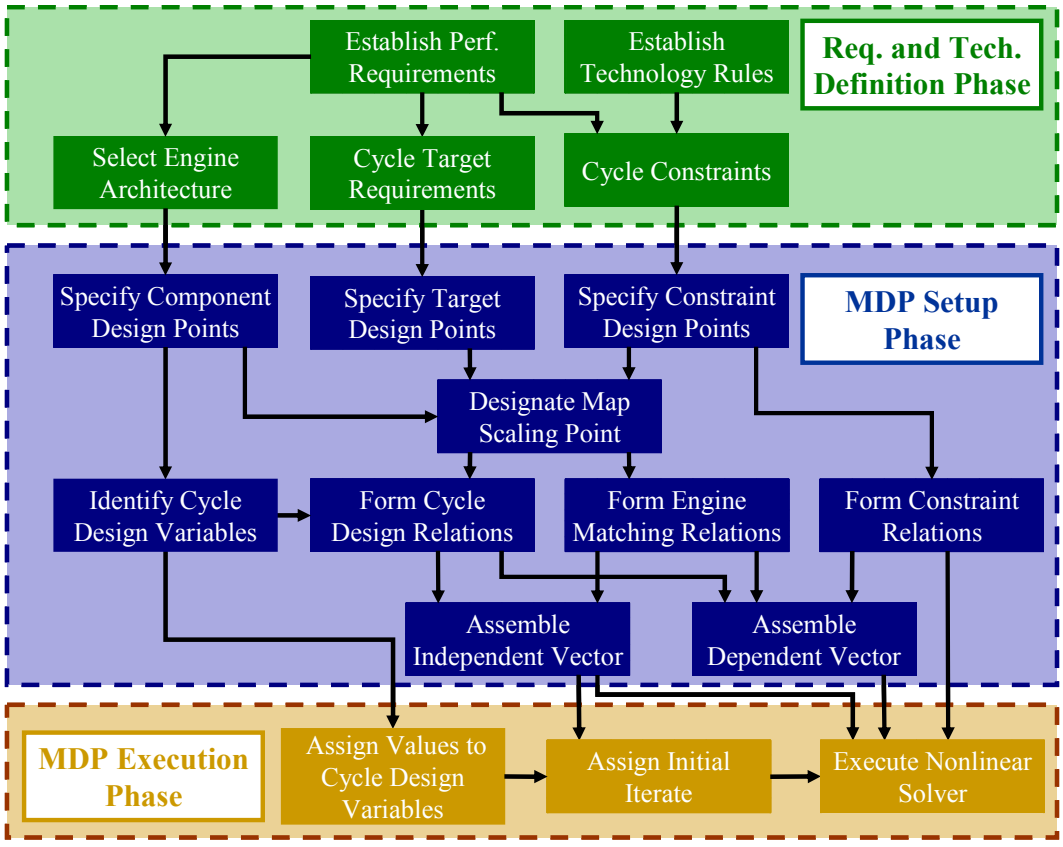

Figure 25: Simultaneous MDP Method Phases and Information Flow for Cycle Analysis[97]

The MDP process begins with the requirement and technology definition phase. In this

phase, the required performance characteristics throughout the operating envelope must be specified. These requirements are typically thrust levels at different operating points. In addition, technology rules which describe how component performance characteristics change with the design variables must be stated. These two pieces of information can be used to determine the cycle target requirements (in the form of equality constraints) and the cycle constraints (in the form of inequality constraints). Finally, the engine architecture is selected in this phase.

The MDP setup phase takes the information from the requirements and technology definition phase and synthesizes it into a system of non-linear equations. At the beginning of this phase, the engine architecture, requirements and constraints are used to determine the required design points for the MDP analysis. From these points, a map scaling point must be specified for each component. One difference between the conventional single point design and MDP, is that maps are required for on-design analysis in the MDP process. The scaling equations described in Section 2.2.4 must be calculated at one design point for each component. After the maps scaling design point has been identified, cycle design, engine matching and constraint relations must be identified. These lead to determining the cycle independent parameters and dependent functions that form a system of non-linear equations. These independent parameters and dependent functions are also referred to as design rules and serve to link the design points together to ensure the requirements and constraints are satisfied. The formation of these design rules also provides a logical, consistent and documented approach for modifying the cycle design to satisfy all the performance requirements and constraints.

The last phase of the MDP methodology is the MDP execution phase. In this phase, values for the cycle design variables are selected. Initial guesses are also made for each of the independent parameters creating the initial iterate. After all this information has been identified, the non-linear system of equations can be solved to identify the feasible engine design.

While Figure 25 shows the information flow and phases for the simultaneous MDP process, it lacks detail about how to complete the entire process. This detail is provided in

an eleven step process shown in Figure 26.[96, 97] One of the details described by this eleven step process is the formation of the design point mapping matrix (DPMM). This matrix relates design variables, performance requirements, component performance estimates and technology limits to their respective design points. A notional DPMM is shown in Figure 27. Readers are referred to the experiments conducted by Schutte for specific examples of the DPMM.[97]

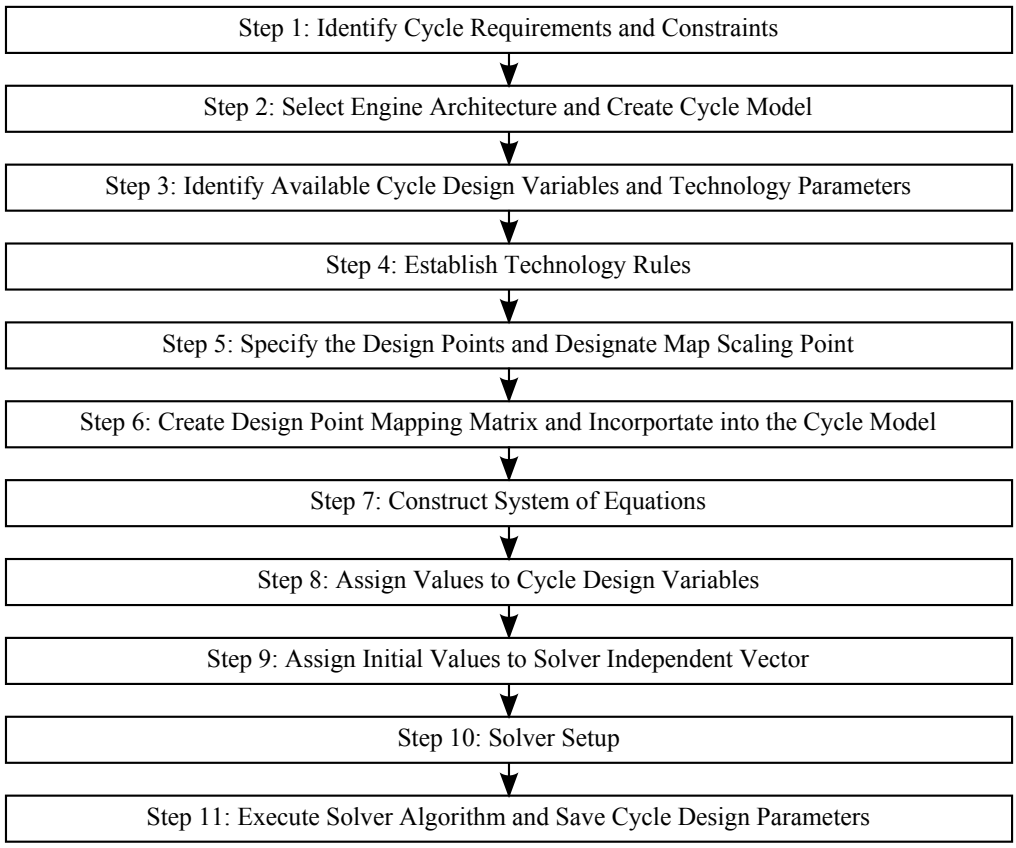

Figure 26: Simultaneous MDP Method Steps for Cycle Analysis[97]

3.1.3 Simultaneous MDP Engine Applications

The developed simultaneous MDP process for on-design cycle analysis is highly capable of modeling a variety of engine architectures with varying numbers of design requirements and constraints. In his thesis, Schutte demonstrated the MDP method using turbofan engines

Design Points		Design Point 1	Design Point 2	Design Point 3	Design Point 4
Comp. Map Scaling Point		**X**			
Design Alternatives (DA)	DA 1	**X**			
	DA 2	**X**			
	DA 3		**X**		
	DA 4				**X**
Performance Requirements (PERF-R)	PERF-R 1	**X**			
	PERF-R 2		**X**		
	PERF-R 3			**X**	
	PERF-R 4				**X**
Component Performance Estimation (CPE)	CPE 1	**X**			
	CPE 2	**X**			
	CPE 3			**X**	
	CPE 4			**X**	
Technology Limits (TLIM)	TLIM 1				**X**
	TLIM 2		**X**	**X**	
	TLIM 3		**X**	**X**	
	TLIM 4		**X**	**X**	

Figure 27: Cycle MDP Design Point Mapping Matrix[97]

for commercial transport aircraft. Using this application, he also examined the ability of the simultaneous MDP procedure to handle large, complicated problems. The method has been successfully applied to a problem with 9 design points with a total of 25 requirements and constraints.[97] The simultaneous MDP method is regularly used as the backbone of EDS to model turbofan engines, typically with five design points.[96] In addition to modeling turbofan engines for commercial aircraft, the simultaneous MDP method has also been applied to other engine concepts. Specific examples include the development of multiple engines with a common core[58] and open rotor engine concepts.[53, 88]

3.1.4 Observations

The review of the simultaneous MDP methodology described the method development, steps in the MDP process and examples of the MDP method application for aircraft engines. From

this review, two notable observations can be made.

The MDP summary provided in this section shows the method is well established and is highly capable of developing designs that meet numerous operating requirements and constraints. The example applications cover conventional turbofan designs as well as unconventional concepts such as the open rotor. The open rotor engine is architecturally similar to the turboprop or turboshaft engine required for tiltrotor aircraft indicating this method would be successful in developing these engine cycle designs. This capability leads to the first observation:

Observation 1: The established simultaneous MDP cycle analysis method addresses the first identified requirement for enabling the conceptual design of tiltrotor engines

This observation makes the simultaneous MDP procedure valuable for determining tiltrotor engine designs.

The second observation relates to other potential applications of the simultaneous MDP method. In the thesis by Schutte, the simultaneous MDP process (both detailed steps and information flow) were developed specifically for cycle analysis. However, there are many other applications where objects must satisfy requirements and constraints at multiple operating conditions. This need for other objects to be designed to meet requirements and constraints at multiple operating points leads to the second observation:

Observation 2: Many steps of the established simultaneous MDP process for cycle analysis could be generalized for application to other problems where requirements and constraints must be met at multiple operating conditions

One relevant example where an MDP method would be beneficial is for the VSPT concept being considered for tiltrotor engines. Using the established cycle MDP method to create a generalized MDP method for other applications would therefore be beneficial for the conceptual design of tiltrotor engines.

3.2 Multi-Fidelity Engine Modeling

The second relatively recent development affecting the engine conceptual design process is research into multi-fidelity engine modeling. The term fidelity in this discussion refers to the complexity of the physics captured by the model. The cycle analysis process described in Section 2.2 uses a low fidelity model for each component based on simple physics relationships and maps which provide relationships that cannot be defined through physics at that fidelity level. The meanline and streamline turbine modeling approaches described in Section 2.5 use more detailed physics to model the performance of the same turbine components as in cycle analysis. Of these two methods, meanline analysis is the lower fidelity (although still higher than cycle analysis) as it assumes the midspan properties are representative of the entire flow. Streamline analysis is the higher fidelity method as it captures the physics associated with the radial variations across the annulus. Other even higher fidelity analyses such as computational fluid dynamics (CFD) are available but are generally overly complex for conceptual design.

Multi-fidelity engine modeling, also commonly referred to as zooming, examines how the various fidelity level analyses can be combined together to form an improved analysis environment that gives more realistic results. As defined by Follen and AuBuchon:

> Zooming means a higher order component analysis code is executed and the results from this analysis are used to adjust the zero-dimensional component performance characteristics within the system simulation. By drawing on the results from a more predictive, physics-based higher order analysis code, cycle simulations are refined to more closely model and predict the complex physical processes inherent to engines.[38]

Claus et al.[26] and Pachidis et al.[83] present similar definitions of the multi-fidelity, zooming analysis capability. Development of zooming capabilities has occurred since the mid-1990s with several demonstrations of the process being completed. Additionally, research has evaluated different approaches for integrating the various fidelity levels with the full engine cycle simulation. The following sections describe the results of this research and

development work.

3.2.1 Multi-Fidelity Capability Development

During the early 1990s it was recognized that the advancement of gas turbine engine technology and design was becoming increasingly difficult. Development of the new technologies and components required expensive experimentation and the resulting designs did not integrate well with other components.[24] Around the same time, advances in computational modeling capabilities were being made enabling analysis and design of new technologies and components with reduced time and cost.[71, 72] This combination of factors lead to the development of a new analysis tool, the Numerical Propulsion System Simulation (NPSS) by NASA, industry and academia. The vision for this tool was to create a virtual test cell for developing advanced propulsion systems and components.[71] The analysis capabilities of the envisioned tool are shown in Figure 28.

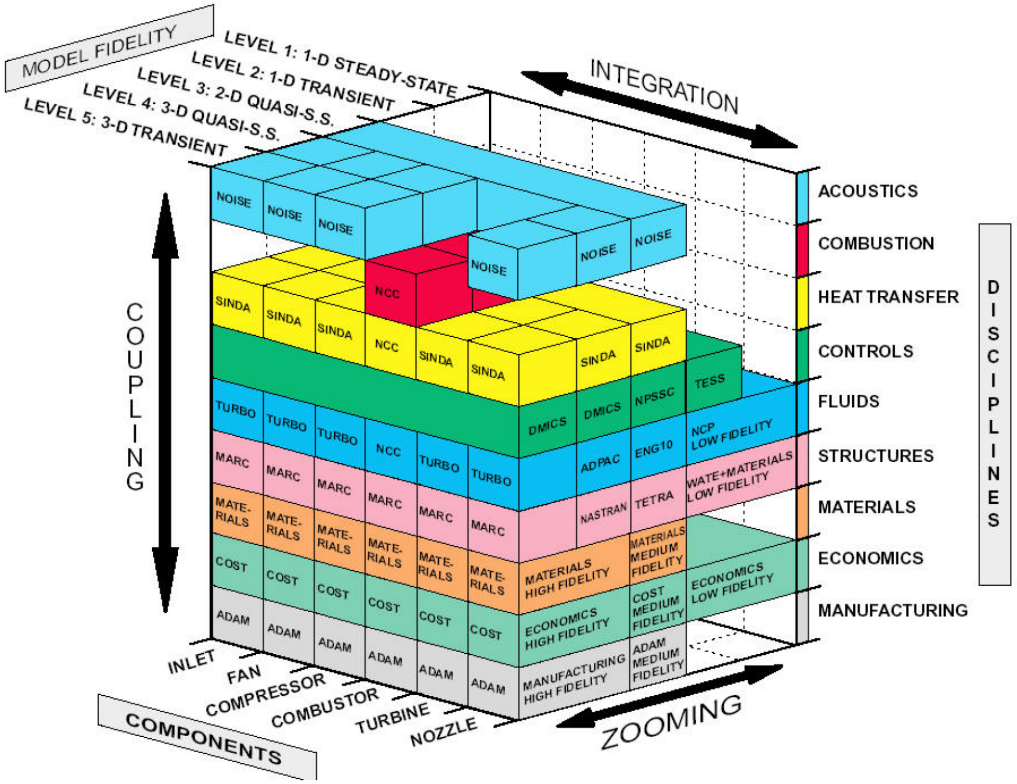

Figure 28: Envisioned NPSS Analysis Capabilities.[71, 89]

The most emphasized of these capabilities in the code development was zooming. The

expected benefits of this zooming capability for the engine design and development process were:[38]

- Rapid component design evaluation in the context of the engine system
- Rapid system-level analysis and optimization
- More predictive results from using first principle component models
- Model fidelity selection to match analysis requirements

The development of the NPSS tool produced a general framework and capability for completing multi-fidelity analysis of engine systems. However, a standardized, full zooming capability was not established for regular use. Despite this limitation, the developed capability was used to perform several demonstrations of the zooming process.

3.2.2 Multi-Fidelity Demonstrations

The foundational capability for zooming developed within NPSS and other similar codes has been used to complete several demonstrations of multi-fidelity engine modeling. A summary of the important features of these studies is presented in this section along with two key observations.

The earliest zooming demonstrations occurred during the development of NPSS and focused on analyzing the engine design produced by General Electric during the Energy Efficient Engine (E^3 or EEE) program.[50, 49] This engine was selected as there was a substantial amount of experimental data available for validation. In this study, high fidelity CFD models of the low pressure engine components were created. These models were coupled with the engine cycle model which included the high pressure and combustion components. The study proved that multi-fidelity analysis of engine components could be completed while also identifying areas for improvement. The analysis of the EEE was later extended to include the high pressure engine components.[48]

Following the initial investigations of zooming on the EEE, a more complete zooming capability was demonstrated by analyzing the General Electric (GE) GE90 engine.[90, 109, 73]

Analysis of the GE90 was completed by again creating CFD models of the engine components. The component models were found to match well with the GE cycle results.[109] These models were used to create component "mini-maps" covering limited operating rages near the selected operating point. Two methods were explored for creating these maps. The first used the CFD simulation to generate the entire map while the second used a single CFD result as input to a meanline analysis code which then generated the mini-map. The second method was preferred as it reduced computational cost and noise in the maps.[90, 109] A number of other key lessons were learned during this study and are reported in several follow-on papers.[23, 25, 108]

Multi-fidelity analysis capabilities were used to model turbomachinery components in support of the Ultra-Efficient Engine Technology (UEET) program beginning in 2002. During the early stages of the research, a General Electric intermediate fidelity tool was first integrated with the cycle analysis to provide new maps.[93] The intermediate modeling capability was then evaluated using existing geometry for highly-loaded turbomachinery components as validation. For a notional 500nm mission, the use of the intermediate fidelity tool resulted in approximately a 3% improvement in mission fuel burn.[93, 89] Following the integration of the intermediate analysis capability, higher fidelity CFD analysis capabilities were added to the analysis. The CFD results were averaged to a meanline value then used to improve the intermediate tool by using an optimizer to find the appropriate settings for empirical parameters in the code. The improved intermediate tool was then used to generate the maps for the cycle analysis.[89]

Finally, recent zooming demonstrations were conducted by Cranfield University on the inlet and fan components.[82, 84, 85, 83] The inlet studies used a commercial CFD package to model the performance while the fan study applied a streamline curvature method. For both of these components, improved performance was achieved through the use of higher-fidelity analyses. The main objective of these studies by Pachidis et al. however was to examine different approaches for integrating the various analysis levels. A review of the integration approaches is provided in the next section.

3.2.3 Integration Approaches

The literature published to date on zooming development and application proposes a number of different strategies for integrating multiple fidelity level analysis. These strategies define the process for executing and passing information between each of the analyses. A brief description of the integration approaches is presented in this section followed by a brief comparison of the approaches.

The de-coupled approach to zooming completely separates the higher fidelity analyses from the engine cycle analysis. In this approach, a range of engine operating conditions are selected and the results from the cycle analysis are used to generate boundary conditions for the component analyses. The component simulations are then run with the outputs used to create a performance map. This map is integrated back into the cycle analysis providing an improved assessment of the engine performance but no further iteration is conducted. This approach is relatively simple and does not require any iteration between the component analyses and the cycle analysis.

The partially integrated approach to zooming provides more coupling between the engine cycle analysis and the component model without going all the way to a fully integrated approach described in the next section. In the partially integrated approach, the cycle analysis is first run and used to provide boundary conditions to the component analysis. The component analysis is then conducted with those boundary conditions and the results are compared with the output from the cycle analysis. If the results do not match, the component results are used to update the cycle analysis which is then rerun. The updated cycle analysis model then provides new boundary conditions to pass to the component model. This process of passing boundary conditions back and forth then running the cycle and component analyses is repeated until convergence is reached.

In the fully integrated approach, the component analysis is directly tied into the cycle analysis and replaces the typical map based component model. For each cycle analysis pass, the component model is also executed providing the exit conditions from the component. As a result, the basic component analysis calculations and the performance map are completely eliminated from the overall cycle analysis for that component. While this approach tightly

couples the cycle and component level analyses, depending on the number of iterations required for the cycle analysis to converge, a large number of executions of the component analysis tool might be required.

The three approaches described in the previous sections focus on different methods for integrating a single component analysis fidelity level with the cycle analysis. When multiple fidelity level tools are available, each of the modeling levels can be included by using a multi-level approach. In this approach, the results from the highest fidelity level analysis are used to update or calibrate an intermediate level analysis to match the higher fidelity results. The calibrated intermediate model can then be used to more quickly predict performance over a wider range of operating conditions.

The decoupled, partially integrated and fully integrated approaches were directly compared in studies by Pachidis et al. that applied the approaches to the analysis of both an inlet and a fan.[82, 84, 85, 83] For both of these test problems, the three methods evaluated produced similar engine performance results. The decoupled approach was found to be fast and computationally inexpensive.[83] The speed of this method resulted from evaluating only the points needed to create the map and not iterating with the cycle. The partially integrated approach ended up being the most computationally intensive, slowest process. Almost 3 times the number of iterations were used compared to the decoupled approach as a result of iteration between the cycle and component models.[83] Finally, the fully integrated approach was found to be the fastest of the three methods directly compared. Rather than produce an entire map, this approach only evaluated the cases needed in the cycle analysis iterative solution. The fully integrated approach may turn out to be more computationally expensive however if a poor initial guess is used in the cycle convergence or if numerous off-design points need to be evaluated.

The multi-level approach is somewhat different than the other three methods and therefore cannot be directly compared. This approach is only valuable when several fidelity level analyses are available for modeling the component. In these situations, however, it was found that coupling the levels together produced the best results as it reduced the computational cost and noise in the maps.[90, 109] In theory, the multi-level approach could

be combined with any of the other three integration approaches that define the interaction between the cycle and component analyses.

3.2.4 Observations

The summary of multi-fidelity analysis capabilities presented in this section describes the development, demonstrations of the capability, and proposed integration methods. The review shows that a solid foundation exists for integrating cycle and higher fidelity component analyses. However, several notable observations can be made regarding the multi-fidelity analysis capabilities in light of the current tiltrotor conceptual design problem.

The first two observations related to multi-fidelity analysis are in regards to the demonstrated zooming capabilities. The demonstrations described above show that results can accurately match known component data and provide improved engine performance for realistic problems. These results show that the zooming capability can be used in the analysis of known designs. However, the developed capability does not describe how to effectively use zooming in the context of design, leading to the first observation of this section:

Observation 3: The demonstrations of multi-fidelity engine modeling to date have been limited to the analysis of known geometries and have not been demonstrated in the context of component and cycle design.

The next observation is closely related to Observation 3. Because the demonstrations have focused on analysis with known geometry, a different set of models were selected than would be used in conceptual design. This observation is formally stated below:

Observation 4: The availability of full 3D geometry allowed for component simulations to be completed with high fidelity CFD but only near a single operating point. Lower fidelity tools commonly used in conceptual design were often either not used or limited to predicting map performance around the converged CFD result.

The last observation related to the multi-fidelity analysis of turbomachinery focuses on the integration approaches. The four methods presented in the review each have benefits and disadvantages that were quantified for several specific applications. These applications

differ from the turbine and tiltrotor engine that are the focus of this thesis leading to the last observation:

Observation 5: Multiple approaches are available for coupling the detailed component analyses with the cycle analysis but it is unclear which approach will work best in the design of tiltrotor engines and their turbines

3.3 Numerical Methods for Solving Systems of Nonlinear Equations

The last key enabler summarized in this chapter is numerical methods for solving systems of nonlinear equations. Engineering models such as the cycle, meanline and streamline analyses described in the last chapter typically contain many complex nonlinear equations that cannot be solved analytically. To solve the nonlinear equations present in these models, numerical methods which focus on finding the roots of the system of equations are commonly applied.[12] Often these numerical calculations are not exposed to the user of the analysis tool as the user is primarily interested in the input and output of the code. However, development of a new method to better design the combined engine and turbine system requires an understanding of these mathematical tools. Therefore, a brief summary of relevant numerical methods for finding the roots for systems of nonlinear equations is warranted.

3.3.1 Newton-Raphson Method

One of the best known numerical methods for finding the roots of a system of nonlinear equations is the Newton-Raphson method (also commonly referred to as simply Newton's Method).[12] This method is popular due to its simplicity and speed in identifying a solution. The method is commonly applied in cycle analysis and meanline analysis codes which are central to this work.

The objective of the Newton-Raphson iterative method is to find the values for independent vector X which makes the dependent system of equations $F(X) = 0$ true. While an exact solution to this system may be possible, it is often impractical and excessive to find the exact independent values. Therefore, application of the Newton-Raphson method

in engineering analyses commonly converts the strict equality to an inequality, $F(X) \leq \epsilon$, such that each dependent function is converged within a specified tolerance ϵ. This tolerance can be specified as either an absolute or relative (fractional) value, and may be unique for each equation in the system.

Once the system of equations and tolerances have been properly defined, the iterative process to find the roots can be started. This process begins by selecting an initial value for each independent parameter giving the initial iterate vector X_0. The dependent functions are evaluate at this point to determine if $F(X_0) \leq \epsilon$ is satisfied. If this expression is true for all equations in the system, the initial guess was close enough to the actual answer and the system is considered converged. If the entire system of equations is not converged, the iterative process continues by determining a new independent vector at which to evaluate the function using Equation 40. In this equation, X_n is the current independent vector and X_{n+1} is the new independent vector being computed. Additionally, $F'(X_n)^{-1}$ is the Jacobian matrix which is defined by Equation 41.

$$X_{n+1} = X_n + F'(X_n)^{-1} F(X_n) \tag{40}$$

$$F'(X) = \begin{bmatrix} \frac{\partial f_1}{\partial x_1} & \cdots & \frac{\partial f_1}{\partial x_m} \\ \vdots & \ddots & \vdots \\ \frac{\partial f_m}{\partial x_1} & \cdots & \frac{\partial f_m}{\partial x_m} \end{bmatrix} \tag{41}$$

Once the new independent vector is determined, the dependent system of equations is again evaluated to determine if all values satisfy the specified tolerance. If convergence is still not reached, the Jacobian (Equation 41) and Newton step (Equation 40) are again computed to determine the next independent vector. This process is repeated until convergence is achieved for all dependent functions. A graphical representation of the Newton-Raphson iterative process for a one-dimensional problem in shown in Figure 29. Here, the green line depicts the function for which the root is trying to be numerically found. The solid blue lines show the steps taken by the Newton solver based on the computed gradient at each iteration.

While the Newton-Raphson iterative process appears relatively simple, there are several

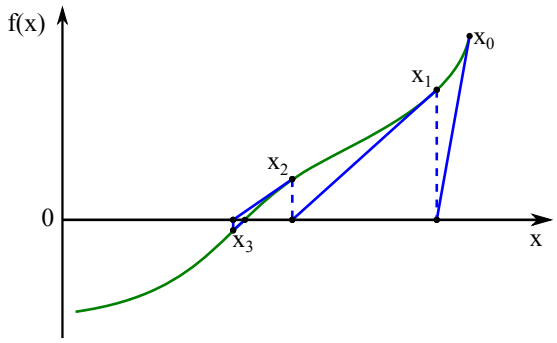

Figure 29: Newton-Raphson Steps for a One-Dimensional Problem.

challenges associated with applying the method in engineering applications. These challenge relate to the Jacobian calculation, convergence issues and constraint application. The following sections describe these challenges as well as modifications to the Newton-Raphson method to address these issues.

3.3.1.1 Jacobian Calculation

An important aspect of applying the Newton-Raphson method in engineering models is computation of the partial derivatives that comprise the Jacobian matrix. In the rare instance that the analysis code provides the partial derivatives for each element of the matrix the Jacobian can be assembled directly. More commonly the partial derivatives needed for the Jacobian matrix are not available from the engineering model and must be approximated. Approximation of the partial derivatives in the Jacobian matrix is commonly achieved through the application of finite difference methods. In these methods, a small perturbation (h) is applied to a single independent value while holding all other independents constant. Applying this perturbation in the positive direction is referred to as a forward difference while a perturbation in the negative direction is a backwards difference. Taking a perturbation step in both the forward and backwards direction is referred to as a central difference approach. Once the perturbation step is taken the model is then re-evaluated with new independent vector thereby determining new values for all dependent variables. The partial derivatives for all dependents can then be determined using Equations 42, 43 and 44 for forward, backward and central differences, respectively. This process is then repeated for

all parameters in the independent vector to determine all elements of the Jacobian matrix.

$$\frac{\partial f}{\partial x} = \frac{f(x+h) - f(x)}{h} \tag{42}$$

$$\frac{\partial f}{\partial x} = \frac{f(x) - f(x-h)}{h} \tag{43}$$

$$\frac{\partial f}{\partial x} = \frac{f(x+h) - f(x-h)}{2h} \tag{44}$$

The accuracy of the gradients computed using these finite difference approaches dependents on several factors. The primary factor influencing the accuracy is the perturbation step size as small step sizes may lead to numeric cancellation errors while a large step size may produce truncation errors.[47] The accuracy of the finite difference approximated gradients is also impacted by any errors (ϵ_f) present in the function evaluation itself.[68, 69] In this case, the function output is actually an approximate, $\hat{f}$, as defined in Equation 45. The gradient computed using the forward finite difference is now based on this approximate function value as defined in Equation 46. As a result, there is a gradient error, ϵ_g, between the values computed with Equations 42 and 46. The magnitude of this gradient error depends on both the function error and the step size with the magnitude of the error defined by Equation 47.[69] This gradient error can be minimized by setting the perturbation step such that $h = O(\sqrt{\epsilon_f})$.

$$\hat{f} = f + \epsilon_f \tag{45}$$

$$\frac{\partial \hat{f}}{\partial x} = \frac{\hat{f}(x+h) - \hat{f}(x)}{h} \tag{46}$$

$$\epsilon_g = O(h + \epsilon_f/h) \tag{47}$$

This propagation of error from the function evaluation to the gradient is similar for the backwards difference approach. For the central difference method, the gradient error magnitude is $O(h^2 + \epsilon_f/h)$ with the gradient error minimized by setting $h = O(\sqrt[3]{\epsilon_f})$.[69]

The use of finite difference gradient approximation techniques is common in engineering tools including those used for cycle, meanline and streamline analyses. The details of how these gradients and the Jacobian matrix are computed is often hidden from the end user of the analysis tool. However, an understanding of these calculations and the potential

sources of error is important for the development and implementation of a combined engine and turbine design methodology as they affect the Newton-Raphson solver convergence characteristics.

3.3.1.2 Convergence Characteristics and Issues

By using the gradient information found in the Jacobian matrix, the Newton-Raphson method is capable of rapidly converging upon the roots of a system of nonlinear equations. The requirements for this convergence are that the gradients be non-zero, the second derivative or Hessian matrix be continuous, and that the initial guess be sufficiently close to the roots of the system of equations. If these conditions are satisfied, it is well documented that the method exhibits a quadratic convergence rate.[12, 17, 41, 86] A quadratic convergence rate implies that the iteration process satisfies Equation 48 where x^* is the actual solution.

$$\|x_{n+1} - x^*\| \leq K\|x_n - x^*\|^2 \tag{48}$$

While the quadratic convergence rate makes solving systems of nonlinear equations with the Newton-Raphson method desirable, there are several additional issues that commonly arise in actual implementation. First, as noted in the convergence rate assumptions the Newton-Raphson method requires that the initial independent vector be sufficiently close to the solution such that the Jacobian matrix and step calculations will move towards the converged solution. The ability of the method to find a solution is therefore heavily dependent on the user providing a quality initial independent vector X_0. Providing a poor initial vector will commonly result in the model diverging from the solution and ultimately failing to converge.

The other issues that may arise in application have to do with special situations encountered during the iterative process. The first of these is the presence of a stationary point in the neighborhood of the root. At this stationary point the partial derivatives for all independent parameters and dependent equations would be zero resulting in no change to the independent vector between iterations. Another special case that may be encountered is a cycle within the iterations. This cycle occurs when the gradients at the current iteration return the independents to the values at a previous iteration. These two issues

are difficult to assess prior to execution of the solver and are best resolved by improving the initial guess. The last issue potentially encountered in the iteration process is that of over shooting the root. In this case, the gradient may be shallow resulting in a large change in the independent values between iterations. This large step sizes can move the iteration outside the neighborhood of the solution and result in divergence from the root. This issue is often addressed by limiting the step size taken in any iteration. This change will improve the stability of the convergence by keeping the iterations in the neighborhood of the root but may reduce the convergence rate.

3.3.1.3 Constraint Application

In addition to these characteristics of the Newton-Raphson method commonly described in texts, another useful development is the ability to add constraints to the solution process.[79] The constraints are formed as supplemental dependent equations to those already in the system of equations. Each constraint equation is then attached to a single dependent equation. In the Newton-Raphson solution process, at each iteration the constraint values are determined in addition to the dependent equation values. If the constraint values are violated, the constraint equation replaces the dependent equation in the system. The iteration continues with the original dependent now serving as a constraint. This functionality allows for a constrained system of equations to be solved and is particularly useful in cycle analysis.

3.3.2 Quasi-Newton Methods

One of the major challenges associated with applying the Newton-Raphson method to systems of nonlinear equations in engineering models is computing the Jacobian matrix on each iteration. Computing the Jacobian can be a difficult and expensive process especially when a finite difference approach is required to determine the partial derivatives. Quasi-Newton methods address this limitation by developing approximations of the Jacobian to use in the iteration. This approximate Jacobian is then used as part of the iteration to find the next independent vector.

One of the most popular quasi-Newton approaches is Broyden's method.[16] The steps

for Broyden's method start out similar to the Newton method with a full Jacobian being computed and applied to find the first step using Equation 40. After this first step, an approximation to the next Jacobian (B_{n+1}) is developed using Equations 49 and 50 with $B_n = F'(X)$.

$$B_{n+1} = B_n + \frac{F(X_{n+1})s^T}{s^T s} \tag{49}$$

$$s = X_{n+1} - X_n \tag{50}$$

These calculations require only the current independent vector (X_n), the current Jacobian or Jacobian approximation (B_n), the next independent vector (X_{n+1}), and the next dependent vector ($F(X_{n+1})$ making determination of a new Jacobian approximation inexpensive to compute. This new approximate Jacobian can then be used to determine the next independent vector using Equation 51.

$$X_{n+1} = X_n + B_n^{-1} F(X_n) \tag{51}$$

While Broyden's method eliminates the need to compute new Jacobians on each iteration, the use of approximate Jacobians effects the rate of convergence of the method. Broyden's method has been shown to have a q-superlinear rate of convergence.[68] This convergence rate is slower than the pure Newton-Raphson method but may provide an overall improvement in computational cost due to removal of the Jacobian calculations at each iteration.

CHAPTER IV

METHODOLOGY FORMULATION

The Introduction and Motivation chapter which opened this thesis examined the design requirements of tiltrotor engines and their power turbines. This examination identified the need for a conceptual design method that considers requirements and constraints for both the cycle and turbine at multiple operating conditions. An assessment of the current engine conceptual design process was presented in Chapter 2 leading to the definition of a generic engine conceptual design process as shown in Figure 30. This assessment found that the process does not effectively produce designs for both the engine cycle and turbine that meet the various requirements and constraints throughout the operating envelope. The main limitation of the current conceptual design process is the three iterative loops that must be converged. For complex problems, such as the tiltrotor engine, there are a number of requirements that are evaluated in each diamond. Modifying the design characteristics in the on-design phases of the cycle and turbine analyses to satisfactorily match these requirements is difficult.

While the current conceptual design process defined in Figure 30 is not considered satisfactory for the design of the tiltrotor engines and power turbines which motivated this thesis, the process contains the proper analyses in a reasonable order. Therefore, this process will serve as a starting point for formulating a new conceptual design method. Chapter 3 presented several recent developments and key enablers which will be combined to address the deficiencies of the current process and produce the new conceptual design method.

4.1 Simultaneous MDP Procedure for On-Design Cycle Analysis

The first convergence loop encountered in the engine design process of Figure 30 considers the requirements and constraints imposed on the engine cycle. The on-design analysis traditionally considers a single engine design point then evaluates other critical design points in the off-design phase. If the requirements and constraints at the off-design points are not

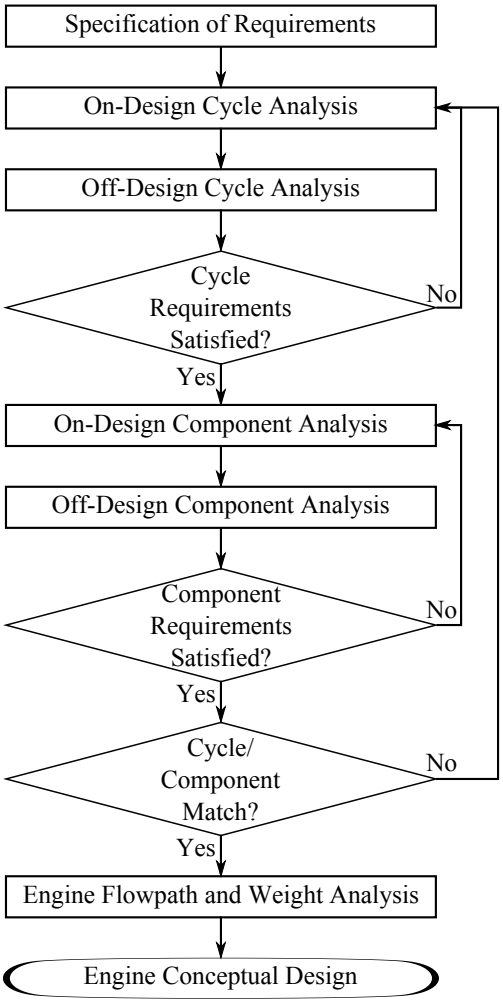

Figure 30: Generic Aircraft Engine Design Process

satisfied by the selected design, a return to the on-design phase is necessary. Changing the cycle design to match the requirements and constraints can be difficult and time consuming, especially when multiple conflicting requirements and constraints are present.

The simultaneous MDP method for on-design cycle analysis presented in Section 3.1 provides a method to capture requirements and constraints at a number of operating conditions during the on-design phase. By considering the requirements and constraints at the critical operating points during the on-design phase the design produced is assured to be feasible. Therefore, the first convergence loop in the conceptual design process is effectively eliminated as shown in Figure 31. In place of this loop is a single step for on-design MDP

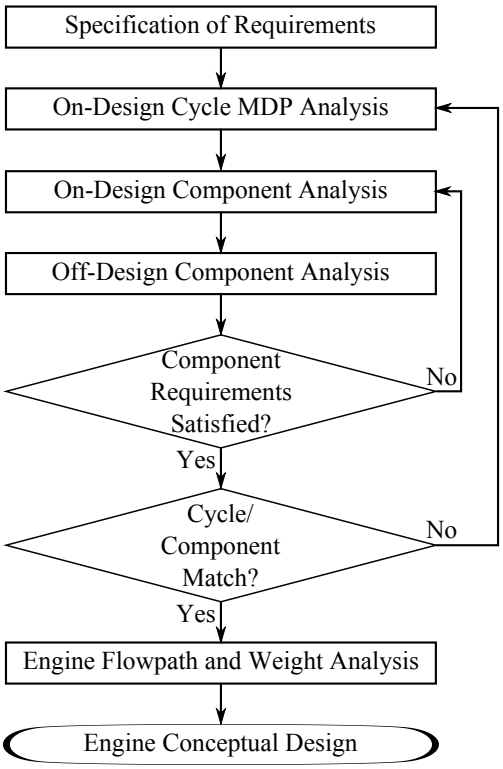

Figure 31: Generic Aircraft Engine Design Process with Cycle MDP

cycle analysis. Implementing the cycle MDP method improves the conceptual design process but still leaves two convergence loops which present challenges for developing turbine designs which satisfy all requirements and constraints as well as matching the cycle and turbine designs.

4.2 Simultaneous MDP Procedure for On-Design Turbine Modeling

With the simultaneous MDP method applied to the cycle analysis, the next area for improving the current process is the second convergence loop that ensures turbine requirements and constraints are satisfied. In the traditional design process, a single design point is considered during the on-design phase with performance at other important operating conditions evaluated later in the off-design phase. Similar to cycle analysis, there are generally a number of requirements and constraints evaluated in the off-design phase that determine if a design is acceptable. Developing satisfactory designs through this iteration is difficult

when numerous conflicting requirements and constraints are present. Addressing this challenging turbine convergence loop will improve the turbine design process and the overall engine conceptual design.

Designing the turbine to meet multiple requirements and constraints at different operating conditions is similar to the challenge faced in cycle analysis. The solution described in the previous section for cycle analysis applies the established simultaneous cycle MDP method. Given the similarities in these problems, the logical solution for ensuring turbine designs meet requirements and constraints at multiple operating points is to develop an analogous turbine simultaneous MDP method for the on-design phase.

In the review of the simultaneous MDP method for cycle analysis presented in Section 3.1, Observation 2 states that cycle MDP method could be adapted and applied to other systems where requirements and constraints must be met at multiple operating conditions. Generalizing the cycle MDP method for application to the turbine leads to the first research question to be addressed in this thesis:

Research Question 1: How can the MDP method established for on-design cycle analysis be generalized and applied to the on-design phase of turbine meanline analysis to generate designs that meet requirements and constraints at multiple operating points simultaneously?

The turbine simultaneous MDP method developed by answering this research question will provide an improved capability to capture requirements and constraints at critical operating points during the on-design analysis phase. Applying the developed turbine MDP method within the engine conceptual design process will streamline the process by removing the turbine convergence iteration as shown in Figure 32.

Applying the turbine simultaneous MDP method will produce designs differing from those generated by the traditional single point turbine design approach. The second research question examines the differences in the turbine designs produced by these two methods and is stated below:

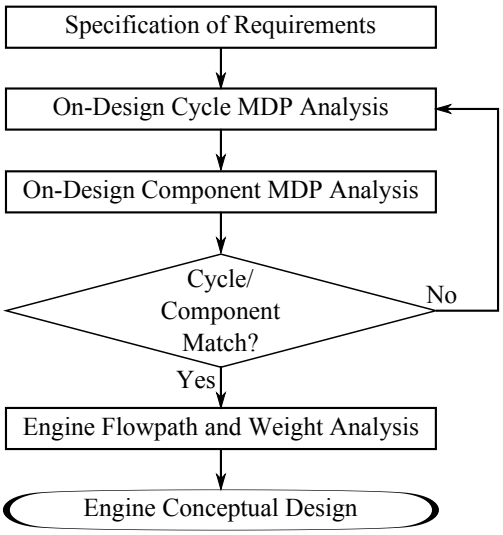

Figure 32: Generic Aircraft Engine Design Process with Cycle and Turbine MDPs

Research Question 2: What are the differences in the turbine design and performance characteristics as a result of using a simultaneous MDP method versus a traditional turbine design approach?

Answering Research Questions 1 and 2 will lead to the development of a new turbine meanline MDP method and determine the benefits of this new approach. The development and evaluation of the turbine MDP method is presented in Chapter 5. Addressing these two research questions also allows for further improvements to be made to the engine conceptual design process to better couple the cycle and turbine analyses.

4.3 Simultaneous Multi-Level MDP Procedure for Engine Conceptual Design

The development of a turbine MDP process to couple with the established cycle MDP process will better identify feasible cycle and turbine designs. While implementing these developments will improve the conceptual design process, there is still a need for additional improvement. Examining the engine conceptual design process in Figure 32, one final convergence loop is shown which matches the engine cycle and turbine performance characteristics. Given the changes that will occur in both the cycle and turbine analyses at multiple operating points, it will be challenging for an engine designer to manually complete

this convergence.

The multi-fidelity (zooming) research reviewed in Section 3.2 provides a starting point for integrating the cycle and turbine analyses. This previous work is only considered a starting point as the multi-fidelity demonstrations focused on analysis of known geometry rather than the conceptual design as stated in Observation 3. However, Observation 5 highlights the different approaches were proposed for integrating the cycle and turbine analyses, but it is unclear which approach will work best for the current problem. Therefore, the third research question addresses how to form a simultaneous multi-level, multi-design point (MLMDP) engine conceptual design method:

Research Question 3: How can the on-design MDP methods for designing the turbine and cycle be merged together to simultaneously generate designs for the both turbine and engine that meet requirements and constraints at multiple operating points?

Successful development of a method in response to this question will allow the cycle MDP analysis, turbine MDP analysis and engine flowpath/weight analysis to be integrated into a simultaneous solution. Such a method would enable the efficient identification of feasible overall engine cycle and turbine designs that meet the requirements and constraints at multiple operating conditions. The simultaneous MLMDP engine conceptual design process is shown in Figure 33.

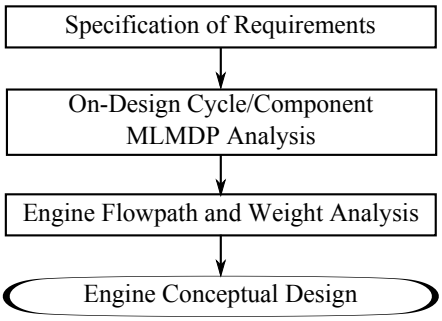

Figure 33: Generic Aircraft Engine Design Process with MLMDP

The simultaneous MLMDP method developed from Research Question 3 will produce

different engine and turbine designs compared to solving the MDP problems for each individual analysis in sequence as shown in Figure 32. The last research question evaluates the differences in the engine cycle and turbine designs between these two approaches:

Research Question 4: What are the differences in the turbine and engine designs and performance characteristics as a result of using the simultaneous MLMDP method versus solving the MDPs at each level individually?

Answering Research Questions 3 and 4 will establish the MLMDP method and evaluate the benefit of this new approach. The development and evaluation of the MLMDP method is presented in Chapter 6. Addressing these two research questions will determine whether the overall research objective stated at the end of Chapter 2 has been satisfied.

CHAPTER V

TURBINE MULTI-DESIGN POINT METHODOLOGY DEVELOPMENT, IMPLEMENTATION AND RESULTS

The previous chapter reviewed the current engine conceptual design methodology and proposed several improvements which could produce better engine and turbine designs while reducing the number of manual convergence loops involved in the process. The first convergence loop which considers the on- and off-design performance of the engine cycle was previously addressed through the development of a multi-design point cycle analysis procedure. The second manual convergence loop in the overall engine conceptual design process involves ensuring the turbine design meets all requirements and constraints at both on-design and off-design conditions. Given the success of the multi-design point method in removing the cycle convergence loop and producing valid cycle designs, Research Question 1 (restated below) inquires if a similar method can be developed for the turbine conceptual design.

Research Question 1: How can the MDP method established for on-design cycle analysis be generalized and applied to the on-design phase of turbine meanline analysis to generate designs that meet requirements and constraints at multiple operating points simultaneously?

Assuming a viable turbine MDP method can be developed during the investigation of Research Question 1, a second research question was posed in the previous chapter which focused on the designs produced by the turbine MDP method. Research Question 2, restated below, investigates the differences in the designs generated by the turbine MDP method in comparison to those determined by the traditional single point design approach.

Research Question 2: What are the differences in the turbine design and performance characteristics as a result of using a simultaneous MDP method versus a traditional turbine design approach?

The investigation of these two research questions is an important first step in the development of the overall multi-level MDP method formulated in Chapter 4. This chapter therefore focuses on answering both of these research questions. The process for answering these two questions started with a thorough examination of the cycle MDP method as described in Section 5.1. Observations made during this examination suggested an approach for generalizing the MDP method for application to a turbine leading to the formation of hypotheses for each of the research questions. Following the formation of these hypotheses in Section 5.2, the turbine MDP method was further developed by adapting several steps of the cycle MDP method to apply to the design of a turbine. With these critical steps addressed, the complete turbine MDP method is described in Section 5.4. While the formulation of this method is important, computational experiments are required to determine if the proposed method indeed ensures that requirements and constraints at all operating conditions are considered, and to assess how the method impacts the turbine design in comparison to the traditional single point design approach. To test both hypotheses, the developed turbine MDP method was applied to three different turbine design problems as described in Section 5.5 with the results from computational experiments using these models presented in Section 5.6.

5.1 Cycle MDP Methodology Examination

The first research question posed in this thesis considers the generalization and adaptation of the cycle MDP methodology for other applications, specifically the design of turbine engine components at the meanline analysis level. The development of a turbine meanline MDP method therefore naturally began with a review of the previously developed cycle MDP method. As summarized in Section 3.1, the cycle MDP method consists of three phases which define the requirements and technology limits, setup the MDP analysis model and execute that model for the given design inputs. To complete these three phases, an 11 step procedure was described as shown in Figure 26. While the details for these steps is specific to cycle analysis, the underlying tasks associated with most steps are identical to

those which would be required for a turbine multi-design point method. However, there are two steps for which the generalization and application of the cycle MDP approach appears to be non-trivial. These steps are those associated with constructing a turbine meanline model that is compatible with the MDP process (Step 2) and determining the system of nonlinear equations which couple design points (Step 7). These two steps are reviewed in more detail below with observations made which guide the generalization of these steps for a turbine MDP procedure.

5.1.1 Cycle Design Parameterization

The first step of the cycle MDP method requiring further investigation for generalization and adaptation to the turbine design problem is that of developing the model to which the MDP method will be applied (Step 2). While this step may seem trivial, the creation of the model, particularly the way that model is parameterized, is critical to the success of the MDP methodology. Here, the term model parameterization refers directly to how the design is specified, specifically in regards to the vector of input parameters used by the analysis tool. While a variety of valid input parameters may be used to define a design in different analysis tools, the selection of an appropriate design parameterization is important for several reasons. First, it determines what parameters are available for coupling the design points where the various requirements and constraints are present. Second, the selection of the design parameterization ensures that the MDP method logically adjusts the design to meet the performance requirements and constraints. Given the importance of the design parameterization for MDP methods, a review of the cycle MDP procedure and examples of its implementation was completed.

Reviewing the written cycle MDP methodology and procedure developed by Schutte[97] revealed little detail on the selection of the design parameters when creating cycle models for the MDP analysis. Therefore, the examination of this step for generalization to other applications was predominantly completed by reviewing the implementation of the method on the examples summarized in Section 3.1.3. Although there were some differences in these examples depending on the engine architecture and design problem, the examination

reveal a similar design parameterization was used in most cases. The models developed for cycle MDP analysis typically define the cycle using parameters such as component pressure ratios, component efficiencies, the extraction ratio (in the case of a turbofan engine), and maximum combustor exit temperature. Within this list, a common theme arises: most of the design parameters used in the cycle MDP examples are non-dimensional values with the primary exception being the combustor exit temperature. While not all these parameters are non-dimensional, they can all be classified as thermodynamic similarity parameters as they uniquely define the thermodynamic process (or path) occurring within the engine.

Specifying the design in terms of these thermodynamic similarity parameters is critical to the success of the cycle MDP method. Although a unique, real Brayton cycle is defined by this parameterization, it is important to note that the determined thermodynamic cycle is independent of the amount of air undergoing those changes. Selection of this design parameterization therefore allows for a unique thermodynamic cycle to be defined and then sized in the MDP method to satisfy the identified performance requirements and constraints. As a result, the following observation can be made:

Observation: The cycle MDP method is enabled by specifying designs in terms of *thermodynamic cycle similarity parameters* (typically non-dimensional values) which allow the method to *size* the engine to satisfy the given performance requirements and constraints.

This observation regarding the design parameterization within the cycle MDP method is important to the development of a general MDP framework for two reasons. First, it indicates that a model which parameterizes the design with similarity parameters is likely to work well with the turbine MDP method. Second, this observation identifies that the MDP method sizes the design specified in terms of these similarity parameters to satisfy the requirements and constraints. Coupled with the analysis of the cycle MDP coupling equations in the next section, this observation will be used to form a hypothesis regarding the generalization of the cycle MDP method for application in the design of the turbine component in Section 5.3.

5.1.2 Cycle MDP Coupling Equations

The second step of the cycle MDP methodology requiring further research for adaptation to a turbine design problem is that of determining the system of nonlinear equations which couple the design points forming the MDP analysis. This step is the central element of the MDP method which makes it different than the traditional single point design approach. The challenge in adapting this step to other design problems is determining the coupling equations, also referred to as design rules, which link the design points allowing for all requirements and constraints to be satisfied. Again for this step, it is informative to reexamine the cycle MDP process for guidance on key features of the design rules which can result in a successful MDP analysis.

The design rules formulated in the cycle MDP method form a system of nonlinear equations which can be converged by a Newton-Raphson solver. This system consists of a set of dependent equations $F(X)$ along with independent parameters X which are varied such that $F(X) = 0$. The requirement for this system is that there must be an equal number of independent parameters and dependent equations, and that the independents must be unique.[97] Although the cycle MDP method does not develop a single set of design rules for all problems, the published examples implementing the method provide insight into the classes of equations and parameters which are likely to produce a valid design. From these published examples, the following observation about the cycle MDP parameter classes can be made:

Observation: The cycle MDP method typically applies design rules which create dependent equations from the performance requirement at each design point and an operating constraint by *sizing* the engine using a single sizing parameter and adjusting the performance at each design point using an operating parameter.

In the cycle MDP method, these performance requirements typically consist of the net thrust at each design point while the operating constraint is commonly a maximum combustor exit temperature at one design point. The independent parameters which form the other half of the design rules typically included the mass flow rate into the engine as

the single sizing parameter with the fuel-to-air ratio of the combustor (or throttle setting) serving as the operating parameter at each design point. These design rules are not the only way to implement the cycle MDP method, but demonstrate the type of independent parameters and dependent equations which have enabled successful implementation of the method. This observation also contributes to the formation of a hypothesis regarding the generalization of the cycle MDP method for application to turbines as described in the next section.

5.2 Turbine MDP Hypotheses

At the beginning of this chapter, two research questions were posed to guide the development and assessment of a turbine MDP methodology. Addressing these questions started by completing a more detailed review of the cycle MDP method in the previous section. From this review, two hypotheses can now be stated regarding the anticipated answer for these questions.

The first research question considered how to generalize the cycle MDP method for application to other design problems, specifically the design of the turbine component within an aircraft engine. The review of the cycle MDP method identified two steps that appeared to be critical for completing this generalization process. In addition, two important observations were made during this review regarding the design parameterization and MDP coupling equations. From these observations, Hypothesis 1 was developed in support of Research Question 1. Hypothesis 1 is stated below:

Hypothesis 1: The MDP method developed for on-design cycle analysis can be applied to the meanline on-design analysis of multi-stage turbines by selecting an appropriate design parameterization and constructing the system of nonlinear equations that couple the design points

Assuming a viable turbine MDP method can be developed in support of Research Question and Hypothesis 1, a second research question related to the designs generated by the turbine MDP method was also posed. This question specifically investigates the differences

in the designs produced by the turbine MDP method in comparison to the traditional single point design approach. With the anticipated formulation of the turbine MDP method with an appropriate design parameterization and set of MDP coupling equations, Hypothesis 2 can also be formulated in response to Research Question 2. This hypothesis, stated below, emphasizes that the difference in the turbine designs produced by the traditional single point design approach and the turbine MDP will differ as a result of the MDP coupling equations.

Hypothesis 2: The MDP generated turbine designs will differ in geometry and performance characteristics from those generated with the traditional approach as a result of the additional equations that consider requirements and constraints across the design points

Evaluation of these two hypotheses will be completed throughout the remainder of this chapter. To start, the first hypothesis will be considered from a theoretical perspective to identify potential turbine design parameterizations and MDP coupling equations. Following this theoretical examination, the turbine MDP procedure will be formulated and applied to several example design problems. Finally, computational experiments will be completed with these models to fully evaluate Hypotheses 1 and 2.

5.3 Turbine MDP Methodology Development

Hypothesis 1, stated in the previous section, identifies two steps of the cycle MDP method requiring investigation and modification for adapting the method to the turbine design problem. These two steps focus on the development of a turbine meanline model compatible with the MDP method and constructing the system of nonlinear equations which couple the design points. Investigation and development of these two steps from a theoretical perspective for the turbine MDP method are discussed in the following sections.

5.3.1 Turbine Design Parameterization

The detailed review of the cycle MDP method completed in Section 5.1.1 identified the selection of an appropriate design parameterization as critical to the success of the MDP sizing process. This observation led to the inclusion of this element in Hypothesis 1 regarding how to generalize the method for application to turbines. The observation and

hypothesis therefore lead to the following question: Is there a set of similarity parameters which uniquely define a turbine meanline design that can facilitate the implementation of an MDP sizing process? This question is answered in this section by first reviewing the turbine meanline literature then formulation of one potential turbine design parameterization. Experimental validation of this design parameterization is completed later in this chapter.

As described in Section 2.5.1, meanline analysis consists of two complementary components: velocity vector calculations and loss model calculations. In order for the sizing process to maintain a consistent design, it is recommended to implement similarity parameters in both parts of the meanline analysis calculation. For the velocity vector calculations, the work of Schobeiri[95] identified a set of five similarity parameters that uniquely define the velocity vectors entering and leaving the rotor of a given stage. These parameters include the standard flow coefficient, loading coefficient and degree of reaction commonly used to characterize turbine designs as defined by Equations 52 through 54. In addition, Equation 55 specifies the axial velocity ratio across the rotor while Equation 56 sets the meanline radius ratio across the rotor. By specifying these five parameters for a given stage, the absolute and relative flow angles entering and exiting the rotor are uniquely defined creating similarity between all turbines with the same values for these parameters.

$$\phi = \frac{V_{z3}}{U_3} \tag{52}$$

$$\psi = \frac{\Delta h_t}{U_3^2} \tag{53}$$

$$R = \frac{\Delta h_{rotor}}{\Delta h_{t,stage}} \tag{54}$$

$$\mu = \frac{V_{z2}}{V_{z3}} \tag{55}$$

$$\nu_{rotor} = \frac{r_{m2}}{r_{m3}} \tag{56}$$

This parameterization can be further extended to facilitate the analysis of multistage turbines by specifying the radius ratio across the vane as defined by Equation 57. Furthermore, for models which include transition ducts between adjacent blade rows, changes to the velocity vectors across the duct can be specified using a meanline radius ratio and axial

velocity ratio as defined in Equations 58 and 59, respectively.

$$\nu_{vane} = \frac{r_{m1}}{r_{m2}} \tag{57}$$

$$\nu_{trans} = \frac{r_{m,in}}{r_{m,out}} \tag{58}$$

$$\mu_{trans} = \frac{V_{z,in}}{V_{z,out}} \tag{59}$$

In addition to parameterizing the design in terms of these velocity vector similarity parameters, characteristics of the blade geometry can also be defined in terms of similarity parameters. While the exact list of similarity parameters required for computing the losses will vary with the loss model, there are several parameters which are likely to be encountered. These parameters are generally non-dimensional values and include the blade aspect ratio, blade thickness-to-chord ratio, solidity and tip clearance-to-blade height ratio.

Specifying the design using similarity parameters such as these provides means for creating a turbine meanline model which is compatible with the MDP sizing process. Defining the design in this way ensures that the design will not exceed accepted design limits during the sizing process. The similarity parameters presented in this section are just one of many sets of design parameterizations which could be compatible with the turbine MDP method. Other parameterizations may also be used as long as they produce designs which maintain similarity throughout the MDP sizing process. Furthermore, this requirement may influence the selection of the meanline analysis tool which is used to implement the MDP method. Analysis tools already defining the model in terms of these similarity parameters are obviously ideal, but non-conforming tools could still be used as long as they can be modified to accept an appropriate set of parameters as inputs.

The use of these similarity parameters to specify both the velocity vector and loss model inputs for the turbine meanline design is an important factor in the ability to adapt the MDP method for application to turbines. With the appropriate model parameterization determined, the next step of the cycle MDP method requiring further investigation for generalization to the turbine MDP is constructing the system of nonlinear equations which couple the design points.

5.3.2 Turbine MDP Coupling Equations

In addition to the development of an appropriate turbine design parameterization, Hypothesis 1 also stated that development of a turbine MDP method would require identification of the required MDP coupling equations or design rules. The review of the cycle MDP method identified the types of coupling equations and independent parameters that typically resulted in the development of valid designs. From this review of the cycle MDP method, the following question can be asked regarding development of the turbine MDP method: Is there a sizing parameter and set of operating parameters for the turbine which will enable a design to be produced which satisfies all performance requirements and operating constraints? This question is addressed in this section from a theoretical perspective with formal validation completed via computational experiments later in this chapter.

As formulated in the cycle MDP method, the MDP coupling equations or design rules ensure that all performance requirements and constraints are satisfied. For the turbine design problem the performance requirements at each design point are typically the power output from the turbine. This output power must match the power required by the component attached to the other end of the shaft such as a compressor or rotor in the case of a turboshaft engine. In regards to the operating limits, several different limits are likely to be present in the turbine design problem. One potential set of limits are those related to material stresses. While the material stresses are highly dependent on the detailed blade and disk geometry, parameters such as AN^2 (the annulus area times rotation speed squared of a blade row) and the rim speed have been found to be proportional to the blade stress and disk stress, respectively.[110] Material limits can therefore be enforced in the meanline analysis by including these AN^2 and rim speed metrics. In addition to these material limits, the turbine is also subject to constraints on the flow thermodynamic properties. These constraints include maximum axial velocities which set the limit load and the maximum pressure ratio across the turbine which must not be exceeded in order to maintain a sufficient total pressure for the downstream engine component. These limits on the thermodynamic properties of the flow provide a means to determine the location of the design points on the turbine performance map.

With these potential dependent equations identified, a set of unique independents must be determined which will allow these equations to be converged. The review of the cycle MDP method found that a single sizing parameter was used in this process along with an operating parameter at each design point. For identifying the sizing parameter, it is helpful to return to the definitions of the similarity parameters identified in the previous step. If the designer were to use this set of similarity parameters (or a similar valid set) and provide values for all the parameters, the overall meanline design is determined when any two of the following three values are set: mean radius at a single station, the shaft speed, or the axial velocity at any station. Of these parameters, the mean radius is a natural choice for the sizing parameter as it directly sets the physical turbine size and affects the power output.

To identify operating parameters at each design point, it is helpful to return to the meanline analysis calculations summarized in Section 2.5.1. In those calculations, Equation 27 shows that the power output from a turbine stage depends on the mass flow rate as well as the change in tangential flow velocity across the rotor. Given this dependence, it is desirable to identify an operating parameter at each design point which varies either the mass flow rate or tangential flow velocity.

At one of the design points, typically the aerodynamic design point, the tangential flow velocities for each blade row are determined by the inputs velocity vector similarity parameters defined in the previous section. With these tangential velocities set, the mass flow rate must be selected as the operating parameter at this design point. For the other design points, selecting an independent operating parameter requires a more detailed understanding of the turbine flow physics as changes to the mass flow rate and tangential flow velocities are coupled. The relationship between these parameters depends on the flow regime in the turbine and is summarized in Figure 34. This figure shows a meanline cut through a notional turbine with important geometry and flow features identified. The important geometry feature shown in this figure is the blade passage throat which is indicated by the green line. Similar to a conventional nozzle, the mass flow rate through this throat is determined by the static pressure downstream of the blade row. If the exit static pressure is relatively high, the mass flow through the blade row remains subsonic and the throat is

unchoked. For this case shown in orange in the figure, the mass flow is set by the downstream static pressure with the flow angle deviating slightly from the metal angle. This deviation angle is independent of the downstream static pressure. However, if downstream static pressure is relatively low, the blade passage throat chokes limiting the amount of mass flow that can pass through the blade row. In the choked case shown in red in the figure, additional expansion occurs downstream of the throat to match the specified exit static pressure. This expansion occurs in a region of Prandtl-Meyer expansion and shock waves shown in blue. The effect of this additional expansion is an increase in the flow Mach number and deviation from the blade metal angle, thereby changing the tangential flow velocity. In both the unchoked and choked flow regimes, the exit static pressure from the turbine is the driving factor setting either the mass flow in the unchoked condition or exit flow angle in the choked regime.[54] As a result, the exit static pressure is an ideal operating parameter selection for the MDP method as it enables matching power across both flow regimes.

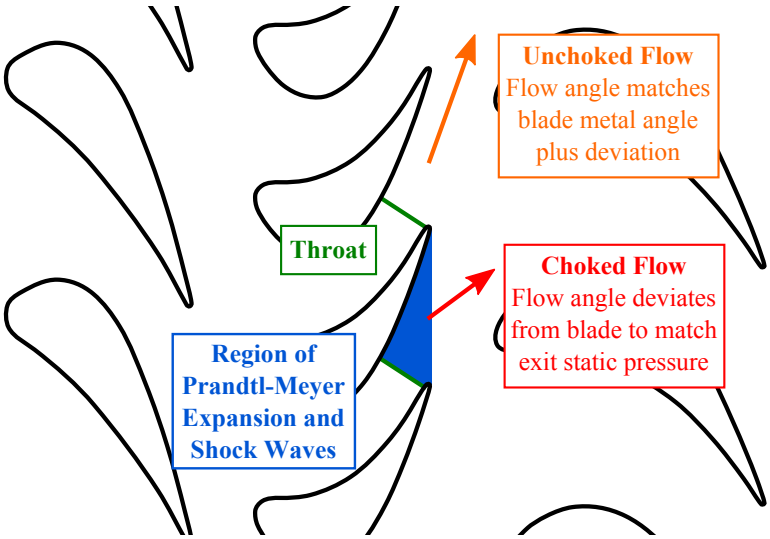

Figure 34: Turbine Flow Characteristics

Finally, if material limits such as AN^2 or rim speed are included in the analysis, an additional operating independent parameter will need to be included to maintain a fully-determined system of nonlinear equations. These operating limits are heavily dependent on another operating parameter: the shaft speed at which the turbine is operating. Therefore,

the shaft speed is also an ideal independent operating parameter to include in the MDP design rules when these types of operating limits are considered.

The analysis completed in this section has identified two classes of dependent equations and two classes of independent parameters which enabled the development of design rules for the cycle MDP method. The identification of these classes of parameters and equations from the cycle MDP is an important realization leading to the identification of similar design rules for the turbine MDP method. These classes can be used along with knowledge of the turbine design parameterization and the meanline analysis equations to identify viable design rules for the turbine design problem. The design rules identified in this section provide one possible approach for coupling the design points in an MDP analysis. Other design rules may be required or desired for different turbine architectures or design philosophies. It should also be recognized that the operating parameters identified in this section are treated as parameters fully controllable by the turbine designer. However, the mass flow rate and shaft speed will ultimately need to be matched with other components in the cycle, serving as further motivation for developing the MLMDP method in the next chapter.

5.4 Turbine MDP Procedure

The previous section examined two steps in the cycle MDP process which were identified by Hypothesis 1 as requiring further investigation to adapt the method to the turbine design problem. In these examinations, key observations regarding the cycle MDP implementation of the step were made which allowed for a similar formulation to be developed for the turbine MDP method. With the turbine MDP formulation of these steps determined, the entire turbine MDP method can now be presented. As described in the introduction to this chapter, this procedure was adapted from the cycle MDP procedure[97] and therefore contains similar steps. The complete procedure is summarized in Figure 35 with the details for each of the steps in the procedure described in the paragraphs below.

Step 1: Identify Turbine Requirements and Constraints

The first step in the turbine MDP process identifies the performance requirements and

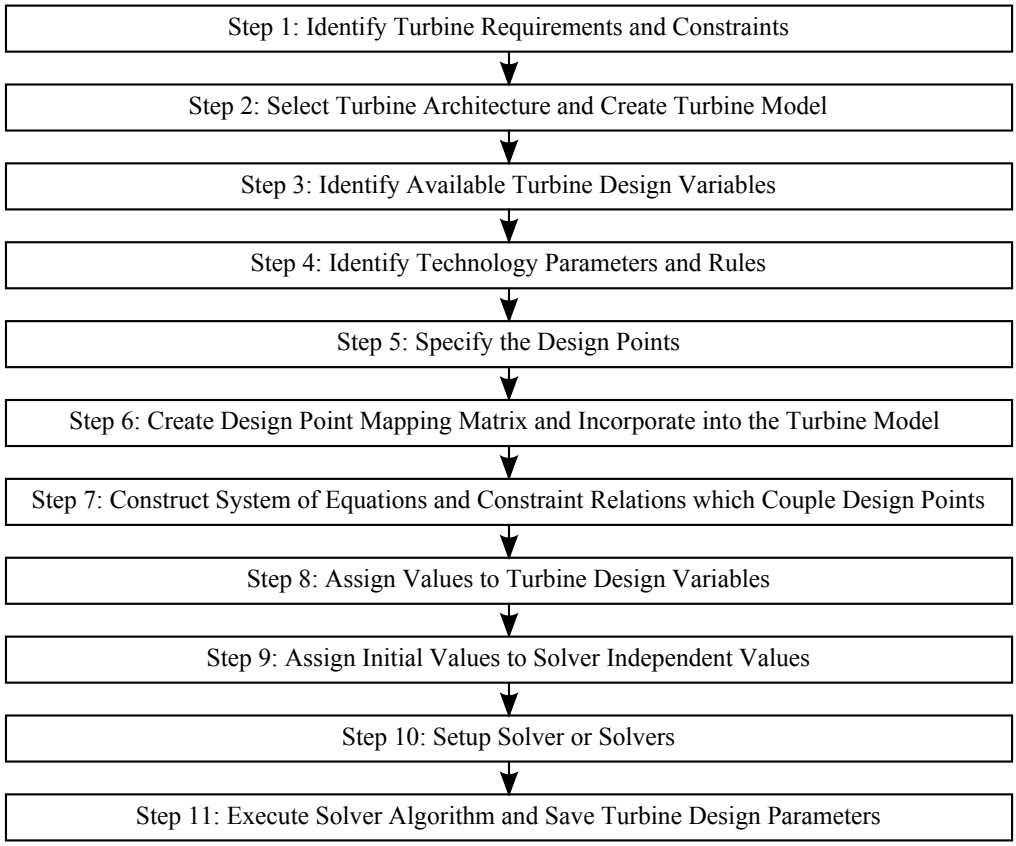

Figure 35: Turbine MDP Procedure

constraints that may influence the resulting turbine design. Performance requirements are defined as metrics which specify the expected performance characteristic of the turbine at a given operating condition. These performance metrics may be derived from the thermodynamic cycle analysis or from other sources. An example performance requirement that is commonly encountered for the turbine is the power delivered to the shaft. Identification of the turbine performance requirements must include both the value of the requirement and a description of the operating condition at which the requirement applies. If an exact value of the requirement is not known as may be the case early in conceptual design, a range of potential values can be specified until a more exact value is determined. Specifying a range of performance requirement values can also be used to study the sensitivity of the

final design to changes in the requirement value.

In addition to specifying the performance requirements to be achieved, constraints also need to be specified during this step. Constraints are limits on the turbine operation or design which may influence the resulting turbine design. The constraints considered in the turbine MDP process generally fall into two categories: operating and geometric design. Operating constraints are limits on the performance of the design at a given operating condition. The definition of these constraints must therefore include both the operating condition and the limiting value. Example operating constraints for the turbine include the maximum allowable pressure ratio and the maximum allowable AN^2. Similar to the performance requirements, the operating constraints may result from the thermodynamic cycle analysis or may come from other sources such as material characteristics. Geometric design constraints are limits which apply to the physical geometry of the design and are not dependent on the operating condition of the turbine. Examples of these constraints may include the maximum radius on the turbine or the flare angle of the annulus in sections of the turbine. While some of these geometric constraints may be hard limits which should be considered in the MDP design process, others such as the flare angle are softer constraints based on best design practices. The designer may choose to implement these softer geometric constraints as hard limits at a single design point in the MDP process or opt to simply note the existence of the limit for post-execution assessment of the design. For both types of constraints, if an exact constraint value is not known a range of potential constraint values can be applied allowing the designer to evaluated the sensitivity of the design to each constraint.

Step 2: Select Turbine Architecture and Create Turbine Model

The second step of the turbine MDP procedure is to select the turbine architecture and create a baseline turbine meanline model. Selecting the turbine architecture primarily includes determining if the turbine is of axial or centrifugal design and identifying the layout of the turbine in terms of number and type of blade rows (stators and rotors). While several different architectures may be capable of satisfying the specified performance requirements and

constraints, the turbine MDP method developed here is applicable to a single architecture. If the designer wishes to consider several different turbine architectures, the turbine MDP procedure should be repeated for each configuration being considered. Once the turbine architecture has been selected, a meanline model of the turbine should be constructed in the selected analysis code. As part of the model construction process, a viable set of meanline similarity parameters should be selected. The selected similarity parameters should also be added to the model as inputs unless the analysis tool already uses these parameters as inputs to the analysis. Examples of acceptable meanline design similarity parameters were presented in the previous section and include the flow coefficient, loading coefficient and reaction of each stage.

Step 3: Identify Available Turbine Design Variables

Following the selection of the turbine architecture and construction of the model, the next step is to identify available turbine design variables. Design variables are parameters which the turbine designer is interested in changing to produce a new design. The list of potential design variables depends on the architecture being considered as well as the design problem under consideration. The selected design variables will commonly include some or all of the velocity vector and blade geometry similarity parameters identified in the previous step.

Step 4: Establish Technology Parameters and Rules Including Loss Models

Step 4 of the method focuses on identifying technology parameters and rules for the turbine design. Technology parameters are similar to design variables but are specifically used to define the technology level of the turbine. Values for these technology parameters can be held constant to develop designs of similar technology level or can be varied to create a technology level trade space.

In addition to individual technology parameters, technology rules should be identified as part of this step. Rather than specifying a single technology parameter, technology rules determine performance characteristics based on the input design variables. These technology rules will commonly include correlations from the selected loss model which related blade

performance to the design blade characteristics. After identifying technology parameters and rules, these rules should be incorporated into the meanline model.

Step 5: Specify the Design Points

The fifth step in the MDP procedure is to determine the design points which must be considered in the turbine MDP analysis. Identifying the necessary turbine design points commonly begins with listing the operating conditions at which the performance requirements and constraints established in Step 1 apply. For each of the design points identified, values defining the turbine operating conditions must also be specified. These values commonly include the inlet thermodynamic flow properties (primarily total pressure and total temperature) as well as the shaft speed. Once all the design points have been identified, each point must be incorporated into the turbine meanline model.

Step 6: Create Design Point Mapping Matrix and Incorporate into the Turbine Model

The sixth step in the procedure collects all the information gathered in the first five steps to form a design point mapping matrix (DPMM). The DPMM relates all the design variables, performance requirements and design limits to their respective design points thereby facilitating the creating of the MDP turbine model.

A notional example of the turbine DPMM is shown in Table 3. The DPMM table is broken up into four sections separated here by the horizontal lines. In the first section the design points identified in Step 5 are enumerated. The second section lists all of the design variables identified in Step 3. Since many of the design variables repeat for each stage, the columns associated with each design point are subdivided by the number of stages allowing for a more condensed, readable DPMM. Baseline design values for each design variable are filled in to these columns as indicated by the "X" marks. The third section lists the performance requirements identified in Step 1 of the procedure. Values for these requirements are again placed under the design point at which they apply as indicated by the "X" marks. The last section of the DPMM lists the operating and geometric design constraints identified in Step 1.

Completion of the DPMM gathers all the information identified in Steps 1 through 5 into a single, easily interpreted table. The DPMM helps document this information, specifically how the performance requirements, constraints and design variables each link to the design points. After completing this table, the turbine designer should incorporate this information into the design points added into the model in Step 5.

Table 3: Notional Design Point Mapping Matrix

Design Point (DP)		DP 1		DP 2		DP 3	
	Stage →	1	2	1	2	1	2
Design Variables (DV)	DV 1	X	X				
	DV 2	X	X				
	DV 3			X	X		
	DV 4			X			X
	DV 5	X	X				
Performance Requirements (REQ)	REQ 1		X				
	REQ 2				X		
	REQ 3						X
	REQ 4				X		
	REQ 5						X
Design Constraints (DC)	DC 1		X				
	DC 2		X				
	DC 3			X			

Step 7: Construct Systems of Equations and Constraint Relations that Couple Design Points

Step 7 of the turbine MDP procedure is the primary step that differentiates the MDP process from the traditional SPD approach. In this step, design rules are developed which form a system on non-linear equations that couple the design points. The role of these design rules is to ensure that all requirements and constraints are satisfied at the various design points. Therefore, construction of the design rules begins with the requirements and constraints identified in Step 1. These requirements and constraints can be used to form the dependent equations in the system. In addition to these dependents, unique independent parameters must be identified which can be used to converge the dependent equations. As discussed in Section 5.3.2, these independents will commonly include a single turbine sizing parameter along with at least one operating parameter at each design point. After defining

the design rules which couple the design points, these rules must be added to the turbine MDP model.

Step 8: Assign Values to Turbine Design Variables

The eighth step in the turbine MDP procedure begins the MDP execution phase. In this step, values must be assigned to each of the design variables and technology parameters. For the development of a specific design, the designer should specify the desired value for each of the design variables identified in Step 3. In most situations, however, the designer will be interested in evaluating a large number of designs spread throughout a defined design space. In this case the designer should specify minimum and maximum values for each design variable to define the design space. Designs throughout this space can then be analyzed by selecting unique combinations of values for each variable.

Step 9: Assign Initial Values to Solver Independent Vector

In addition to specifying values for each of the design variables, the ninth step determines initial values for each independent parameter in the MDP model. This includes the independents which form part of the design rules in Step 7 as well any other independents which are used by the analysis tool in its solution process. Values for these independent parameters cannot be assigned randomly as the Newton-Rapshon method for solving systems of nonlinear equations is locally convergent meaning the initial iterate values must be in the neighborhood of the final solution. A poor initial iterate can therefore result in convergence failures or excessive convergence iterations. The cycle MDP procedure proposed a method which can be used to help generate the initial iterate[97] which is also applicable to the turbine MDP and is summarized below:

1. Create a SPD turbine model with design variable and technology parameter values within the design space identified in Step 8.

2. Evaluate the SPD model in on-design mode at a single design point corresponding to one of the turbine MDP points.

3. Evaluate the SPD model in off-design mode at points with similar operating conditions as the other turbine design points identified in Step 5.

4. Save the independent values from each of these design points to serve as the initial iterate.

For the cycle MDP method, this simple procedure was found to provide a good first guess for the initial iterate. This initial iterate could later be improved by saving the independent values from a converged MDP model. While generating the initial iterate can be time consuming, once a viable initial iterate is obtained the process does not need to be repeated even when exploring a design space. The reusability of the initial iterate stems from the postulate developed as part of the cycle MDP process.[97] This postulate has been generalized for application to the turbine and is state below:

Initial Iterate Postulate: A single initial iterate can be utilized to efficiently and robustly find solutions within the design space provided that the initial iterate is itself a solution to one of the designs within the space.

Applying this postulate allows for a single initial iterate to be used for all designs considered in a design space exploration as long as the initial iterate is valid for a design in that space.

Step 10: Setup Solvers

The tenth step of the turbine MDP procedure focuses on properly setting up the Newton-Raphson solver or solvers required to converge the non-linear equations present in the model. Setting up the solver(s) primarily involves specifying values for parameters which control the iteration and convergence characteristics. These parameters are likely to include the convergence tolerances, step size limits, and iteration limits. If the implemented solver includes the ability to use quasi-Newton approaches in conjunction with the pure Newton-Raphson method, parameters defining when and how each approach is used should also be specified.

Step 11: Execute Solver Algorithm and Save Turbine Design Parameters

The final step of the turbine MDP procedure is to execute the MDP model for the selected design variables values. After the model execution has been completed, output data describing the final design should be saved for later analysis. It is recommended that the recorded output include all design characteristics and the converged iterate as these values will be needed to reproduce the design in a single point model for evaluation at operating conditions other than those used for the design points.

5.5 Implementation on Example Turbine Design Problems

In order to assess the capabilities of the developed turbine MDP methodology and compare the designs it produces to the traditional SPD approach, the method needs to be implemented on several example turbine design problems. Three such problems were identified which cover a range of performance requirements, constraints, design points, and turbine architectures to give a thorough assessment of the method. The first example problem is to reexamine the design of the low pressure turbine for the E^3 turbofan engine. The second and third sample problems draw from the tiltrotor aircraft engine design problem described in the motivation for this research. The second problem examines the design of a conventional power turbine (CPT) for this engine. The CPT configuration would require the use of a multi-speed transmission to match the desired rotor speeds throughout the flight envelope. The third problem considers the design of a variable speed power turbine which would be capable of operating over a wider speed range without the need for a multi-speed transmission. This section presents the implementation of the turbine MDP method on each of these three example design problems.

Before presenting the implementation of the turbine MDP method on these design problems, one other consideration needs to be discussed: the selection of the meanline analysis tool to be used. While the turbine MDP process described in the previous section is intended to be independent of the analysis code selected, the selection of an appropriate analysis tool can facilitate the implementation of the method. One desirable feature of the

analysis code is that it be written in an object-oriented programming language. An object-oriented code allows for the analyst to create multiple instances of the meanline model, with one for each design point. Next, it is also desirable for the analysis code to have already implemented a Newton-Raphson solver for the convergence of the meanline analysis equations. If such a solver is present and available to the user, the amount of effort required to implement the MDP method is greatly reduced as the analyst does not need to write their own Newton-Raphson solver code. Finally, a third desirable characteristic of the selected meanline analysis code is that it specify the design in terms of the similarity parameters or can be modified to accept similarity parameters as input.

For the meanline analysis of the turbine in this research, the Object-Oriented Turbomachinery Analysis Code (OTAC) was selected as it has all the desirable features described above. OTAC is a newly developed code from NASA Glenn Research Center and is an extension of the object-oriented NPSS cycle analysis code.[65] OTAC takes advantage of the NPSS thermodynamic packages as well as its modified Newton-Raphson solver by adding newly developed objects for analyzing blade rows, blade segments and transition ducts. These objects can be combined to consider compressors and turbines with any number of stages. While the code provides the basic components for analyzing turbomachinery, it remains flexible by allowing the user to define the loss model used for each blade row. OTAC also has the ability to conduct streamline analysis with an arbitrary number of streamlines but this capability is not used in this research. OTAC has been validated by modeling several compressors and turbines for which NASA has experimental data or analysis results from codes with similar capabilities.[66] As part of this research for developing the turbine MDP method, the author made several improvements to the tool to enable analysis of choked flow in the turbine.[54] Finally, while OTAC does not use similarity parameters by default for most inputs, the code can be easily modified to accept these inputs through the use of additional independent parameters and dependent equations that are converged by the solver. With the analysis tool selected, implementation of the turbine MDP method on the three example problems was completed as summarized in the next three sections with detailed descriptions of the implementation provided in Appendices D through F. Finally,

Section 5.5.4 describes an implementation challenge for all three models regarding the solver setup for converging the system of nonlinear equations within each model.

5.5.1 E^3 Low Pressure Turbine

During the 1970s the United States suffered fuel shortages and high fuel prices which placed significant stress on the aviation industry. In response to these challenges for the nation and aviation industry, NASA began the Aircraft Energy Efficiency Program to research aircraft and engine technologies to reduce fuel consumption. One of the projects within this program was the Energy Efficient Engine (E^3) project which focused on developing an entirely new turbofan engine capable of providing significant fuel consumption improvements.[13]

The E^3 project focused on the development of a large, conventional two-spool turbofan engine. The research conducted during this project on both the overall engine and its individual components was well documented, including for the low pressure turbine (LPT).[18, 15] This extensive documentation provided sufficient data to support the use of the E^3 LPT for validating OTAC[66] and makes it an ideal example problem. For this research, a redesign of the LPT was completed using turbine MDP methodology as summarized in the next paragraph. Additional detailed of the turbine MDP method's application to the E^3 LPT design problem can be found in Appendix D.

For the E^3 LPT design problem, performance requirements and operating constraints were identified at three different operating conditions. These operating conditions represented the turbine aerodynamic design point (ADP), the turbine operation at the top-of-climb flight condition, and the turbine operation at the sea-level static (SLS) flight condition. The performance requirements and constraints included the power output at each operating condition along with the maximum AN^2 and SLS pressure ratio. The values defining the performance requirements and operating conditions for this turbine were derived from an MDP model of the E^3 engine which is described in Appendix A. A five stage turbine architecture was also selected to match the original architecture of the E^3 LPT. Given this architecture, a set of design variables was selected that focus on changes to the mean-line velocity vectors. These design variables therefore included the flow coefficient, loading

coefficient, degree of reaction and rotor axial velocity ratio for each stage.

5.5.2 Conventional Power Turbine

The second example design problem used to test the turbine MDP method comes from the tiltrotor engine design challenge which served as motivation for this research. As discussed in Chapter 1, the rotor performance during cruise for a tiltrotor aircraft is significantly improved by reducing the rotor speed. One of the options for achieving this reduced rotor speed while maintaining high turbine efficiency is to connect the power turbine to the rotor using a multi-speed transmission. With this configuration, the gear ratio setting the relative speeds of the turbine and rotor can be varied throughout the flight to obtain near optimal performance for both engine components at different flight conditions. The performance requirements and operating constraints at each of these flight conditions must be considered during the turbine design process supporting the use of the MDP method. The design problem summarized in this section considers a clean sheet design of a conventional power turbine for this tiltrotor engine configuration. Additional details of the turbine MDP method's application to the conventional power turbine design problem can be found in Appendix E.

Implementation of the turbine MDP methodology on the conventional power turbine design problem started with determining the performance requirements and constraints on the turbine. Power requirements were identified at seven different engine operating conditions including the aerodynamic design point (ADP), top of climb (TOC), hover out of ground effect (HOGE), one engine inoperative (OEI), start of climb (Climb), pre-shift (Shift1) and post-shift (Shift2). In addition, target and constraining values for AN^2 , pressure ratio and degree of reaction were specified at many of the design points. Values for the power requirements and pressure ratio limits were derived from an MDP model of a turboshaft engine with a conventional power turbine which is described in Appendix B. The architecture selected for the conventional power turbine was a three stage axial configuration. This architecture was selected based on previous studies[91, 113] which identified a three stage axial architecture as the most likely turbine architecture. The

turbine design variables selected for this design problem included those used for the E^3 LPT design problem. In addition, design parameters specifying the meanline radius throughout the turbine and design characteristics of the blades such as the thickness-to-chord ratio, aspect ratio, and solidity. This expanded set of design variables significantly expands the size of the design space and allows for more variation in the turbine designs produced.

5.5.3 Variable Speed Power Turbine

The third and final example design problem for evaluating the turbine MDP methodology is also drawn from the tiltrotor engine which served as motivation for this research. While the design problem described in the last section focused on a conventional power turbine attach to the rotor via a multi-speed gearbox, the design problem of interest in this section is a variable speed power turbine (VSPT) which is connected to the rotor with a single speed gearbox. In this configuration, the turbine must be designed to produce the required power over an extremely wide speed range while maintaining high efficiency. These requirements at several different operating conditions make this design problem an ideal candidate for the implementation of the turbine MDP method. The design problem presented in this section considers a clean sheet design of a variable speed power turbine for the tiltrotor engine. The step-by-step implementation of the turbine MDP method for this design problem is described in Appendix F with a summary of the key elements provided in this section.

The requirements and constraints for the VSPT that were identified are similar to those identified for the CPT. The primary difference is that the turboshaft engine with a VSPT is not required to go through the complex shifting procedure as the VSPT is designed to operate efficiently over the entire speed range. This eliminates the pre-shift and post-shift design points resulting in a total of 5 design points being considered in this design problem. As for the VSPT architecture, a four stage axial design was selected as previous research identified this architecture as best candidate for satisfying the performance requirements.[91, 113] The same list of design variables as selected for the conventional power turbine were also used for the VSPT design problem.

5.5.4 Turbine MDP Solver Setup

While the previous three sections summarize the implementation of the turbine MDP method on the three design problems, there is one important step of the implementation process that requires an extended description. The second to last step of the turbine MDP process is to setup the solver or solvers which converge the system of nonlinear equations present in the MDP turbine meanline model. The implementation of this step differs significantly from the implementation used for the cycle MDP method. In the cycle MDP method, the user defined independents and dependents forming the MDP design rules are added to the existing independents and dependents from the cycle match equations. This large system is then converged with a single Newton-Raphson solver. Solving this large system of equations with a single solver is viable and efficient as a result of the limited correlation between many of the independents and dependents in the system. When the independents and dependents are organized by design point, Schutte[97] showed that a structured, sparse Jacobian matrix was produced with the form given in Equation 60.

$$F'(X) = \begin{bmatrix} \frac{\partial F_{DP1}}{\partial X_{DP1}} & 0 & 0 & 0 & 0 \\ \frac{\partial F_{DP2}}{\partial X_{DP1}} & \frac{\partial F_{DP2}}{\partial X_{DP1}} & 0 & 0 & 0 \\ \frac{\partial F_{DP3}}{\partial X_{DP1}} & 0 & \frac{\partial F_{DP3}}{\partial X_{DP1}} & 0 & 0 \\ \frac{\partial F_{DP4}}{\partial X_{DP1}} & 0 & 0 & \frac{\partial F_{DP4}}{\partial X_{DP1}} & 0 \\ \frac{\partial F_{DP5}}{\partial X_{DP1}} & 0 & 0 & 0 & \frac{\partial F_{DP5}}{\partial X_{DP5}} \end{bmatrix} \tag{60}$$

However, applying a similar solver setup for the turbine MDP method in OTAC is difficult for two reasons. First, the solution of OTAC meanline models requires the convergence of a significantly larger number of dependent equations. In these OTAC models, each vane blade row adds four independent-dependent pairs to the system of equations while each rotor blade row adds five independent-dependent pairs. Furthermore, the transition ducts add another 3 independent-dependent pairs. Taking the E^3 LPT model as an example, this means with five stages each analyzed at three design points a total of 234 independent-dependent pairs must be converged as part of the base meanline analysis. The use of additional independent-dependent pairs to enable specification of the design in terms

of similarity parameters and the MDP coupling equations themselves grow this system even larger. The second issue preventing the use of a single Newton-Raphson solver in the turbine MDP analysis is the inaccurate computation of partial derivatives for some elements in the Jacobian. These inaccurate partial derivatives result in iteration steps which do not progress towards the true solution ultimately leading to convergence failures.

Given these issues, the solver setup implemented for the turbine MDP procedure in OTAC is to subdivide the system of equations and solve each one with a separate Newton-Raphson solver. This division creates a nested solver hierarchy with three different levels as shown in Figure 36. At the lowest level of this hierarchy, a solver is created for each blade row and transition duct to converge the dependent equations local to that component. These solvers are referred to as the internal solvers. The middle level in this hierarchy is a set of solvers which converge the systems of equations local to each of the design points and are therefore referred to as the design point solvers. For each of the passes through these design point solvers, the internal solvers are reconverged. Finally, the top level solver referred to here as the MDP solver contains only the independents and dependents which couple the design points. Again here, for each pass through this MDP solver all of the solvers in the lower two levels must be reconverged.

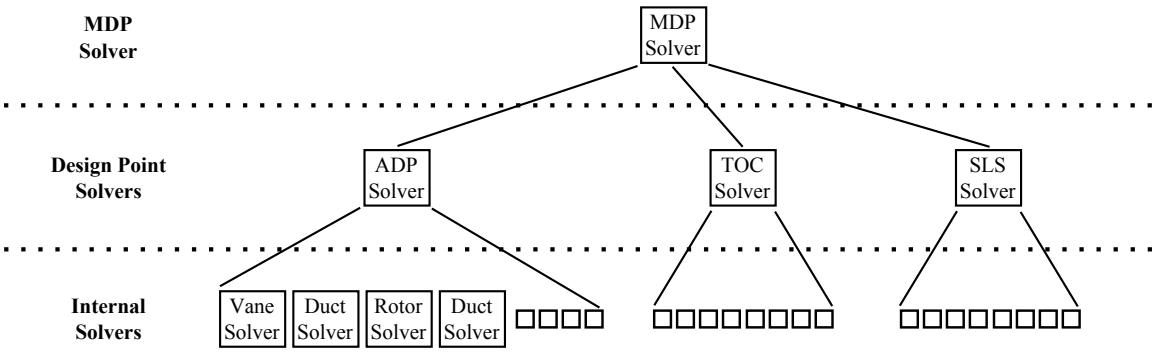

Figure 36: E^3 LPT Nested Solver Setup

This solver structure was selected for several reasons. First, splitting up the system of

equations into smaller blocks where a known relationship between independents and dependents exists results in rapid convergence for these smaller systems. Furthermore, splitting up the system of equations takes advantage of these known relationships to eliminate the inaccurate partial derivatives which were causing convergence failures in the single solver approach. Although these smaller systems must be converged a large number of times in the nested solver structure, the overall convergence of the model can benefit resulting in a reduction to the overall convergence time. One reason for this potential improvement is that fewer passes through the entire model are required to calculate the Jacobian elements with the finite difference scheme implemented in the OTAC solver. Instead, finite difference calculations must only be completed on small portions of the model for each of the lower level solvers. A second reason for the improvement in the convergence time is that the OTAC solvers use the previously converged independent values as the initial guess for each new convergence of a solver. These values are likely to be close to the final solution for the next convergence resulting in a relatively quick convergence, especially when the higher level solver is doing perturbation steps as part of its finite difference Jacobian calculations.

While there are advantages to splitting up the system of nonlinear equations and using a nested solver hierarchy, implementation also presents a significant challenge for selecting the appropriate solver settings at each level. The presence of a lower level solver results in uncertainty or error in the exact value of the converged independent and dependent values from this lower level. Since these values impact the calculation of the dependents in a higher level solver, this error will propagate through the nested system, particularly when a finite difference scheme is used to calculate the Jacobian matrix. The details of this propagation were presented in Section 3.3.1.1 along with suggestions for how the higher level Jacobian error can be minimized by reducing the error in the lower level values and selecting appropriate step sizes.

For the implementation of the MDP method on all three design problems, a constant fractional perturbation step size was maintained for the finite difference calculation in all of the nested solvers. This step size was 0.001 of the current independent value. With this step size, a small study was conducted using the E^3 LPT model to approximate the error

in the Jacobian matrix at the design point and MDP solver levels as a function of the lower level solver tolerances. Figure 37 shows the error in the design point solver Jacobians as a function of the internal solver tolerance. In this figure the error is defined by Equation 61 with the real Jacobian values assumed to be those produced by a tolerance of 10^{-10} on the internal solver. From the resulting figure, it can be seen that the ADP Jacobian error is highly dependent on the internal solver tolerance while the TOC and SLS Jacobians have low error for all internal tolerance levels.

$$R = \frac{\|F'_{real}(X) - F'_(X)\|_2^2}{\|F'_{real}(X)\|_2^2} \tag{61}$$

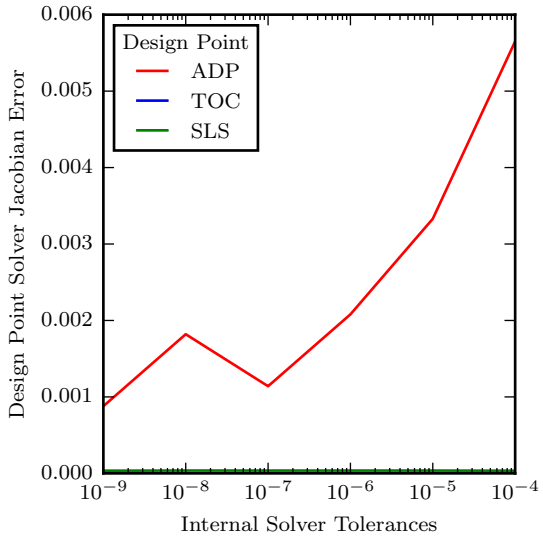

Figure 37: E^3 LPT Design Point Jacobian Errors vs. Internal Solver Tolerances

A similar process was repeated for the MDP solver Jacobian with the results shown in Figure 38. Here the real Jacobian values were assumed to be sufficiently captured by a solver tolerance of 10^{-9}. In this figure, it can be seen that there is significant variation in the MDP solver Jacobian error when a design point tolerance of 10^{-4} was used. However, for design point solver tolerances less than 10^{-5} the MDP solver Jacobian became almost insensitive to the tolerance of the internal solvers.

These two figures generated from the solver study help identify the appropriate tolerances for each solver level to minimize the error in the Jacobians. Computing accurate

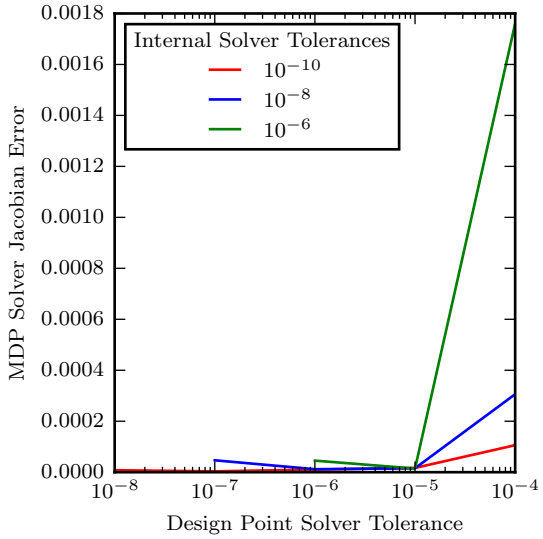

Figure 38: E^3 LPT MDP Solver Jacobian Error vs. Design Point and Internal Solver Tolerances

Jacobians is important for the overall convergence of the system of equations. While the tolerances could be set extremely tight for the internal solvers to eliminate the error, converging to these excessively tight tolerances will increase the overall execution time of the model. Therefore, a balance must be struck between sufficiently tight tolerances to produce accurate Jacobian matrices at all levels while not drastically increasing the execution time. Weighing both of these factors, a relative solver tolerance of 10^{-6} was selected for the internal solvers with a tolerance of 10^{-5} for the design point solvers and a tolerance of 10^{-4} for the MDP solver.

5.6 Turbine MDP Computational Experimental Results

At the beginning of this chapter, two research questions and hypotheses were posed which guided the development of a turbine MDP design methodology. This methodology was then implemented for three example problems which considered different architectures, performance requirements and constraints. This section presents the results of computational experiments conducted with these models to numerically test the stated hypotheses. The first experiment presented below focuses on assessing the turbine MDP method to ensure that it produces results which satisfy all performance requirements and constraints. The

second experiment is designed to test Hypothesis 2 and focuses on comparing the designs produced with the new turbine MDP methodology to the designs generated with the traditional SPD approach.

5.6.1 Experiment 1: Assessment of the Turbine MDP Method

The first research question and hypothesis stated at the beginning of this chapter focused on adapting the cycle MDP methodology to the design of turbines. The hypothesis proposed that the method could be adapted by focusing on two specific steps in the process: constructing the turbine meanline model and identifying the design rules which couple the design points forming a system of nonlinear equations. Sections 5.3.1 and 5.3.2 examined these steps and identified approaches for each which enable the application of the MDP method to turbines.

While these sections determined how to adapt these steps from a critical examination of the cycle MDP process and a review of applicable literature, these individual steps as well as the overall method require experimental testing to fully accept or reject the stated hypotheses. Therefore, a computational experiment was developed to test these steps and the overall method. The primary objectives of this first experiment is to demonstrate that the formulated turbine MDP method produces designs which maintain similarity during the sizing process and that those resulting designs satisfy all performance requirements and constraints. A secondary objective of the experiment is to evaluate the complete turbine MDP method to ensure that it finds those valid designs in an efficient and robust manner.

5.6.1.1 Experiment 1 Setup

The focus of Experiment 1 is to evaluate the developed turbine MDP method. Specifically, the evaluation aims to assess the design parameterization and the coupling equation formulation presented at the beginning of this chapter. To test these two elements, Experiment 1 is divided into two parts.

In the first part of Experiment 1, the definition of the design in terms of similarity parameters is examined. For this part of the experiment, the VSPT model was selected as its architecture (number of stages), number of design points and design requirements

are about average for the three design problems considered. To test if the turbine MDP method maintains similarity during the sizing process, a sensitivity study was conducted by varying several performance requirements and constraints one at a time. During this study, the design variable values were held constant at their baseline values given in Table 47. The results from this sensitivity study will be shown in terms of the flowpath geometry as well as the meanline velocity vectors.

The second part of the experiment considers the coupling equations which ensure that all performance requirements and constraints are satisfied. For this part of Experiment 1, all three example design problems presented in Section 5.5 were considered. To evaluate the ability of the coupling equations to ensure that all performance requirements and constraints are satisfied, each model was executed for designs throughout the design spaces identified in Step 8 of the MDP method implementation. To thoroughly evaluate these high-dimension design spaces, a design of experiments (DoE) analysis was completed which consisted of 10,000 randomly selected designs. To determine and execute this DoE, the OpenMDAO software framework was utilized. OpenMDAO is an open source framework for facilitating the solution of multidisciplinary design, analysis and optimization problems, including design of experiments analyses.[46, 6] This framework provided a built-in DoE generator and facilitated the execution and recording of results for each case on a high performance computing cluster. The results from each of these DoE's will be analyzed to determine if the formulated coupling equations ensure that all performance requirements and constraints are satisfied. These results will also be used to evaluate efficiency and robustness of the overall method in finding valid turbine designs.

A successful Experiment 1 will show that the MDP maintains similarity in the turbine design throughout the sizing process. Furthermore, a successful test will show that for a wide range of design inputs on each of the design problems, the design rules will produce designs that satisfy all performance requirements and constraints. Finally, a successful test will prove that the MDP method efficiently and robustly finds valid solutions throughout the design space.

5.6.1.2 Experiment 1 Results

The first part of Experiment 1 focuses on assessing formulation of a turbine MDP process which defines the design in terms of similarity parameters. For this part of the experiment, only the VSPT MDP model was considered. To complete this part of Experiment 1, sensitivity studies were conducted in which several performance requirement and constraint values were varied one at a time to determine their affect on the MDP design. The performance requirement and constraint values changed were the HOGE power, OEI power, HOGE pressure ratio and OEI AN^2 .

Assessing the formulation of the turbine MDP process around a similarity based design parameterization is first considered in terms of the flowpath or annulus geometry produced with different performance requirement and constraint values. Figure 39 shows how the flowpath of the VSPT changes for three different values of the HOGE power requirement. From this figure it can be seen that the flowpath remains geometrically similar as the HOGE power requirement changes. The different flowpaths have been formed by shifting the radial location of the meanline, scaling the blade heights around this meanline, and scaling the axial length of the turbine. The change to the meanline radius results from the MDP coupling equations used to ensure the required performance characteristics are satisfied. The blade heights are scaled around this meanline based on the mass flow rate also determined by the MDP coupling equations. Finally, the axial lengths of each blade row and transition duct are scaled to maintain the input aspect ratio for the blades as well as a constant duct length relative to the to upstream blade row's axial chord. This ratio of the duct length to axial chord of the upstream blade was held constant at 0.25 based as suggested by Walsh and Fletcher.[110] The effect of changing the power requirement at this design point on the flowpath can also be summarized from the results in this figure. For an increase in the HOGE power, the meanline radius decreases while the blade heights and overall turbine length increase.

In addition to examining the affect of the power requirement at the HOGE design point, a second sensitivity study was completed to examine the influence of the power requirement at the OEI design point. The results for this study are shown in Figure 40 and indicate

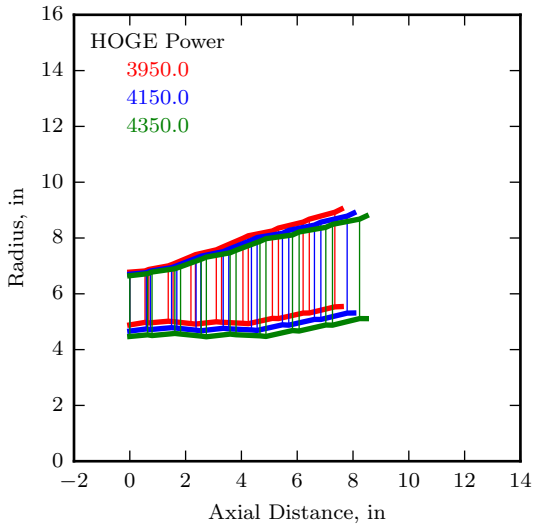

Figure 39: Flowpath Variation with HOGE Power

there is no change to the geometry for the three different power levels. At this design point, changes to the required power have no effect on the geometry as the power requirement could be achieved by simply adjusting the exit static pressure at that operating point. This result is important as it shows that the turbine MDP methods identifies and sizes the design based on the most limiting requirements and constraints.

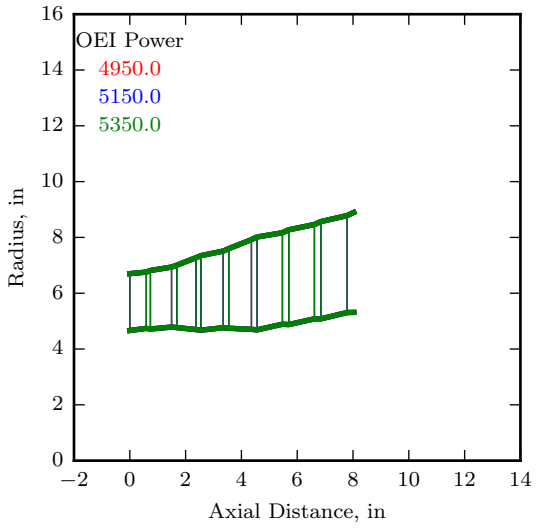

Figure 40: Flowpath Variation with OEI Power

Beyond varying the power requirements at several design points, a sensitivity study on the HOGE pressure ratio requirement was completed with results presented in Figure 41. For changes to the HOGE pressure ratio, similarity in the flowpath geometry is again maintained by adjusting the meanline radius, scaling the blade heights and scaling the axial length of each component. The design trends from this plot indicate that increasing the HOGE pressure ratio results in an increase in the meanline radius, decrease in the blade heights and a decrease in the axial length.

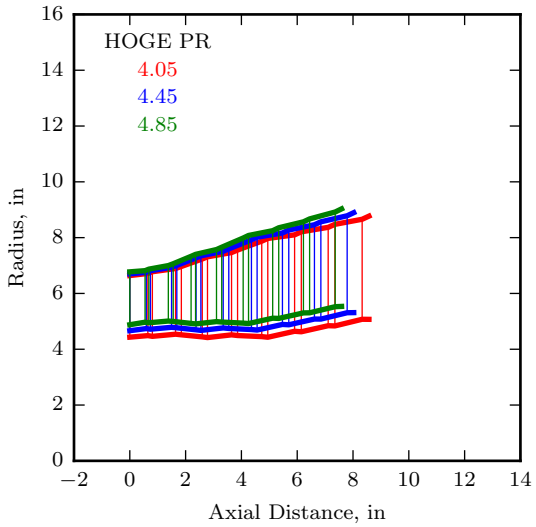

Figure 41: Flowpath Variation with HOGE Pressure Ratio

Finally, the AN^2 requirement at the OEI design point was varied as shown in Figure 42. The figure again shows that turbine design similarity is maintained throughout the sizing process. The design trends from this figure indicate that for an increase in AN^2 the meanline radius will decrease while the blade heights and axial length of the turbine both increase.

On top of examining similarity in the flowpath geometry, the meanline velocity vectors for each of these sensitivity studies were evaluated. Figure 43 shows the velocity vectors for the sensitivity study on HOGE power. In this figure, the resulting velocity vectors exiting each blade row are shown for all five design points. Examining the velocity vectors for the ADP point reveals a similar geometry for all three power levels. These velocity triangles have

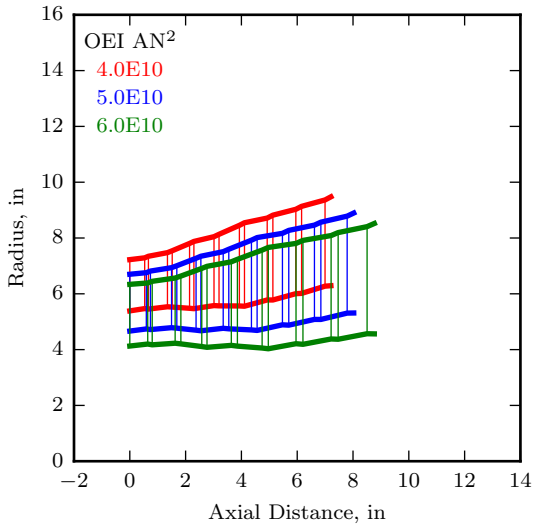

Figure 42: Flowpath Variation with OEI AN^2

the same shape with identical angles, but have been scaled to match the power requirement. Similarity at the ADP point is assured as a result of the similarity parameter inputs all being specified at this design point. At the other design points, however, velocity vector similarity is not guaranteed. For example, significant differences are observed in the HOGE velocity vectors, especially for the last stage comprising Vane 4 and Rotor 4.

For the OEI power sensitivity study, the flowpath geometry shown in Figure 40 remained the same as the required output power could be achieved by changing only the operating parameter value at that design point. The velocity vector diagram for this sensitivity study shown in Figure 44 confirms this result. Here, the velocity vectors are identical for all design points other than OEI. At the OEI design point, the various power levels result in different velocity triangles especially in the last stages of the turbine.

Velocity vector diagrams were also produced for the HOGE pressure ratio and OEI AN^2 sensitivity studies as shown in Figures 45 and 46, respectively. These figures again show that the velocity vectors maintain similarity at the ADP point as the design is sized to satisfy performance requirements.

The results from these velocity vector and flowpath plots complete the first part of Experiment 1. For three of the four sensitivity studies completed, the overall design was

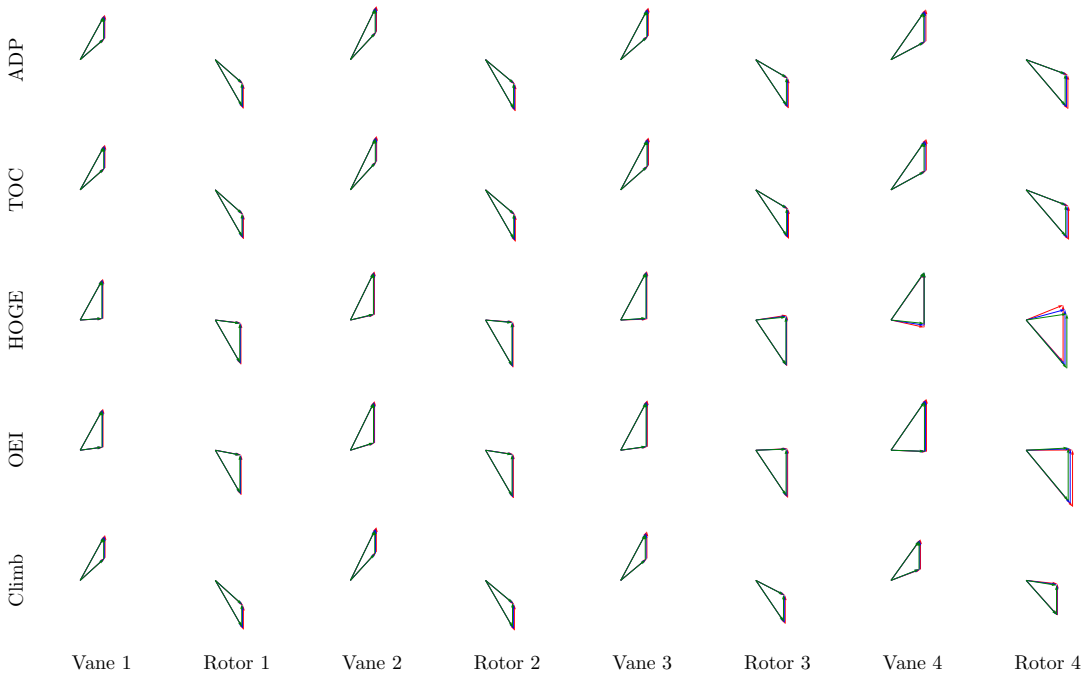

Figure 43: Velocity Vector Variation with HOGE Power

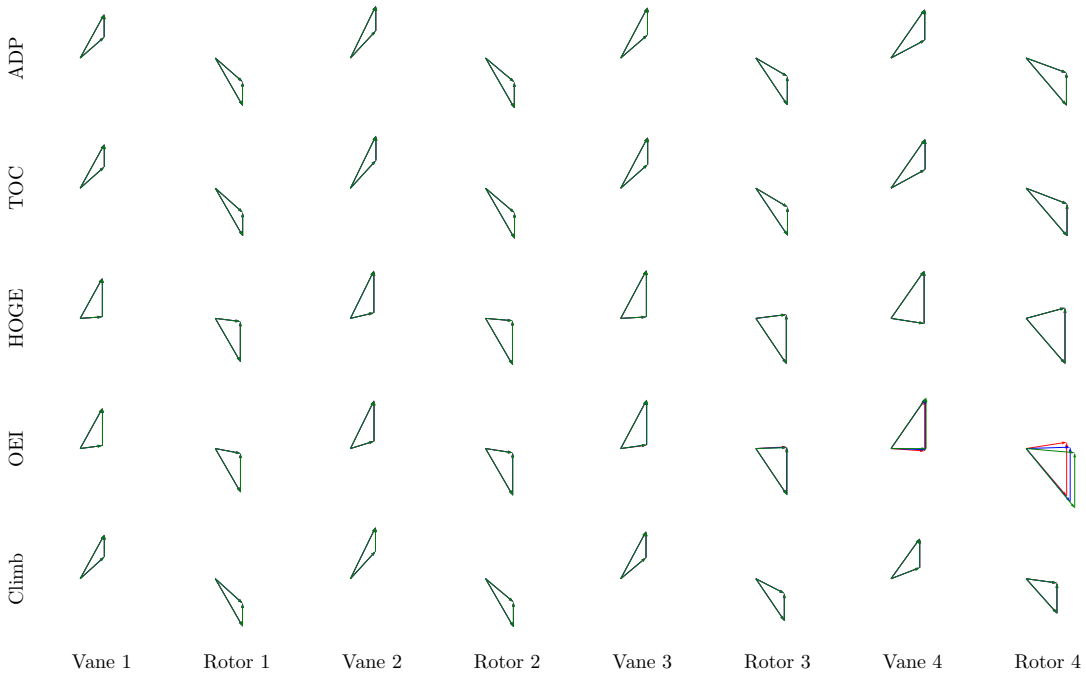

Figure 44: Velocity Vector Variation with OEI Power

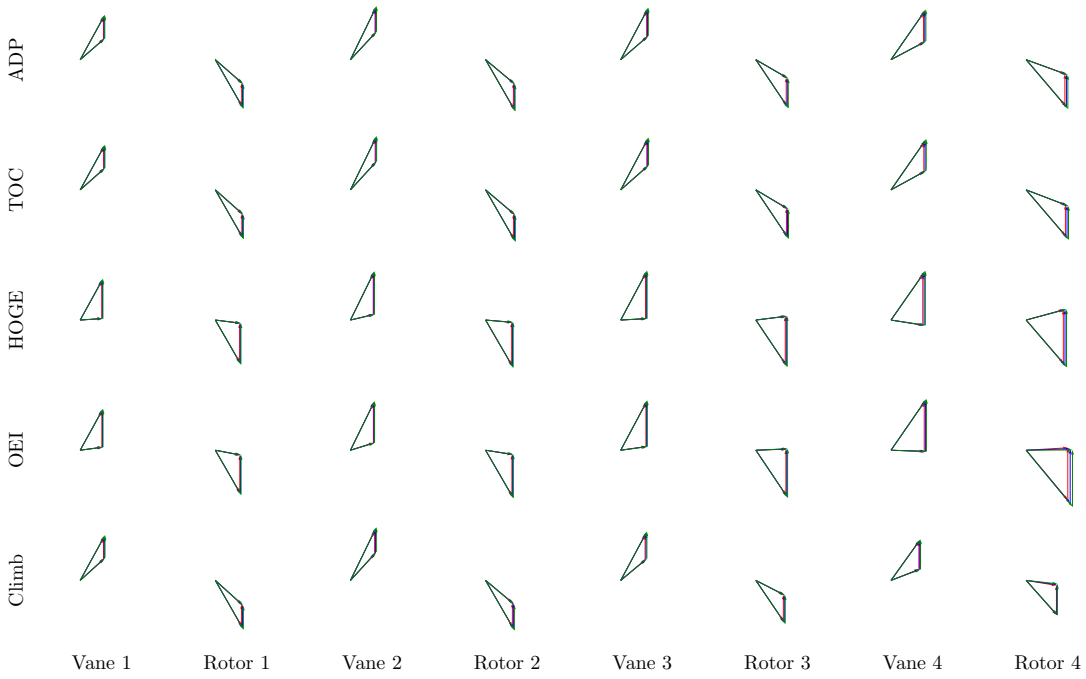

Figure 45: Velocity Vector Variation with HOGE Pressure Ratio

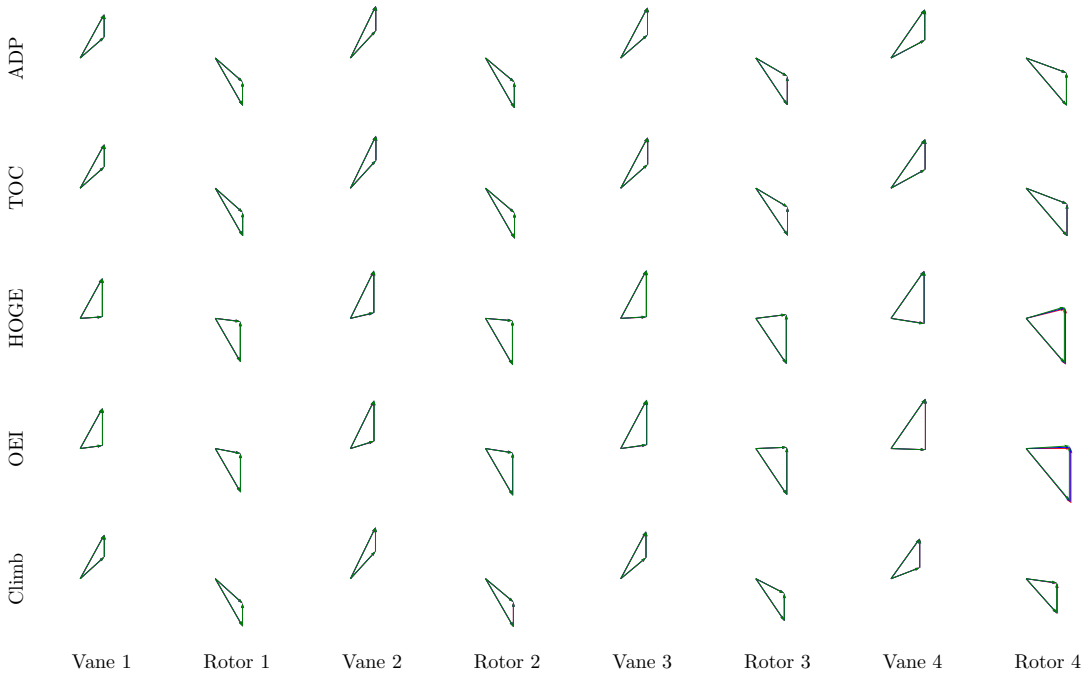

Figure 46: Velocity Vector Variation with OEI AN^2

affected by the change in the performance requirement. The study involving the OEI power requirement however found that the MDP method did not need to adjust the size of the turbine as the required power output could be achieved by simply changing the operating parameter at that point. These results show that as the various performance requirements and constraints are varied, the turbine MDP method sizes the turbine appropriately while maintaining a geometrically similar design. This validates the similarity parameter based approach taken to adapt Step 2 of the cycle MDP method for application to a turbine MDP design problem.

The second part of Experiment 1 is designed to test the system of nonlinear coupling equations formulated for the turbine MDP method. As mentioned in the experiment setup, all three turbine design problems were considered in this part of the experiment. Each of these models was evaluated throughout the design space defined in the implementation section using a large design of experiments (DoE). Results from these DoE runs were analyzed to assess whether the cases satisfied the specified performance requirements and constraints. The results from this assessment of the large DoE runs with each model are summarized in Table 4. For all three design problems, the table shows that approximately 95% or more of the DoE cases converged to feasible solutions. This high success rate across three different design problems validates the formulated turbine MDP coupling equations based on the performance requirements, operating constraints, sizing parameter and operating parameters.

Table 4: Experiment 1 DoE Results Summary

Metric	**E^3 LPT**	**CPT**	**VSPT**
Total Cases	10000	10000	10000
Feasible Cases	9906	9492	9680
Convergence Rate	99.1%	94.9%	96.8%

For the small percentage of the cases which did not converge to a feasible solution, convergence errors were commonly encountered throughout the solution process. These convergence errors often first arose in the internal solvers for the OTAC blade rows and transition ducts. The hierarchical solver structure used in the models resulted in these

solvers needing to be reconverged for each pass through the MDP and design point solvers. The convergence errors for these internal solvers presented problems for the design point solvers specifically as inaccurate Jacobian matrices were produced based on the unconverged values. These inaccurate Jacobians likely drove the design point and ultimately the MDP solver away from the actual solution. With all the internal solver convergence errors and bad Jacobians, these failed cases had excessively long execution times and were stopped after a certain timeout limit was reached in the DoE execution.

A secondary objective of this part of the Experiment 1 was to evaluate the overall solution process to determine if it finds the feasible designs in an efficient and robust manner. Tables 5 through 7 provide an overview of the solver statistics for the three different turbine design problems. For the converged cases in all three design problems, the tables show that the solution was found by the MDP solver in less than 10 iterations on average. From these tables, it can also be seen that the ADP solvers generally takes the most iterations, passes and Jacobians to converge as a result of the significantly larger system of equations at this point. The system of equations for this design point solver is larger primarily due to the use of dependent equations to define similarity parameter inputs in OTAC.

Table 5: Solver Summary for E^3 LPT MDP

Metric	Mean	Standard Deviation	Minimum	Maximum
Wall Time (sec)	43.36	45.75	5	302
MDP Solver Iterations	3.73	0.74	2	10
ADP Solver Iterations	254.05	262.89	42	2011
TOC Solver Iterations	60.97	13.75	36	162
SLS Solver Iterations	85.71	65.55	46	6225
MDP Solver Model Passes	8.87	1.29	7	25
ADP Solver Model Passes	4322.88	5122.29	288	34119
TOC Solver Model Passes	151.65	55.89	60	533
SLS Solver Model Passes	206.44	123.26	82	9522
MDP Solver Jacobians	1.03	0.16	1	3
ADP Solver Jacobians	49.62	59.30	3	395
TOC Solver Jacobians	4.32	2.16	1	19
SLS Solver Jacobians	5.75	3.32	1	157

Overall, the results in this part of Experiment 1 show that the coupling equations formulated for the turbine MDP method and implemented on these sample problems produce

Table 6: Solver Summary for CPT MDP

Metric	Mean	Standard Deviation	Minimum	Maximum
Wall Time (sec)	33.01	32.41	8	298
MDP Solver Iterations	9.31	7.07	3	103
ADP Solver Iterations	302.82	345.08	49	3699
TOC Solver Iterations	160.44	100.27	54	1436
HOGE Solver Iterations	226.16	159.99	98	2740
OEI Solver Iterations	234.76	161.28	95	2554
Climb Solver Iterations	206.49	152.43	87	2473
Shift1 Solver Iterations	241.64	201.96	77	8674
Shift2 Solver Iterations	244.67	184.42	81	3306
MDP Solver Model Passes	28.62	23.32	15	349
ADP Solver Model Passes	2480.48	3621.18	119	38713
TOC Solver Model Passes	239.91	152.33	67	3750
HOGE Solver Model Passes	347.34	234.78	124	4248
OEI Solver Model Passes	373.85	247.14	133	4025
Climb Solver Model Passes	306.34	210.93	112	3474
Shift1 Solver Model Passes	449.12	442.18	104	23319
Shift2 Solver Model Passes	454.94	359.02	115	6803
MDP Solver Jacobians	1.61	1.4	1	21
ADP Solver Jacobians	42.7	64.39	1	689
TOC Solver Jacobians	6.11	5.18	1	178
HOGE Solver Jacobians	9.32	6.52	1	180
OEI Solver Jacobians	10.7	7.42	1	171
Climb Solver Jacobians	7.68	5.04	1	77
Shift1 Solver Jacobians	15.96	20.84	1	1297
Shift2 Solver Jacobians	16.17	14.04	1	299

designs which satisfy all performance requirements and constraints. Furthermore, the MDP method efficiently and robustly finds solutions throughout the design space. Combined with the results from the first part of the experiment which examined the similarity parameter formulation, the experiment supports the first hypothesis that the cycle MDP method can be adapted and applied to the turbine problem by selecting an appropriate design parameterization, constructing the system of nonlinear equations that couple the design points.

5.6.2 Experiment 2: Comparison of MDP and SPD Turbine Meanline Analysis Methods

The second research question presented at the beginning of this chapter inquires about the differences in the designs produced by the newly developed turbine MDP methodology and

Table 7: Solver Summary for VSPT MDP

Metric	Mean	Standard Deviation	Minimum	Maximum
Wall Time (sec)	116.00	60.33	23	599
MDP Solver Iterations	154.09	69.31	32	598
ADP Solver Iterations	1196.97	579.71	229	5787
TOC Solver Iterations	1063.49	503.75	165	5623
HOGE Solver Iterations	997.36	658.11	202	18371
OEI Solver Iterations	1084.31	434.77	251	3518
Climb Solver Iterations	832.15	361.75	151	2879
MDP Solver Passes	384.04	170.34	74	1381
ADP Solver Passes	4006.47	2914.74	417	24927
TOC Solver Passes	1221.57	589.23	182	6881
HOGE Solver Passes	1267.88	1678.01	269	39372
OEI Solver Passes	1396.83	568.74	345	4636
Climb Solver Passes	949.28	412.30	185	3124
MDP Solver Jacobians	16.43	7.36	3	62
ADP Solver Jacobians	39.02	33.90	2	278
TOC Solver Jacobians	9.30	6.56	1	93
HOGE Solver Jacobians	15.91	64.65	1	1570
OEI Solver Jacobians	18.38	10.86	1	87
Climb Solver Jacobians	6.89	4.67	1	35

the traditional SPD approach. Hypothesis 2 conjectures that the individual designs and the overall design space topology will be altered as a result of the additional requirements and constraints which are considered in the MDP methodology. The objective of Experiment 2 is to test this hypotheses and answer Research Question 2 by comparing results generated from both the MDP and SPD methods. The setup and results from this experiment are presented in the sections below.

5.6.2.1 Experiment 2 Setup

Experiment 2 uses all three example design problems presented in Section 5.5. All three designs were considered in this experiment as they implement a range of architectures, design points, requirements and constraints which may impact the resulting design spaces. With these models selected, the next step in this experiment was to evaluate each of the design with both the MDP and SPD methods.

Prior to defining the data generation and comparison process for the MDP and SPD methods, it is important to first describe the SPD method assumed for this analysis. The

SPD method designs the turbine considering only the performance requirements and constraints present at a lone design point. For all three problems considered in this experiment, the single point design was assumed to correspond to the aerodynamic design point used in the MDP analysis. This point was selected as it is representative of a cruise operating condition where the turbine is likely to spend the most time operating and therefore benefits most from a high efficiency. In order to satisfy the power requirement present at this single design point, it was also assumed that the designer would adjust the mean radius of the turbine similar to the design rule utilized in the MDP analysis. Values for the shaft speed and mass flow rate at the on-design point were assumed to be set by the engine cycle and therefore held constant. Following the development of a valid design at the ADP point, the turbine was then evaluated in an off-design mode for the other operating conditions of interest to determine if the performance requirements were satisfied while remaining within the constraint limits.

With the SPD method defined, the details of the Experiment 2 setup can be presented. Experiment 2 is broken down into two parts with the first part focusing on the comparison of the turbine design spaces produced by the two methods. To complete this comparison, several sets of design space explorations were conducted for each design problem using both the newly developed turbine MDP approach and the traditional SPD method. The first set of DoEs evaluated with both models considered very small design spaces. These design spaces consisted of only two design variables: the flow coefficient and loading coefficient for a given stage. These two design variables were selected as they are commonly used in the conceptual design process to identify candidate designs from the Smith chart.[99] These charts depict the design space for a single stage in terms of the flow coefficient and loading coefficient with contours for the stage efficiency as shown in Figure 47. Given these small design spaces, a full factorial DoE was evaluated with 20 levels per variable for a total of 400 cases. These cases were then analyzed and used to create plots similar to the Smith chart for each turbine. This process was repeated for all stages in each of the three design problems.

The second set of DoEs considered in this first part of Experiment 2 explored the full

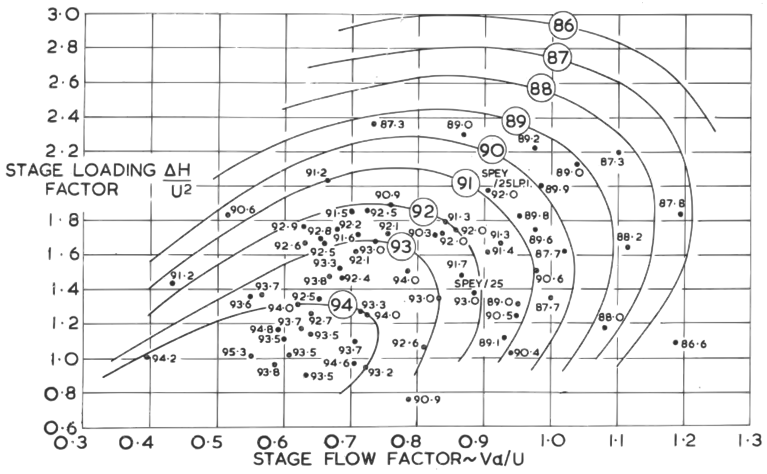

Figure 47: Example Smith Chart[99]

design space specified for each design problem in Section 5.5. Given this high-dimensional design space for each design problem, a random sample DoE was used to fill the design space with 10,000 cases. These 10,000 cases were analyzed with both the MDP method and the SPD method so that for every MDP case evaluated there was an equivalent SPD case. Visualizing the topology of this high-dimension design space is difficult leading to a numerical comparison approach being used to evaluate the differences between the design spaces. This large DoE run was also used to examine the changes to the independent vector values between the MDP and SPD methods.

The second part of Experiment 2 focuses on comparing individual designs produced by the two design methods. For this part of the experiment, individual designs were randomly selected from the 10,000 case DoEs used in part 1 of this experiment. The selected cases were compared in terms of the flowpath geometry and velocity vectors. In addition, the saved designs from each method were evaluated in off-design mode to produce the performance maps for comparison.

A successful Experiment 2 will be defined by several different outcomes. First, a successful experiment will show that the MDP method alters the design space specifically in terms of the efficiency contours and feasible design space relative to the SPD generated design space. It will also show that the MDP method adjusts the independent vector values

differently than the SPD method to satisfy all performance requirements and constraints. Third, a successful test will show that individual designs produced by the MDP and SPD methods were altered in terms of geometry and performance map characteristics. Given that the same design inputs will be evaluated with both the MDP and SPD methods, this experiment will prove that the differences shown in the design space and individual design comparisons are a result of the design rules included in the MDP method.

5.6.2.2 Experiment 2 Results

The first part of Experiment 2 focuses on comparing the design spaces that result from applying the MDP and SPD methods to the same design problem. As described in the experiment setup, this design space comparison uses three different techniques to evaluate the differences in the spaces. Each of these three comparison techniques will be presented one at a time with a selection of results shown for all models before moving on to the next comparison technique. Additional results for each comparison technique are provided in the appendices. For clarity throughout this experiment, when results from the two methods are shown on the same plot the results from the MDP method will be shown in red in all figures while result produced using the SPD method will be shown in blue.

Part 1: Design Space Comparisons

The first design space comparison technique examines the small design spaces described in the setup section. These small design spaces are formed by varying the flow coefficient and loading coefficient for a single stage of each design. The results produced from evaluating these design spaces were plotted to visually analyze the differences between the two methods. These plots are similar to the classical Smith chart, however the efficiency contours shown are for the overall turbine efficiency and are not the efficiency for that particular stage. In addition, for the design spaces generated from the SPD method, constraint lines and shading have been added to the diagrams indicating infeasible portions of the design space.

To demonstrate the differences in design spaces in terms of the Smith charts, the CPT design problem will be primarily used. Figure 48 shows the design spaces produced with

the MDP (on the left) and SPD methods (on the right) for the first stage flow and loading coefficients. The blue/green contours in these plots are the overall turbine efficiency which have trends that generally match those found in the Smith chart. Examining the efficiency contours in this figure reveals that the MDP and SPD methods produce similar efficiency trends throughout the design spaces. However, there are some minor differences in efficiencies predicted by the two methods with the SPD generated designs having higher efficiency over most of the design space. The more significant difference in this design space comparison, however, is the feasible design space produced by the two design methods. For the MDP method, the inclusion of all performance requirements and constraints produces designs throughout the entire design space that are feasible. In comparison, significant portions of the SPD generated design space are infeasible as indicated by the black constraint lines and gray shading. For this analysis, the limits for both maximum AN^2 and pressure ratio at the HOGE operating condition render large portions of the design space infeasible. A designer using the SPD method that chose flow and loading coefficient values in this infeasible range would therefore be required iterate on the SPD design inputs to generate a feasible turbine.

A similar comparison can be made for the second stage of the conventional power turbine as shown in Figure 49. For the second stage, the trends in the efficiency contours throughout the design space are similar with the SPD efficiency values being higher throughout the design space. Again for this stage, a significant portion of the design space produced by the SPD method is infeasible as a result of the AN^2 and HOGE pressure ratio constraints.

The design space comparison for the third and final stage of the CPT is shown in Figure 50. For this third stage, there is a noticeable difference in the efficiency contour trends compared to the first two stages. Here, the efficiencies for the MDP generated designs are higher than the SPD generated designs throughout the design space. In addition, the increased separation in the contour lines in the SPD design space shows that the gradient of the design space is also different, particularly at low flow coefficient values. The design space resulting from the SPD analysis is also largely infeasible with both the AN^2 and HOGE pressure ratio again serving as the limiting constraints. By comparison, the designs

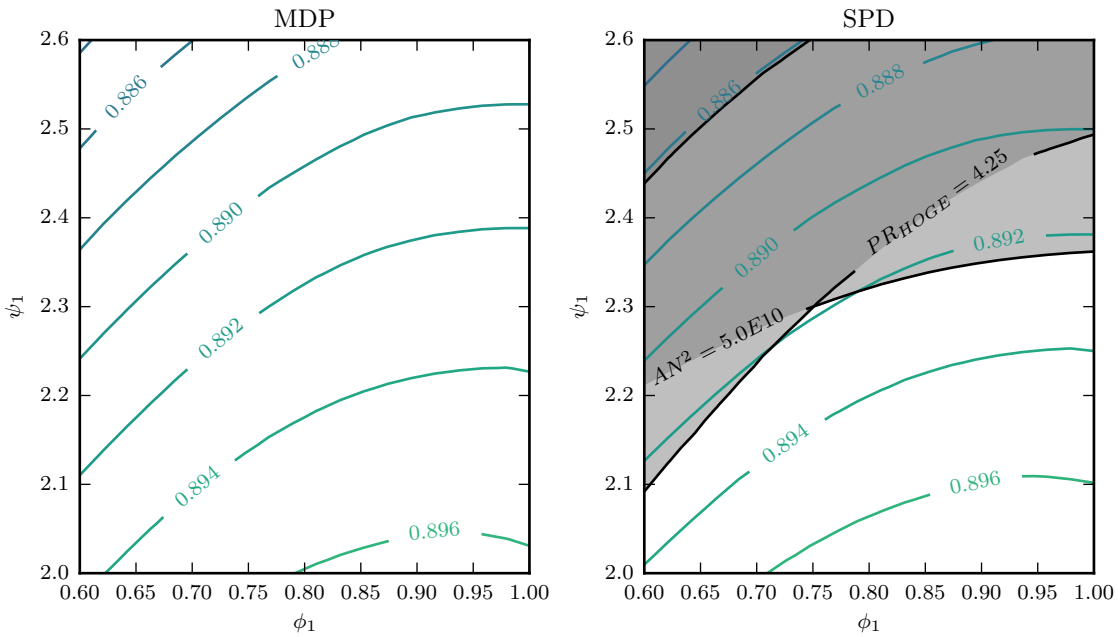

Figure 48: Comparison of the MDP and SPD Generated Design Spaces for the CPT Stage 1 Flow and Loading Coefficients

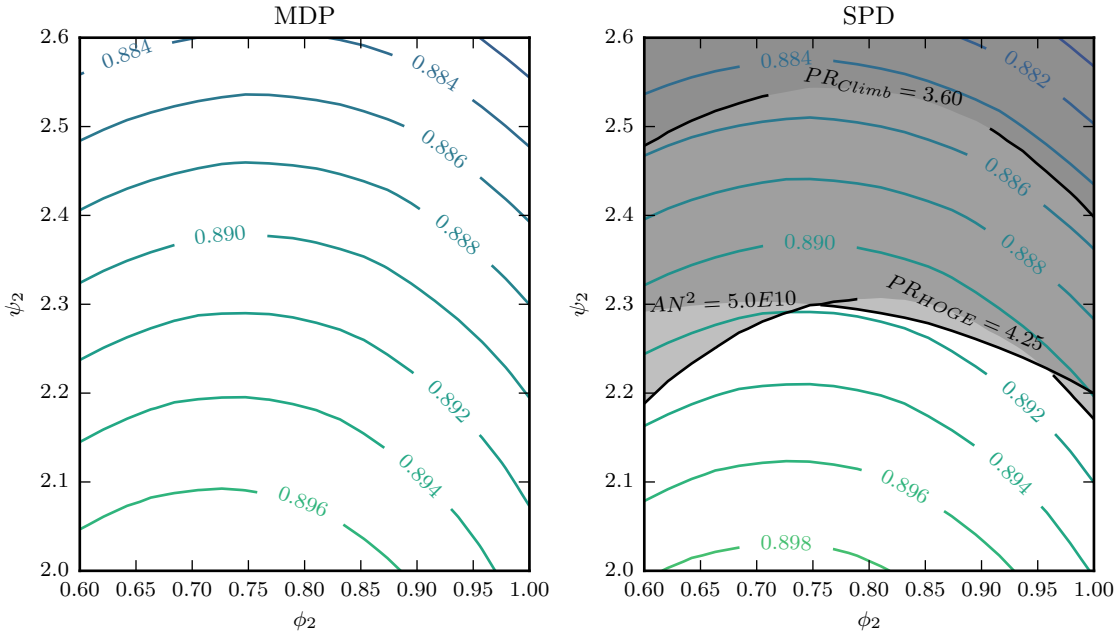

Figure 49: Comparison of the MDP and SPD Generated Design Spaces for the CPT Stage 2 Flow and Loading Coefficients

produced by the MDP method take these constraints into account during the on-design phase resulting in a design spaces which is completely feasible.

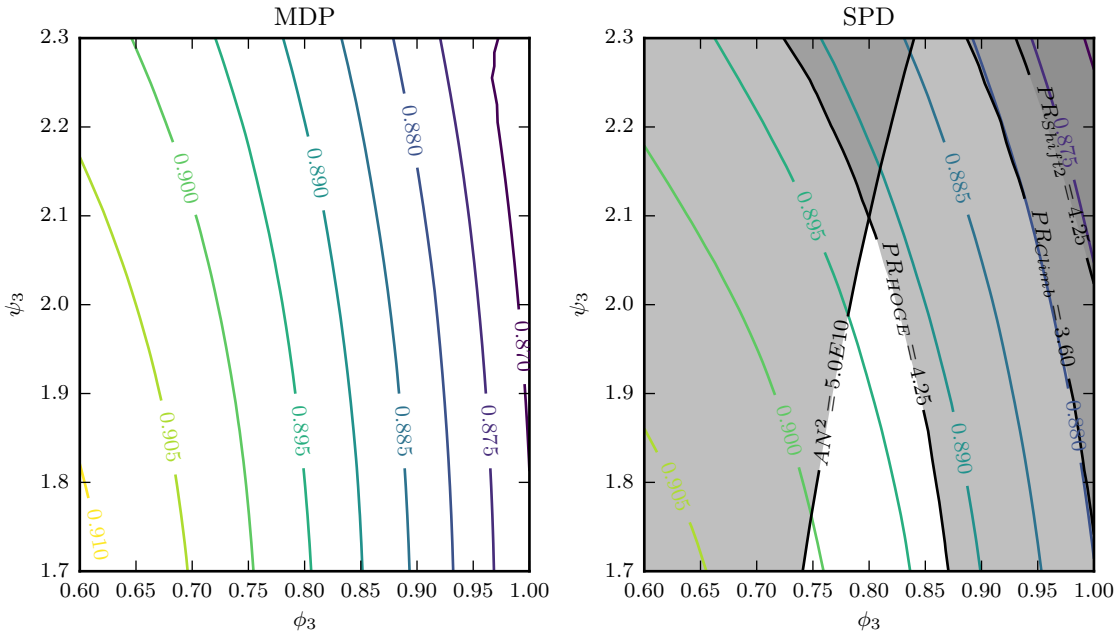

Figure 50: Comparison of the MDP and SPD Generated Design Spaces for the CPT Stage 3 Flow and Loading Coefficients

Similar assessments of the flow and loading coefficient design spaces for each stage were also completed for the other two design problems. The MDP and SPD generated designs spaces for these problems generally display similar characteristics as the CPT results shown in Figures 48 through 50. The analysis of the E^3 LPT and VSPT are therefore presented in Appendix J. However, there are two stages from these models that when analyzed exhibited trends worthy of discussion here. These two stages are the fourth stage of the E^3 LPT and third stage of the VSPT. The comparison of the MDP and SPD generated design spaces for these two stages are shown in Figures 51 and 52 respectively. For both of these stages there is a significant difference in the efficiency contours produced by the two methods for cases with low flow coefficients. The results from the MDP method show a sharp change in the efficiency contours at these low values. In addition, the results from the SPD analysis for both stages show a sharp break in the AN^2 constraint. These two characteristics are the result of the same phenomenon. The stages considered in these figures are the second to last

stages of their respective turbine architectures. When a low flow coefficients is specified for these stages, the axial velocity entering the rotor is reduced leading to an increased annulus height to pass the required mass flow. This larger annulus height makes the annulus area of these stages greater than that of the last stage of each design. Since the AN^2 limit is set by the largest value for any stage in the turbine, these sharp changes in the efficiency contours and AN^2 constraints correspond to changes in the AN^2 limiting blade row. While this change in the limiting AN^2 blade row is not captured by the SPD method until the off-design analysis, the MDP method includes this constraint allowing for the turbine design to be adjusted resulting in a completely feasible design space.

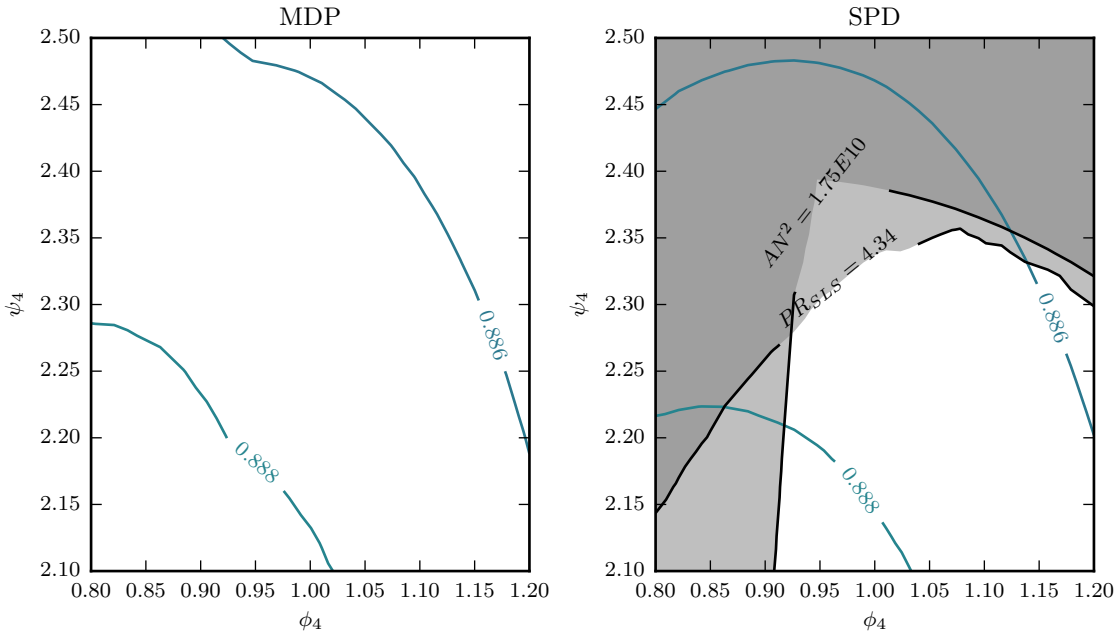

Figure 51: Comparison of the MDP and SPD Generated Design Spaces for the E^3 LPT Stage 4 Flow and Loading Coefficients

The second technique for comparing the design spaces produced by two methods examines a larger set of design variables for each problem. As described in the experiment setup, for each problem the design spaces identified in Step 8 of the implementation were evaluated with a large random sample DoE. Given the dimensionality of these design spaces, visual comparison of the topology of the resulting spaces is difficult. Therefore, a numerical comparison of the resulting designs produced by each method was completed. Since the

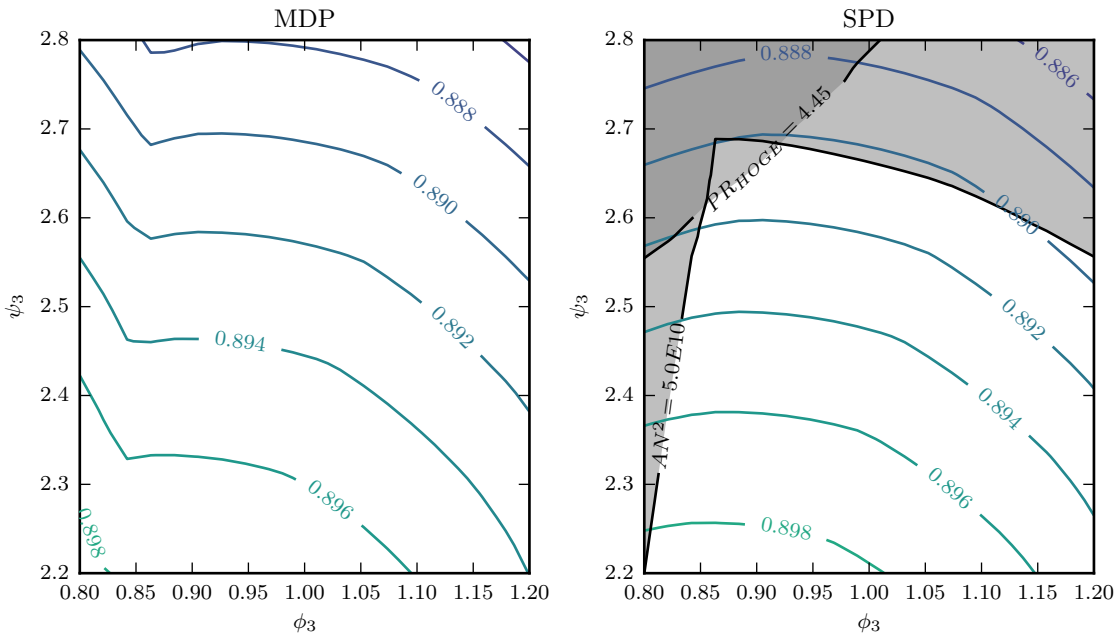

Figure 52: Comparison of the MDP and SPD Generated Design Spaces for the VPST Stage 3 Flow and Loading Coefficients

same random sample DoE was analyzed by both the MDP and SPD methods, differences between each corresponding case can be computed. Examining these differences across the entire design space allows for a statistical comparison between the two methods.

The first design problem examined with this numerical comparison technique is the E^3 LPT. Figure 53 shows a box plot comparing the turbine efficiencies produced by the two design methods at all three design points. In this figure, the horizontal red line defines the mean difference between the MDP and SPD produced designs. The black box encompasses the interquartile range (the middle 50% of the cases) with the the dashed lines showing the upper and lower quartiles. In this analysis, the difference between the MDP and SPD generated designs was computed using Equation 62. With this definition, difference values that are positive indicate the SPD value exceeded the MDP value while negative values indicate that the MDP value exceeded the SPD value.

$$Difference = SPD\ Value - MDP\ Value \tag{62}$$

The numerical comparison in this figure shows that the mean difference in efficiency between the MDP and SPD generated designs is close to zero with SPD being slightly higher than the MDP value. The largest differences in efficiency between the two methods occur at the ADP and TOC design points. However, the minimum and maximum differences at these design points are relatively small at less than 0.2%. The similarity in efficiency between the MDP and SPD generated designs is a result of the design parameterization and loss model implemented for this study. The Kacker-Okapuu model computes losses based flow angles and non-dimensional parameters such as thickness-to-chord ratio, blade aspect ratio and tip clearance-to-blade height ratio. Since these values are determined by the similarity parameters used to define the design, the efficiency is nearly identical between the MDP and SPD results. The small differences that do arise are due to changes in the Reynolds number and the hub-to-tip ratio.

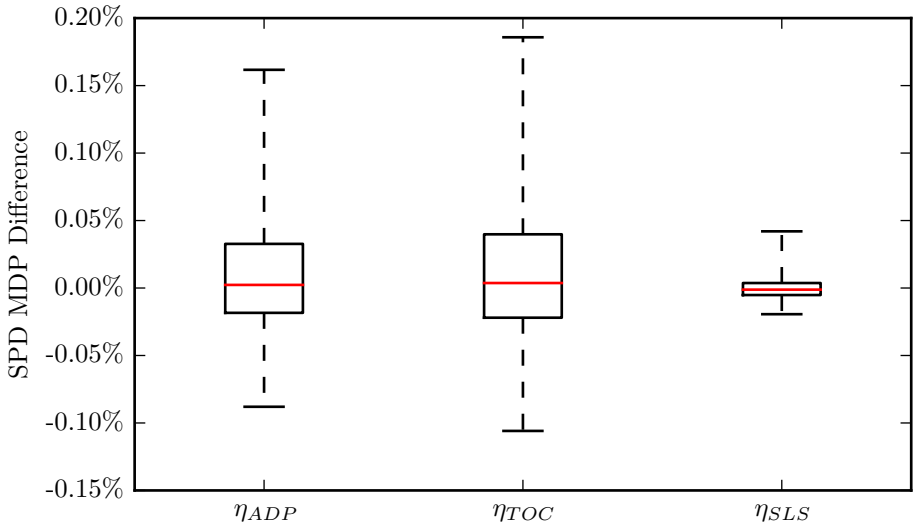

Figure 53: Efficiency Comparison of the MDP and SPD Generated E^3 LPT Design Spaces

In addition to numerically evaluating the differences in terms of efficiency, the design spaces were also examined relative to the performance requirements and constraints. For the MDP method, all cases within the design spaced that converged satisfied the performance requirements and constraints as shown in Figure 54. In this figure the metric values have

been normalized by the required values such that all requirements and constraints can be shown on the same figure. The presence of only the red mean bar without interquartile boxes and whiskers indicates that all designs matched the specified requirement values. Evaluation of the SPD results relative to the performance requirements and constraints is shown in Figure 55. In comparison to the MDP results, many of the designs produced with the SPD method do not satisfy the AN^2 and SLS pressure ratio requirements as indicated by the segments of the box plots lying above a normalized value of 1. In total, only 4,635 of the 10,000 designs (46.35%) produced with the SPD method in this experiment satisfied all performance requirements and constraints simultaneously.

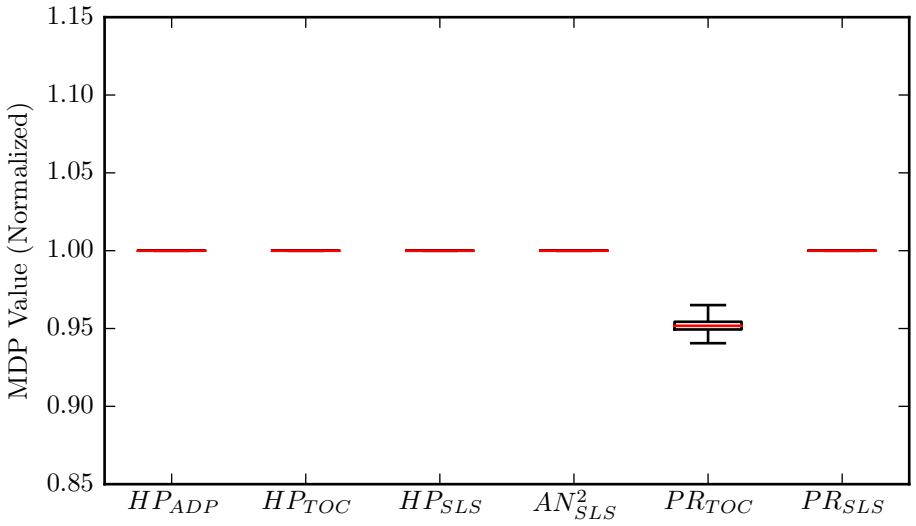

Figure 54: Requirement and Constraint Values from the MDP Generated E^3 LPT Design Space

A similar numerical analysis to compare the MDP and SPD generated design spaces for the CPT problem was also completed. This design problem had more design points, performance requirements and constraints compared to the E^3 LPT problem presenting different challenges for the MDP and SPD design methods. Figure 56 show the difference in efficiency between the MDP and SPD generated designs within the large design space for the CPT. Most of the designs evaluated from this design space had similar efficiency characteristics as indicated by the small interquartile range for each design point efficiency. However, the

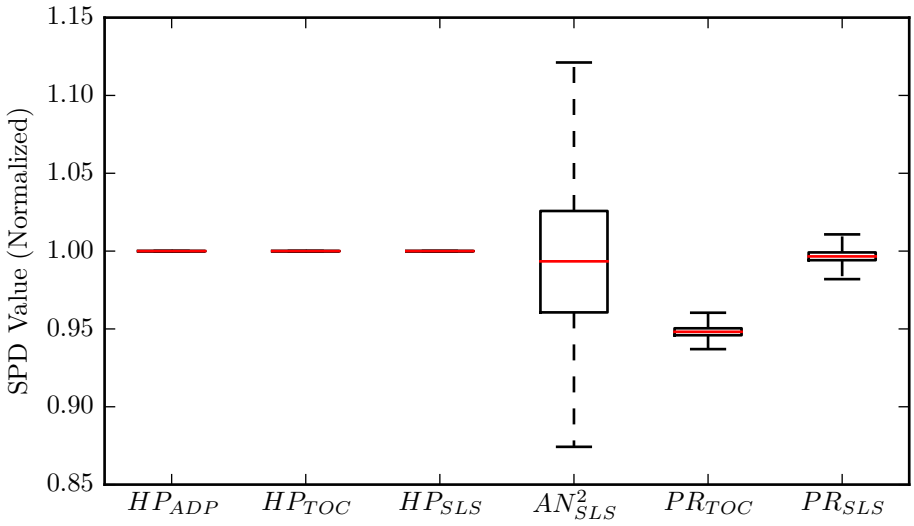

Figure 55: Requirement and Constraint Values from the SPD Generated E^3 LPT Design Space

upper and lower quartile bars show that there are larger differences between some MDP and SPD results, especially for the Shift1 and Shift2 efficiencies. These larger difference are the result of the MDP method taking into account requirements and constraints not considered by the SPD method, particularly those related to the Shift1 minimum reaction. The constraints for these values result in modifications to the input design parameters for the ADP stage reactions leading to the larger differences in the performance characteristics.

The design spaces produced by both methods were also evaluated in terms of the feasibility of the results. Figure 57 shows box plots for the MDP generated design space against all performance requirements and constraints. The requirements and constraints have been normalized by the value in Table 37 such that a value of 1 indicates the constraint value for all metrics. As can be seen in the top part of the figure, the power requirements and AN^2 requirement are exactly satisfied for all converged cases. The lower part of the figure shows that the pressure ratio values for all cases are acceptable as indicated by the normalized values being less than 1. For Shift1 reaction constraints, the figure shows that the minimum value for all designs in the lower quartile satisfy the constraint by being greater than 1.

For the SPD generated design space shown in Figure 58, the power requirements can be

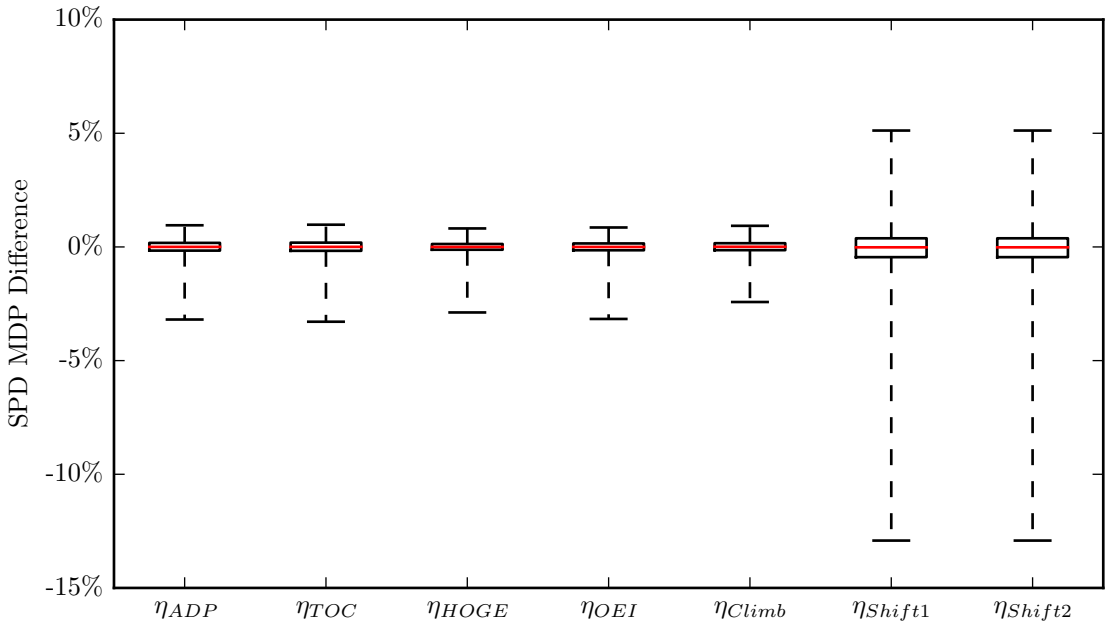

Figure 56: Efficiency Comparison of the MDP and SPD Generated CPT Design Spaces

satisfied by all designs as indicated by the red bars in the upper part of the figure. However most of the other constraints have portions of the design space that violate the constraint values. For the AN^2 and HOGE pressure ratio constraint about half of the designs exceed the allowable value (have values greater than 1). The other pressure ratio constraints have portions of the upper quartile above 1 showing the some designs violate these constraints as well. Lastly, the figure shows that portions of the design space violate the Shift1 reaction limit as the lower quartile line extends below the unity value. In total, 4,935 of the 10,000 designs produced with the SPD method satisfied all requirements and constraints for a success rate of just under 50%. By comparison, almost 95% of the 10,000 MDP evaluated designs resulted in a converged, feasible design.

The last problem analyzed to determine the numerical differences in the design spaces which result from the MDP and SPD design methods is that of the VSPT. Comparison of the VPST efficiency at each design point for the two different methods is shown in Figure 59. For this design problem, the efficiency of the turbine at the HOGE and OEI design points predicted by the two methods are nearly identical. Larger variations are observed

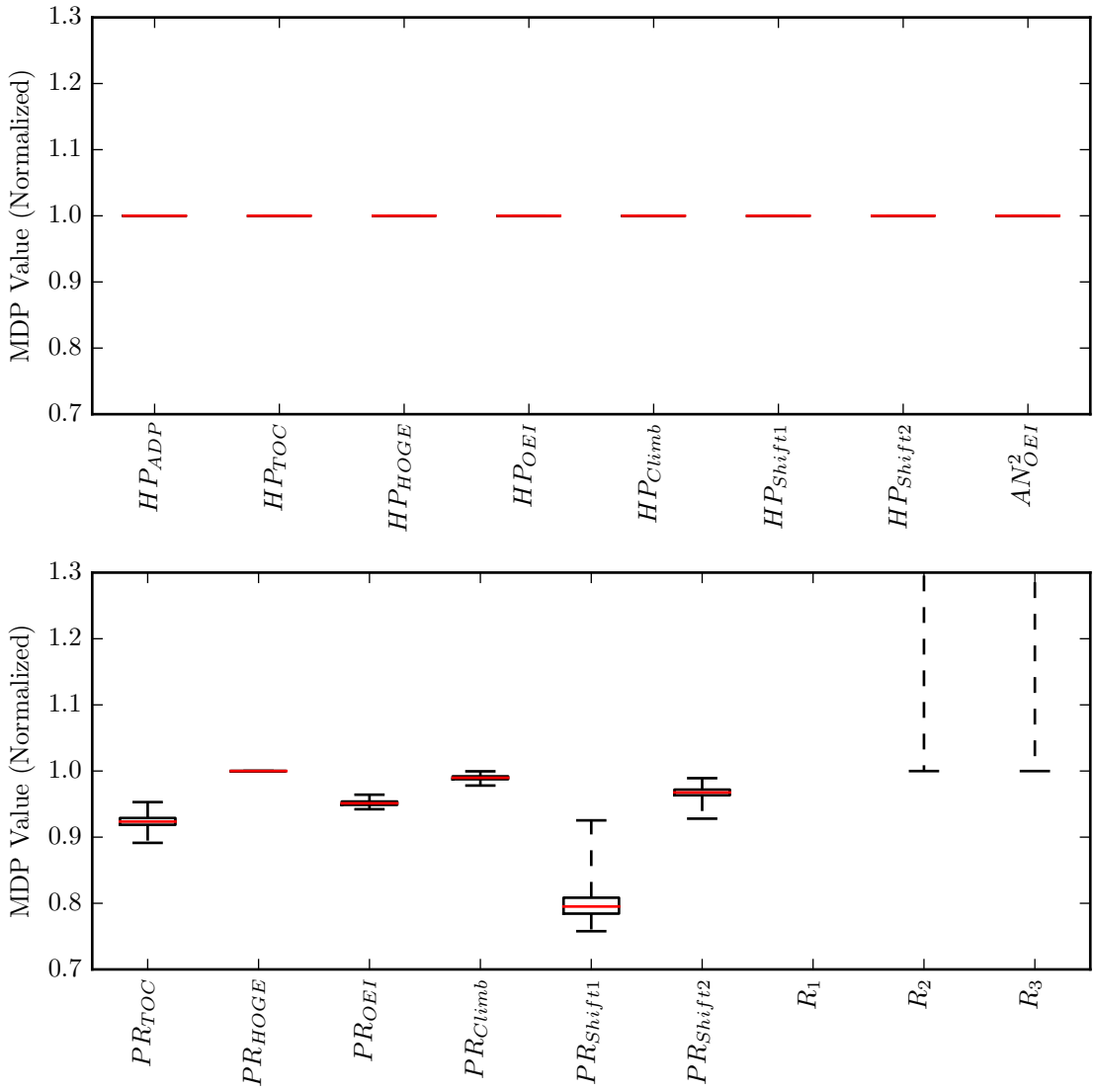

Figure 57: Requirement and Constraint Values from the MDP Generated CPT Design Spaces

at the other operating conditions with the efficiencies for the SPD generated designs on average falling below the efficiencies for the corresponding MDP generated design. These larger variations are generally less than 0.75% as a result of similar inputs into the loss model calculations.

Figures 60 and 61 show the VSPT design spaces in terms of performance requirements and constraints for the MDP and SPD methods, respectively. As expected, the designs produced by the MDP method satisfy all performance requirements and constraints as

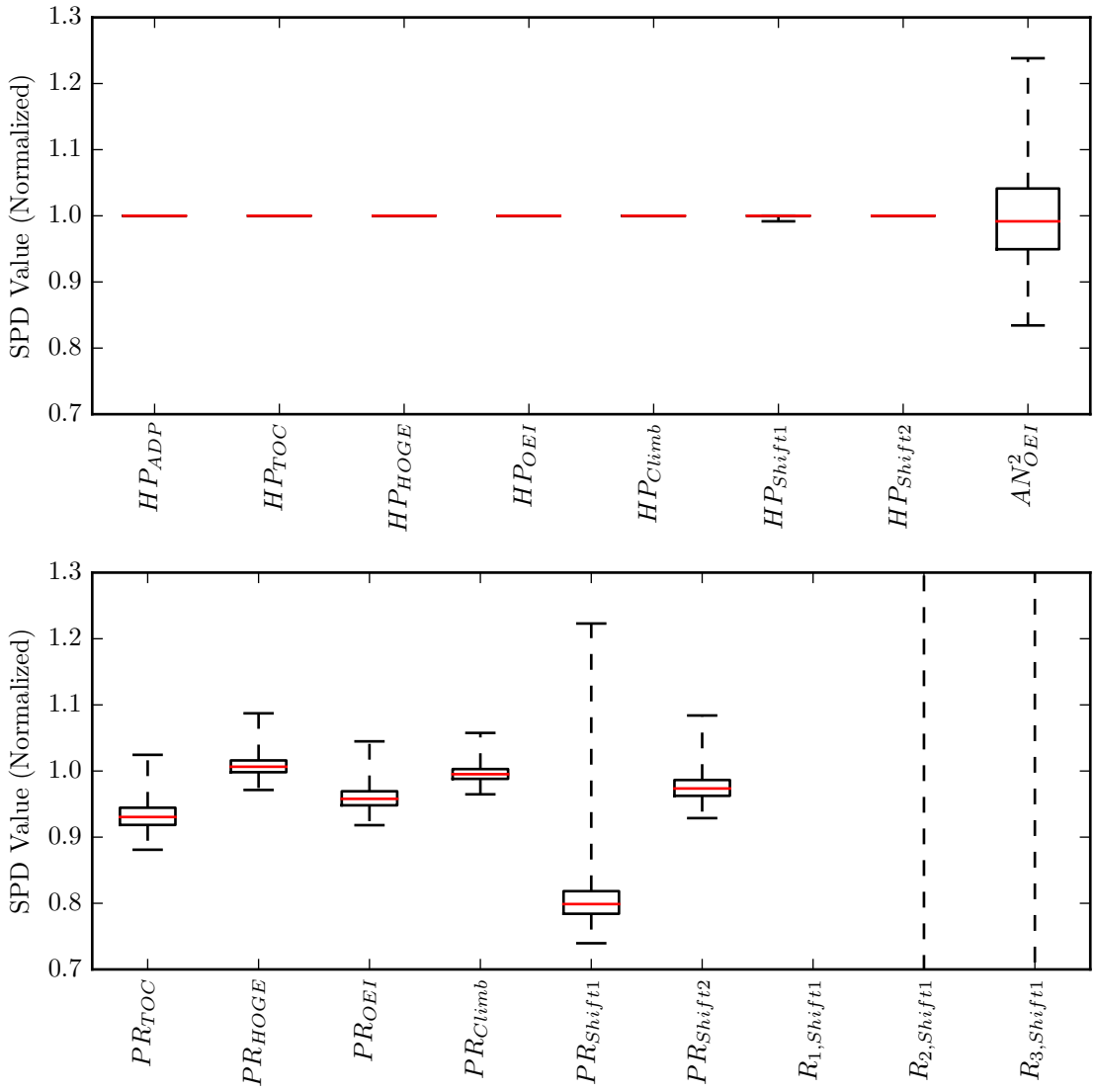

Figure 58: Requirement and Constraint Values from the SPD Generated CPT Design Spaces

indicted by the red bars at the normalized value of 1 for each metric. For the SPD generated designs, the power requirements can be exactly matched but the AN^2 and HOGE pressure ratio constraints are violated for most of the designs. For this design problem, of the 10,000 different design cases analyzed with the SPD only 1,491 satisfied all performance requirements and constraints.

The third technique used to evaluate differences in the design spaces produced by the MDP and SPD methods was to examine the independent vector values that form one half

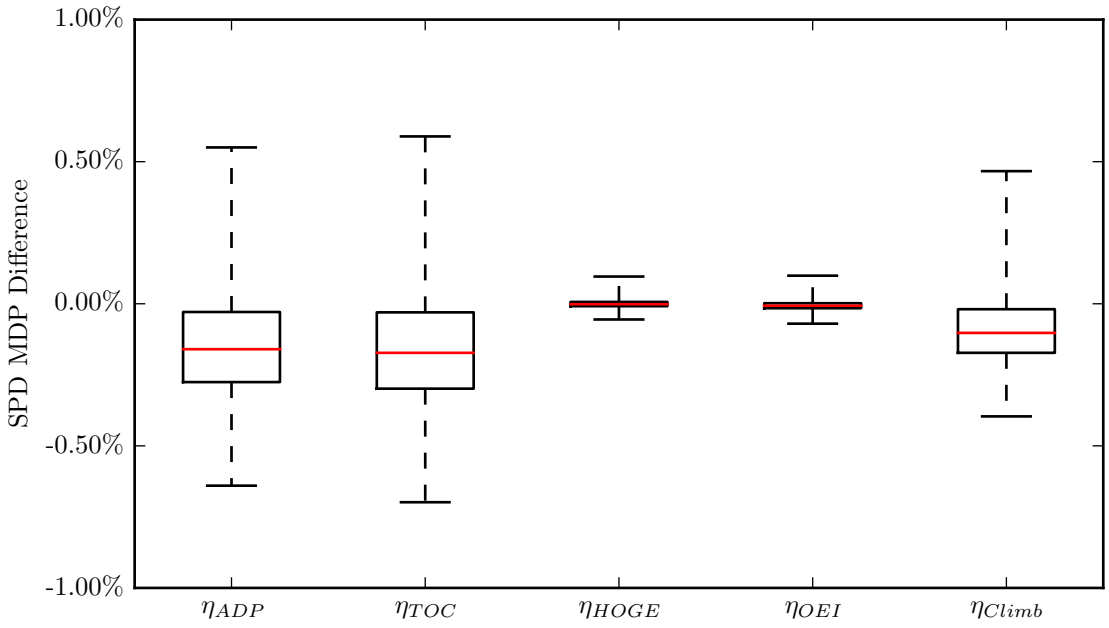

Figure 59: Efficiency Comparison of the MDP and SPD Generated VSPT Design Spaces

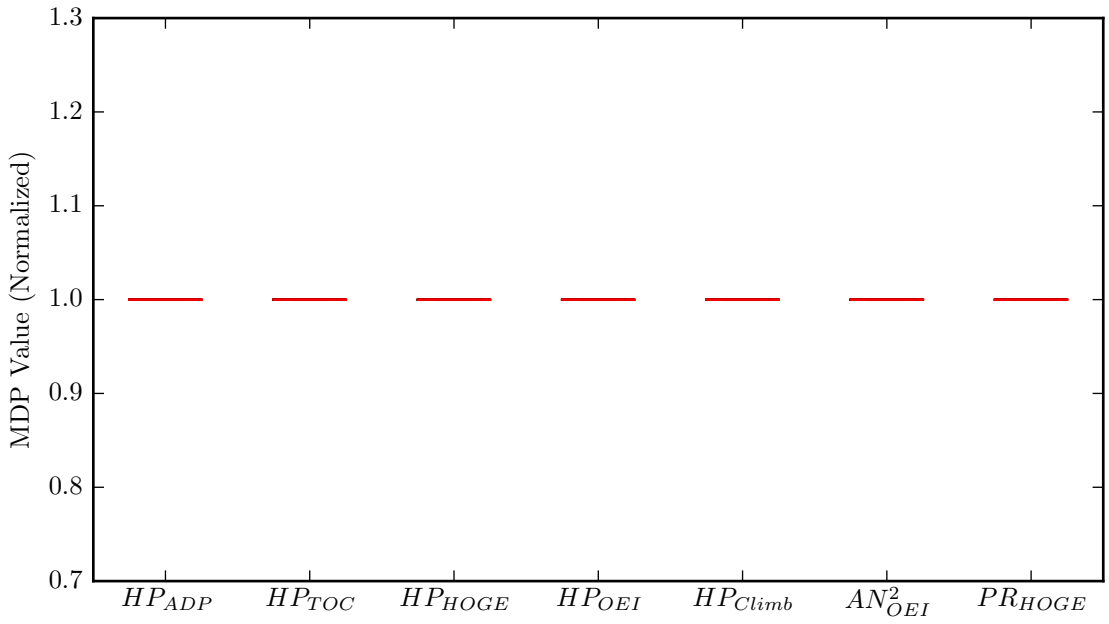

Figure 60: Requirement and Constraint Values from the MDP Generated VSPT Design Spaces

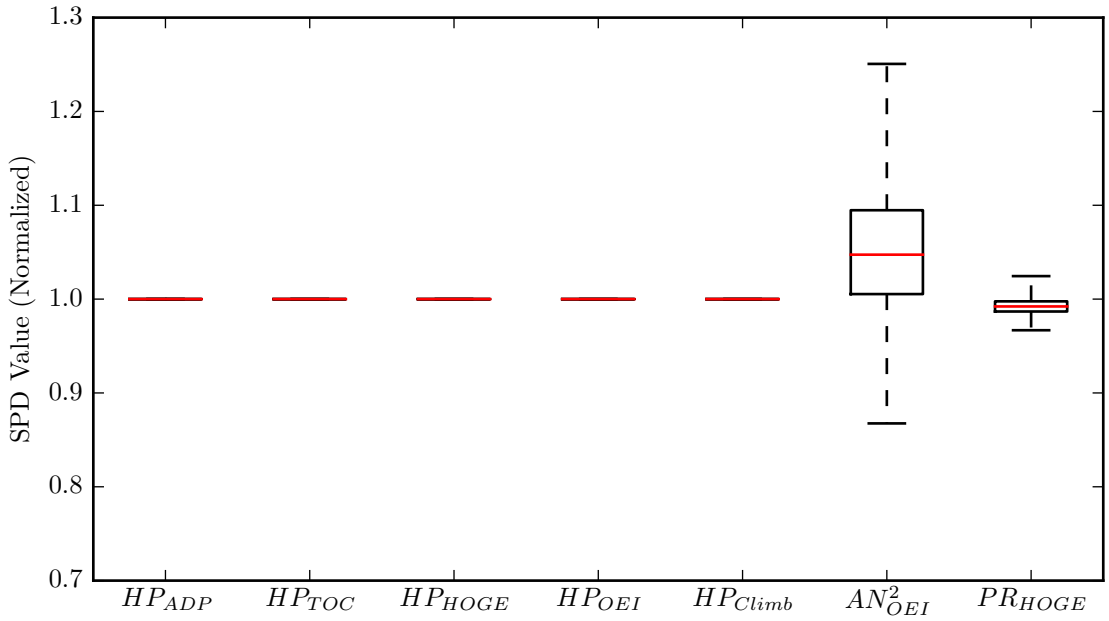

Figure 61: Requirement and Constraint Values from the SPD Generated VSPT Design Spaces

of the MDP design rules. These independent parameters are varied in the MDP method to ensure the design satisfies all performance requirements and constraints. In the SPD method, the sizing of the turbine by varying the mean radius is completed using information available only in the on-design phase at the lone design point. Other on-design parameters such as the mass flow rate and shaft speed are held constant as information from the off-design operating conditions which affect these values is not available. In the off-design phase, the exit static pressure operating parameters at each operating condition are varied such that the performance requirements at these conditions are satisfied. However, the constraints at these off-design operating points may be violated and the turbine design is not resized. Therefore, comparing the values for these independents parameters from the MDP and SPD methods shows the influence of the MDP design rules on the designs produced. For this part of the experiment, all three design problems were analyzed using multivariate plots. These plots were selected as they not only show changes to the individual parameter values between the methods, but they also show changes in the correlation between these parameter values.

The first multivariate plot examined is for the E^3 LPT design problem and is shown in Figure 62. In this figure, each square in the scatter plot matrix shows the relationship between two of the independent parameters. The independents for each block are specified by the labels along the diagonal of the matrix. The independent on the x-axis for each block in the matrix corresponds to the label in that column while the independent on the y-axis for each block is identified by the label in that row. The minimum and maximum values defining the scale of each axis of the block are defined by the numbers below the labels on the diagonal. Within each block, every red point in the scatterplot shows the values for those independent parameters for a single design out of the 10,000 run for this experiment with the MDP approach. The blue points in the scatterplot correspond to 10,000 designs evaluated with the SPD method. Examining the differences between the red and blue points shows the effect of the MDP coupling equations. For example, in the SPD method the ADP shaft speed and mass flow rate were set to a constant value during the on-design analysis phase as indicated by the straight lines of blue dots in those columns and rows. In the MDP method however, these parameters are part of the design rules used to ensure that all performance requirements and constraints are satisfied. As a result, the scatter plots for these parameters show that a range of values are required. The variation of the these parameters by the MDP method also results in changes in the other independent values used by both the MDP and SPD methods. This is particularly obvious in regards to the change in correlation between the mean radius and exit static pressure values at both TOC and SLS between the MDP and SPD produced designs. These results show that the MDP method alters the independent values differently than the SPD method to assure that all performance requirements and constraints are satisfied.

A similar multivariate plot can be created for the CPT as shown in Figure 63. For the CPT, the figure again shows that the ADP shaft speed and mass flow rate are held constant in the SPD method with the other parameters varied to size the turbine and satisfy the power requirements. Using the MDP method to design the CPT results in variations to these parameter values and effects the values and correlations for the other independent parameters. Of particular interest in this figure for the CPT is the row and

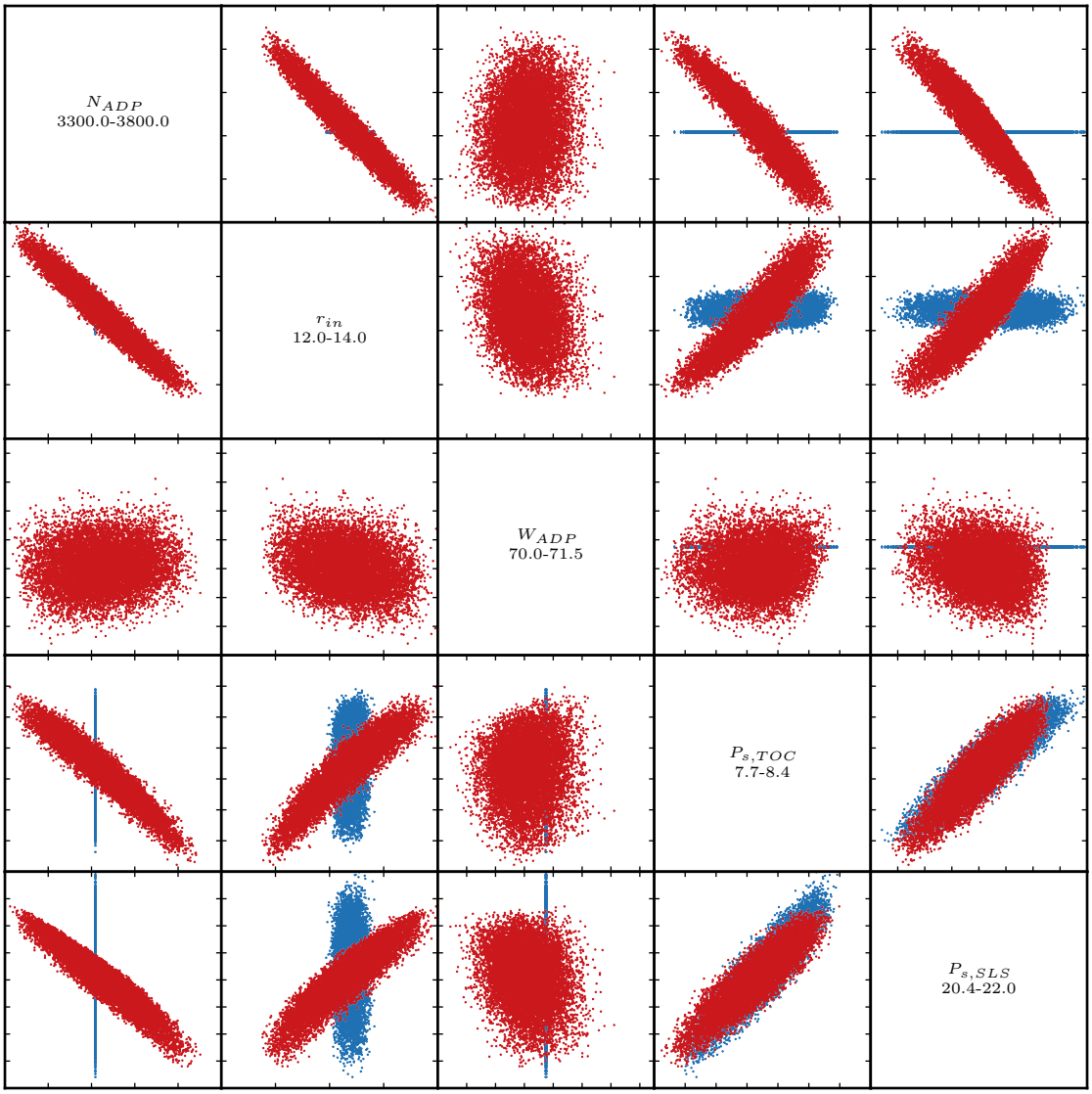

Figure 62: Multivariate Comparison of the MDP (Red) and SPD (Blue) Determined E^3 LPT Coupling Independents

column associated with the Shift1 exit static pressure. In these plots, there is a small cluster of SPD generated results that have lower exit static pressures than most of the MDP and SPD results. The SPD generated designs in this offset cluster have lower exit static pressures due to negative reaction values at Shift1 operating point when the power requirements are satisfied. A negative reaction for a given stage indicates that one of the blade rows in that stage is compressing the flow. The exit static pressure for these cases must be further reduced at the Shift1 operating point to expand the flow to achieve the

desired power output.

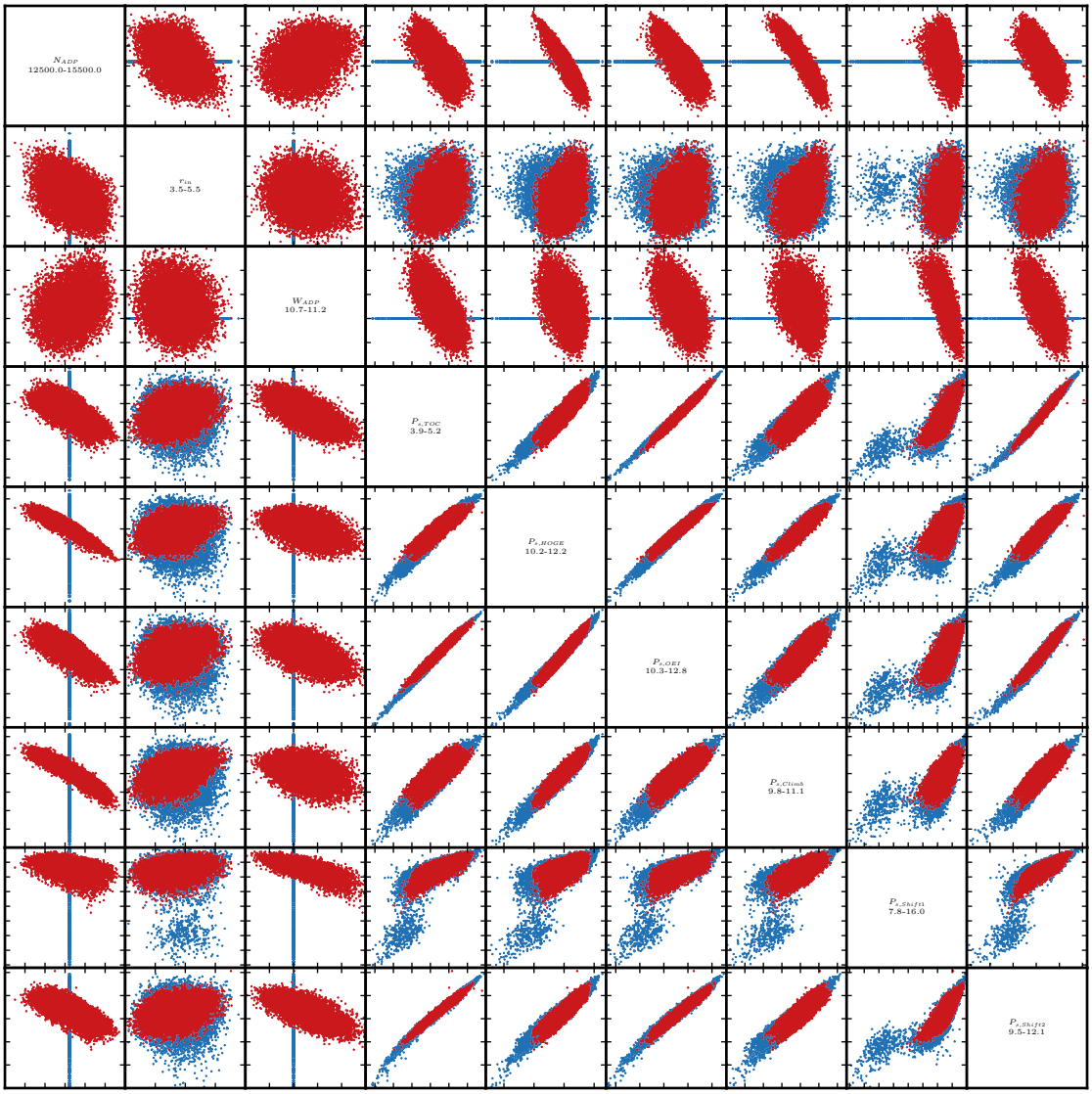

Figure 63: Multivariate Comparison of the MDP (Red) and SPD (Blue) Determined CPT Coupling Independents

Finally, a multivariate plot was also created for the MDP independents of the VSPT design problem as shown in Figure 64. The results shown in the multivariate plot for the VSPT are similar to those shown in for the other two design problems. Again, the multivariate plot for this problem show that the design rules implemented in the MDP methodology result in a different relationship between the independent values in the MDP method compared to the relationships observed in the SPD approach.

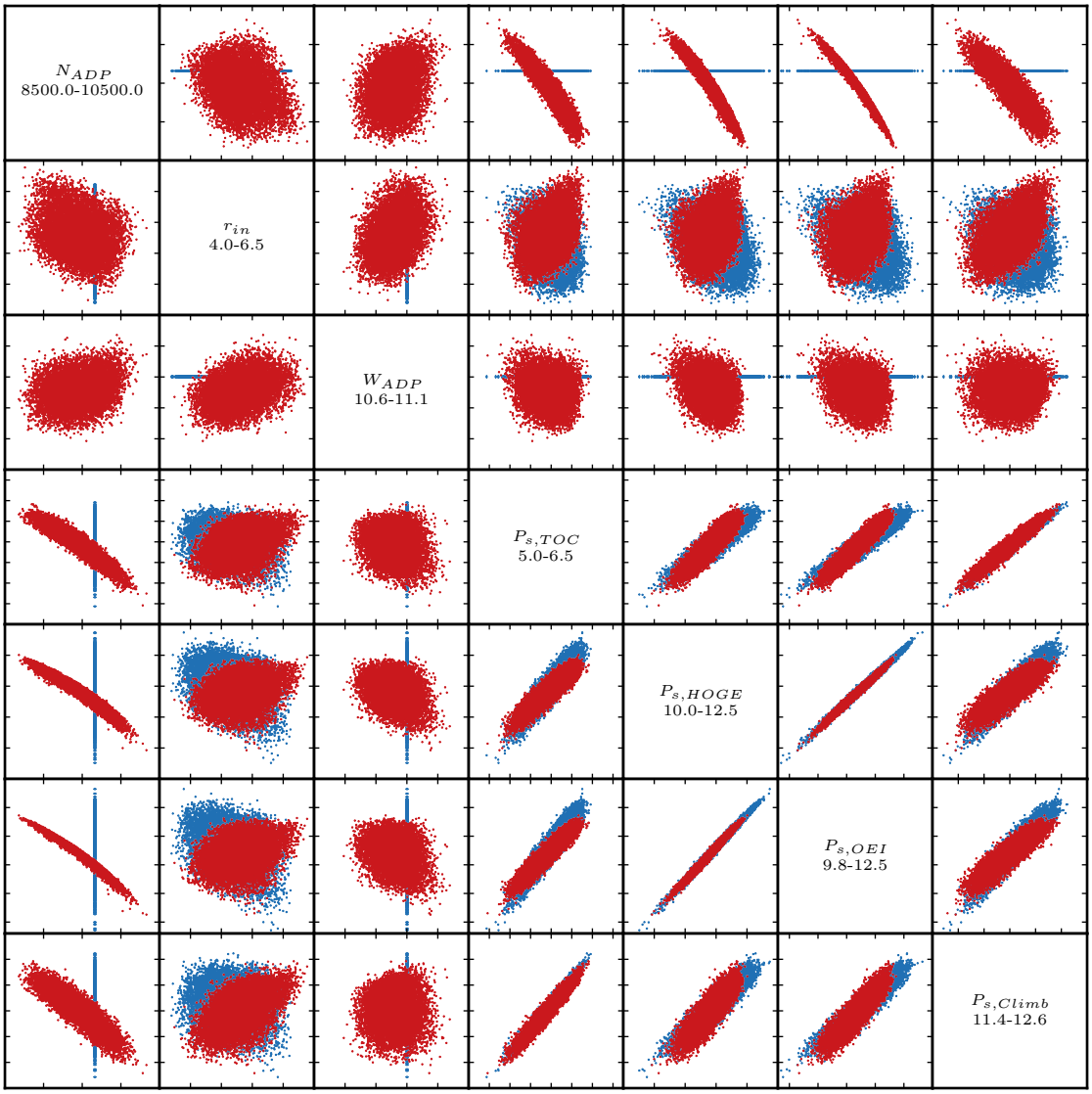

Figure 64: Multivariate Comparison of the MDP (Red) and SPD (Blue) Determined VSPT Coupling Independents

For Part 1 of Experiment 2, three different techniques were used to compare the design spaces generated by the MDP and SPD methods for all three design problems. The first technique examined small stage design spaces consisting of flow and loading coefficients using contour plots. The stage design spaces from each method showed minor differences in the efficiency contours except for the last stage of each problem which exhibited larger changes to the efficiency contours. Across all stages, the biggest difference between the two design spaces was the feasible space produced. Large portions of the SPD generated stage

design spaces were infeasible while the entire MDP design space satisfied all performance requirements and constraints. The second technique numerically compared much larger design spaces for each problem since visualizing these high-dimensional spaces is difficult. The results of the numerical comparison show that the MDP and SPD generated efficiencies for the E^3 LPT and CPT are similar at all design points. For the CPT design problem, the efficiencies predicted for the shift points differed between the MDP and SPD methods as a result of the input reaction being modified to maintain positive stage reactions at these points. These numerical analyses again showed that all designs from the MDP method meet all performance requirements and constraints while portions of the SPD generated design space violate one or more of the constraints. The third technique for comparing the MDP and SPD generated design spaces examined the changes to the independent vector values. These multivariate plots showed that the MDP method changes the relationship between these independent values in comparison to the SPD method. In total, these three comparison techniques show that the MDP method generates design spaces which differ from those produced by the SPD method as a result of the additional MDP coupling equations.

Part 2: Individual Design Comparisons

The second part of Experiment 2 focuses on evaluating the differences between individual designs produced by the MDP and SPD methods. For this part of the results section, the comparison between methods will be completed one case at a time for all metrics. This change in organization is done to better show the connection between the flowpath, velocity vector and map for a given set of design variables. To complete the comparison of individual designs, results from applying the MDP and SPD methods will be shown in terms of the flowpath geometry, velocity vectors and performance maps. For each design problem, several example comparisons are presented below with additional comparisons available in Appendix J.

The first two individual design comparisons presented come from the E^3 LPT design problem. Figures 65 through 67 show the flowpath, velocity vectors and performance map for the first E^3 LPT comparison. The flowpath comparison shown in Figure 65 indicates that

the MDP and SPD generated designs are geometrically similar. This similarity is expected as both methods are developing the design based on the same values for all similarity parameter inputs. The differences in the flowpath geometry result from the consideration of additional performance requirements and constraints by the MDP method. In this example, the MDP method decreases the mean radius while slightly increasing the blade height and overall length of the turbine in comparison to the SPD generated design. For this set of design inputs, the SPD method produces an infeasible design as the AN^2 constraint is violated. While the flowpath geometry produced by the two methods for the same design inputs is different, the velocity vectors shown in Figure 66 are identical. Given that the designs being developed by the two methods have the same similarity parameter values and are producing the same power at each design point, this similarity is again expected at all design points. Lastly, Figure 67 shows the performance maps for the turbine designs generated with each design method. The left plot shows the corrected flow through the turbine as a function of the pressure ratio with the lines representing different corrected speeds. Similarly, the right plot shows the efficiency as a function of the pressure ratio for lines of different corrected speeds. The dots in both figures indicate the locations of each of the three operating points on the map. For this particular design, the MDP method produced a design with lower mass flow for all speed lines and at each operating point. The efficiency characteristics of both designs are similar for all speed lines and operating points.

The second individual design comparison for the E^3 LPT is shown in Figures 68 through 70. For this set of design inputs, the flowpath geometries produced by the MDP and SPD methods are again geometrically similar as shown in Figure 68. However, in this case the MDP method has increased the mean radius of the turbine while decreasing blade height and overall length to satisfy the performance requirements and constraints. The velocity vectors are shown in Figure 69 and as was the case for example 1 are identical between the two design approaches. Finally, the performance map for the design produced by each method is shown in Figure 70. In this example, there is very little difference in the performance characteristics for the designs produced with each method. The designs produced by the MDP and SPD methods shown in this example are both valid as each satisfy the specified

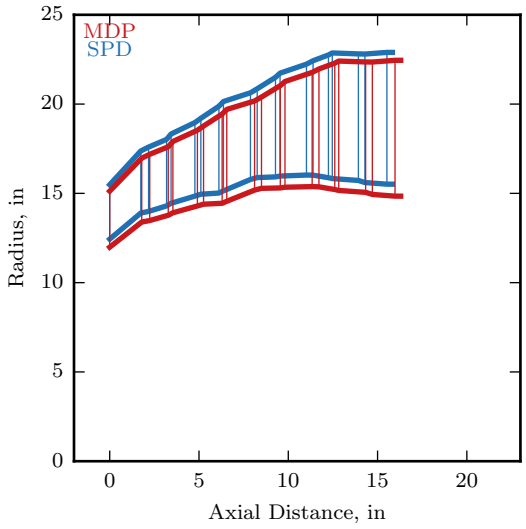

Figure 65: E^3 LPT Example 1: Flowpath Geometries for MDP and SPD Generated Designs

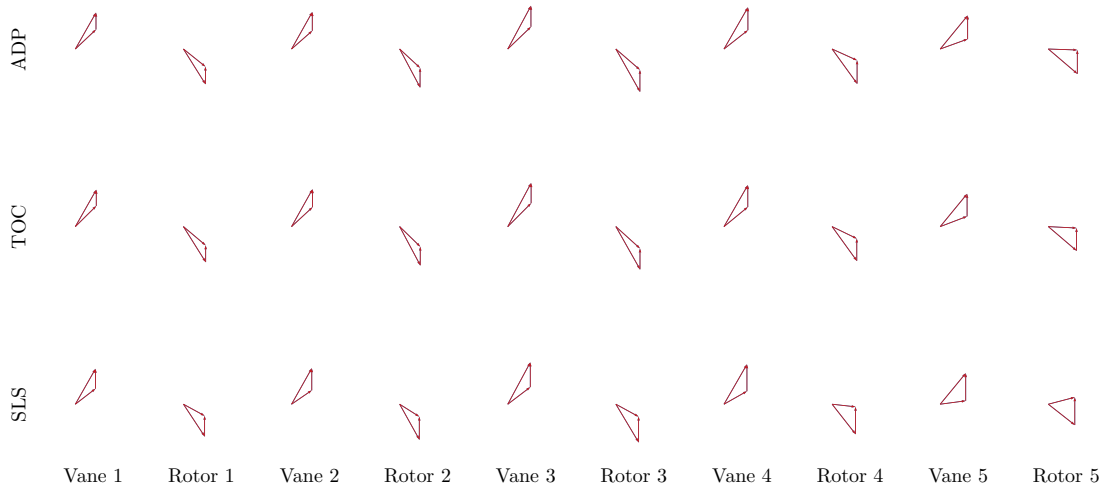

Figure 66: E^3 LPT Example 1: Velocity Vectors for MDP and SPD Generated Designs

performance requirements and constraints.

The next two individual design comparisons for this part of Experiment 2 come from the CPT design problem. The flowpath geometry for the first CPT design compared is shown in Figure 71. The flowpath geometries for the MDP and SPD produced turbines are

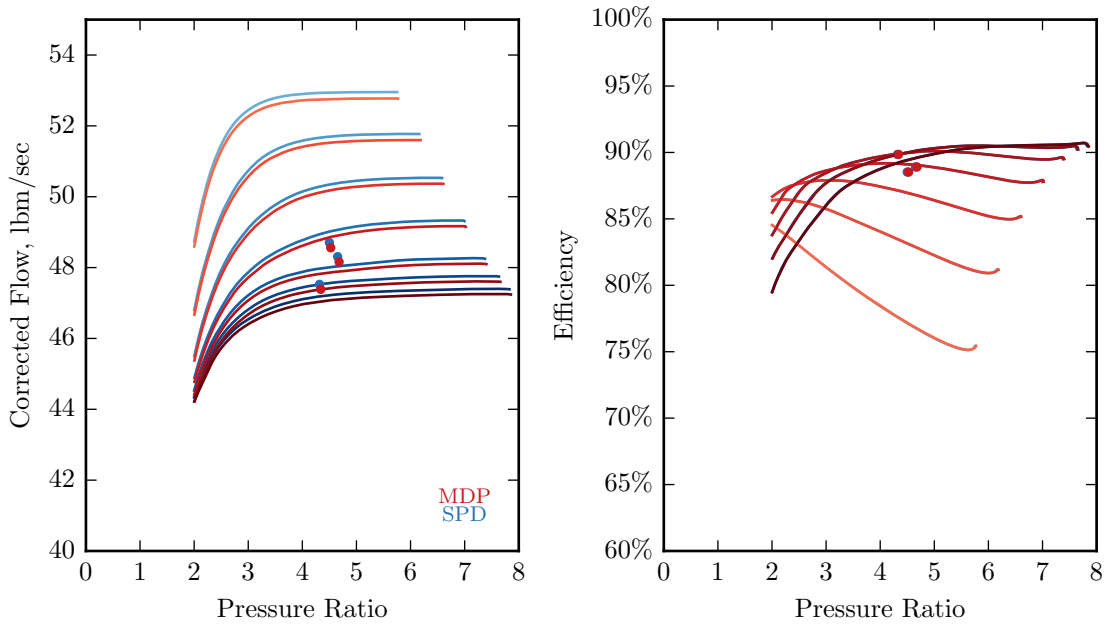

Figure 67: E^3 LPT Example 1: Performance Maps for MDP and SPD Generated Designs

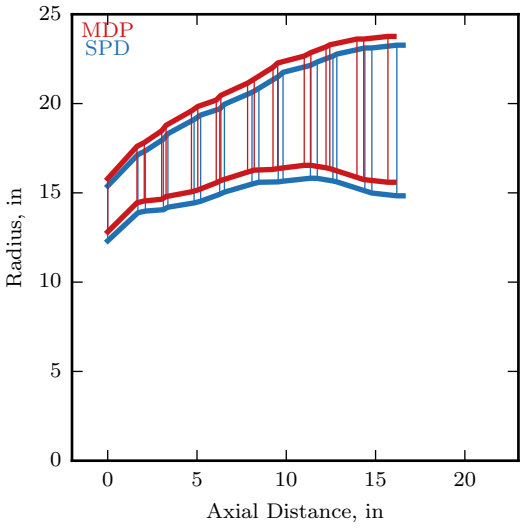

Figure 68: E^3 LPT Example 2: Flowpath Geometries for MDP and SPD Generated Designs

also very similar with only minor changes to the radial and axial dimensions. The velocity vectors at each design point for the MDP and SPD designs are shown in Figure 72 and are again identical between the methods as a result of the same design input, performance

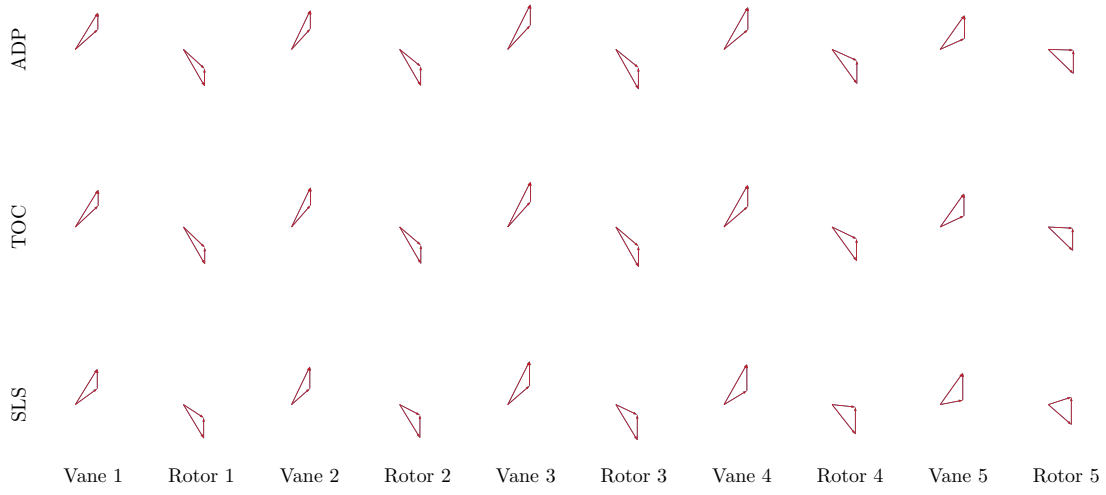

Figure 69: E^3 LPT Example 2: Velocity Vectors for MDP and SPD Generated Designs

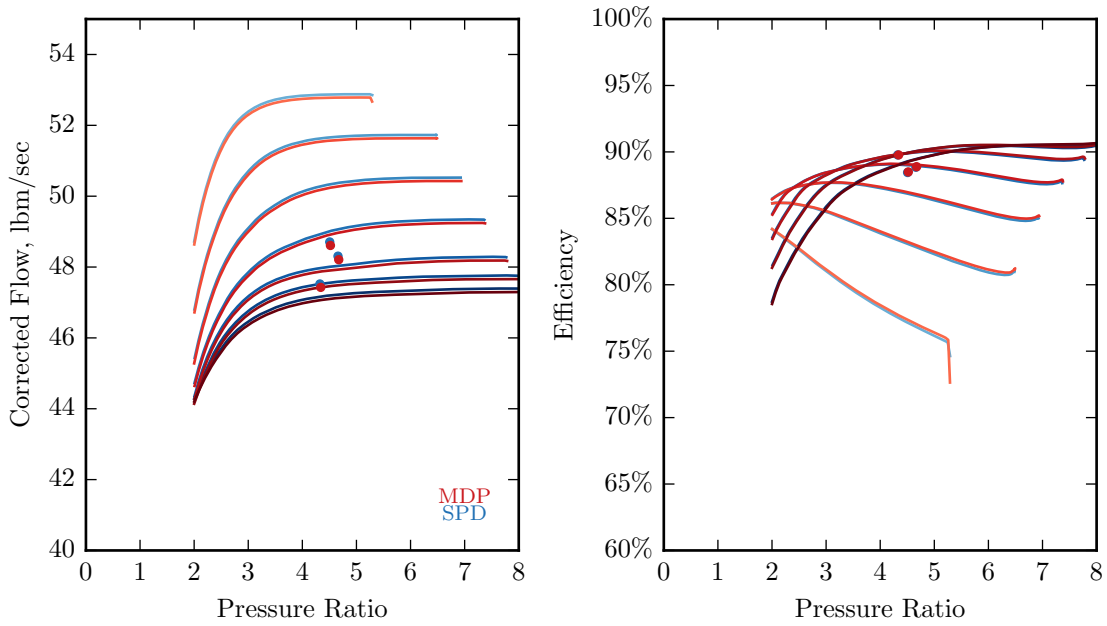

Figure 70: E^3 LPT Example 2: Performance Maps for MDP and SPD Generated Designs

requirement and constraint values. Finally, Figure 73 shows the performance map for MDP and SPD generated turbines. These two turbines generally exhibit similar performance characteristics with the higher corrected flows and lower efficiencies for the MDP speed

lines and operating points.

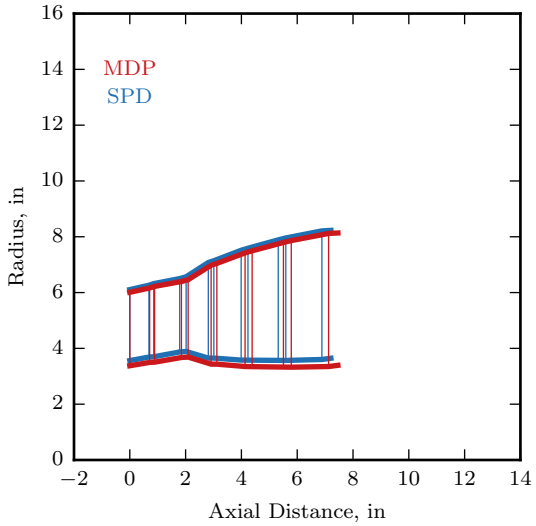

Figure 71: CPT Example 1: Flowpath Geometries for MDP and SPD Generated Designs

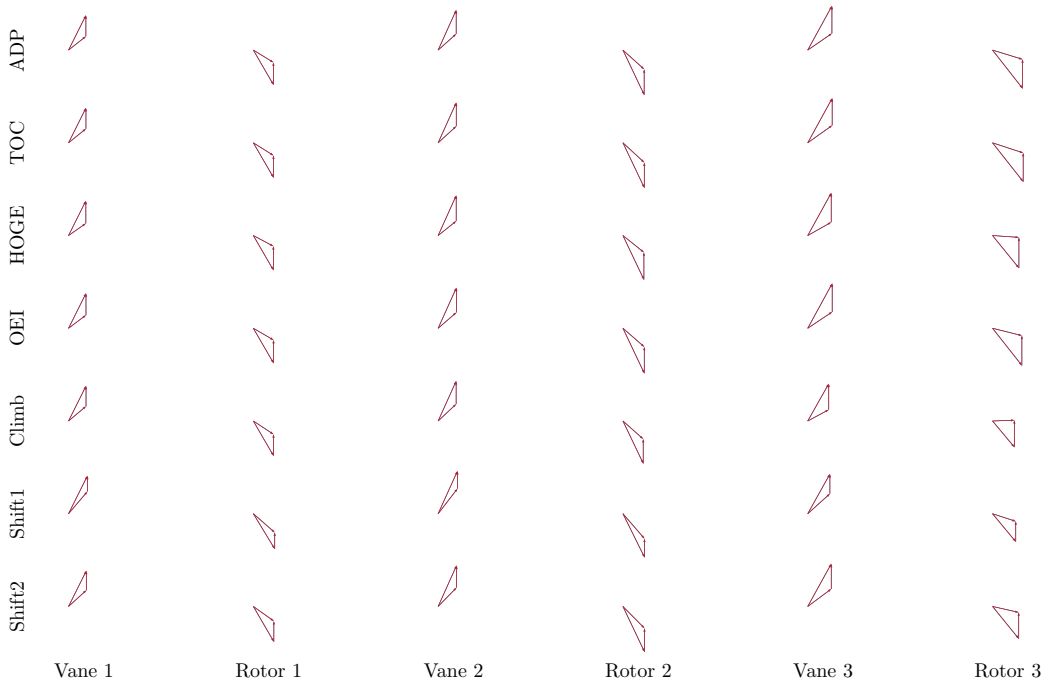

Figure 72: CPT Example 1: Velocity Vectors for MDP and SPD Generated Designs

The second comparison of CPT designs produced by the MDP and SPD methods is

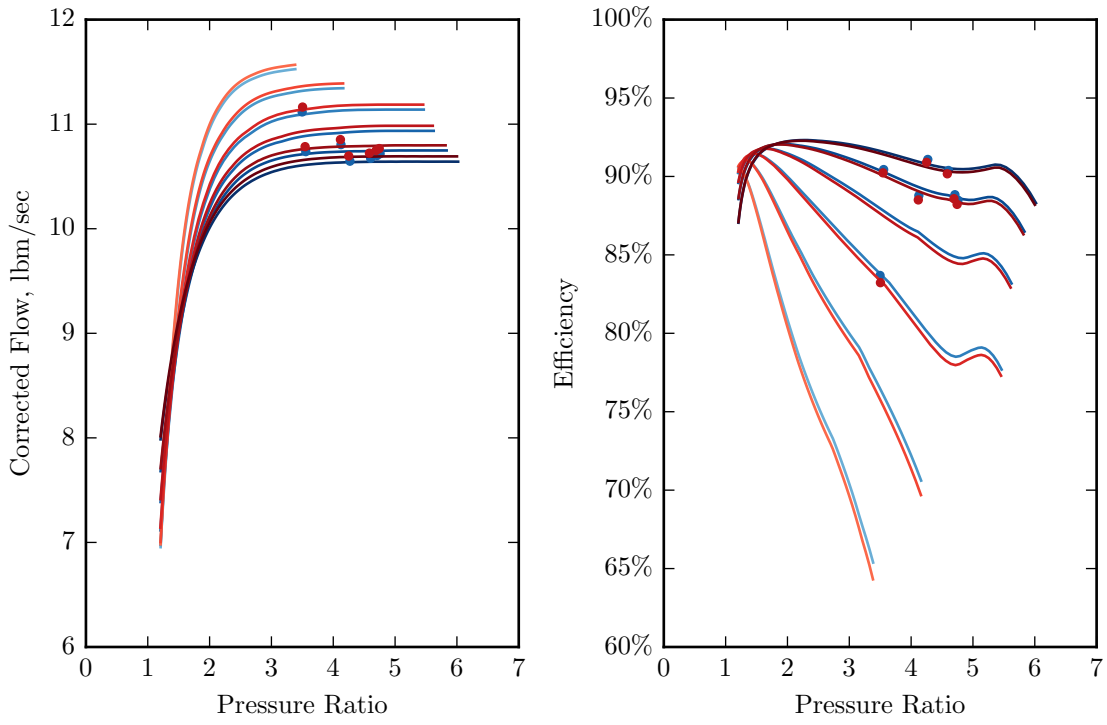

Figure 73: CPT Example 1: Performance Maps for MDP and SPD Generated Designs

shown in Figures 74 through 76. For this set of design inputs, the flowpath geometries determined by the MDP and SPD design methods are nearly identical as shown in Figure 74. Despite having the extremely similar flowpath geometries and identical velocity vectors, the performance maps produced by the MDP and SPD generated designs exhibit some differences in the corrected flows as indicated by Figure 76. Here, the corrected flow for the MDP design is lower than that of the SPD design for all speed lines and operating points.

The final two individual design comparisons selected come from the VSPT design problem. The first of these VSPT design comparisons is shown in Figures 77 through 79. In this example, the flowpath geometry is altered by the MDP method to match the performance requirements and constraints by varying the mean radius, blade heights and overall length. While the flowpath is altered by the MDP method, the velocity vectors again remain identical as shown in Figure 78. In addition, for this design the MDP and SPD methods produce similar performance maps as shown in Figure 79.

The second comparison between the MDP and SPD generated VSPT designs is presented

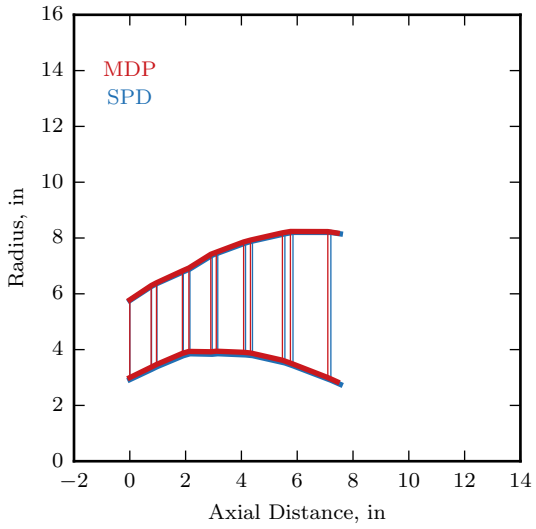

Figure 74: CPT Example 2: Flowpath Geometries for MDP and SPD Generated Designs

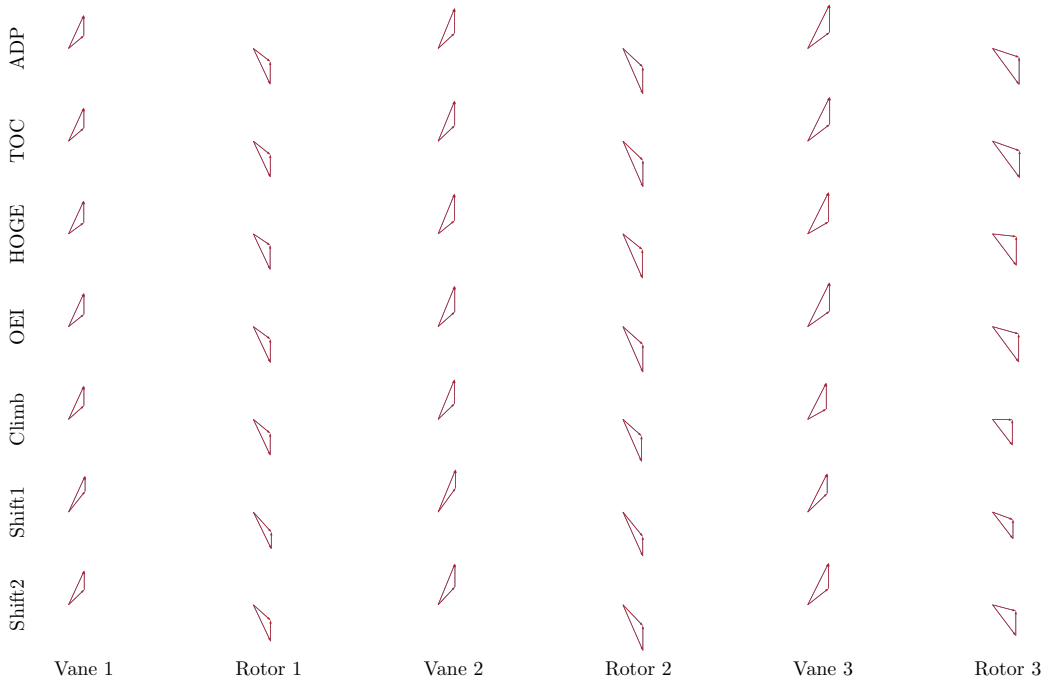

Figure 75: CPT Example 2: Velocity Vectors for MDP and SPD Generated Designs

in Figures 80 through 82. Similar to the other turbines examined in this section, the flowpath geometry is altered by the MDP method to satisfy the performance requirements and constraints. The similarity parameters used to specify the design also result in the

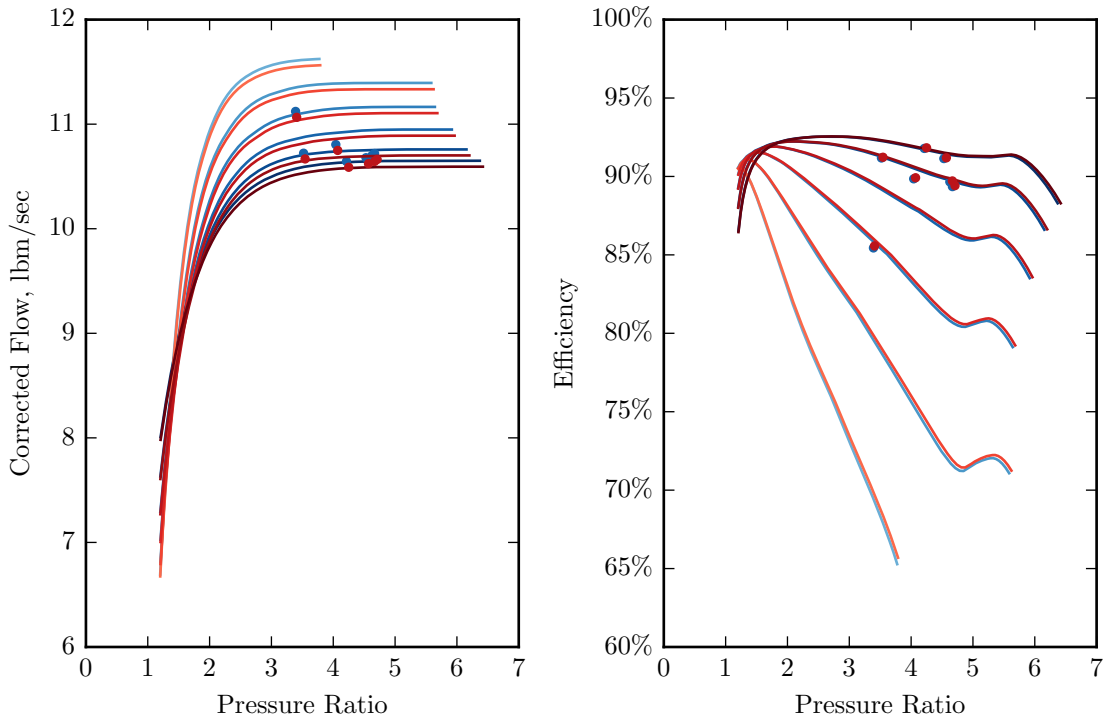

Figure 76: CPT Example 2: Performance Maps for MDP and SPD Generated Designs

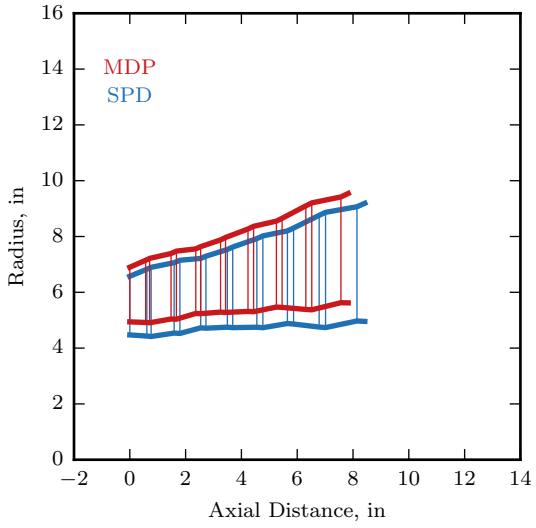

Figure 77: VSPT Example 1: Flowpath Geometries for MDP and SPD Generated Designs

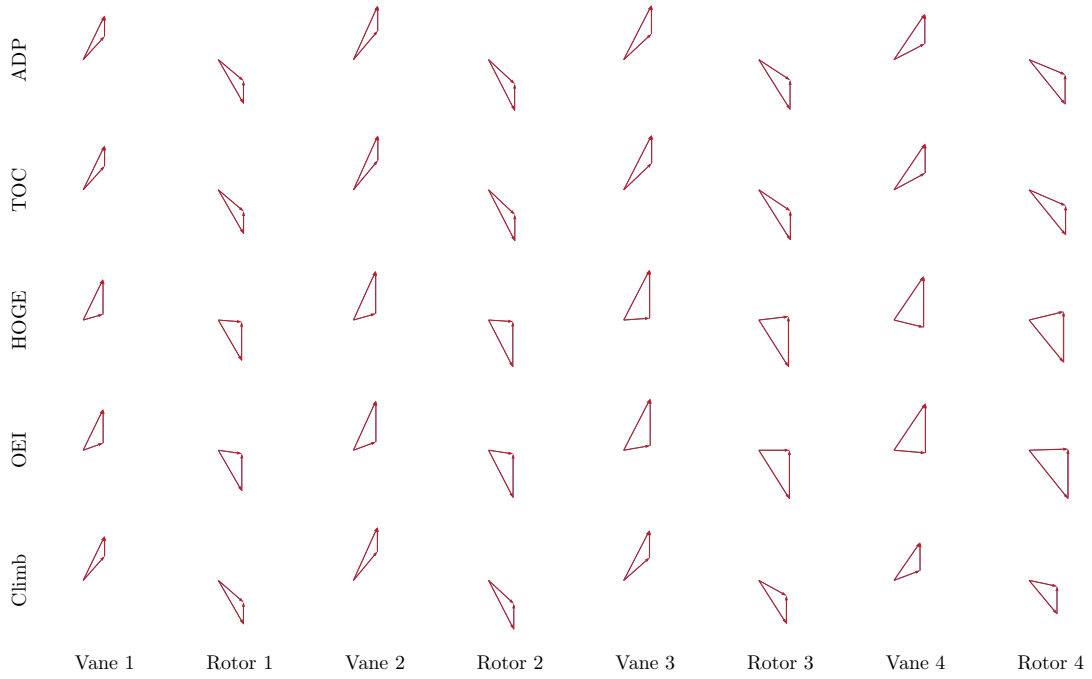

Figure 78: VSPT Example 1: Velocity Vectors for MDP and SPD Generated Designs

velocity vectors for the designs produced by each method being identical. The performance map for this example, however, shows differences between the corrected flow values for each speed line and operating condition on the map. There is a less pronounced difference between the MDP and SPD generated designs in terms of the turbine efficiency.

The six individual design comparisons presented here give a snapshot of the differences commonly observed between the MDP and SPD generated designs for the three turbine design problems. Additional individual comparisons for all three models are provided in Appendix J. Overall, the MDP and SPD methods typically generate flowpath geometries which are geometrically similar but have been scaled following the process identified in Experiment 1. The magnitude of the scaling between the MDP and SPD results depends on the performance requirements and constraints that must be satisfied in the MDP process. While the flowpath geometry produced commonly varied between the two methods, the velocity vector diagrams were identical in all cases. This similarity between the MDP and SPD velocity vectors is expected as the vectors are determined by the similarity parameter

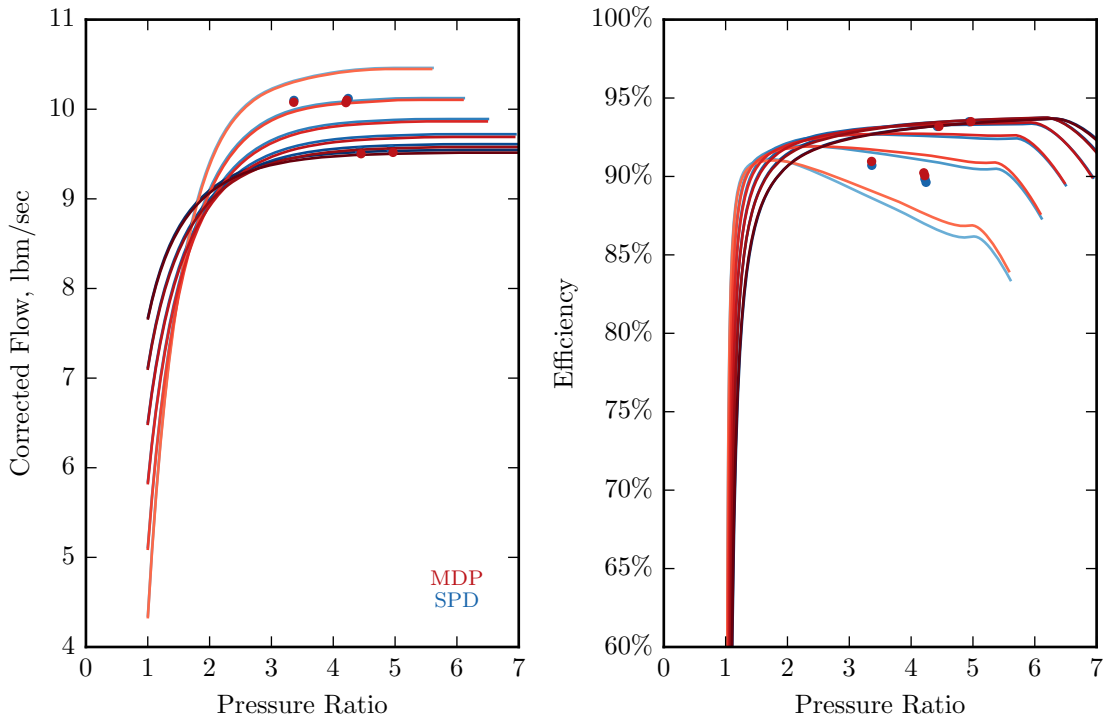

Figure 79: VSPT Example 1: Performance Maps for MDP and SPD Generated Designs

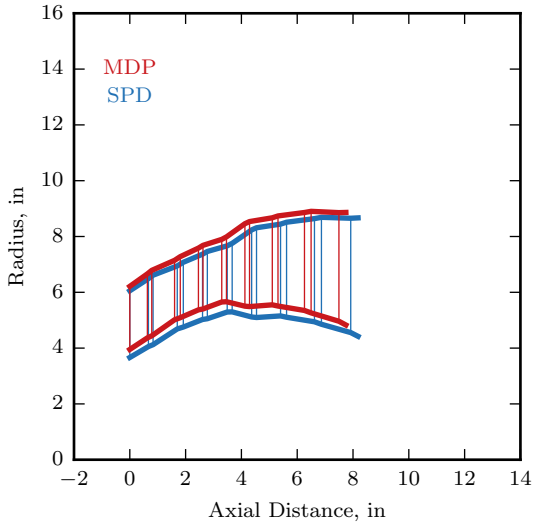

Figure 80: VSPT Example 2: Flowpath Geometries for MDP and SPD Generated Designs

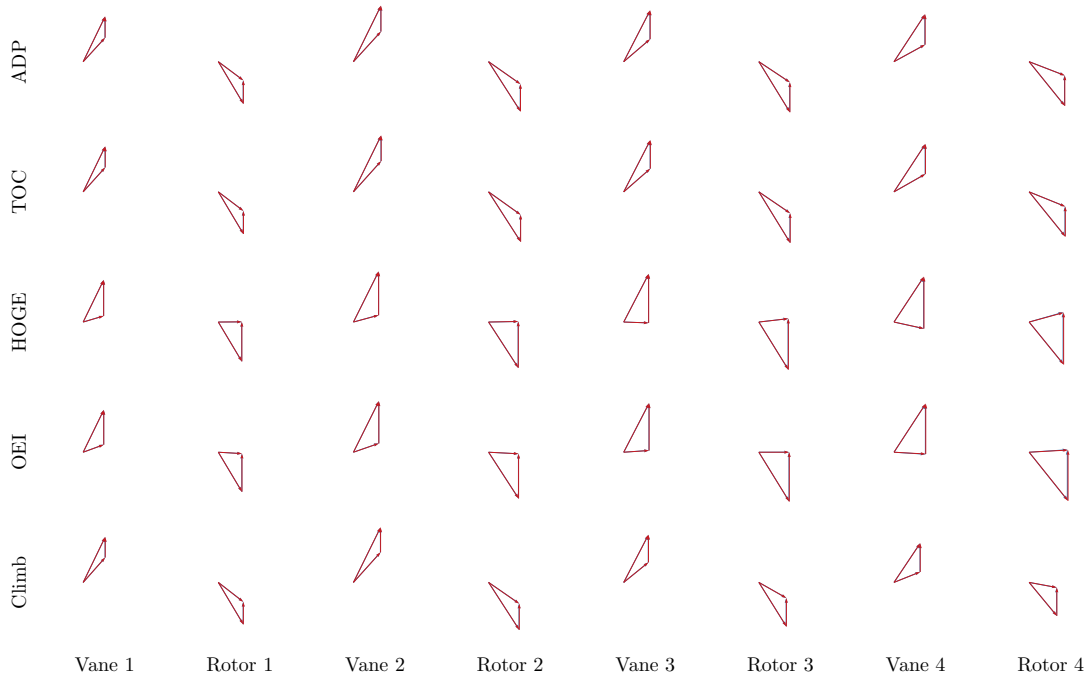

Figure 81: VSPT Example 2: Velocity Vectors for MDP and SPD Generated Designs

values input to both methods. Finally, the performance maps for designs produced by the two methods are generally similar in topology, with largest changes observed in the corrected flow values of the speed lines and operating points. Little difference is commonly observed in the efficiencies for all speed lines and operating points. The similarity in the efficiency between the two designs can be explained by examining the loss model used in these design studies. The Kacker-Okapuu loss model relies primarily on the defined turbine meanline similarity parameters as inputs to the loss prediction calculations. With these parameters remaining the same for both the MDP and SPD design process, the loss computations are not significantly effected. For this loss model, the only calculations which are effected by changes to the physical size of the machine are those related the Reynolds number and hub-to-tip ratio. These two factors have a minor effect on the overall loss calculations resulting in similar efficiencies in the designs produced by the two methods. Implementation of a different loss model which depends more heavily on dimensional geometric characteristics may result in more variation in the performance maps.

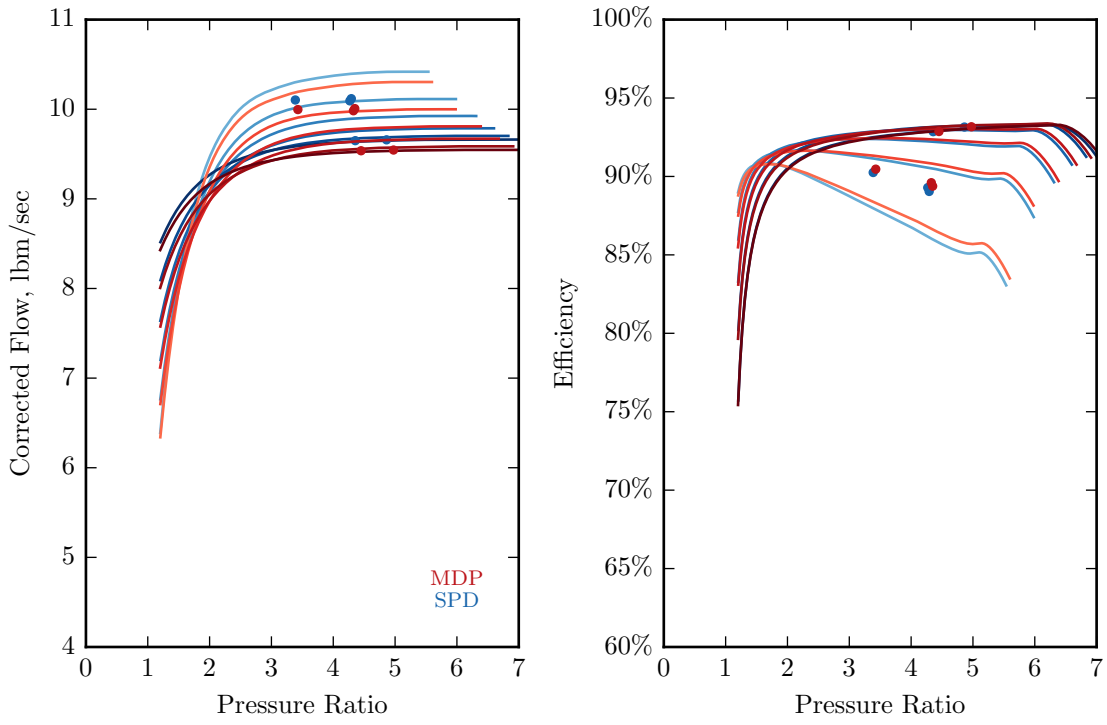

Figure 82: VSPT Example 2: Performance Maps for MDP and SPD Generated Designs

5.7 Summary

The focus of this chapter has been the development and evaluation of a turbine MDP methodology. At the beginning of the chapter, two research questions and hypotheses were presented which guided the development and evaluation process. Based on the research presented throughout this chapter, it is now prudent to return to these research questions to confirm or reject the hypotheses.

The first research question in this chapter focused on how a turbine MDP methodology could be developed from the previously formulated cycle MDP method. The hypothesis for this question state that the cycle MDP method could be adapted to the turbine by focusing on two key areas: constructing the model with an appropriate design parameterization and determining the MDP coupling equations. These two key areas were first investigated using logic and a literature review providing a theoretical basis for confirming the first hypothesis. In this development process, it was determined that a turbine model that has been specified

in terms of similarity parameters is compatible with the previously developed MDP method. The MDP method uses this design specified in terms of similarity parameters and sizes it to satisfy the performance requirements and constraints by forming design rules which couple the design points. For these design rules, adaptation of the cycle MDP method was completed by identifying classes of different independent parameters and dependent equations from the cycle MDP method which were found to produce a valid MDP setup. Potential independent parameters and dependent equations fitting into these classes were then identified for the turbine meanline design problem. With these steps addressed from a theoretical perspective, the full turbine MDP method was then developed and presented. The method consists of similar steps as the cycle MDP method with minor modifications to the details for applying each step to a turbine design problem.

To evaluate the capabilities of the developed turbine MDP method, the method was implemented on three example problems: a redesign of the E^3 LPT, the design of a CPT for the tiltrotor engine, and the design of a VPST for the tiltrotor engine. These three design problems differ in the turbine architectures, number of design points, performance requirements and constraints which will thoroughly test the MDP method. Using these design problems, Experiment 1 computationally assessed the developed turbine MDP method. Part 1 of this experiment examined the use of similarity parameters within the MDP method. Results from this part of the experiment showed that geometric similarity is maintained for the flowpath during the MDP sizing process for different values of the performance requirements and constraints. Similarity is also maintained in the velocity vectors as the performance requirements and constraints are varied. The second part of Experiment 1 evaluated the design rules which were formulated to couple the design points and ensure that all performance requirements and constraints were satisfied. For this part of the experiment all three example design problems were evaluated using a large random sample DoE. The MDP method was found to converge upon a valid solution for a high percentage of these cases across all three problems. In addition, the results show that the MDP method converges efficiently and robustly to the valid solutions.

With the results from the initial examination of the key steps as well as the computational experiments, an assessment of the first hypothesis can be made. The results presented in this chapter confirm Hypothesis 1 that the cycle MDP can be adapted to the turbine design problem by determining an appropriate model parameterization and by forming the system of nonlinear equations which couple the design points. This confirmation closes out Research Question 1 and enables further assessment of the turbine MDP method by comparing it to the SPD approach.

The second research question inquired about the differences between the MDP generated designs and the designs produced with the traditional SPD method. The hypothesis for this research question stated that the design spaces and individual designs would differ as a result of the MDP method including design rules that couple the design points. To test this hypothesis, an experiment was completed in which the three turbine design problems were evaluated over a large number of DoE cases with both methods. Examination of the DoE results from each design problem was completed by comparing the overall design space as well as individual designs produced by each method.

The first part of Experiment 2 evaluated the differences between the MDP and SPD methods by comparing the design spaces produced by the two methods. Three different techniques were used with the first one visually examining small slices of the design space using Smith plots. These plots showed that the design spaces produced by the two methods generally had similar efficiency characteristics but differed significantly in regards to how much of the design space satisfied all performance requirements and constraints. In addition to the visual comparison of slices of the design space, a numerical comparison was completed on results throughout the full, high-dimension design space. The numerical comparison confirmed the results visually observed for the small design space slices were consistent throughout the larger design spaces with minor differences to the turbine efficiencies but significantly changed the feasible boundaries. The last technique for the design space comparisons examined the changes introduced by the MDP method to the independent parameters used in the coupling equations. The independent parameter evaluations showed that changes to these parameters produced by the MDP method not only effected

their values, but also the correlation of these parameters. The changes to these correlations introduced by the MDP method depend on a number of different factors including the design input values indicating it would be difficult to determine the proper values for these parameters in the SPD approach.

The second part of Experiment 2 examined differences in the individual designs produced by the two methods. Results in this section showed that the turbine flowpath geometry was typically altered by the MDP method although geometric similarity was maintained due to the identical input values being supplied to both methods. Given the same inputs and performance requirements between the methods, the velocity vectors produced with both methods were identical. Lastly, the developed designs were further evaluated in terms of the complete turbine map. The maps generated by the two methods were again similar in terms of efficiency and corrected flow. The closeness of the efficiency predicted by the two methods results from the loss calculations relying heavily on the similarity parameter inputs with largest changes resulting from changes to the Reynolds number and Mach numbers.

By considering the results from both parts of Experiment 2 an assessment can be made of Hypothesis 2 which states that the designs and design spaces produced by the MDP and SPD methods will differ as a result of coupling equations linking the design points. The experimental results show that the design space topology in terms of performance characteristics is generally similar between the methods. However, there is significant difference between the methods in terms of feasibility as the MDP design space is completely feasible while large portions of the SPD space is infeasible. The individual design comparisons show that the differences mostly arise in the determined flowpath geometry with little difference in the velocity vectors and performance maps. These results can therefore be considered a partial confirmation of Hypothesis 2. The MDP method does change the design flowpath and feasible space as a result of the coupling equations. However, the design space topology and performance characteristics of individual designs do not change significantly between the methods. With development and assessment of the turbine MDP method completed, the next part of this thesis will focus on integrating the cycle and turbine MDP methods to form a multi-level MDP method.

CHAPTER VI

MULTI-LEVEL MULTI-DESIGN POINT METHODOLOGY DEVELOPMENT, IMPLEMENTATION AND RESULTS

The engine conceptual design process, as described in Chapter 2, considers the design of the engine thermodynamic cycle as well as the individual components. Traditionally, each of these disciplines or analysis levels is analyzed in two modes, on-design and off-design, to assess the performance characteristics of the selected design. The cycle MDP method defined by Schutte and the turbine MDP method developed in the previous chapter provide a means for assuring all designs developed in the cycle and turbine component steps satisfy the requirements and constraints imposed at a number of operating points. These methods therefore eliminate the need to complete the off-design analysis as part of the overall design process. However, reexamining Figure 32 shows there is one additional iterative loop which ensures the engine cycle and turbine design and performance characteristics match. Converging this iterative loop requires appropriately modifying both the cycle and turbine designs. The presence of requirements and constraints at multiple operating conditions within each level further complicates the modification of these designs to achieve convergence. This challenging convergence process was therefore the motivation for the third research question which is restated below.

Research Question 3: How can the on-design MDP methods for designing the turbine and cycle be merged together to simultaneously generate designs for the both turbine and engine that meet requirements and constraints at multiple operating points?

This question examines the means by which the cycle and turbine MDP analysis can be integrated together to form a multi-level MDP method. Development of such a method in Research Question 3 should eliminate the computationally expensive, manual cross-level convergence loop from the overall engine conceptual design process. Assuming a multi-level

MDP method can be successfully developed, the last research question explored in this thesis examines the differences in the cycle and turbine designs generated using the new method compared to a more traditional approach of evaluating each analysis level independently.

Research Question 4: What are the differences in the turbine and engine designs and performance characteristics as a result of using the simultaneous MLMDP method versus solving the MDPs at each level individually?

The remainder of this chapter focuses on answering these two research questions. First, an examination of existing methods for integrating the analysis levels is completed in Section 6.1. This examination specifically focuses on the capabilities of the existing approaches when MDP methods are applied within the individual analysis levels. Following this assessment, a hypothesis is formed for each of the research questions based on the observations made during the examination of the existing integration approaches. Next, from these hypotheses a new multi-level MDP specific integration approach is formulated and tested on a proof-of-concept problem in Section 6.3. Following this development and assessment of key integration elements, Section 6.4 presents the complete MLMDP method and procedure. This MLMDP method is then implemented on three example design problems covering a range of design requirements, constraints and system architectures is described. Finally, two computational experiments are completed in Section 6.6 using these design problems to test the two hypotheses stated above.

6.1 Current Integration Approach Examination

Answering Research Question 3 began by first examining previously developed approaches for integrating different analysis methods within the overall analysis of a gas turbine engine. Integrating different analysis techniques with different fidelity levels in the analysis of gas turbines is commonly referred to as zooming as described in Section 3.2. From the review completed in that section, two different approaches where identified which are potentially applicable to the integration of cycle analysis and turbomachinery meanline analysis: the

decoupled and partially integrated methods. The fully integrated approach was not selected for assessment as it is impractical in most situations to directly replace the component calculations in the cycle analysis with a separate component analysis code. Therefore, the focus of this assessment was the decoupled and partially integrated methods.

The decoupled integration approach was briefly summarized in Section 3.2 but is reviewed in more detail here. A schematic of the steps in the method are shown in Figure 83. The method begins by completing cycle analysis with an input turbine performance map. The source of this map is left up to the analyst with a representative reference map typically chosen. Using this map, the cycle on-design and off-design analyses are completed to assess the performance of the selected engine design over the entire operating envelope. From these results, the expected operating ranges and performance requirements of the turbine component can be determined. The operating ranges along with turbine design inputs are then used to complete both the on- and off-design meanline turbine analyses. The result of the turbine off-design analysis is the generation of a new turbine performance map that covers the expected turbine operating range. This improved performance map is then fed into a second execution of the on-design and off-design cycle analysis. The decoupled approach ends after this execution of the cycle analysis without further iteration with the turbine meanline analysis.

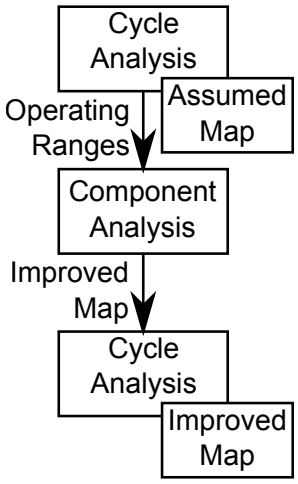

Figure 83: Decoupled Integration of Analysis Levels

The partially integrated approach was also summarized in Section 3.2 with a visual depiction of the process shown in Figure 84. The partially integrated method is generally similar to the decoupled approach. It starts with the on-design and off-design analysis of the engine cycle which supplies the operating ranges to the turbine meanline analysis. The on-design and off-design turbine meanline analysis is then executed to generate an improved turbine performance map which is passed back to the cycle. Instead of stopping after the second execution of the cycle analysis with this improved map, the partially integrated approach continues to alternate executing the cycle and turbine meanline analysis. This iteration between the analysis levels continues for a set number of analysis passes or until the turbine operating ranges, performance requirements and performance maps reach a stable, converged state. Overall, the partially integrated and decoupled methods are similar with the partially integrated approach attempting to more tightly converge the analysis levels.

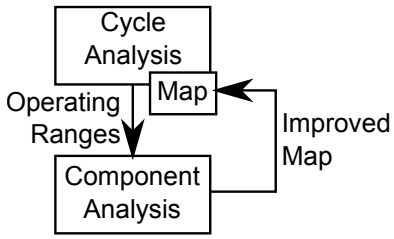

Figure 84: Partial Integration of Analysis Levels

The development process for the decoupled and partially integrated approaches focused on coupling analysis levels that each use traditional single point sizing process. Off-design analysis therefore also had to be completed at each level to ensure the design satisfied all performance requirements and constraints. In addition, the off-design analysis is used to generate the operating ranges and performance characteristics (in the form of a performance map) which must be passed to the other analysis level. Given the development of the cycle and turbine MDP methods using the traditional single point design method coupled with off-design analysis, the question then becomes how do these MDP methods for the individual analysis levels fit into the different integration approaches?

The MDP methods previously developed for each analysis level are formulated to improve the on-design phase of the design process and eliminate the iterations between the on-design and off-design phases to assure that the requirements and constraints at that level are satisfied. As a result, the following observation can be made regarding the use of MDP methods within an integrated analysis process considering more than one analysis level:

Observation: The decoupled and partially integrated approaches can be used to integrate analysis levels in which MDP methods are applied to the on-design phase provided off-design analysis is also completed at each level to generate the data (operating ranges, performance requirements and performance maps) which must be passed between the levels.

To assess capabilities and performance of the decoupled and partially integrated methods when applied with MDP analysis levels, an assessment was completed using the VSPT turbine design problem coupled to a turboshaft engine. For this assessment, the on-design MDP method was applied at each level to ensure that all performance requirements and constraints at that level were satisfied. Once the on-design performance was completed, the off-design analysis phase was performed to generate the data required to be passed to the other analysis level. This process was repeated at each analysis level and several iterations were run according to the previously described decoupled and partially integrated methods. Throughout this section, the decoupled MDP and partially integrated MDP will be referred to as the DCMDP and PIMDP methods, respectively.

To evaluate the DCMDP and PIMDP methods, the same design inputs for the VSPT problem were evaluated by each approach. Figure 85 shows the cycle and turbine design and performance characteristics across five different design points identified for turboshaft engine and turbine. The charts in the left column show the cycle design and performance characteristics of effective power specific fuel consumption, combustor exit temperature and total mass flow rate. These cycle results are nearly identical for the two methods showing that when only considering the cycle performance, the two methods are generally equivalent. However, the turbine design and performance characteristics shown in the right column of Figure 85 differ more substantially. Here, the decoupled method has only executed a single

pass of the turbine analysis level and therefore does not capture changes to the turbine design as a result of the updated operating conditions from the cycle analysis. For the turbine efficiency and flow, the difference between the integration approaches is approximately constant across all the operating points evaluated. This difference can therefore easily be overcome by the application of scalars to the efficiency and flow characteristics of the turbine map. The differences in the turbine pressure ratio between the methods however is not a simple scaling as trend across design points is different between the methods as operating conditions move the design points on the map. This result shows the benefit of completing additional iterations between the analysis levels in the partially integrated approach compared to the decoupled approach.

In addition to looking at these design and performance metrics at each design point, the final turbine performance map and annulus geometry were also generated. The performance maps shown in Figure 86 again display similar performance characteristic trends as a result of the same design inputs being used by both methods. The efficiency contours are almost identical while the corrected flow and pressure ratio values differ more substantially. The differences in the corrected flow and pressure ratio are also a result of the decoupled approach only evaluating the turbine design a single time. Given the similar trends however, it is clear that the map produced in the decoupled approach could be scaled in the second execution of the cycle analysis to generate cycle performance characteristics similar to the partially integrated approach.

The turbine annulus geometries produced by the two methods are shown in Figure 87. These annuli are geometrically similar owing to the same design inputs being used for both methods. The differences result from changes to the operating conditions in the partially integrated approach resulting from additional iterations between the cycle and turbine analyses. Again here, one can see that the DCMDP geometry could be sized or scaled to match eventual design produced by the PIMDP method.

Overall, the assessment of the DCMDP and PIMDP methods showed that the methods produce similar results. These similar results are expected as both methods are integrating the same analyses which are evaluating the same design inputs. While the design and

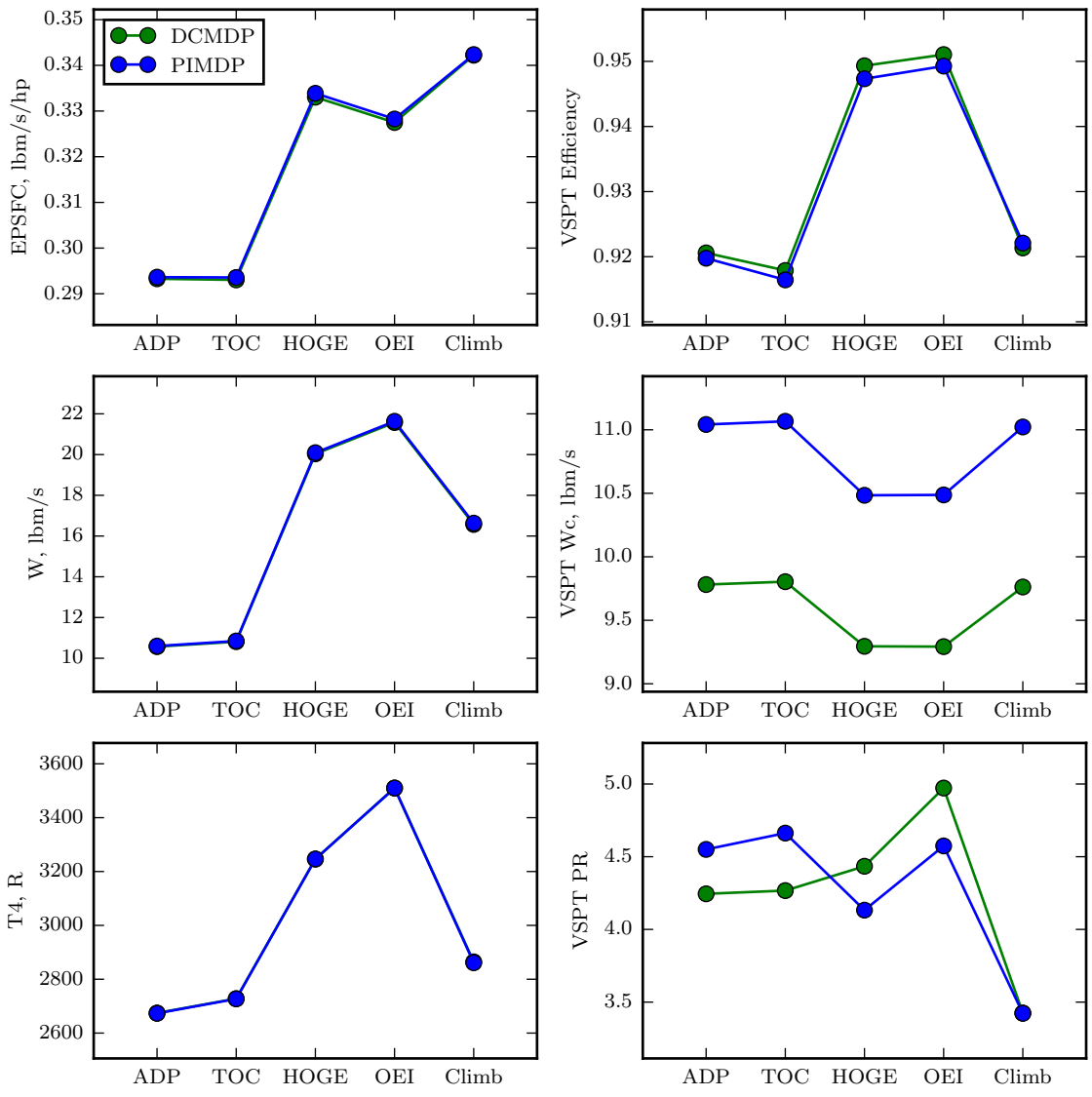

Figure 85: DCMDP and PIMDP Predicted Performance Characteristics at Each Design Point

performance results that are produced are similar, the methods differ in their convergence characteristics and computational cost. For the DCMDP method, convergence between the analyses is not a primary driver as the method limits the number of executions of each analysis level. The PIMDP method attempts to achieve tighter convergence between the levels by completing additional iterations. To measure the convergence between the levels in the PIMDP method, the error between a number of values at each analysis level were evaluated. For this analysis, these values included the turbine corrected flow and efficiency

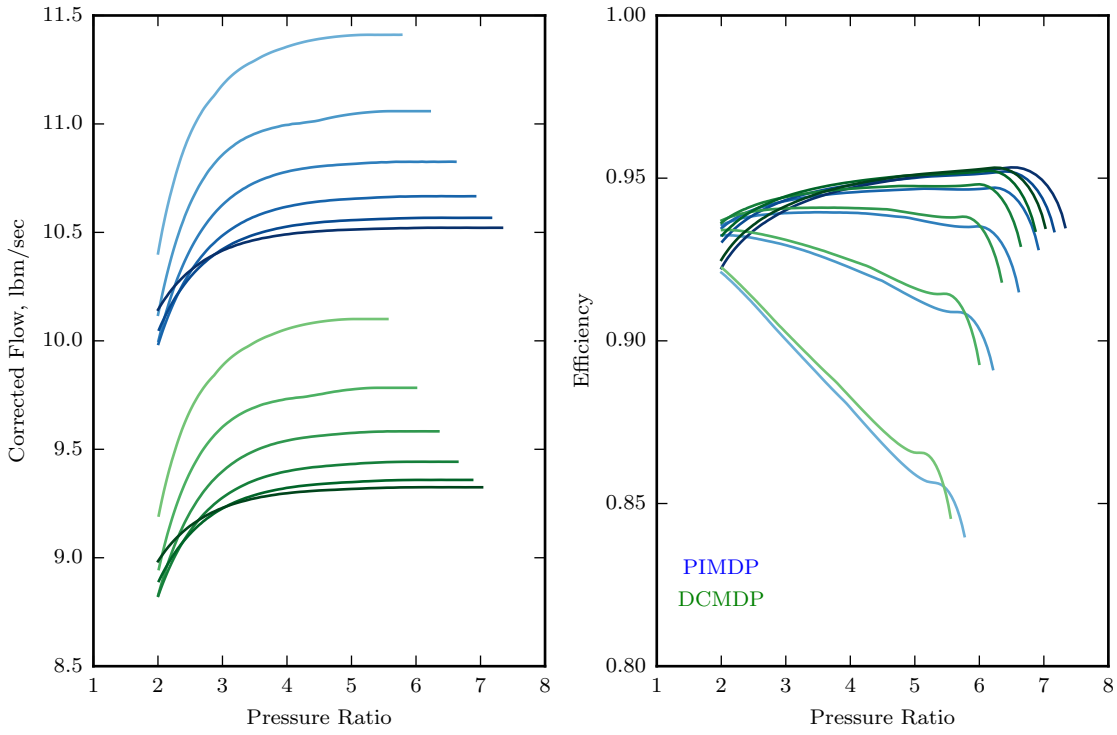

Figure 86: Turbine Performance Maps Produced by the DCMDP and PIMDP Approaches

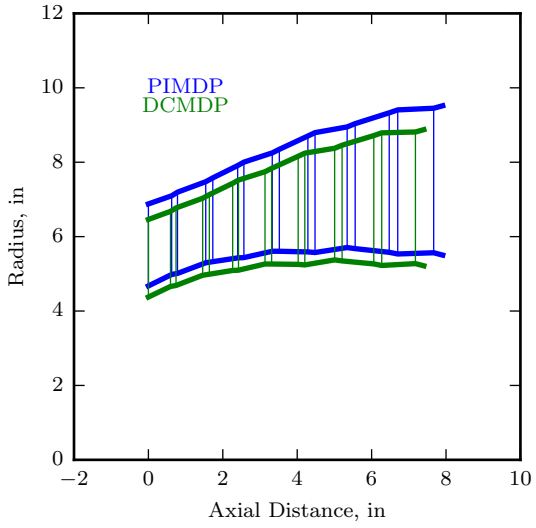

Figure 87: Turbine Flowpath Geometry Produced by the DCMDP and PIMDP Approaches

at each design point used in the models at both levels. In this analysis, the turbine power was specified at each design point for both levels making the error between the levels zero. Differences in the turbine pressure ratios between the levels were also not considered as the pressure ratio error is captured by the error in the efficiency and correct flow when the power output is known. This relationship is between the power, flow, efficiency and pressure ratio is expressed by Equations 63 and 64 below. In these equations, the ideal change in total enthalpy is a complex function of the change in total pressure across the turbine. While a complex function was used throughout this research, a simplified relationship for ideal total enthalpy and pressure ratio can be defined as in Equation 65 for the assumption of a calorically perfect gas.

$$\dot{W} = \dot{m} * \eta * \Delta h_{t,ideal} \tag{63}$$

$$\Delta h_{t,ideal} = f(PR) \tag{64}$$

$$\Delta h_{t,ideal} = C_P(T_{t,in} - T_{t,out,ideal}) = C_P \left(1 - \left(\frac{1}{PR}\right)^{\frac{\gamma-1}{\gamma}}\right) \tag{65}$$

To evaluate the PIMDP method, the error in efficiency and corrected flow at each design point were tracked for eight iterations of the integrated analysis. The root-mean-square of this error for each iteration is plotted in Figure 88. The PIMDP method reduces the error in these values significantly over the first few iterations as the operating ranges and performance maps at the respective levels are updated However, after iteration three the convergence stalls with no additional progress made in reducing the corrected flow and efficiency errors over the remaining iterations. As a result, tight convergence was not achieved between the analysis levels with some errors in the corrected flow values between the levels being as large as 0.165 pounds mass per second, or approximately 1.5% of the corrected flow at that operating condition.

Based on the assessment of the DCMDP and PIMDP integration approaches completed in this section, the following observation was made:

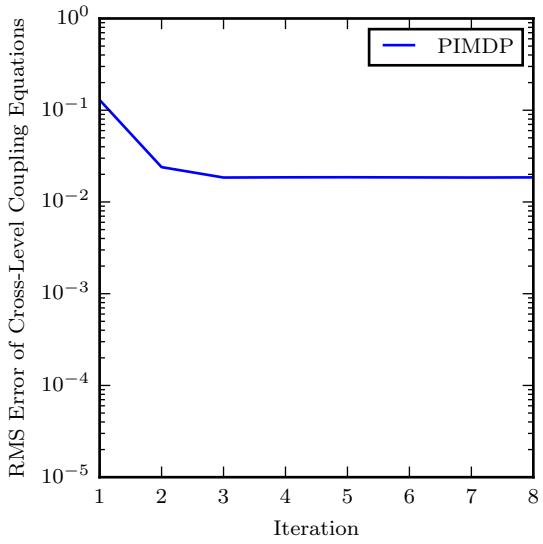

Figure 88: Convergence Characteristics of the PIMDP Approach

Observation: The decoupled and partially integrated MDP approaches produce nearly identical designs at the cycle level with similar designs produced by the turbine analysis, however neither method achieves tight convergence on the turbine operating conditions and performance metrics at all critical operating conditions across the levels.

In addition, the decoupled and partially integrated methods do not allow for a truly simultaneous process as both on-design and off-design analysis phases must be completed at each level. As a consequence of these issues, the existing integration approaches were deemed unsatisfactory for simultaneously developing cycle and turbine meanline designs that satisfy all design requirements and constraints. However, the analysis and observations made in this examination led to the formulation of a hypothesis for Research Question 3 related to an alternate approach for integrating the analysis levels when MDP methods are applied at each level. This hypothesis and the hypothesis for Research Question 4 are presented in the next section.

6.2 MLMDP Hypotheses

At the beginning of this chapter, two research questions were posed to guide the development and assessment of a multi-level MDP methodology. Addressing these questions started

by completing a more detailed examination of existing approaches for integrating cycle and turbine analysis when requirements and constraints are present at multiple operating conditions for each level. Based on the results of this assessment, hypotheses can now be stated for each of these questions.

First, the assessment of the existing integration approaches in the previous section identified several key characteristics of these integration approaches. These characteristics included the definition of a converged state, what information is passed between the analysis levels, and how that information is passed. The review of these integration approaches also identified several weaknesses for the application to MDP problems therefore supporting the development of a new multi-level MDP methodology. The hypothesis for this question supposes that a system of cross-level coupling equations directly linking the design points at each level can be added to the cycle and turbine MDP coupling equations to ensure that all requirements and constraints are simultaneously satisfied at each level.

Hypothesis 3: A method will simultaneously satisfy the requirements and constraints at multiple operating points for both the on-design cycle and turbine analyses by constructing a single system of nonlinear equations consisting of the cycle MDP equations, turbine MDP equations, and cross-level coupling equations

Assuming a viable MLMDP method can be developed in support of Research Question and Hypothesis 3, a second research question related to the designs generated by the MLMDP method was also posed. This question specifically investigates the differences in the designs produced by the MLMDP method in comparison to a traditional approach. The traditional engine design process treats the cycle and turbine analyses as separate process that are typically considered isolated steps in the overall process. As indicated by the question, comparing the results from this traditional process to the multi-level MDP method results can be completed by analyzing the differences in the cycle and turbine designs and performance characteristics. The hypothesis for this question states that the cycle and turbine design and performance characteristics will differ as a result of the cross-level coupling equations which couple the design points at each level.

Hypothesis 4: The MLMDP generated engine and turbine designs will differ in geometry and performance characteristics from those generated with the individual MDP approaches as a result of the additional cross-level coupling equations included in the multi-level method

Evaluation of these two hypotheses will be completed throughout the remained of this chapter. First, the Hypothesis 3 will be considered from a theoretical perspective to formulate a new MDP specific integration approach. Following this theoretical examination, key elements of the MDP specific integration will be tested on a proof-of-concept problem. With a successful proof-of-concept completed, the MLMDP procedure is formally defined and implemented on three example design problems Finally, computational experiments will be completed with these models to fully evaluate Hypotheses 3 and 4.

6.3 MLMDP Methodology Development

The first research question related to the MLMDP method (Research Question 3) inquires about how to integrate the cycle and turbine MDPs in order to simultaneously develop designs at both levels that satisfy all requirements and constraints. Hypotheses 3, stated in the previous section, proposed the development of a system of cross-level coupling equations to supplement the cycle and turbine MDP coupling equations. This new approach was proposed after evaluation of existing integration approaches in Section 6.1. This section focuses on the development of this new integration approach specifically for the use of MDP methods at each level. First, the new approach is formulated with details of the cross-level coupling equations identified. Following the formulation of this approach, a assessment was completed to compare the new integration method to the current approaches on the same problem used in Section 6.1. The formulation and initial assessment of the multi-level MDP coupling approach in described in the ensuing sections ultimately leading to the formal description of the Multi-Level MDP method in Section 6.4.

6.3.1 Formulation of an MDP Specific Multi-Level Coupling Approach

To address the limitations of the previously developed decoupled and partially integrated approaches when applied with MDP analyses at each level, a new MDP specific multi-level coupling approach was formulated. There were two primary goals for this method formulation. The first goal was to develop a method for coupling of the MDP analysis levels which would enable tighter convergence of the operating conditions and performance characteristics at the different design points evaluated at each level. The second goal was to formulate a process that would simultaneously satisfy the performance requirements and constraints at both levels as well as the cross-level coupling. Specifically, this second goal aims to eliminate the separate off-design execution within the level which is required to generate the operating ranges and performance map. These two goals were addressed by first examining the details of the coupling present in the decoupled and partially integrated approaches then combining that knowledge with the structure of the MDP analyses at each level.

Formulation of the MDP specific integration approach started with a review of the coupling between the analysis levels present in the decoupled and partially integrated methods. Specifically, the focus of this review was to identify the details of the parameters which are shared and ultimately must match across the analysis levels. In both the decoupled and partially integrated methods, the final product of the cycle analysis is a set of turbine operating ranges which will be used by the ensuing turbine analysis. The operating ranges generated are typically defined in terms of turbine inlet total pressures, total temperatures, mass flow rates, and fuel-to-air ratios throughout the cycle's operating envelope. For the turbine analysis, the final output is typically a turbine performance map which covers those cycle defined operating ranges. As described in Chapter 2, this turbine performance map defines the physical relationships between the turbine corrected flow, shaft speed, pressure ratio and efficiency for the specified turbine design. The identification of these specific parameters which comprise the general operating ranges and performance maps is an important first step in formulating the new multi-level MDP integration approach.

With the details of the cross-level coupling examined, the next part of formulating the

multi-level MDP integration approach was to examine the differences in the structure of the analysis when using an MDP at each level. In the original formulation of the decoupled and partially integrated methods, the methods use a single design point on-design phase followed by an off-design phase at each level to generate the required data for the ensuing analysis level. When the MDP on-design analysis was added to each level as shown in the previous section, the DCMDP and PIMDP methods still completed both the on-design and off-design analyses as shown in Figure 89. The only change from the original implementation was the conversion of the on-design phase from a single point methodology to the MDP methodology. As a result, there is still a need to generate the operating range or performance map to pass between the levels. The presence of this off-design phase requires additional executions of the models at each level to generate these results and prevents the methods from simultaneously developing designs at both levels that satisfy all requirements and constraints while also converging the two levels.

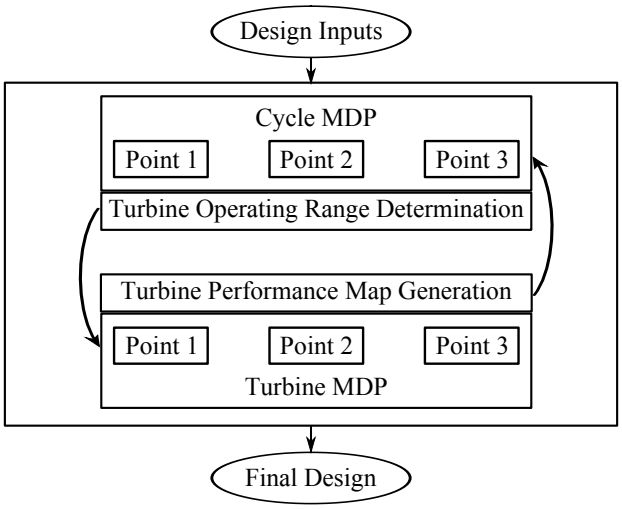

Figure 89: Partial Integration Approach with MDP Analyses

In this setup, the off-design analysis at each level serves as an important intermediary step for the analysis levels to communicate with each other. While these off-design analyses are necessary in this analysis setup, focusing on only the on-design MDP portions allows the following observation to be made:

Observation: The MDP methods applied at each analysis level only require the turbine operating conditions and performance characteristics at a limited number of design points at each level.

This observation is important as it means that most of the operating ranges and performance map ranges that were evaluated in the off-design phase are irrelevant for the ensuing MDP analysis at the other level. As a result, the following question is raised: can the design points at each level be directly coupled to each other with operating condition and performance information? A method which couples the individual design points would eliminate the intermediary off-design analysis and potentially allow for a simultaneous solution of both levels. The resulting method would therefore have a structure such as that shown in Figure 90 for three design points at each analysis level. If the design points used at both analysis levels correspond to the same overall operating conditions, the design points can be directly coupled with only the operating conditions and performance characteristics specific to that point being passed. These coupling parameters are those identified in the detailed review of the cross-level coupling earlier in this section.

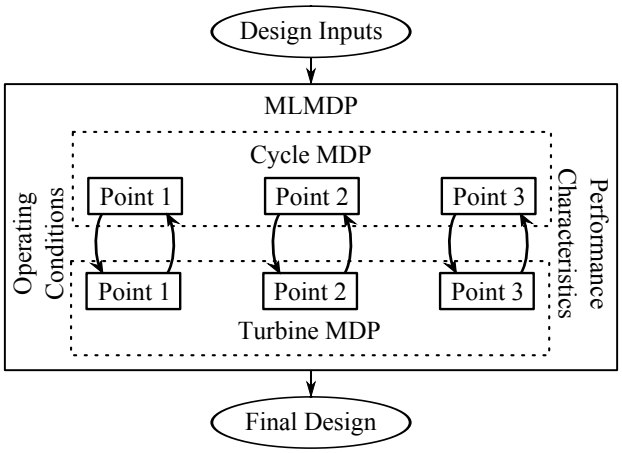

Figure 90: Multi-Level Integration of MDP Analyses

Formulating a multi-level MDP (MLMDP) method in this way eliminates the expensive and unnecessary off-design analysis which was previously required at each level. In addition, this solution allows for a simultaneous solution approach to be developed. The previously

developed cycle and turbine MDP methods each form a system of nonlinear equations which couple the design points within those analysis levels. As proposed in Hypothesis 3, an additional set of nonlinear equations can now be defined which couple the design points at each level. The aim of these cross-level coupling equations is to ensure that the turbine operating conditions and performance characteristics at the corresponding design points at each level match. Given this objective for the cross-level coupling equations and the identified coupling parameters from earlier in this section, typical equations for each design point pair (cycle and turbine design point at the same operating conditions) are anticipated to be those defined in Equations 66 to 72. These cross-level coupling equations connecting design points at each level provide a mechanism for converging on a design that simultaneously satisfies all requirements and constraints at each level and ensures the turbine performance at each level matches.

$$P_{t,in,cycle} = P_{t,in,meanline} \tag{66}$$

$$T_{t,in,cycle} = T_{t,in,meanline} \tag{67}$$

$$FAR_{in,cycle} = FAR_{in,meanline} \tag{68}$$

$$\dot{m}_{in,cycle} = \dot{m}_{in,meanline} \tag{69}$$

$$N_{cycle} = N_{meanline} \tag{70}$$

$$\dot{W}_{cycle} = \dot{W}_{meanline} \tag{71}$$

$$\eta_{cycle} = \eta_{meanline} \tag{72}$$

Up to this point, the formulation of the MLMDP method has focused on developing the analysis structure and cross-level coupling equations. During this formulation, it was initially assumed that corresponding design points at the same operating conditions were added at level. The last remaining element of the method formulation is to determine the process for identifying and selecting the design points included in the analysis. For the cycle and turbine MDP analyses, the required design points are determined by the operating conditions where performance requirements and constraints are present. To assure that all

the requirements and constraints at each level are satisfied, the MLMDP method needs to include all of these design points at each level at a minimum. It is likely that many of these design points at each level will occur at the same operating points allowing these points to be coupled. However, there may be some design points identified in the cycle or turbine MDP analysis for which a corresponding design point in the other analysis level was not identified. In this scenario, an additional design point must be added in the other level. This design point will not have a requirements or constraints that directly affect the sizing at that level, but will serve to determine either the operating condition parameters or performance parameters needed by the corresponding design point in the other level.

For example, the notional model in Figure 91 shows that three design points were identified for both the cycle MDP and turbine MDP. Here, the first and second design point identified at each level occur at the same operating conditions, respectively, allowing these design points to be directly coupled. However, the last design point required at each level do not have the same operating conditions. As a result, an additional design point is added at each level as indicated by the design point boxes with dashed lines to provide either the turbine operating conditions or performance characteristics. With this setup, there will be a total of four design points evaluated at each analysis level.

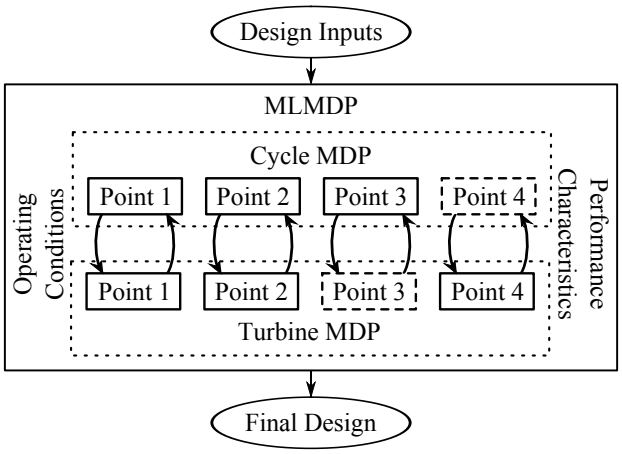

Figure 91: Multi-Level MDP Setup with Non-Corresponding Design Points.

The identification of the design points along with the coupling equations and model

structure completes the initial formulation of the new MLMDP method. The next section assesses this formulated MLMDP method and compares the results to the previously examined decoupled and partially integrated MDP approaches.

6.3.2 Assessment of the MDP Specific Multi-Level Coupling Approach

The formulation of the MLMDP method described in the previous section proposed an approach for simultaneously developing cycle and turbine designs which consider requirements and constraints at multiple operating points. This formulation focused on addressing limitations of the decoupled and partially integrated approaches which were not capable of tightly converging the analysis levels and did not allow for a simultaneous solution. The formulated MLMDP method addresses these issues by directly coupling the design points through the formation of a system of nonlinear cross-level coupling equations. In this section, the new MLMDP method is assessed with results compared to the other integration approaches examined in Section 6.1.

The assessment of the MLMDP method was again completed by examining the design of the VSPT coupled to a turboshaft engine. For this assessment, the same design points, performance requirements, constraints and design inputs as those used in the previous PIMDP and DCMDP assessment were considered. The assessment of the different methods again focused on comparing the resulting cycle and turbine designs along with the convergence characteristics of the methods.

First, the MLMDP method was assessed in terms of the engine and turbine design and performance characteristics produced by each of the methods. Figure 92 shows design characteristics resulting from all three methods. The left column of plots shows the engine effective specific fuel consumption, inlet mass flow rate and combustor exit temperature. The results show that all three methods produce similar engine performance characteristics. In the right hand column of plots, the turbine efficiency, corrected flow and pressure ratio at each operating condition is shown. For these turbine design and performance characteristics, the MLMDP method results are generally similar to those produced by the PIMDP approach. The turbine efficiencies are nearly identical with the slight differences between

the PIMDP and MLMDP methods observed in the turbine corrected flow and pressure ratio at each design point. These results indicate that the coupling equations utilized in the MLMDP produce engine and turbine designs with similar performance characteristics to the PIMDP approach across all the design points.

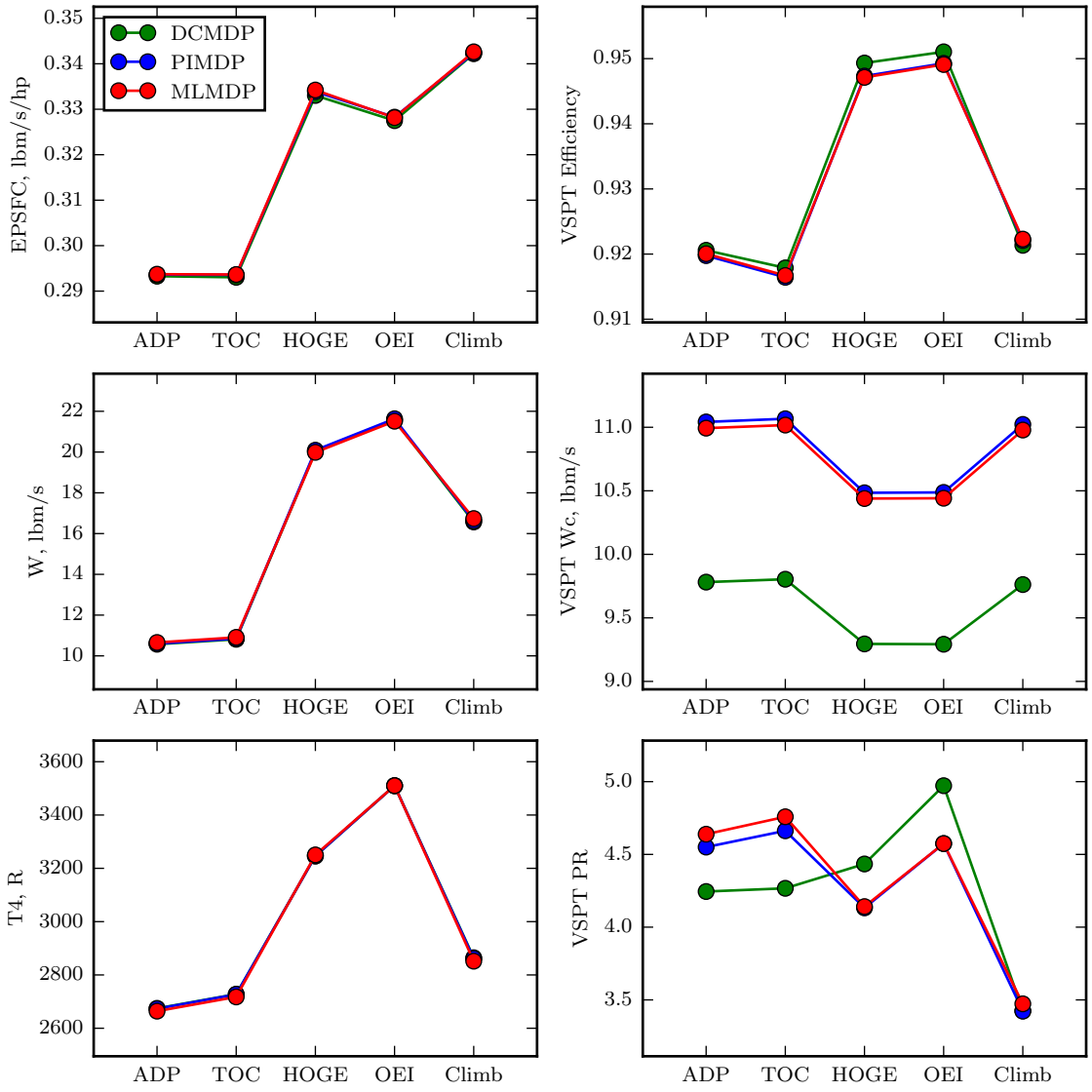

Figure 92: DCMDP, PIMDP and MLMDP Predicted Performance Characteristics at Each Design Point

In addition to examining design and performance characteristic at the design points for the cycle and turbine, the resulting turbine performance maps and annulus geometries were also evaluated. Figure 93 shows the turbine performance maps produced by all three

methods. In these maps, the performance characteristics of the turbines are generally similar across all three approaches. The corrected flow versus pressure ratio plot shown on the left indicates there are small differences in the corrected flow and pressure ratio between the PIMDP and MLMDP methods. While there are some small differences in these parameters, the efficiency contours shown in the right plot are nearly identical between those two integration methods. The similar turbine efficiencies are a result of nearly identical turbine annulus geometries being produced by both approaches as shown in Figure 94. Again, these results indicate that the coupling equations formulate for the MLMDP provide the same coupling of the analysis levels as the PIMDP approach which relies on passing large operating ranges and performance maps between the levels.

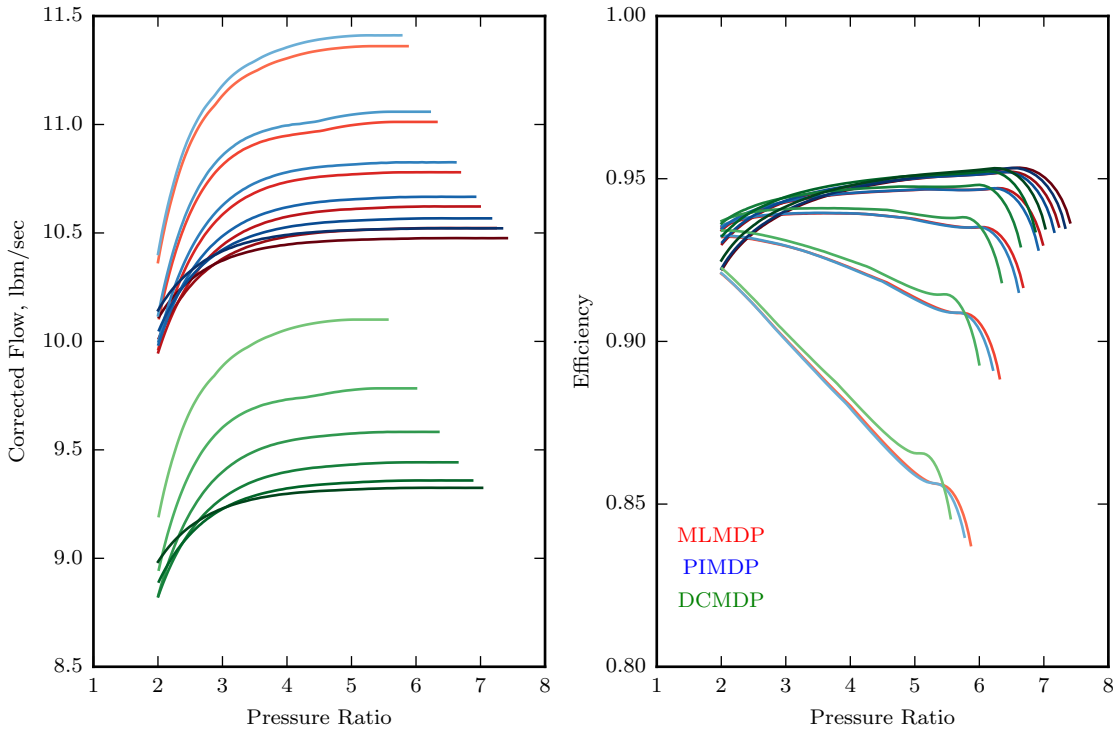

Figure 93: Turbine Performance Maps Produced by the DCMDP and PIMDP Approaches

Overall, these results show the PIMDP and MLMDP integration approaches produce similar design and performance characteristics when given the same design inputs, design

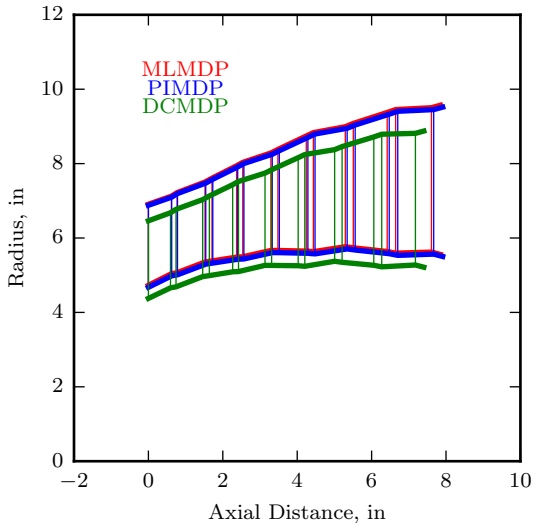

Figure 94: Turbine Flowpath Geometry Produced by the DCMDP, PIMDP and MLMDP Approaches

points, performance requirements and constraints. While the designs produced are similar, the convergence characteristics of the PIMDP and MLMDP methods are significantly different. As shown in Section 6.1, the PIMDP fails to tightly converge the analysis levels resulting in substantial error in the turbine corrected flow and pressure ratio between the levels. The formulation of the cross-level coupling equations and the elimination of the off-design analysis phase in the MLMDP method allows the levels to converge to a much tighter tolerance as shown in Figure 95. Here, the error in the cross-level coupling equations is continually decreased with all equations solved to within a 1.0E-4 relative tolerance after 8 iterations. This tight convergence on all cross-level coupling equations ensures that both the cycle and turbine analyses are consistent and is the source of the small differences in the turbine designs produced by the PIMDP and MLMDP methods

In addition to altering the cross-level convergence characteristics, the MLMDP method provides a benefit in terms of the overall computational cost of the cross-level integration and convergence. Table 8 details the number of function calls to various portions of the model used in this assessment. The first two rows of the table show the total number of function calls to the cycle MDP and turbine MDP portions of the model. The MLMDP

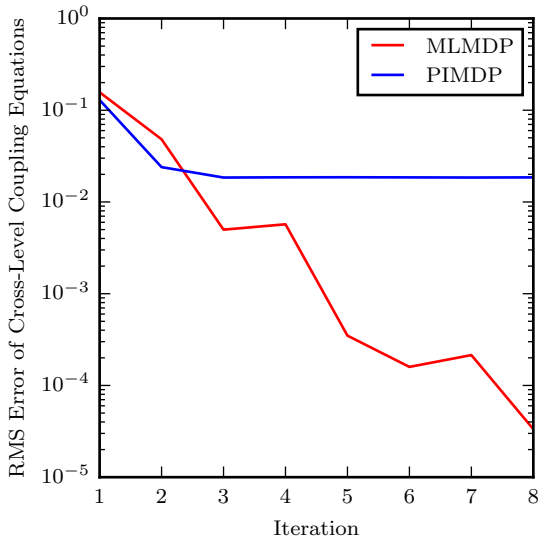

Figure 95: Convergence Characteristics of the PIMDP and MLMDP Approaches

method requires are larger number of cycle and turbine MDP evaluations as a result of the need to compute the Jacobian matrix with a finite difference approach for the cross-level coupling equations as part of the Newton solver. The breakdown of the function calls in the main iterations and as part of the finite difference calculations is given in rows 3 through 6. Finally, the last row of the table shows the number of function calls made to the turbine off-design analysis to generate the performance maps during each iteration of the DCMDP and PIMDP methods. The map generation process is computationally intensive requiring approximately 650 evaluations to generate each new map. Elimination of the map generation in the MLMDP method offsets the additional cycle and turbine MDP evaluations required for generating the Jacobian matrix for the Newton solver. Furthermore, the generation of this map in off-design mode and formatting the resulting data for use in the cycle analysis can often be a challenging task to automate thereby requiring human interaction. The elimination of this map generation step in the MLMDP method therefore produces a process that is able to simultaneously develop the cycle and turbine designs to satisfy all requirements and constraints.

The assessment of the formulated MLMDP method completed in this section evaluated several key elements of the formulated MDP integration approach. Specifically, the

Table 8: Computational Cost of the DCMDP, PIMDP and MLMDP Methods.

Metric	DCMDP	PIMDP	MLMDP
Cycle MDP Calls (Total)	2	8	38
Turbine MDP Calls (Total)	1	8	38
Cycle MDP Calls (main iteration)	2	8	8
Turbine MDP Calls (main iteration)	1	8	8
Cycle MDP Calls (finite difference)	0	0	30
Turbine MDP Calls (finite difference)	0	0	30
Turbine Map Calls (Off-Design)	649	5262	0

assessment showed that the use of cross-level coupling equations which directly linked the design points at each level produced designs equivalent to those produced by the PIMDP method. Furthermore, the assessment results showed that the MLMDP approach is capable of achieving significantly tighter convergence between the analysis levels than either of the other two methods. Lastly, an added benefit of the MLMDP method is a reduction in the overall computational cost as the large number of function calls required to produce the turbine performance map is eliminated. With this initial assessment of the key MLMDP integration approach completed, the next section will describe the steps for the complete MLMDP method.

6.4 Multi-Level MDP (MLMDP) Procedure

The multi-level MDP formulation described in the previous section focused on examining the critical elements of how MDP analyses at multiple levels could be merged together to enable simultaneous development of engine and turbine designs. In this assessment, these critical elements centered on the analyses completed at each level along with the data passed between the levels. Although several integration approaches had been previously studied, an assessment of these approaches showed they did not allow for truly simultaneous design development and did not tightly converge on the turbine operating conditions and performance requirements across the levels. Therefore, a new integration approach for use when MDP analyses are present at each level was formulated and evaluated. With a successful evaluation of this multi-level integration approach for MDP problems, a more detailed multi-level MDP procedure can now be described. The MLMDP procedure described in this

section draws heavily from the previously defined cycle and turbine MDP procedures and therefor consists of similar set of steps. The complete MLMDP procedure is summarized in Figure 96 with the details for each of the steps in the procedure described in the paragraphs below.

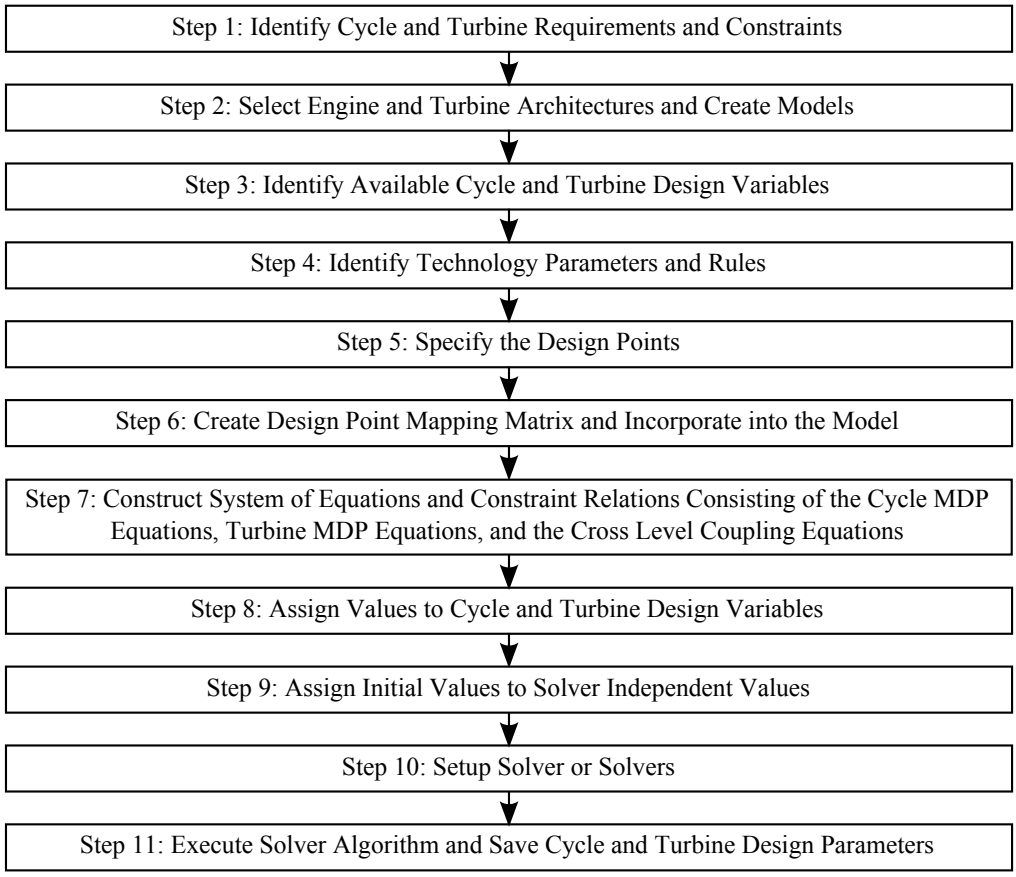

Figure 96: MLMDP Method

Step 0: Identify the Coupled Cycle and Turbine Design Problem to be Evaluated

The MLMDP procedure starts with a prologue step to generally identify the coupled cycle and turbine design problem to be evaluated. While this may seem like a trivial step, it is important to have a clear understanding of the engine and turbine design to be evaluated. Completing this step requires having some initial understanding of the design requirements at each level (formally identified in Step 1) along with the engine and turbine architectures

which will be explored (formally determined in Step 2). This step therefore is required for determining the turbine within the engine which will be studied with the multi-level analysis as well as the requirements and constraints that may be present.

Step 1: Identify Cycle and Turbine Requirements and Constraints

The first step in the MLMDP process is to identify the performance requirements and constraints that both the engine and turbine designs must satisfy. The performance requirements are defined as metrics which specify the expected performance level of either the engine or turbine at a certain operating condition. These requirements are typically identical to those which would be identified in the first step of either the cycle or turbine MDP processes. In addition to identifying the performance metrics to be considered, the values for the requirements along with the operating condition at which that requirement is evaluated must also be specified in this step. Typical examples of these performance requirements are the output thrust or shaft power for the engine and the output power for the turbine.

While performance requirements specify exact targets which must be matched, constraints are defined as limits on the operation or physical design which may potentially alter the design produced. Limits on the operation of either the engine or turbine specify minimum or maximum performance of the design at a given operating condition. Example operating constraints for the cycle include the maximum combustor exit temperature at various operating conditions with a turbine operating constraint being the maximum allowable AN^2 . Physical (geometric) design constraints are limits which apply to the physical geometry of the engine or turbine and are not dependent on the operating condition of the turbine. Examples of these constraints may include the maximum fan diameter for the engine or a maximum radius on the turbine.

Step 2: Select Engine and Turbine Architectures and Create Models at Each Level

The next step of the MLMDP procedure is to select architectures for the engine and turbine to be used in the design development. Selecting these architectures primarily includes

determining the fundamental components which comprise each system. For the engine this means selecting the type of engine to be analyzed (i.e. turbojet, turbofan, and turboshaft) as well as the determining layout of the internal components of this engine. Similarly, for the turbine under consideration the type of turbine (axial or centrifugal) and the layout of the turbine in terms of number and type of blade rows (stators and rotors) must be determined. If the designer wishes to consider several different engine and turbine architectures, the MLMDP procedure will need to be repeated for each unique configuration being considered. Once the engine and turbine architectures have been determined, baseline models of each system can be constructed in the selected analysis codes. In this model construction, it is important to define the models in terms of similarity parameters to enable the sizing of these systems in the MLMDP evaluation.

Step 3: Identify Available Cycle and Turbine Design Variables

Following the selection of the engine and turbine architectures and construction of the associated models, the next step is to identify the available design variables at each level. The design variables are engine and turbine parameters which the designer is interested in changing to produce a new design which satisfies all the requirements and constraints. The list of potential design variables depends on the architecture being considered at each level as well as the design problem under consideration. The selected design variables at each level will commonly include some or all of the similarity parameters identified in the previous step.

Step 4: Identify Technology Parameters and Rules

The fourth step of the MLMDP method focuses on identifying technology parameters and rules for both the engine and turbine. These technology parameters are similar to design variables but are specifically used to define the technology level of the system components. Values for these technology parameters can be held constant to develop designs of similar technology level or can be varied to create a technology trade space.

In addition to individual technology parameters, this step also identifies technology rules

which will be included in the analysis. These technology rules set the value of a technology parameter as a function of the input design variable values or output design and performance characteristics. Once the technology parameters and rules have been identified they should be incorporated into the meanline model.

Step 5: Identify the Design Points at Each Level and Determine the Multi-Level Set of Design Points

Step 5 of the MLMDP procedure determines the design points which must be considered by both levels of the MLMDP analysis. This step begins by identifying the necessary design points at each level. Identification of these points commonly begins with listing the operating conditions at which the performance requirements and constraints determined in Step 1 are enforced. For the cycle design points identified, values defining the operating conditions at each must also be specified. For the turbine design points, nominal values for the operating conditions for each design point can also be specified. However, these turbine operating condition values will ultimately be determined through the coupling to the cycle analysis.

Once the design points at each level have been identified, the next part of this step is to determine the multi-level set of design points. In the identification of the design points at each level, it is likely that there will be several design points at each level that have a corresponding design point in the other level. Identification of these corresponding design points is important as it allows these design points to be coupled in the MLMDP analysis. For cycle and turbine design points that do not have a corresponding point in the other level, a corresponding design point in the other level must be added to provide the operating conditions or turbine performance characteristics. Once the multi-level set of design points across the levels has been identified, each point must be incorporated into the cycle and turbine meanline models.

Step 6: Create Design Point Mapping Matrices and Incorporate into the Models at Each Level

The next step in the procedure collects all the information gathered in the first five steps to form a design point mapping matrix (DPMM) for each analysis level. These design point mapping matrices are similar to those developed in the cycle MDP and turbine MDP methods. These relate all the design variables, performance requirements and design limits to their respective design points thereby facilitating the creating of the MLMDP model. Notional DPMMs for the cycle and turbine analysis levels are shown in Tables 9 and 10, respectively.

Table 9: Notional Cycle Design Point Mapping Matrix

Design Point (DP)		DP 1	DP 2	DP 3
Map Scaling Point		X		
Design Variables (DV)	DV 1	X		
	DV 2	X		
	DV 3			X
	DV 4			X
	DV 5		X	
Performance Requirements (REQ)	REQ 1	X		
	REQ 2		X	
	REQ 3			X
	REQ 4		X	
	REQ 5			X
Design Constraints (DC)	DC 1	X		
	DC 2	X		
	DC 3		X	
Component Performance Estimates (CP)	CP 1	X		
	CP 2	X		
	CP 3		X	

While a single DPMM covering both analysis levels could be formed in this step, creating a separate DPMM for each analysis level is suggested to provide a more readable format. With two separate tables, the design variables, requirements and constraints associated with each level are clearly identified. Combining the tables has the potential to confuse this information across the levels and could also result in a large, overwhelming table that is difficult to comprehend.

Although two separate DPMMs that are similar to those produced in the cycle and turbine MDP methods are recommended, the DPMMs at each level require one important

Table 10: Notional Turbine Design Point Mapping Matrix

Design Point (DP)		DP 1		DP 2		DP 3	
	Stage →	1	2	1	2	1	2
Design Variables (DV)	DV 1	X	X				
	DV 2	X	X				
	DV 3			X	X		
	DV 4			X			X
	DV 5	X	X				
Performance Requirements (REQ)	REQ 1		X				
	REQ 2				X		
	REQ 3						X
	REQ 4				X		
	REQ 5						X
Design Constraints (DC)	DC 1		X				
	DC 2		X				
	DC 3			X			

change. As described in Step 5, for the MLMDP method there may be design points in one of the levels that do not have a corresponding design point the other level. In this case an extra design point needs to be added to the deficient level to ensure that the points can be coupled across the levels. With this requirement on the design points, it is highly recommended that the cycle and turbine DPMMs produced in this step contain columns for all multi-level design points identified in Step 5.

Step 7: Construct the MLMDP Systems of Equations and Constraint Relations

The seventh step of the MLMDP procedure may be the most critical of all the steps as it constructs the system of nonlinear equations that couple all of the design points at the different analysis levels. In this step, design rules are defined which will ensure that all requirements and constraints present at both levels are satisfied at the various design points and that the two levels match.

Development of the design rules that couple the design points to each other at the cycle and turbine levels follows a similar process to that used in the cycle and turbine MDP methods, respectively. In this process, the requirements and constraints identified for a given analysis level in Step 1 can be used to form the dependent equations in the

system. In addition to these dependents, unique independent parameters must be identified which can be used to converge the dependent equations. These independents will commonly include a single sizing parameter along with at least one operating parameter at each design point.

In addition to these equations, cross-level coupling equations must be developed. As discussed in Section 6.3.1, the role of these cross-level coupling equations is to ensure that the turbine operating conditions and performance characteristics match across the levels. Therefore, the dependents in the system of equations will likely be those defined by Equations 66 to 72. The independents parameters used to converge these are typically the operating conditions or performance characteristics of the turbine which were assumed in the analysis levels. Specifically, the parameters defining the operating conditions for the turbine design points can be used as independents to match the operating conditions determined in the cycle analysis. The parameters defining the turbine performance characteristics in the cycle model can also be used as independents to match the turbine performance determined in the meanline analysis.

Defining the cycle MDP coupling equations, turbine MDP coupling equations and the cross-level coupling equations forms the complete MLMDP system of equations. After defining these design rules which couple the design points within and across the levels, these rules must be added to the MLMDP model. Constraint relations based on the limits identified in Step 1 should also be added to the model at this point.

Step 8: Assign Values to Cycle and Turbine Design Variables

The eighth step in the MLMDP procedure begins the execution phase of the method. In this step, values must be assigned to each of the design variables and technology parameters previously identified. To develop a specific design, the designer will specify the value for each of the design variables and technology parameters. However, if the designer is interested in evaluating a large number of designs spread throughout a defined design space, the designer will need to specify minimum and maximum values for each design variable. Designs throughout this space can then be analyzed by selecting unique combinations of

values for each variable.

Step 9: Assign Initial Values to Solver Independent Vector

Step 9 of the method determines initial values for independent parameters used throughout the MLMDP model to converge the system of nonlinear equations. The independent parameters considered in this step are those required for the cycle MDP equations, turbine MDP equations, cross-level coupling equations, and any independents created internal to the cycle and turbine models at each design point. Initial values for these independent parameters must be carefully selected as the Newton-Rapshon method for solving systems of nonlinear equations will only converge if the initial guess is in the neighborhood of the final solution. A poor initial iterate can therefore result in convergence failures or excessive convergence iterations.

Development of the initial iterate for the cycle MDP and turbine MDP coupling independents can be completed following the process successfully used in both the cycle and turbine MDP methods. This process is summarized the steps below:

1. Create a SPD cycle or turbine model with design variable and technology parameter values within the design space identified in Step 8.

2. Evaluate the SPD model in on-design mode at a single design point corresponding to one of the design points.

3. Evaluate the SPD model in off-design mode at points with similar operating conditions as the other design points identified in Step 5.

4. Save the independent values from each of these off-design evaluations to serve as the initial iterate.

In addition to determining the initial values for the cycle and turbine MDP independent parameters, the initial iterate must also be developed for the cross-level coupling equations. To develop this initial iterate, it is recommended to execute the cycle and turbine MDP analyses in isolation. In this execution, reasonable values for the turbine performance at

each design point must be provided to the cycle MDP analysis while reasonable values for the turbine operating conditions must be provided to the turbine MDP analysis. Based on the results of the isolated cycle and turbine MDP analysis, these values can then be updated. This manual execution of the cycle and turbine MDP models with the passing of operating conditions and performance characteristics can be completed several times until reasonable agreement is achieved at all design points.

Once the initial iterate is developed for these three portions of the system of equations, the overall initial iterate can be assembled. This initial iterate can be later refined by saving the independent values from a converged MDP model. While generating the initial iterate can be time consuming, once a viable initial iterate is obtained the process does not need to be repeated even when exploring a design space. The reusability of the initial iterate stems from the postulate stated below developed as part of the cycle MDP process.[97]

Initial Iterate Postulate: A single initial iterate can be utilized to efficiently and robustly find solutions within the design space provided that the initial iterate is itself a solution to one of the designs within the space.

Applying this postulate within the MLMDP method allows for a single initial iterate to be used for all designs considered in a design space exploration as long as the initial iterate is valid for a design in that space.

Step 10: Setup Solvers

The tenth step of the MLMDP procedure focuses on setting up the Newton-Raphson solver or solvers required to converge the non-linear equations present in the model. Setting up the solver(s) primarily involves specifying values for parameters which control the iteration and convergence characteristics. These parameters are likely to include the convergence tolerances, step size limits, and iteration limits. If the implemented solver includes the ability to use quasi-Newton approaches in conjunction with the pure Newton-Raphson method, parameters defining when and how each approach is used should also be specified.

Step 11: Execute Solver Algorithm and Save Design Parameters

The final step of the MLMDP procedure is to execute the MLMDP model for the selected design variables values. After the model execution has been completed, output data describing the final cycle and turbine design should be saved for later analysis. It is recommended that the recorded output include all design characteristics and the converged iterate as these values will be needed to reproduce the design in a single point model for evaluation at operating conditions other than those used for the design points.

6.5 Implementation on Example Engine and Turbine Problems

The MLMDP method described in the previous section is intended to be applicable to a wide variety of engine and turbine design problems. However, to assess the capabilities of the developed MLMDP methodology it needs to be implemented on several example engine and turbine design problems. Three representative design problems were selected for this assessment and the implementation of the methods in their evaluation will be described in this section. The three design problems selected cover a range of engine and turbine architectures, performance requirements, constraints, and design points to thoroughly assess the capabilities of the MLMDP method. The design problems selected are similar to those used in the turbine MDP method evaluation. The first example problem examines the design of the E^3 mixed flow turbofan and its low pressure turbine. The second and third sample problems again draw from the tiltrotor aircraft engine design problem described in the motivation for this research. These two problems therefore examine the design of a turboshaft engine with either a conventional power turbine (CPT) or a variable speed power turbine (VSPT). The details of the implementation of the MLMDP method on each of these problems is described in the sections below.

Prior to describing the implementation of the MLMDP method on these design problems, it is also necessary to discuss the selection of the analysis tools to be used at each level. The MLMDP process was developed as a generic process that can be implemented with a variety of different analysis codes. However the selection of appropriate analysis tools

can facilitate the implementation of the method. As described for the cycle and turbine MDP methods, there are several desirable features for the analysis codes selected to possess. These desirable features include being written in an object-oriented programming language, implementation of a Newton-Rapshon solver, and the ability to specify the design in terms of similarity parameters. An additional consideration in the selection of analysis tools that is unique to the MLMDP method relates to the thermodynamic models or packages used in each code. The analysis of the engine cycle and turbine meanline are both highly dependent on the thermodynamic properties of the gases passing through the system. Differences in the thermodynamic properties between the selected analysis tools may therefore lead to differences in the computed turbine operating conditions and performance characteristics. It is therefore desirable to select analysis tools with compatible thermodynamic models or packages to limit this source of error. Finally, while the selection of the analysis tools at each level can be made independently these tools must ultimately be integrated to form the MLMDP analysis. Selection of analysis tools with common programming languages is therefore beneficial as it may facilitate integration. If the analysis tools selected are incompatible an additional code might be required to integrate the analysis levels and execute a Newton-Raphson solver to converge the system of nonlinear equations coupling the analysis levels.

Given this list of desirable features, two compatible analysis codes were selected for the implementation of the MLMDP method on these example problems. As described in the turbine MDP implementation, the Object-Oriented Turbomachinery Analysis Code (OTAC) was selected for the meanline analysis as it contains all the desirable features listed above. For the cycle analysis, the Numerical Propulsion System Simulation (NPSS) code was selected. The code was originally developed at NASA Glenn Research Center during the 1990s[22] and is a powerful tool for analyzing thermodynamic cycles for aerospace applications. As a result, NPSS received the NASA Software of the Year Award in 2001.[1] The NPSS code is now a collaborative effort between NASA, other government agencies, industry and academia[72] with the NPSS Consortium managing code maintenance and development.[102] NPSS was selected for this implementation as it again possesses all of

the desirable features listed above. These two tools are also compatible in terms of the thermodynamic packages as OTAC was developed within NPSS itself. Furthermore, the selection of these two codes facilitated the integration of the analysis levels as a result of the compatible programming language. With these analysis tools selected, implementation of the MLMDP method on the three example problems was completed as summarized in the sections below.

6.5.1 E^3 Engine and Low Pressure Turbine

The first example design problem considers the design of the E^3 mixed flow turbofan along with its low pressure turbine. As described in Section 5.5.1, this engine and LPT were the subject of significant research efforts within government and industry leading to a wealth of documentation on the design of each. This design problem therefore considers a redesign of both the engine and the LPT. A brief summary of the key elements of the implementation of the MLMDP method is presented in this section with a more detailed description provided in Appendix G.

The E^3 engine and turbine design problem identified a number of performance requirements and constraints at each analysis level. At the engine level, thrust requirements were identified at operating conditions specified as the cruise aerodynamic design point (ADP), the top of climb point (TOC) and the sea-level static (SLS) point. In addition, a maximum combustor exit temperature target was specified at the SLS point. For the turbine, the performance requirements and constraints were the same as those identified for the turbine MDP problem. However, the values for the turbine power requirements and pressure ratio limit were coupled to corresponding parameters in the cycle model. With these performance requirements and constraints, the engine and turbine architectures were selected to be those originally used in the E^3 engine development program. The engine architecture was therefore a two-spool mixed flow turbofan with the turbine architecture being a five stage axial flow configuration. The design variables for this design problem included those used in the E^3 LPT turbine MDP study describe in Section 5.5.1 along with the fan pressure ratio (FPR) and overall pressure ratio (OPR) of the engine. Finally, a design rule

was implemented which varied the bypass ratio (BPR) of the engine in order to maintain a constant mixer extraction ratio. This extraction ratio was defined as the ratio of the total pressures from each stream entering the mixer.

6.5.2 Tiltrotor Engine and Conventional Power Turbine

The second design problem used for evaluating the MLMDP method draws from the motivation for this thesis: the design of engines for a tiltrotor aircraft. This example problem focuses on developing designs for the turboshaft engine along with a conventional power turbine which is connected to the rotor through a multi-speed gearbox. Again, a brief summary of the key elements of the implementation of the MLMDP method on this design problem is presented in this section with a more detailed description provided in Appendix H.

For the conventional power turbine and turboshaft engine design problem, performance requirements and constraints were identified for both levels at seven different design points. These design points matched those identified in the analysis of the conventional power turbine in Section 5.5.3 and included the aerodynamic design point (ADP), top of climb (TOC), hover out of ground effect (HOGE), one engine inoperative (OEI), start of climb (Climb), pre-shift (Shift1) and post-shift (Shift2). The engine performance requirements included the shaft power output at each design point along with maximum combustor exit temperature and minimum nozzle pressure ratio limits at select design points. These shaft power requirements were also used in the design of the turbine with additional turbine design requirements being the target AN^2 and pressure ratio. Furthermore, constraints were added to ensure a minimum degree of reaction was maintained at each design point. The engine architecture selected for this design was a two spool gas generator with free power turbine. The high pressure compressor was assumed to consist of several axial stages followed by a centrifugal stage to achieve higher pressure ratios with a high efficiency. As described in the conventional power turbine design study for the turbine MDP method, a three stage power axial configuration was selected for the turbine architecture based on previous research results. Finally, the design variables for this problem included the cycle overall pressure

ratio and nozzle pressure ratio, along with all of the turbine design parameters specified in Section 5.5.3.

6.5.3 Tiltrotor Engine and Variable Speed Power Turbine

Finally, the last multi-level design problem considers the design of a turboshaft engine with variable speed power turbine for the tiltrotor aircraft. This configuration differs from the conventional power turbine described in the previous section as the engine uses a single speed gearbox thereby requiring the power turbine to operate efficiently over a wide range of shaft speeds. Appendix I provides a detailed description of the implementation of the MLMDP method on this design problem with a brief summary provided in this section.

The performance requirements and constraints for the turboshaft and VSPT are similar to those for the conventional power turbine and turboshaft engine described in the previous section. Power requirements for both the cycle and turbine were identified at five different operating conditions with additional requirements for the combustor exit temperature, turbine AN^2 and turbine pressure ratio. The operating points identified led to the creation of five design points including the aerodynamic design point (ADP), top of climb (TOC), hover out of ground effect (HOGE), one engine inoperative (OEI) and start of climb (Climb). Also, the design variables selected for both the cycle and turbine were the same as those used in the conventional power turbine design problem.

6.5.4 MLMDP Solver Setup

The three previous sections summarize the key elements of the implementation of the MLMDP method to the three engine and turbine design problems selected for this research. However, similar to the implementation of the turbine MDP in Section 5.5, the solver setup for the MLMDP design problems requires additional discussion. As described for the turbine MDP implementation, the system of nonlinear equations that must be solved for the turbine MDP using the OTAC analysis code is relatively large but has known correlation structure. Furthermore, OTAC computes the partial derivatives required to solve the system of equations using finite difference approximations with some of these computations producing inaccurate partial derivatives.

To address these issues, a nested solver structure was implemented as shown in Figure 97. This solver structure is similar to that used in the turbine MDP method with Newton-Raphson solvers being used at multiple levels to converge the equations specific to that level. In this example for the E^3 engine and LPT, each of the design points in the cycle and turbine MDPs gets its own solver with many of the components inside the turbine design points also having their own internal solvers. Two MDP level solvers are then used to converge the coupling equations for the cycle and turbine MDPs respectively, with a multi-level solver converging the cross-level coupling equations.

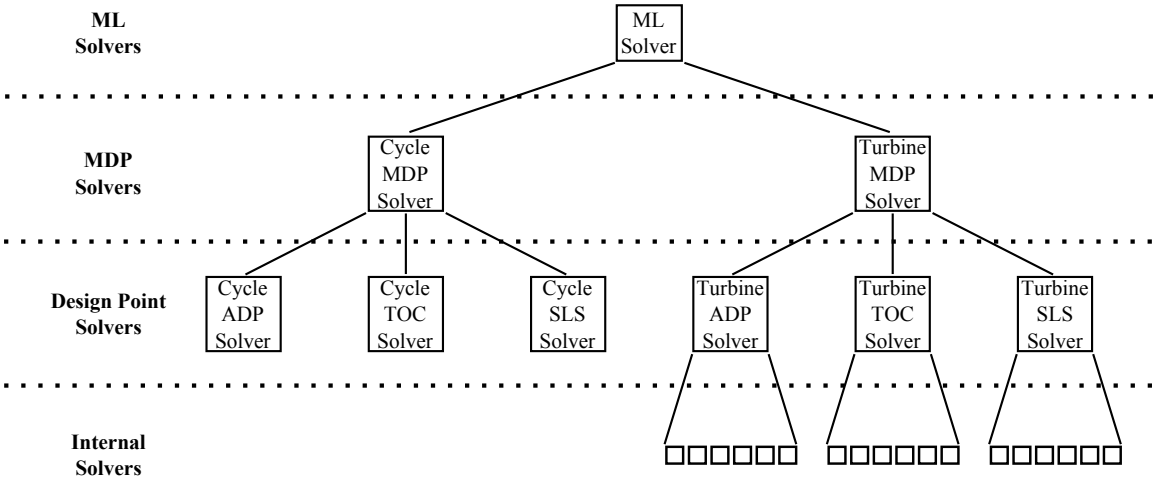

Figure 97: E^3 Engine and Turbine Nested Solver Setup

As with the nested solver setup for the turbine MDP, applying this approach in MLMDP models requires extra attention be paid to the solver tolerances and step sizes used at each solver level. These values must be carefully set to ensure that errors in the converged values at one solver level do not significantly alter the computation of partial derivatives through finite difference approaches in the higher level solvers. Based on the solver tolerance study presented in the turbine MDP implementation, a relative solver tolerance of 10^{-6} was selected for the internal solvers with a tolerance of 10^{-5} for the design point solvers. For both the MDP solvers and the multi-level solver, a relative tolerance of 10^{-4} was selected.

6.6 MLMDP Computational Experimental Results

The beginning of this chapter posed two research questions and hypotheses which guided the development of a multi-level MDP design methodology. This methodology was formulated by assessing current approaches for integrating analysis levels then developing a new integration approach specifically applicable when MDP methods are applied within each analysis level. This methodology was then implemented on three example problems which considered different engine and turbine architectures, performance requirements and constraints. This section presents the results of two computational experiments conducted with these models to numerically test the stated hypotheses. The first experiment presented below focuses on assessing the MLMDP method to ensure that it produces results which satisfy all performance requirements and constraints across both analysis levels. The second experiment is designed to test Hypothesis 4 and focuses on comparing the designs produced with the new MLMDP methodology to the designs generated when the cycle and turbine MDP methods are applied without coupling to the other analysis level.

6.6.1 Experiment 3: Assessment of the Multi-Level MDP Method

Research Question 3 stated at the beginning of this chapter inquired about how the MDP methods at the cycle and turbine analysis levels could be integrated to allow for simultaneous development of the engine and turbine designs to satisfy all performance requirements and constraints. Hypothesis 3 supposed that the cycle and turbine MDP analyses could be merged by adding a system of nonlinear equations which couple the design levels to the systems of equations already developed for the cycle and turbine MDP analyses. Sections 6.1 through 6.3.2 examined this integration of the analysis levels and formulated the system of equations which would be required to couple the analysis levels.

As part of the examination in these sections, an initial assessment of the MLMDP approach was completed. This assessment focused on only the turboshaft and VSPT design problem and considered a single set of design input values for both the cycle and turbine. The results of this assessment indicated that the new MLMDP method had the potential to

provide tighter convergence on the turbine operating conditions and performance characteristics while also developing the designs with fewer overall function calls. These positive initial results were then used to develop the formal MLMDP methodology described in Section 6.4.

While the initial assessment of the integration approaches produced promising results, a formal computational experiment is required to fully assess the capability of the method to simultaneously develop engine and turbine designs for problems with a variety of different architectures, performance requirements, constraints and design points. The primary objectives of this experiment is to demonstrate that the formulated MLMDP method produces engine and turbine designs which have consistent turbine operating and performance characteristics across the levels while also satisfying all performance requirements and constraints at each level. Furthermore, a secondary objective of the experiment is to evaluate the MLMDP method to ensure that it finds those valid designs in an efficient and robust manner.

6.6.1.1 Experiment 3 Setup

Given the objectives stated in the overview of Experiment 3, an experiment was designed to evaluate the developed MLMDP methodology and specifically the use of the cross-level coupling equations. The initial evaluation of cross-level coupling equations in Section 6.3.2 indicated the approach had promise but the assessment was limited to a single design problem with a single set of design inputs. Experiment 3 expands this evaluation to consider several design problems with different combinations of model architectures, design points, performance requirements, constraints and design inputs. Therefore, all three example design problems presented in Section 6.5 were considered providing a range of different design points, requirements and constraints. To evaluate the performance of the method with different design inputs, a combined cycle-turbine design space was specified for each problem by specifying minimum and maximum values for each design variable. Given the large number of design variables in combined cycle and turbine design space, each design space was explored using a design of experiments (DoE) approach. This DoE analysis for

each design problem evaluated 10,000 randomly selected designs from the design space. To determine the design inputs and execute this DoE, the OpenMDAO software framework used in the turbine MDP assessment was again utilized. This framework provided a built-in DoE generator and facilitated the execution and recording of results for each case on a high performance computing cluster. The results from each of these DoE's will be analyzed in the next section to determine if the formulated cross-level coupling equations provide a valid approach to integrating the analysis levels. These results will also be used to evaluate efficiency and robustness of the overall method in finding valid turbine designs to address the secondary objective of the experiment.

A successful Experiment 3 will show that for a wide range of architectures, design inputs, design points, performance requirements and constraints across the design problems, the MLMDP design rules (system of equations) will produce designs that satisfy all performance requirements and constraints at each level and are consistent across the levels. A successful test will also prove that the MLMDP method efficiently and robustly finds valid solutions throughout the design space.

6.6.1.2 Experiment 3 Results

As described in the experiment setup section, Experiment 3 examines the effectiveness of the MLMDP and specifically the cross-level coupling equations. This was completed by running a large DoE on three different engine and turbine models and evaluating the results based on several metrics in support of the primary and secondary experiment objectives.

The primary objective of the experiment was to show that the MLMDP method produces valid designs for a range of different design problems. Given this primary objective, the results from each DoE case were evaluate to first ensure that the performance requirements and constraints at both the cycle and turbine levels were satisfied. Second, the results from each case were evaluated to make sure that the turbine operating and performance characteristics are consistent across the analysis levels. In this experiment, consistency across the levels means that the turbine mass flow rate, inlet total pressure, inlet total temperature, fuel-to-air ratio, efficiency, pressure ratio and speed have values that match

within solver tolerance.

The results from assessing the cases from each design problem based on these metrics are summarized in Table 11. For all three design problems, the table shows that a high percentage of the DoE cases (well over 90%) converged to feasible, valid solutions. Each of these feasible, valid solutions had consistent turbine operating and performance characteristics across the analysis levels while also satisfying the performance requirements and constraints at each level. This high success rate across three different design problems further validates the initial assessment of the cross-level coupling equations completed in Section 6.3.2. More importantly, the results show that for a range of different model architectures, design points, performance requirements, constraints and design inputs the overall MLMDP methodology works well.

Table 11: Experiment 3 DoE Results Summary

Metric	**E^3 LPT**	**CPT**	**VSPT**
Total Cases	10000	10000	10000
Feasible Cases	9721	9269	9878
Convergence Rate	97.2%	92.7%	98.8%

While the DoE results show that a high percentage of the cases converged to valid solutions, there were some cases where the MLMDP method failed to produce valid results. In assessing the reasons behind these failed cases, several potential issues were identified. The first potential issue that may have led to failed cases relates to the combination of design inputs selected for the case. The design space formed for each problem and evaluated using the random sample DoE assumed a minimum and maximum value for each design variable. However, some combinations of these design variable values, especially in the corners of the design space, may have resulted in a set of similarity parameters that could not be sized to satisfy the performance requirements and constraints.

Another potential issue that may have led to failed cases was convergence errors which were commonly encountered throughout the process of solving the systems of equations at the various solver levels in the models. These convergence errors often first arose in the lower level internal and design point solvers in the hierarchical solver structure. With these

lower level solvers re-converged for each pass through the higher level solvers, convergence errors at the lower levels often had a detrimental impact on the overall convergence of a case. Specifically, lower levels solver convergence failures particularly during finite difference calculations for the higher level solvers resulted in inaccurate Jacobian matrices. These inaccurate Jacobians would therefore result in the Newton-Raphson solver potentially moving away from the actual solution. For these cases, the solver convergence errors and inaccurate Jacobians at the various levels led to excessively long execution times and were stopped after a specified timeout limit was reached in the DoE execution.

The issues of poor design input combinations and lower level solver convergence errors are intertwined making it difficult to precisely determine the issue that ultimately led to the failure of a case. For the design input combination issue, there is little that could be done to improve the MLMDP method as the design inputs selected would not result in a physically valid design regardless of the design method used. For the internal solver convergence issue, some improvements potentially could be made to the hierarchical solver structure implementation in the selected analysis codes. Despite these two issues, the overall high convergence rate of the MLMDP method across the three design problems shows the formation of a system of cross-level coupling equations successfully enables the simultaneous development of engine and turbine designs that satisfy all performance requirements and constraints.

In addition to examining the ability of the MLMDP method to find feasible solutions, the secondary objective for Experiment 3 was to evaluate the overall solution process to determine if it finds the feasible designs in an efficient and robust manner. Tables 12 through 14 provide an overview of the solver statistics for the three different engine and turbine design problems. For the converged cases in all three design problems, the tables show the details of the multi-level solver which exclusively handled the cross-level coupling equations. They show that for all three models a solution was typically found in less than 10 iterations of the Newton-Raphson solver. Furthermore, the process for completing the Newton iterations typically required the computation of a limited number of Jacobian matrices at this level with the remaining iterations using the Broydan update process. As

a result, the total number of passes through the entire MLMDP model was reduced.

Table 12: Solver Summary for E^3 LPT MLMDP

Metric	Mean	Standard Deviation	Minimum	Maximum
Wall Time (sec)	247.14	175.91	49.00	1018.00
Multi-Level Solver Iterations	7.14	0.94	5.00	14.00
Multi-Level Solver Passes	13.45	2.15	11.00	37.00
Multi-Level Solver Jacobians	1.05	0.26	1.00	4.00

Table 13: Solver Summary for CPT MLMDP

Metric	Mean	Standard Deviation	Minimum	Maximum
Wall Time (sec)	162.67	214.02	34.00	2854.00
Multi-Level Solver Iterations	4.67	1.20	3.00	18.00
Multi-Level Solver Passes	20.81	6.97	17.00	113.00
Multi-Level Solver Jacobians	1.15	0.44	1.00	7.00

Table 14: Solver Summary for VSPT MLMDP

Metric	Mean	Standard Deviation	Minimum	Maximum
Wall Time (sec)	1003.81	483.92	105.00	3010.00
Multi-Level Solver Iterations	5.91	0.86	4.00	12.00
Multi-Level Solver Passes	19.49	5.44	14.00	51.00
Multi-Level Solver Jacobians	1.36	0.50	1.00	4.00

Overall, the results presented for Experiment 3 in this section show that the cross-level coupling equations formulated for the MLMDP method and implemented on these sample problems produce designs which satisfy all performance requirements and constraints. Furthermore, the MLMDP method efficiently and robustly finds solutions throughout the design space. Combined with the results from the assessment of the current approaches for integrating analysis levels, the experiment supports the first hypothesis that the analysis levels can be coupled by forming a system of equations consisting of the cycle MDP equations, turbine MDP equations and the cross-level coupling equations.

6.6.2 Experiment 4: Comparison of the MLMDP and Individual Cycle and Turbine MDP Methods

The final experiment completed in this thesis focused on addressing the fourth research question which was posed at the beginning of this chapter. This question inquires about

the differences in the engine and turbine designs produced by the newly developed MLMDP methodology and those produced by applying the MDP methods at each level individually. Hypothesis 4 states that the designs produced by the MLMDP method will be different than those produced by the individual MDP analyses as a result of the cross-level coupling equations. The objective of Experiment 4 is therefore to test this hypothesis and answer Research Question 4 by comparing results generated from both the MLMDP and individual MDP methods. The experimental setup and results are presented in the sections below.

6.6.2.1 Experiment 4 Setup

Research Question and Hypothesis 4 provide clear guidance for the setup of the fourth experiment. Experiment 4 needs to compare the designs produced by MLMDP method to those produced by the cycle MDP and turbine MDP methods. This comparison was completed by applying the three MDP methods to the design of the engine and turbine of all three design problems described in Section 6.5. These three design problems were again selected as they implement a range of architectures, design points, requirements and constraints which may impact the resulting designs and design spaces. The evaluation completed in Experiment 4 is divided into two parts, focusing on the cycle and turbine designs respectively.

The first part of Experiment 4 compares the engine and cycle designs produced by the MLMDP method to those produced with the cycle MDP method. In this comparison, the cycle MDP method assumes standard cycle design practices relating to turbine performance would be followed. Predominantly, use of standard cycle design practices means that a reference performance map is selected for the turbine. This map can then be scaled in the cycle MDP sizing process to match the input turbine design efficiency and speed as well as the computed turbine corrected flow and pressure ratio. For the MLMDP portion of this analysis, the turbine design was completed by specifying a vector of baseline design input values. These values were selected to be approximately in the middle of the turbine design space identified in Step 8 of the method.

To compare the MLMDP and cycle MDP methods, the two methods were applied in

the evaluation of the cycle design space for each design problem. The cycle design spaces identified for the three design problems considered a small number of design variables. For the E^3 engine the design space consisted of the fan pressure ratio and overall pressure ratio variables while for the CPT and VSPT engine design problems the cycle design space consisted of the overall pressure ratio and nozzle pressure ratio variables. Given the limited dimensionality of these design spaces, a full factorial DoE was used to explore the entire space. This exploration of the relatively small design space allowed for the creation and visual comparison of contour plots showing the changes to the specific fuel consumption across the design space.

To supplement this visual comparison of the overall design space, an optimization was also completed with the MLMDP and cycle MDP models to examine the difference in the optimum designs produced by each method. For the optimization of each design problem with both the cycle MDP and MLMDP methods, the optimization objective function was to minimize a form of specific fuel consumption metric applicable to that engine at the ADP point. For the E^3 engine, this meant that the thrust specific fuel consumption (TSFC) value was minimized. For the CPT and VSPT engines a variation of the power specific fuel consumption (PSFC) known as the effective power specific fuel consumption (EPSFC) was selected. The EPSFC metric defined in Equation 73 combines the output shaft power with the thrust power from the nozzle to better capture the overall power output of the engine. [56] Selection of the EPSFC metric for the CPT and VSPT engines therefore recognizes the benefit of nozzle thrust to the overall vehicle propulsion and helps to prevent unacceptably low nozzle pressure ratios from being selected. Finally, while the various SFC values for each design problem can be computed at any design point, the values at the ADP point were selected for the objective function as these design points are representative of the cruise flight conditions where the engines would spend the most time operating. With the objective functions defined for each design problem, the last setup element for the optimization was the selection of an appropriate optimization algorithm. This selection will be address later in this section as the comparison of the turbine MDP and MLMDP methods also utilized a similar optimization.

$$EPSFC = \frac{\dot{m}_f}{\dot{W}_{out} + F_{net} V_0} \tag{73}$$

Following the comparison of the designs produced by the cycle MDP and MLMDP methods, the second part of Experiment 4 compares the turbine designs produced by the MLMDP and the turbine MDP methods. The approach used in this part of the experiment is similar to that used in the first part to compare the cycle designs. As in the cycle comparison, the turbine MDP comparison requires defining the assumptions which will be used in each method. First, in the turbine MDP method the operating conditions at each design point were assumed fixed based on the results of the preceding cycle analysis with a scalable reference map. By contrast in the MLMDP method, the turbine operating conditions were coupled to the cycle and allowed to vary as the cycle model reacted to the computed turbine performance characteristics. Furthermore, for the MLMDP method the cycle design inputs were set to baseline values near the middle of the identified cycle design space.

Similar to the cycle design space comparison, the turbine design comparison was first investigated through the use of DoE methods to explore the design space. Because of the larger number of design variables for the turbine, visually comparing the full design space with contour plots was not possible. Therefore, only slices of the high-dimensional design space for each problem were examined. The design space slices were formed by varying the flow and loading coefficients for each stage while holding the remaining design inputs at nominal values. These design space slices therefore are similar to the traditional Smith chart which shows contours of efficiency as function of the flow and loading coefficient for a single turbine stage.

While the examination of the design space slices provides some understanding of differences in the designs produced by the methods, it does not capture the full magnitude of the differences produced throughout the design space. Therefore, an optimization was also completed for this part of the experiment to show the differences in the best designs. For the optimization of the turbines in all three design problems, the objective function was selected as the efficiency at the ADP point. This point was again selected as it is

representative of the cruise condition of the engine and turbine.

With the comparisons of the cycle MDP and turbine MDP results to the MLMDP results both relying on the examination of the optimum engine and turbine designs, it is necessary at this point to discuss the selection of an appropriate optimization algorithm which can be applied to these problems. The selection of an optimization algorithm to support the comparison of the individual MDP analyses and the MLMDP analysis started with an assessment of the features of the design problems. First, the design problems examined in this experiment do not specify constraints other than minimum and maximum input values which must be considered by the optimization algorithm. Hence, the optimization of the cycle and turbine designs can be completed using algorithms for unconstrained optimization. Second, although the slices of design spaces will be explored with DoE cases as part of this experiment it is unclear if the full design spaces explored are unimodal or multimodal. With this uncertainty in the modality of the design space, global optimization algorithms are preferred to reduce the possibility of finding a local optimum. Furthermore, the dimensionality of the design spaces, particularly the turbine space, make the computation of derivatives with finite difference approaches a time consuming endeavor. Therefore, gradient free optimization approaches which can evaluate cases in parallel were also considered beneficial.

Given these characteristics of the design problems to be optimized, a gradient-free, unconstrained global optimization approach was deemed appropriate for this study. While there are a number of optimization algorithms that fit into this category are available, the Augmented Lagrangian Particle Swarm Optimization (ALPSO) algorithm was selected for this study.[59] Implementation of this algorithm was also facilitated by its availability within the OpenMDAO framework. The OpenMDAO implementation of the ALPSO algorithm was also done in such a way to allow for parallelization on a computing cluster to reduce the overall computation time. For each of the optimizations performed in this experiment, default settings within the pyOpt[87] implementation were used with the swarm size increased to 200 particles.

Lastly, before presenting the results of Experiment 4 it is important to define what

will constitute a successful experiment. First, a successful experiment will show that the MLMDP method alters the engine design space specifically in terms of the SFC contours. Supporting this comparison of the design spaces, the optimization results from each approach will show that the optimum designs are different between the approaches. Second, a successful experiment will show that the MLMDP method alters the examined slices of the turbine design space specifically in terms of the efficiency contours. Furthermore this comparison will be supported by differences in the optimum turbine designs identified by the optimization portion of the experiment.

6.6.2.2 Experiment 4 Results

As described in the Experiment 4 setup, the assessment of the MLMDP was completed in two parts. The first part of Experiment 4 focuses on comparing the engine designs produced by the MLMDP methodology with those produced by the cycle MDP method. In this part of the experiment, the cycle design spaces were explored and the optimum designs are compared. For the second part of the experiment the focus shifts to comparing the turbine designs produced by the MLMDP and turbine MDP methods. This part of the experiment also examines the turbine design space and the optimum design which results from each method.

Part 1: Cycle Design Space Comparisons

The first part of the Experiment 4 compares the cycle designs generated by the cycle MDP and MLMDP methods for each design problem. As described in the setup, the analysis with the isolated cycle MDP method used a reference turbine map for the component of interest. In comparison, the MLMDP analysis coupled in the meanline design for this turbine of interest with the turbine design variables set at nominal values. The evaluations in this section specifically focus first on comparing the trends in the cycle design spaces for each design problem produced by each design method. These design space comparisons are then supplemented by a more detailed comparison of the optimum designs identified with the design space.

The first problem examined in the section is the design of the E^3 engine. The design space for this problem was formed by varying the fan pressure ratio and overall pressure ratio with a full factorial DoE being used to explore the space. Examination of the results across the design spaced focused in on two performance metrics of the engine: the TSFC and primary bypass ratio. The trends for these two metrics throughout the MLMDP and cycle MDP produced design spaces are shown in Figures 98 and 99 respectively. Overall, the design space trends (contours) for both ADP TSFC and ADP BPR are similar between the two methods. The main difference in the design spaces is a slight shift in both the TSFC and BPR levels for the two methods.

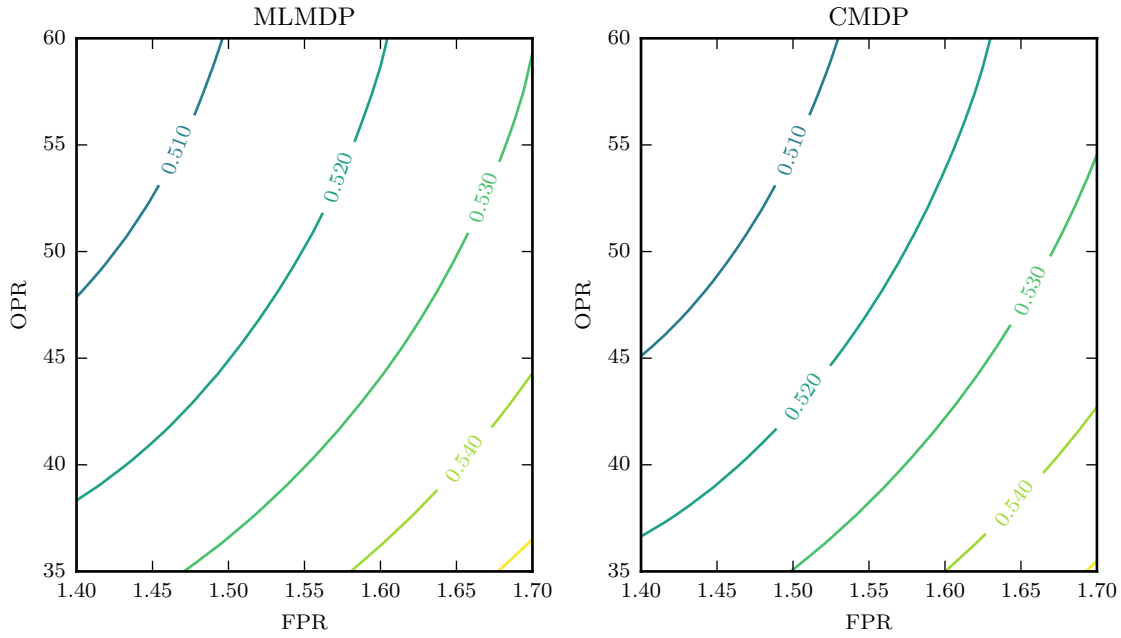

Figure 98: TSFC Variation in the Cycle Design Spaces Produced by the MLMDP and Cycle MDP Methods for the E^3 Engine.

To better understand these minor differences in the design spaces produced by the two methods, a more detailed examination of the optimum designs was completed. As is clear from Figure 98, the minimum ADP TSFC occurs with the highest OPR and lowest FPR inputs. Details of the design and performance characteristics of these two engines across all three design points are shown in Figure 100. The plot in the left hand column show that the TSFC, total engine mass flow and the OPR are similar at all three design

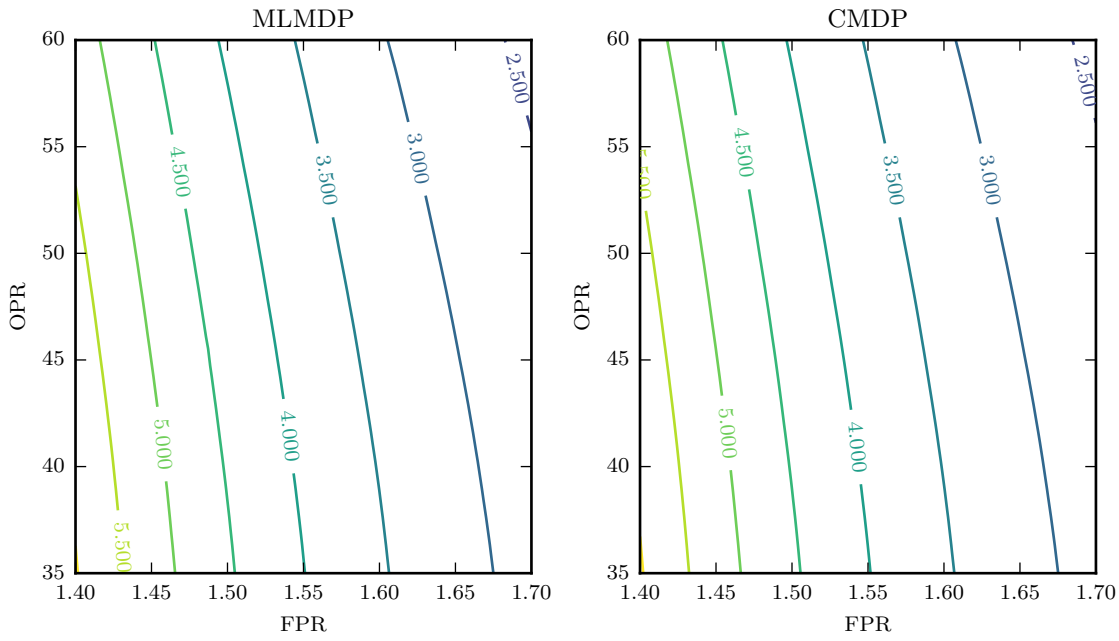

Figure 99: BPR Variation in the Cycle Design Spaces Produced by the MLMDP and Cycle MDP Methods for the E^3 Design Problem.

points. While these values are similar, the plots in the right hand column show some differences in the design and performance characteristics. Specifically, the LPT efficiency in the upper right plot shows about a 1% difference at both the ADP and TOC points with nearly identical performance at SLS. As a product of this difference in efficiency, both the maximum combustor exit temperature and the primary BPR are altered at ADP and TOC to produce feasible designs.

While there are some differences in the optimum cycle designs and design spaces produced by the two methods, overall the E^3 engine results from both methods are generally similar. One factor likely contributing to this similarity was the LPT reference map selected in the cycle MDP analysis. This LPT performance map was based on data for the actual design developed for the LPT during the E^3 development program.[18, 15] For the MLMDP method, the LPT model and nominal design inputs selected were also representative of this turbine design leading to similar turbine performance characteristics. These results therefore indicate that if a turbine performance map representative of the actual geometry for the cycle MDP can be selected, it can serve as an acceptable alternative to completing the

design with the MLMDP method.

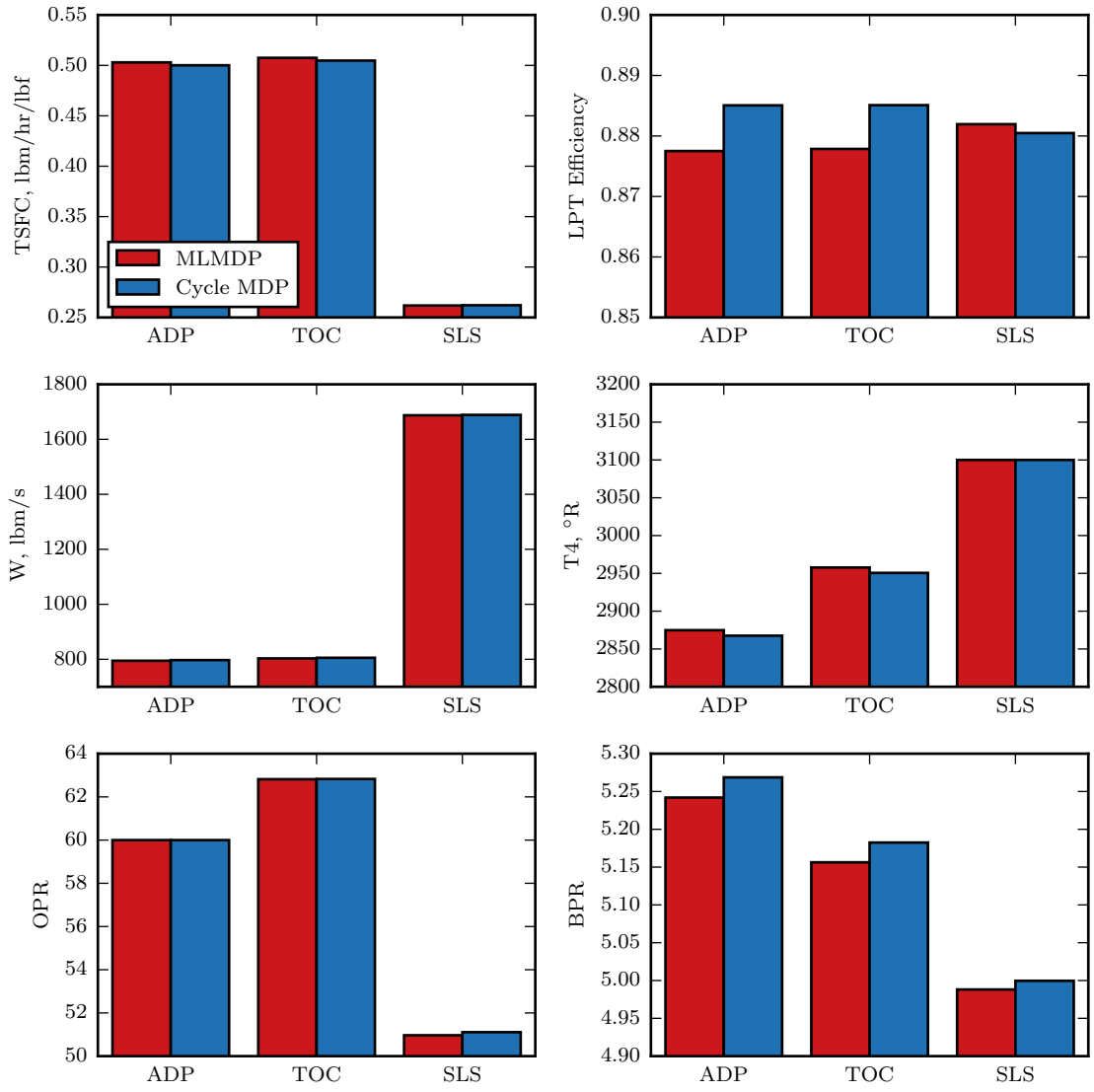

Figure 100: Optimum Cycle Designs Produced by the MLMDP and Cycle MDP Methods for the E^3 Design Problem.

While a representative LPT performance map was available for the E^3 engine problem, the other two conceptual design problems examined in this thesis did not have that luxury. One of those problems, the design of an engine with conventional power turbine for the tiltrotor aircraft, is examined next in this section. For this problem, a reference power turbine map was used for the cycle MDP based on the previous work of Snyder[100] while in the MLMDP a three stage turbine model with a set of baseline design inputs was

implemented. Similar to the E^3 analysis, a design space for this engine was first explored by varying the ADP overall pressure ratio and the ADP core nozzle pressure ratio. Figure 101 shows the changes to the engine EPSFC throughout the design spaces produced by the cycle MDP and MLMDP methods. As observed in this figure, the EPSFC contours produced by both methods have a similar topology throughout the design space with the MLMDP method producing lower EPSFC values throughout the space. In both of these design spaces, there is a noticeable break in the contour trends at nozzle pressure ratios of approximately 1.04. This break results from a minimum nozzle pressure ratio constraint applied within the cycle MDP to maintain a nozzle pressure ratio greater than 1.02 at all design points. While the overall design space topology produced by the two methods is similar, there is a distinct shift in the location of optimum design produced by the two methods. This shift in the optimum cycle design values was further explored by examining the details of these optimum designs.

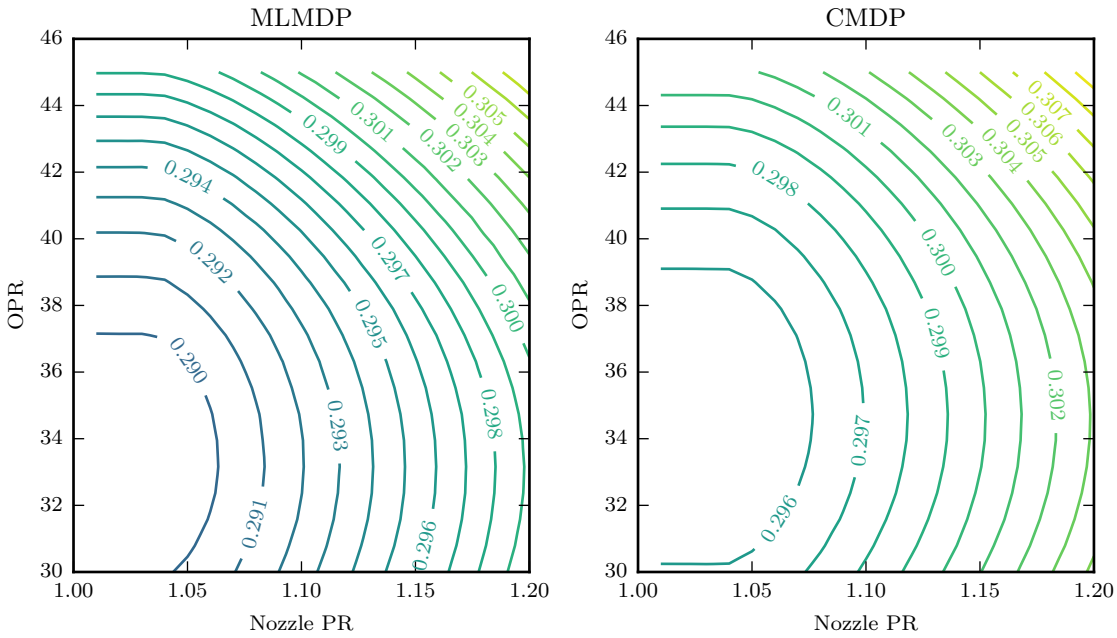

Figure 101: EPSFC Variation in the Cycle Design Spaces Produced by the MLMDP and Cycle MDP Methods for the CPT Design Problem.

The results of this optimum design evaluation are shown in Figure 102. As depicted in the bottom two charts in this figure, there is a difference in both the optimum ADP OPR

and ADP nozzle pressure ratio identified by the two methods. This shift in the optimum cycle design variables was the result of differences in the turbine performance characteristics between the methods which are shown in the upper right plot. This plot shows that the turbine performance characteristics in the MLMDP method have much less variability across the design points in comparison to the cycle MDP method with the selected reference map. Specifically, the turbine efficiency for the MLMDP model is significantly higher at the ADP, TOC and Shift1 operating points while also being slightly lower at the HOGE, Climb and Shift 2 points. These differences in the turbine performance characteristics across the design points also affected the other cycle design and performance characteristics. The more efficient turbine at ADP allowed for the engine to be sized to a slightly smaller overall mass flow rate with a lower combustor exit temperature (T4) at the ADP point. These changes to the cycle design and performance characteristics are significant as a smaller mass flow rate is usually correlated with a smaller engine diameter and lower weight while lower combustor temperatures affects the material selection and life of hot section parts. In total, the results for this engine show that the MLMDP method alters the design and performance characteristics relative to the isolated cycle MDP method as a result of the cross-level coupling.

The last problem examined in this section considers the design of a turboshaft engine with a variable speed power turbine, also for the tiltrotor aircraft. Similar to the previously described turboshaft with CPT problem, a reference power turbine map was used for the cycle MDP based on the work of Snyder[100] while in the MLMDP a four stage turbine model with a set of baseline design inputs was implemented. Also in this problem, the cycle design parameters forming the design space were identical to the previous problem. With these inputs, the cycle design spaces produced by the cycle MDP and MLMDP methods were evaluate and are show in Figure 103. The EPSFC topology shown in these plots is generally similar to that observed in the turboshaft and CPT problem. The one noticeable difference is the lack of a break in the contours at low nozzle pressure ratios as the minimum nozzle pressure ratio constraint was not active. Comparing the cycle MDP and MLMDP generated spaces for this problem again shows that the MLMDP method produces more efficient, lower

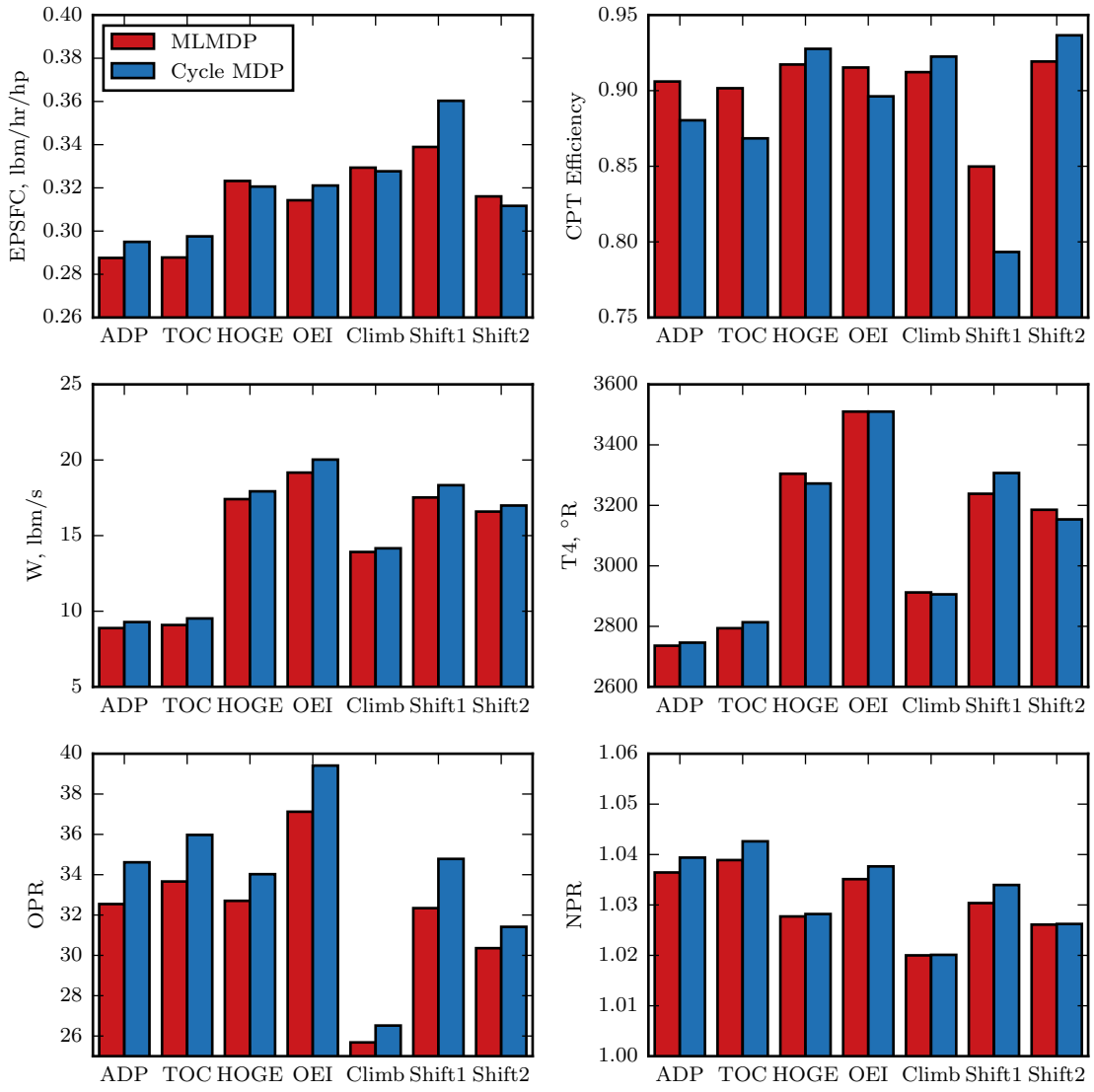

Figure 102: Optimum Cycle Designs Produced by the MLMDP and Cycle MDP Methods for the CPT Design Problem.

EPSFC designs throughout the design space. Furthermore, there is a noticeable shift in the location of the optimum cycle design values between the methods.

To further evaluate these differences, the optimum designs produced by the two methods were also examined with results shown in Figure 104. The differences in the optimum cycle design parameters, ADP OPR and ADP NPR, are shown in the lower two plots. Similar to the turboshaft with a conventional power turbine, the MLMDP method for the turboshaft with a VSPT generates turbine designs with a more consistent efficiency level across the

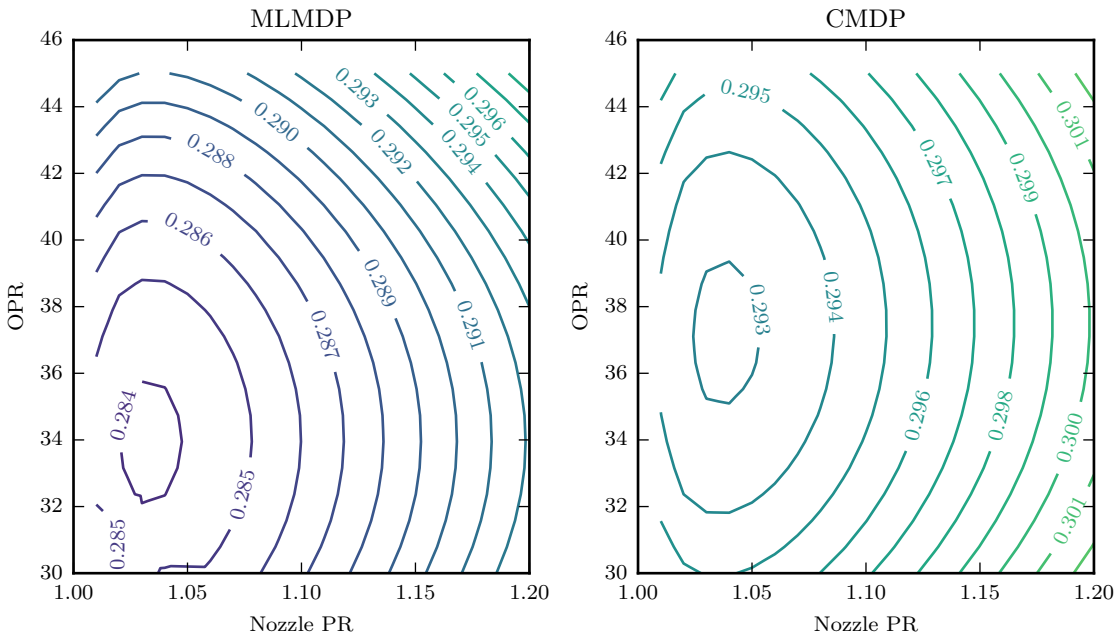

Figure 103: EPSFC Variation in the Cycle Design Spaces Produced by the MLMDP and Cycle MDP Methods for the VSPT Design Problem.

different design points. These differences in the turbine performance characteristics also propagate through the rest of the engine design influencing other cycle characteristics such as the overall mass flow rate and combustor exit temperature. For the optimum designs examined here, some of these changes to the cycle are significant. Particularly, the approximately 100 degree Rankine decrease in the ADP combustor exit temperature for the MLMDP generated engine could notably alter turbine material selections, engine weight and hot section part life. Overall, the results shown in Figure 104 for the turboshaft and VSPT design problem indicate that the cycle MDP method and MLMDP method produce different designs as a result of the cross level coupling equations.

The computational results presented in the first part of this experiment show that the cycle MDP and MLMDP methods generally produce different cycle design spaces and optimum designs for all three design problems. While there were differences observed in the cycle designs for each design problem, the magnitude of the differences varied across the problems. For the E^3 engine design, the differences between the design spaces and optimum designs were relatively small. In this model, the influence of the coupling to the turbine

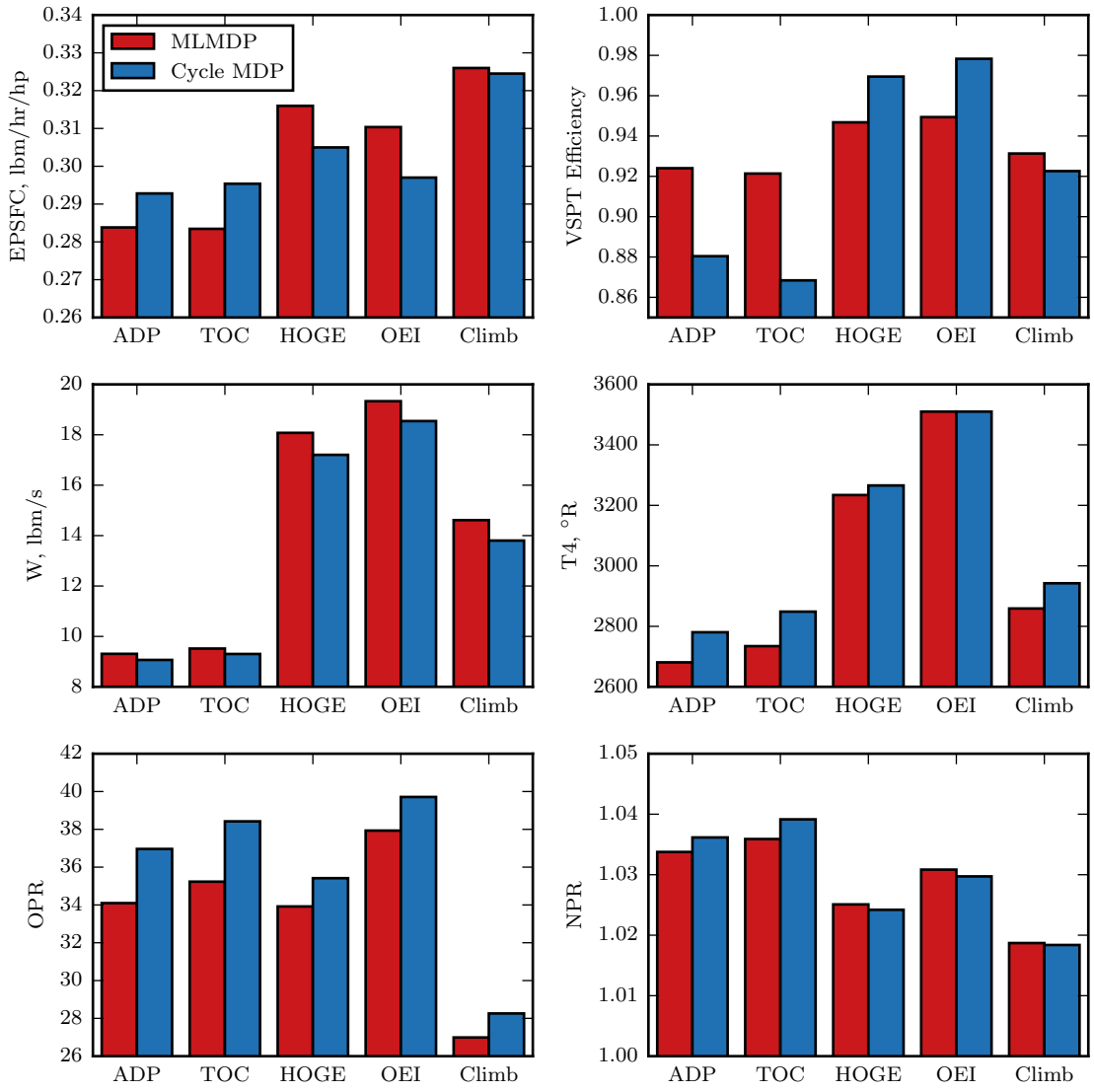

Figure 104: Optimum Cycle Designs Produced by the MLMDP and Cycle MDP Methods for the VSPT Design Problem.

MDP analysis in the MLMDP method was partially mitigated by the use of a representative LPT performance map based on experimental data. For the turboshaft engine design problems with both the conventional and variable speed power turbines, the differences in the cycle designs produced by the two methods were more significant. In these models, the cross-level coupling introduced improved turbine performance predictions altered the topology of the cycle design spaces as well as the cycle design characteristics associated with an optimum design.

Part 2: Turbine Design Space Comparisons

The second part of Experiment 4 examines the turbine designs produced by the MLMDP method in comparison to those produced by the isolated turbine MDP approach. As described in the setup, the analysis with the isolated turbine MDP method considered design points at fixed operating conditions while the MLMDP analysis changed the operating conditions as the cycle responded to changes in the turbine design and performance characteristics. The evaluations in this section specifically focus first on comparing the trends in slices of the turbine design spaces for each design problem produced by each design method. These design space comparisons are then supplemented by a more detailed comparison of the optimum designs identified within the full turbine design space.

The first problem examined in the section is the design of the LPT for the E^3 engine. Given the large number of design variables in the E^3 LPT, the design space was examined by plotting slices of the space in terms of flow and loading coefficients for one stage at a time. For each slice of the design space examined, all other design variables where held constant at values near the middle of the design space. The resulting slices are shown in Figure 105 starting with stage 1 at the top and working down to stage 5 at the bottom. Comparing the design space slices produced by the MLMDP method in the left column with those produced by the isolated turbine MDP method in the right column reveals that they are generally similar. Across all the stages, the two methods produce similar contour shapes with slight shifts in the efficiency levels between the two methods. Overall, this similarity is due to the loss models in the turbine meanline analysis primarily depending on the non-dimensional similarity inputs which are the same for both methods. The small shift in the efficiency levels between the methods are the result of secondary effects captured in the loss model related to the physical size of components. Specifically, changes in the chord of each blade row alter the computed Reynolds numbers which are then applied as a correction factor to the blade row losses.

To evaluate the full E^3 LPT design space, an optimization was completed using all turbine design variables. The resulting designs produced by this optimization were evaluated

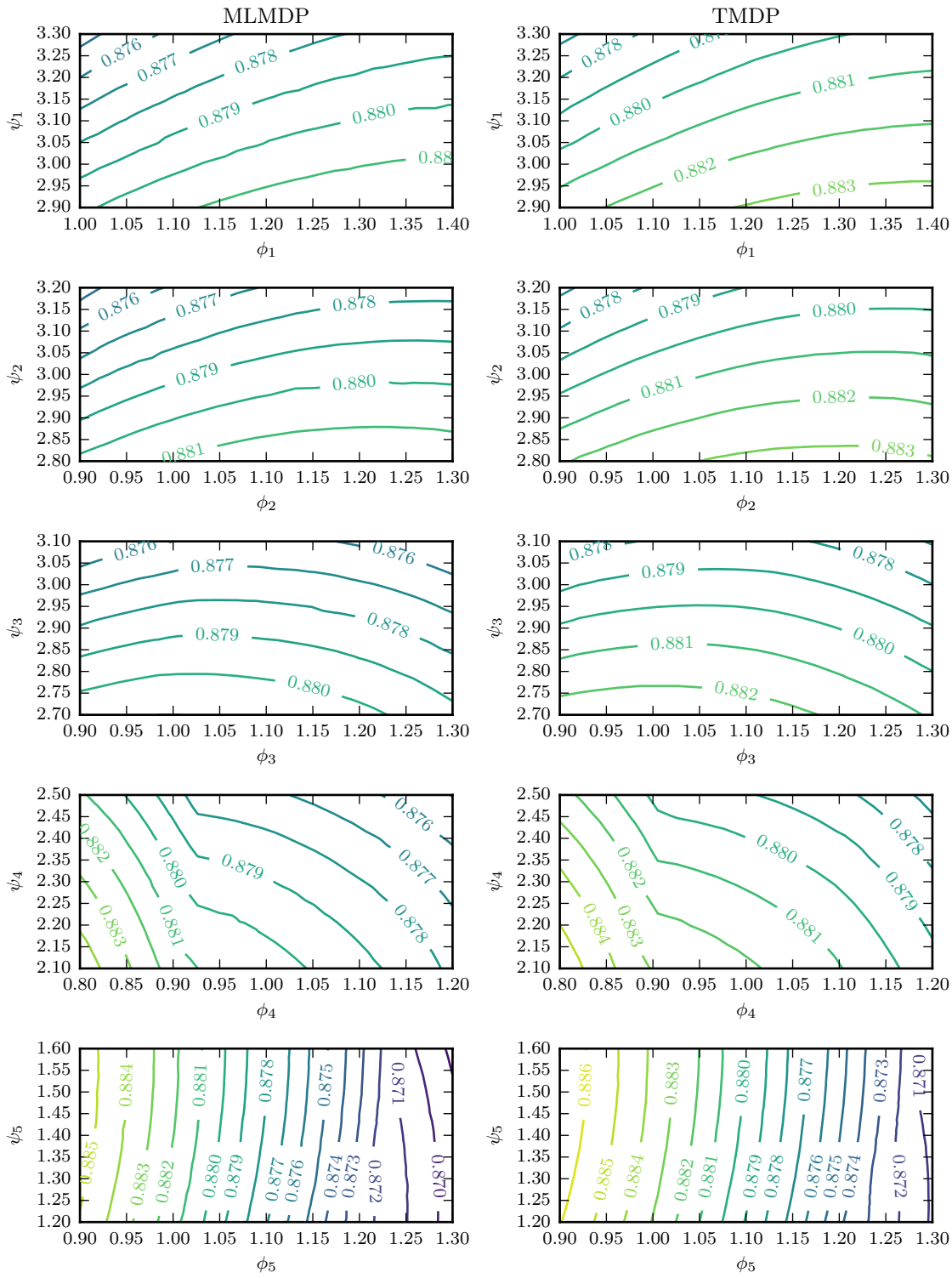

Figure 105: Efficiency Variations in the Turbine Design Spaces Produced by the MLMDP and Turbine MDP Methods for the E^3 LPT Design Problem.

by examining the resulting turbine flowpaths and performance maps. The resulting turbine flowpath designs produced by the MLMDP and turbine MDP methods are shown in Figure 106. This figure shows that the optimum designs for both methods have similar geometries with only minor differences. Given the similarity of the E^3 LPT design spaces and flowpaths produced by the two design methods, it is also expected that the performance map for these turbines would also be similar. Figure 107 shows the E^3 LPT performance maps produced by the two methods and confirms that they in fact are similar. In this figure, the lines of constant corrected speed are nearly identical in both the corrected flow plot on the left and the efficiency plot on the right. Furthermore, the maps show that the performance characteristics and operating conditions at the design points do not change significantly between the design approaches. These limited changes to the design points stems from the accurate turbine performance map used in the cycle MDP analysis which was used to determine operating conditions at each point.

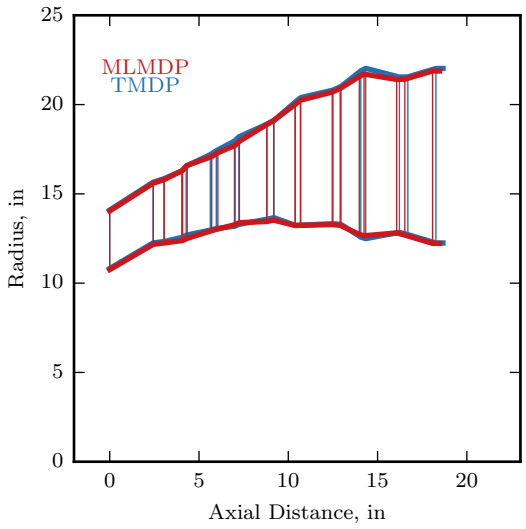

Figure 106: Optimum E^3 LPT Flowpath Produced by the MLMDP and Turbine MDP Methods.

The next problem examined in this section is the design of a conventional power turbine for the tiltorotor turboshaft engine. Similar to the E^3 LPT evaluation, the design space for the CPT was examined in terms of flow and loading coefficient slices for each stage. Figure

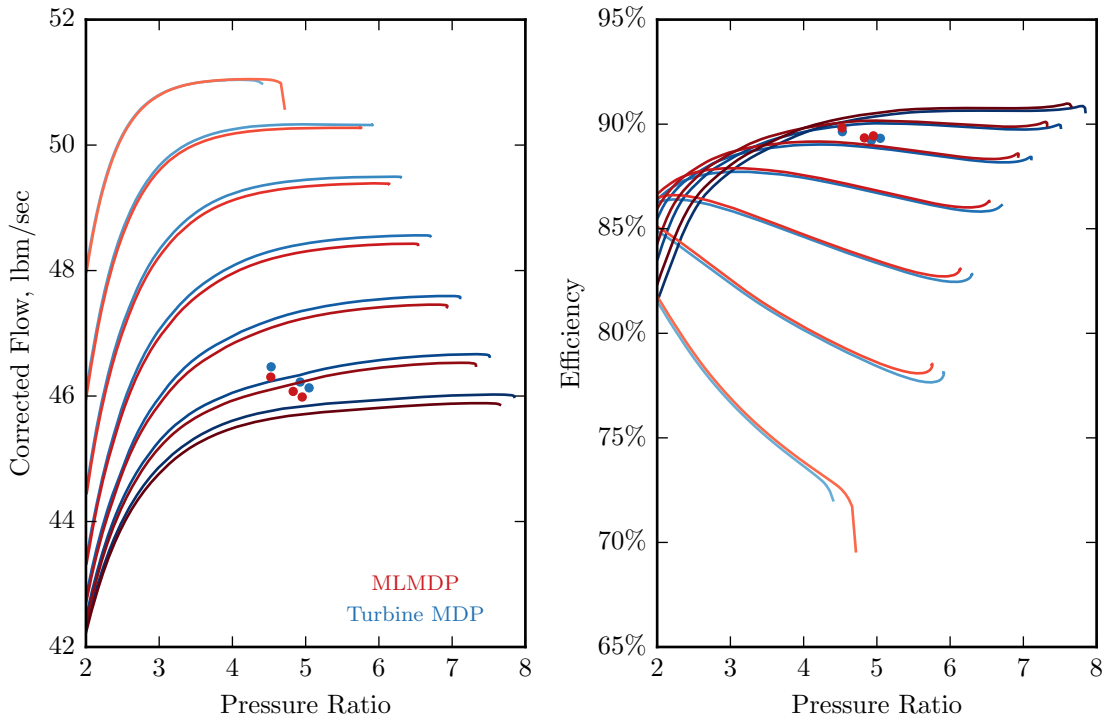

Figure 107: Optimum E^3 Performance Map Produced by the MLMDP and Turbine MDP Methods.

108 shows these slices for each stage produced by the MLMDP method in the left column and the turbine MDP method in the right column. For the first and second stages of this turbine, the efficiency contours are generally similar with a small shift in the efficiency levels throughout the spaces. However, for the last stage there is a more significant difference in the spaces produced by the two methods at high flow and loading coefficients. In the MLMDP method there is a sharp break in the efficiency contours which is not present in this design space from the turbine MDP method.

After examining these slices of the turbine design space produced by the MLMDP and turbine MDP methods, an optimization was again completed to compare the best designs. The optimum flowpath and map produced by each method are shown in Figures 109 and 110, repsectively. The flowpaths produced in the optimization are again generally geometrically similar However, the MLMDP method produced a design that was shorter with a larger radius in comparison to the turbine MDP design. For the turbine maps shown in Figure 110,

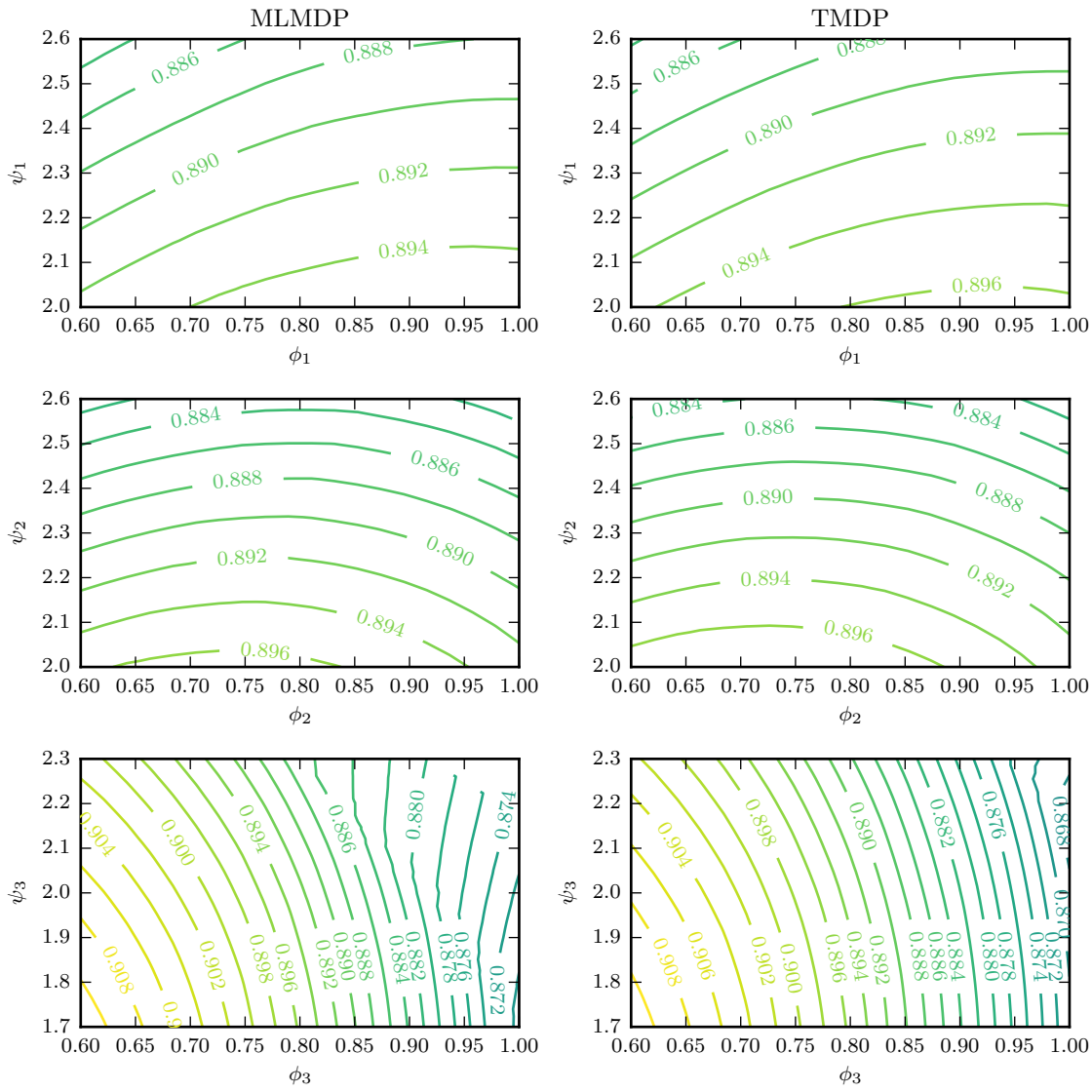

Figure 108: Turbine Design Spaces Produced by the MLMDP and Turbine MDP Methods for the CPT Design Problem.

the colored lines represented different corrected speeds (with the lightest shade representing the lowest speed and darkest shade representing the highest speed) and the dots indicated the turbine performance at each design point. Within these maps, there is a notable shift in both the location of the speed lines for the corrected flow and turbine efficiency between the two methods. These changes are the result of the cross-level coupling which alter the turbine design point operating conditions to match those determined by the cycle analysis with the meanline predicted turbine performance. These changes in the operating conditions can

be observed by comparing the relative positions of the operating points (dots) in the map figure. For example, consider the Shift1 design point which has higher corrected flow with lower corrected speed and efficiency than the other design points. Comparing the location of this point to the other design points shows that the cross-level coupling equations MLMDP method shifts this point to higher turbine pressure ratios to match the required turbine operation within the overall cycle. This shift in the operating conditions for the various design points effects the ability to satisfy the turbine performance requirements in the MLMDP and shows the importance of coupling the two analysis levels.

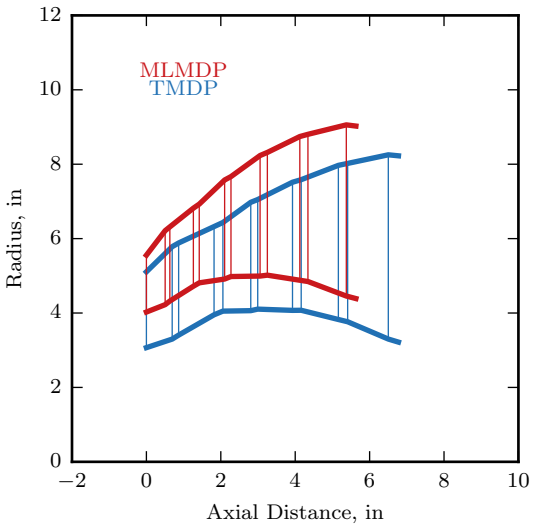

Figure 109: Optimum CPT Flowpath Produced by the MLMDP and Turbine MDP Methods.

Finally, the last problem examined in this section compares the VSPT designs produced by the MLMDP and turbine MDP methods. Again, slices of the design spaces in terms of the stage flow and loading coefficient produced by these methods were examined as shown in Figure 111. The design space plots in this figure show that the MLMDP generated spaces in the left column have similar topology to the turbine MDP generated results in the right column. The primary difference between the spaces produced by the two methods is a slight decrease in the turbine efficiency for the MLMDP method.

An optimization which considered the full turbine design space was also completed for

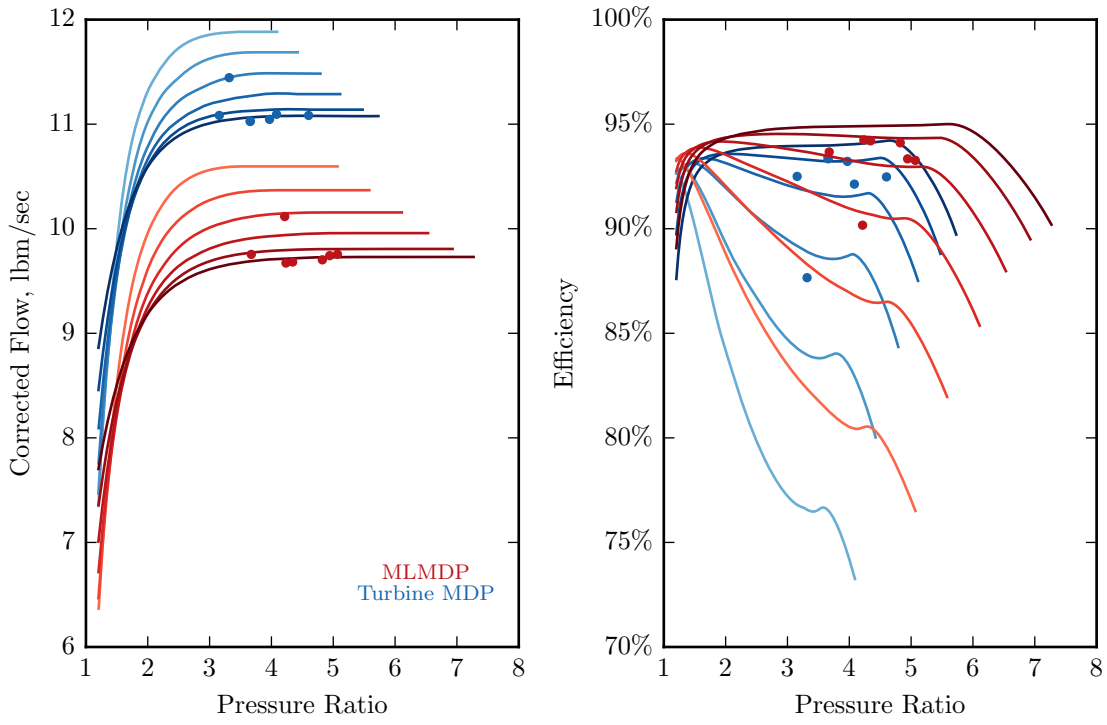

Figure 110: Optimum CPT Performance Map Produced by the MLMDP and Turbine MDP Methods.

the VSPT design problem using both design methods. The VSPT flowpaths determined through this optimization are shown in Figure 112. These flowpaths are geometrically similar with the mean radius and annulus flare following similar contours for both designs. However, the turbine design produced by the MLMDP method is shorter in length than the turbine MDP generated design. This change in turbine length is important as it potentially reduces the weight of the turbine and overall engine.

The turbine maps for these optimum VSPT designs were also examined as shown in Figure 113. Overall, the contours of the speed lines for these maps are similar with the largest difference being a decrease in the turbine flow for the MLMDP design. Also, similar to the CPT design problem, these map plots note the location of the turbine design points (dots) used in both analyses. Assessing the positions of these points shows that the cross-level coupling equations present in the MLMDP method shift the relative location of these design points.

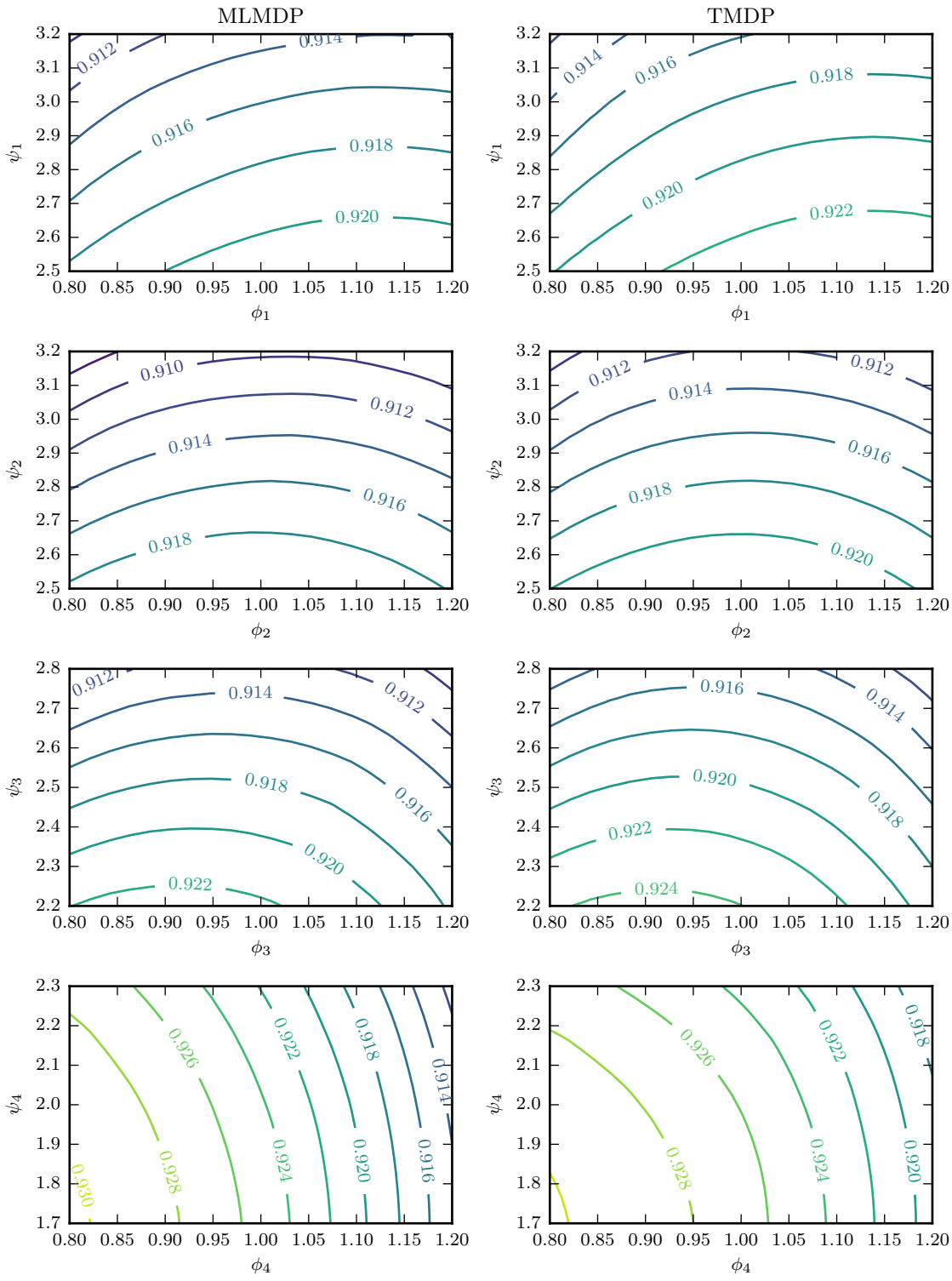

Figure 111: Turbine Design Spaces Produced by the MLMDP and Turbine MDP Methods for the VSPT Design Problem.

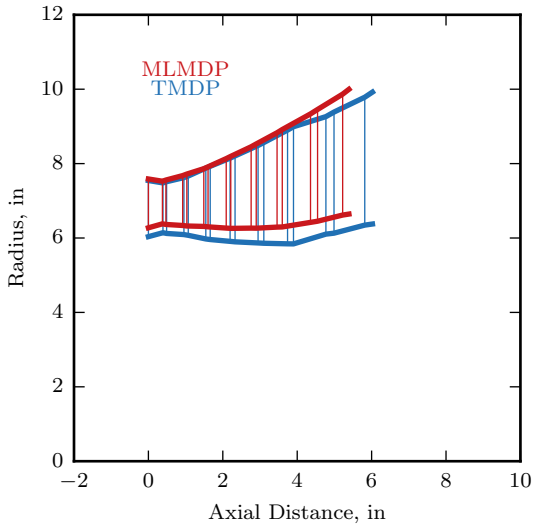

Figure 112: Optimum VSPT Flowpath Produced by the MLMDP and Turbine MDP Methods.

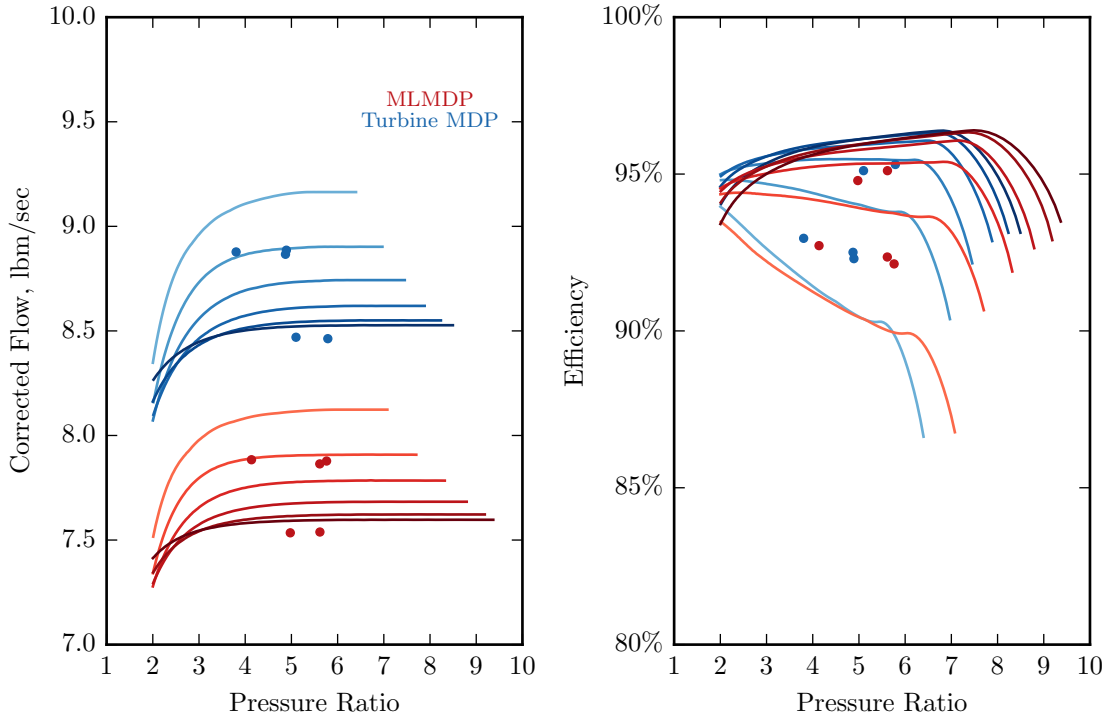

Figure 113: Optimum VSPT Performance Map Produced by the MLMDP and Turbine MDP Methods.

In summary, the second part of Experiment 4 examined the turbine designs produced by the MLMDP method and the isolated turbine MDP method. The computational results for the three problems examined slices of the design space as well as the optimum turbine designs produced by each method. Generally, the design spaces slices for the three problems have similar topologies with small changes to the overall turbine efficiency levels predicted by the methods. This closeness in the turbine performance is the result of the loss model used in the meanline analysis depending primarily on the values for the input similarity parameters which are the same for both methods. The small differences in efficiency result from changes to secondary effects in the loss model based on the physical turbine size and changes to the operating conditions for each design point. The changes in the operating conditions were observed by plotting the design points on the turbine maps produced by each method. In total, the results from all three models show that the cross-level coupling equations applied in the MLMDP method altered the turbine operating points, flowpath designs and the performance maps.

6.7 Summary

At the beginning of the chapter, two research questions and hypotheses were presented which considered the potential for developing a multi-level multi-design point (MLMDP) methodology for simultaneously creating engine cycle and turbine designs. The contents of this chapter then explored these two research questions and formulated a new MLMDP methodology. Based on the research presented throughout this chapter, it is now prudent to return to these research questions to confirm or reject the hypotheses.

Research Question 3 presented at the beginning of this chapters focused on how to combine the previously developed cycle and turbine MDP methods to simultaneously develop designs at both levels. The hypothesis for this question stated that the two MDP methods could be combined by forming an additional set of cross-level coupling equations to supplement the design point coupling equations found in the cycle and turbine MDP methods. To begin assessing this question and hypothesis, a review and assessment of existing approaches for integrating the cycle and turbine meanline analysis levels was completed. This

assessment focused on the decoupled and partially integrated approaches and attempted to apply the approaches in an example design of a turboshaft engine with a variable speed power turbine. The investigation of these approaches showed that they can be used when MDP methods are applied at each analysis level. However, these two integration approaches did not allow for tight convergence on the turbine operating conditions and performance characteristics. In addition, the overall design process was not truly simultaneous in nature as expensive off-design calculations were required to define the turbine operating envelope and performance map which couple the levels.

Based on the results of this assessment of existing integration approaches, a new approach using cross-level coupling equations directly connecting the design points at each level was formulated and explored. This approach requires that design points be added to the two analysis levels in pairs then directly couples the turbine operating conditions and performance characteristics at these points. The assessment of this integration approach on the turboshaft and VSPT example problem showed that significantly tighter convergence could be achieved between the analysis levels compared to the partially integrated approach. Furthermore, the direct coupling of the design points at each level eliminated the need for off-design analysis at each level to compute the turbine operating ranges and turbine performance map. Eliminating these steps therefore allowed for a simultaneous development of both the engine cycle and turbine designs. Following the development and initial assessment of this new integration approach specifically designed for coupling MDP methods at each level, the complete MLMDP procedure was described.

To evaluate the capabilities of the developed MLMDP method, the method was implemented on three example problems: the redesign of the E^3 engine and its LPT, the design of turboshaft engine with a conventional power turbine for a tiltrotor aircraft, and the design of turboshaft engine with a variable speed power turbine, also for a tiltrotor aircraft. These three design problems were selected as they differ in the engine and turbine architectures, number of design points, performance requirements and constraints which will thoroughly test the MLMDP method. With these three design problems identified, Experiment 3 was conducted to validate the capabilities of the MLMDP on this range of

problems. In this experiment, design spaces consisting of both cycle and turbine design variables for each problem were explored with a 10,000 case random sample DoE. The results from these DoEs showed that the MLMDP method generated valid designs in well over 90% of the cases. In addition, examining the solver statistics for these results showed that the cross-level coupling equations were generally converged in less than 10 iterations. This high success rate across a range of design problems coupled with the expedient convergence between the analysis levels confirmed Hypothesis 3 that cycle and turbine designs can be simultaneously developed to satisfy all performance requirements and constraints by forming a system of equations consisting of the cycle MDP, turbine MDP and cross-level coupling equations.

Next, Experiment 4 was completed to address Research Question and Hypothesis 4. This research question inquired about the differences in the engine and turbine designs produced by the MLMDP method versus those produced by the individual cycle and turbine MDP methods. The hypothesis for this experiment stated that the designs produced by the respective methods would differ as a result of the cross-level coupling equations present in the MLMDP method. Experiment 4 evaluated this hypothesis by first comparing the cycle designs produced by the cycle MDP and MLMDP methods. In this part of the experiment, it was found that the topology of the cycle design space, particularly for the turboshaft design problems, is altered in the MLMDP method as a result of coupling to the turbine MDP analysis. In these problems, the effective PSFC of the MLMDP generated designs was lower and the OPR and nozzle pressure ratio of the optimum design were also shifted. The E^3 engine did not experience as significant of a change in the cycle design space topology and optimum location as the LPT performance map used in the cycle MDP was extremely close to the turbine performance characteristics predicted by the turbine MDP in the MLMDP method. For all three design problems, a more detailed comparison of the optimum cycle designs produced by all three methods was also completed.

The second part of Experiment 4 compared the design of the turbines produced by the MLMDP method and isolated turbine MDP methods for all three problems. In this comparison, slices of the design space were first evaluated to compare the topology of the turbine

efficiency over the design space. These slices generally showed that the overall efficiency topology of the design space is not significantly impacted by the coupling of the analysis levels. This is the result of the efficiency computed by the turbine meanline models primarily depending on non-dimensional similarity parameters with secondary effects for the physical turbine size. However, examining the optimum flowpath designs and performance maps reveals more significant differences in the turbine designs produced by the two methods. In all three example problems, coupling the turbine design to the cycle with the cross-level equations altered the sizing of the turbine annulus and flowpath. Furthermore, the coupling changed the turbine performance map, predominantly by changing the corrected flow characteristics as a function of speed. Examining the turbine operating points on the performance map for each level also showed that the MLMDP method altered the relative location of these points in response to changes in the cycle from the turbine performance prediction.

The results from both parts of Experiment 4 allow for an assessment to be made regarding Hypothesis 4. This hypothesis stated that the engine and turbine designs produced by the individual cycle and turbine MDP methods will differ from those developed by the MLMDP method as a result of the cross-level coupling equations. The first part of the experiment showed that coupling the cycle MDP to the turbine analysis in the MLMDP method changed the cycle design space resulting in different optimum designs from the two methods. This change was particularly notable in the design of the two turboshaft engines as a representative power turbine map was not selected for the cycle MDP model. In the second part of the experiment, the comparison of the turbine design spaces showed that coupling the analysis levels did not have a significant impact on the efficiency contours within the space. However, coupling in the cycle analysis in the MLMDP method did alter the operating conditions for the turbine design points, ultimately resulting in different turbine flowpath designs and performance maps. These results therefore confirm the fourth hypothesis that the cycle and turbine designs generated with the MLMDP method will be altered relative to the cycle and turbine MDP generated designs due to the cross-level coupling equations.

CHAPTER VII

CONCLUSION

The research contained in this thesis examined the development of a turbine multi-design point (MDP) methodology along with a coupled cycle and turbine multi-level, multi-design point (MLMDP) methodology. Development of these MDP methods was motivated by ongoing research within NASA's Revolutionary Vertical Lift Technology Project to investigate engine concepts for tiltrotor aircraft. The design of these engines and their associated power turbines places a number of stringent requirements and constraints on both the engine and turbine designs throughout the operating environment. The turbine MDP and MLMDP methods developed in this thesis allow for determining feasible engine and turbine designs by simultaneously considering the requirements and constraints at multiple operating conditions in the design process. These two methods were developed and evaluated in this thesis through the examination of four research questions, hypotheses and experiments as summarized in the next section. Following this review of the research questions, hypotheses and experiments, significant contributions from this work and areas for further research are discussed.

7.1 Review of Research Questions, Hypotheses and Experiments

The primary objective of this thesis stated at the end of Chapter 2 was to develop a combined engine and turbine design process that simultaneously considers the requirements and constraints present at multiple operating conditions for both the turbine and engine cycle. This objective was addressed by first focusing on the development of an approach for designing the turbine that simultaneously considered the turbine requirements and constraints at all operating conditions. Development and assessment of this turbine MDP method was guided by the first two research questions. This turbine MDP method then served as a starting point for formulating a design approach that simultaneously considered the engine cycle and turbine design. Development and assessment of this multi-level MDP

methodology was guided by the third and fourth research questions contained in this thesis.

The first research question posed in this thesis inquired about how the MDP method previously developed for the cycle analysis of gas turbine engines could be generalized and applied to other engine components, specifically the turbine. The hypothesis for this question stated that the existing MDP method could be generalized and applied to the turbine by identifying the appropriate parameterization for the turbine design and determining the design rules to form a system of equations that couple the design points. Evaluation of this hypothesis began by completing a detailed review of the cycle MDP method and making several key observations regarding the design parameterization and coupling equations. These observations served as a critical step for defining these two key steps in the turbine MDP process. With the turbine MDP process defined, Experiment 1 was completed to assess the ability of the selected parameterization and coupling equations within the overall method to produce designs which satisfied all turbine performance requirements and constraints. The first part of the experiment specifically analyzed the turbine design parameterization to assure that similarity in the flowpath and velocity vector design was maintained over different design inputs and requirements. The second part of the experiment applied the complete method to three selected design problems to ensure that the coupling equations produced designs that satisfied all requirements and constraints. The results from these three design problems showed that the turbine MDP method and specifically the coupling equations selected produced feasible designs in approximately 95% or more of cases throughout the turbine design spaces. This high success rate confirmed the first hypothesis that the existing cycle MDP method could be generalized and applied to the turbine by identifying the proper design parameterization and design point coupling equations.

The second research question investigated in this thesis examined the differences in the turbine designs produced by the traditional single point design approach and the new multi-design point methodology. The hypothesis for this question stated that the designs produced by these two methods would differ as a result of the design rules which coupled the turbine design points. Experiment 2 evaluated this question in two parts. The first part of the experiment examined the turbine design spaces produced by both methods for

all three sample problems used in Experiment 1. This evaluation compared slices of the high-dimensional design space representative of the Smith chart for each stage, the ability to satisfy the requirements and constraints, and the changes to the coupling independents between the methods. These results showed that the turbine MDP method altered the turbine design space and coupling independent values to satisfy all the requirements and constraints. However, when the traditional single point design approach was used significant portions of the design space were determined to be infeasible. The second part of this experiment compared the resulting designs from each method from selected inputs within the design space. This comparison considered the flowpath geometry, velocity vectors and performance maps for each design. For all three of these metrics, the designs generated by each method generally produce similar results with the largest differences being in the sizing of the turbine flowpath. This similarity results from the primary dependence of the velocity triangles and performance on the input similarity parameters with only secondary effects from the physical turbine size. While the differences between the individual designs selected for comparisons were small, the evaluation of the completed design space showed the turbine MDP changes the overall space by making the entire space feasible. Therefore, the second hypothesis stating that the designs produced by the turbine MDP method differ from those produced by the traditional single point approach as a result of the design rules that couple the design points.

Following the development and assessment of the turbine MDP method, the second half of this thesis examined the development of a MLMDP method to simultaneously design the cycle and turbine to satisfy all performance requirements and constraints. Research Question 3 inquired about how the existing cycle MDP method and the newly developed turbine MDP method could be combined to produce this method. The hypothesis for this question stated that the methods could be combined by forming an additional system of equations which coupled the design points at each level. To evaluate this hypothesis, a review and assessment of current approaches for integrating the cycle and turbine analysis levels was completed. In this assessment, two approaches were evaluated with an MDP method applied within the levels. While the partially integrated approach did converge the

analysis levels, it was not able to do so to a tight tolerance. Furthermore, this method required extensive off-design evaluation at each level to define the turbine operating ranges and performance map making the approach not simultaneous. Therefore, a new approach which used cross-level coupling equations to directly couple design points at each analysis level was developed and assessed. This assessment showed that the MLMDP method using cross-level coupling equations enabled tighter matching across the analysis levels in a simultaneous process that did not require any off-design analysis. Experiment 3 further evaluated this developed MLMDP method by applying it to the design of three engine and turbine combinations. The high percentage of cases converged throughout the design spaces for each problem supported Hypothesis 3 that the MDPs at each level could be combined with cross-level coupling equations to generate designs that simultaneously satisfy all performance requirements and constraints.

Finally, the fourth research question inquired about the differences in the engine and turbine designs produced by the MLMDP method and those produced by the cycle and turbine MDP methods respectively. The hypothesis for this question stated that the designs produced by these methods would differ as a result of the cross-level coupling equations. Experiment 4 evaluated the hypothesis by again examining the results produced by each method for three different engine and turbine design problems. The first part of the experiment evaluated the cycle designs and design spaces and showed that the cross-level coupling in the MLMDP method altered the cycle designs, particularly when the turbine performance map selected in the cycle MDP model did not closely match the turbine performance predicted by the meanline model. For two of the problems examined, the MLMDP method changed the overall pressure ratio and nozzle pressure ratio of the optimum design, highlighting the importance of this coupling. The second part of the experiment compared the turbine designs produced by the turbine MDP and MLMDP methods. The results from this part of the experiment showed that in the slices of the design space examined only minor differences in the design space topology existed. However, when comparing the optimum designs produced by each method for the three design problems, larger differences were observed. These differences altered both the turbine flowpath and performance map

as a result of the turbine operating conditions determined by the cycle changing in the MLMDP method. Overall, the results from Experiment 4 confirmed the fourth hypothesis that the cross-level coupling equations used in the MLMDP method would alter the engine and turbine designs produced relative to those generated by the individual cycle and turbine MDP methods.

7.2 Summary of Contributions

The research work completed in this thesis provide a number of contributions to the field of aerospace engineering. The first principle contribution of this research was the development of a turbine MDP method to enable generation of turbine designs that simultaneously satisfy all performance requirements and constraints present throughout the turbine operating envelope. This method identifies these critical performance requirements and constraints leading to the formation of individual design points which must be included in the analysis. The performance requirements and constraints are then transformed into a set of design rules which couple the design points enabling the simultaneous solution. Also, documentation and implementation of these design rules within the model provides a consistent, repeatable approach for modifying the design inputs to ensure the performance requirements and constraints are satisfied.

The second principle contribution from this research was the formulation of a multi-level MDP method which merges the cycle and turbine MDP process to simultaneously design the engine and turbine. The coupling of these two MDP methods was completed by forming an additional set of design rules which ensure the turbine performance matches across the engine cycle and turbine meanline analysis levels. Development of these cross-level coupling equations allows for both the cycle and turbine to be designed in a simultaneous approach to satisfy all engine and turbine performance requirements and constraints which may be present at different operating conditions. Overall, the coupling of these MDP methods at the two analysis levels produces engine and turbine designs which differ from those which would be produced by completing the MDP analyses at each level separately. Furthermore, the MLMDP method and specifically the coupling equation approach for integrating the

analysis levels provides a new multi-fidelity integration (zooming) method to the existing integration techniques. This method can be used in the conceptual design of new engines where the component geometry is not yet known and was shown to enable tight convergence across the analysis levels.

In addition to these principle contributions, a supporting contribution of this work was the identification of the fundamental elements required to enable MDP approaches to be applied to a variety of problems. These fundamental elements include the appropriate parameterization of the design to be developed and the various classes of parameters required to solve the MDP coupling equations. Identification of these elements stemmed from the critical observation that MDP methods are sizing processes requiring the model to be specified in terms of similarity parameters with a sizing parameter included in the design rules.

Finally, the last significant contribution of this thesis was the decomposition of the system of equation solved as part of the MDP method into a set of smaller systems. This decomposition takes advantage of the known relationships between the independent parameters and dependent equations in these models and creates a hierarchical solver structure. Development of this structure also identified important factors which must be considered when using this structure coupled with a finite difference derivative calculation approach. These factors included setting the appropriate solver tolerances and perturbation step sizes at each level.

7.3 Recommendations for Further Research

While the research presented in this thesis contains several important contributions, several areas prime for further investigation can be identified. First, the turbine MDP and MLMDP methods developed in this thesis specifically focused on the design of the low pressure or power turbine engine components. These components, specifically the power turbines, were selected for this preliminary design investigation as a result of the motivating problems presented at the beginning of this document. However, the methods developed in this research are expected to be easily adaptable to other turbomachinery components in

gas turbine engines. One turbomachinery component that could be of particular interest for generalizing and applying these methods would be the compressor. In particular, compressors with variable vanes present a unique design challenge as the vane angle provides an additional operating parameter which can be used to satisfy the performance requirements and constraints present at different operating points. Another component that may benefit from the application of these MDP methods is the high pressure turbine, especially if the turbine models incorporate cooling flows that must be matched with the rest of the cycle.

A second area for further development of the turbine MDP method (and by extension the MLMDP method) is the application of the methods to turbomachinery models with higher fidelity levels. The research presented in this thesis focused exclusively on the uses of meanline analysis methods to evaluate the turbine performance. However, as discussed in Chapter 2 there are other turbomachinery analysis approaches that could be used that are often considered higher fidelity such as streamline analysis. Further research is required to validate that the turbine MDP and MLMDP methods could be applied to these types of analyses. It is expected that the primary challenge associate with extending methods to these types of analyses will be identifying an appropriate model parameterization that will be consistent with the MDP sizing process.

The next area for potential further research focuses on the details of how the systems of equations in the turbine MDP and MLMDP method are solved. As noted in the implementation section for each method, the solution process in the OTAC and NPSS analysis codes required computing elements of the Jacobian matrix with finite difference techniques. This process can be time consuming and can introduce errors in to the partial derivatives, especially when internal solvers are present. Emerging approaches for analytically computing the required derivatives and combining them together to solve the complete system of equations in these methods may improve the overall performance.

Another area for future research is the development of loss models for unconventional turbine designs such as the VSPT. The research on the VSPT design conducted over the past few years has included examination of blade geometries for reducing losses due to high incidence angles through both computational and experimental approaches.[113, 10, 37, 106, 39]

While this extensive research has quantified the performance characteristics of these specially designed blades, the knowledge gained from this research has not yet been incorporated into the meanline analysis. The analysis completed in this thesis used the best existing loss models as the focus of the research was on the MDP method development. To capture the new VSPT design characteristics in the meanline design process, the computational and experimental data needs to be used to revise existing loss models or develop new loss correlations. Translating this data into new or improved loss model correlations is a difficult task as it requires attributing the losses to different sources and identifying the design characteristics affecting each loss source. While this process could be completed manually by an experienced turbomachinery designer, the process of developing the new or revised loss models may benefit by the application of modern machine learning techniques.

The final area for further research is the incorporation of the engine MLMDP design methodology into the overall vehicle design. The process developed in this thesis focused on designing the engine and turbine in isolation from the rest of the aircraft. As a result, the critical operating conditions, performance requirements such as thrust or shaft power, and design points were identified a priori and held constant throughout the design process However, the design, performance characteristics and weight of the engine determined in the MLMDP analysis will undoubtedly influence the resulting vehicle design. This is similar to how the design of the cycle and turbine changed by integrating the analysis levels together as was completed in Experiment 4. Integrating the engine MLMDP method with the overall vehicle design is therefore expected to alter the vehicle, engine and component designs. Integration of the vehicle and engine analyses currently is completed by generating a tabular engine performance deck which specifies the engine thrust/power and fuel consumption as a function of Mach number, altitude and throttle setting. In addition, the design of the vehicle is commonly completed using a single design mission with other performance requirements and constraints evaluated later in the design process. The coupled design process of the vehicle and engine could therefore potentially be improved by adapting the MDP method for the vehicle design and extending the MLMDP method to cover both disciplines. Formulating such a method would facilitate the convergence of the vehicle, engine and component designs

and allow for simultaneous design development.

APPENDIX A

E^3 ENGINE MDP MODEL

In order to facilitate the development of the E^3 LPT MDP model and the E^3 engine/LPT MLMDP model, a cycle model of the E^3 engine needed to be first constructed. This model could then be used to determine turbine operating conditions and performance requirements for the LPT MDP analysis and serve as a starting point for the MLMDP analysis. Therefore, an MDP model of the E^3 thermodynamic cycle was developed in NPSS.

The starting point for the E^3 cycle MDP model development were two previously constructed SPD models of the engine by Claus[21] and Denney.[1] The models from these two sources were generally consistent and produced similar output. However, these models were developed in older versions of NPSS, therefore requiring a new E^3 SPD engine model to be developed. The new model blends elements from both of these previous models, with results from the new model closely matching output at three operating conditions provided with the Claus model. This SPD model was then convert to an MDP model following procedure developed by Schutte.[97] The following sections briefly describe how steps 1 through 7 of the cycle MDP procedure were applied to the E^3 engine.

Step 1: Identify performance requirements and constraints

Based on the engine model developed by Claus, four performance requirements and constraints were developed for the E^3 engine and are defined in Table 15. The requirements capture the required engine thrust at the engine aerodynamic design point (cruise), top of climb operating condition and sea level static. Additionally, a maximum allowable combustor temperature is specified for all flight conditions.

[1] Unpublished NPSS model from Russell Denney, Research Engineer II in the Aerospace Systems Design Laboratory at the Georgia Institute of Technology, October 2015.

Table 15: Performance Requirements for E^3 Engine

Name	Value	Description
ADP Thrust	8500 lbf	Minimum net thrust at cruise (ADP) condition
TOC Thrust	9100 lbf	Minimum net thrust at top of climb (TOC) condition
SLS Thrust	40000 lbf	Minimum net thrust at sea-level static (SLS) condition
Maximum T4	3100 °R	Maximum allowable combustor exit temperature

Step 2: Select engine architecture and create cycle model

The E^3 engine is a high BPR mixed flow turbofan engine.[30] In addition to the primary splitter following the fan, an additional splitter is located aft of the LPC, with the bypass flow from both splitters combining in a mixer in the bypass duct. This bypass flow is mixed with the core flow prior to exiting the engine nozzle. This engine architecture was captured in the NPSS model by linking together components as shown in Figure 114.

Step 3: Identify cycle design variables and technology parameters

For the E^3 engine, the design variables are defined in Table 16. Since the E^3 engine is an existing engine with a specific technology level, no technology parameters were selected for inclusion in the MDP model.

Table 16: Design Variables for E^3 Engine

Name	Description	Design Point
FPR	Fan Pressure Ratio	ADP
LPCPR	LPC Pressure Ratio	ADP
HPCPR	HPC Pressure Ratio	ADP
BPR	Bypass Ratio	ADP
CDF	Core Stream Dump Fraction	ADP
T4max	Maximum Combustor Exit Temperature	All

Step 4: Establish technology rules

The establishment of technology rules for the E^3 engine primarily involved selection of performance maps for each of the engine components. The performance maps for this model

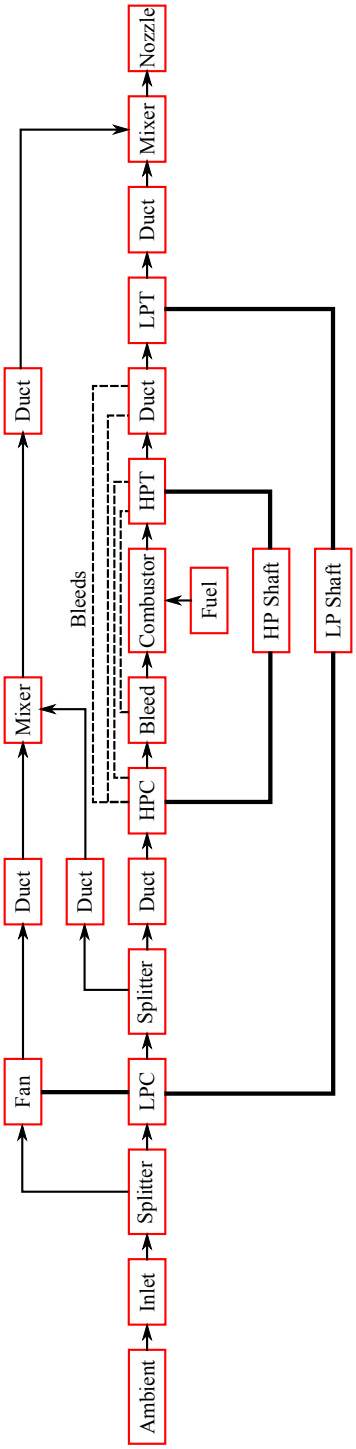

Figure 114: Block Diagram of E^3 Engine.

were taken from the E^3 model by Denney.

Step 5: Specify design points and map scaling point

From the performance requirements and constraints determined in step 1, a set of three design points were identified and are listed in Table 17. These design points are at the cruise condition which is the aerodynamic design point, the top of climb condition and the sea level static condition.

Table 17: Design Points for E^3 Engine

Design Point	**Label**	**Mach**	**Altitude**	**ΔT**
Aero Design Point	ADP	0.8	35000 ft	+18 °R
Top of Climb	TOC	0.8	35000 ft	+18 °R
Sea-Level Static	SLS	0.0	0 ft	+27 °R

Step 6: Create design point mapping matrix

The information gathered in the previous steps was combined to form the DPMM as shown in Table 18. This information was then incorporated into the SPD cycle model to form the MDP model.

Step 6: Construct system of nonlinear equations

Step 7 of the cycle MDP process defines the design rules which are used to construct a system of nonlinear equations forming the MDP analysis. The design rules establish a set of independent values which are varied by the solver to match the performance requirements and constraints. The design rules formulated for the E^3 engine are defined in Table 19.

Table 18: Design Point Mapping Matrix for E^3 Engine

		Design Point		
		ADP	TOC	SLS
Map Scaling Point		ADP		
Design Variables	FPR	1.64		
	LPCPR	1.66		
	HPCPR	22.4		
	BPR	3.484		
	CDF	0.81196		
	T4			3100 °R
Performance Requirements	ADP Thrust	8500 lbf		
	TOC Thrust		9100 lbf	
	SLS Thrust			40000 lbf
Component Performance	Inlet Pressure Recovery	1.0		
	Fan Adiabatic η	0.894		
	LPC Adiabatic η	0.906		
	HPC Adiabatic η	0.861		
	Burner η	0.98		
	HPT Adiabatic η	0.927		
	LPT Adiabatic η	0.925		
	Nozzle Cv	1.0		
Technology Limits	T4 Max			3100 °R
	DL 2			
	DL 3			

Table 19: Independent-Dependent Set for E^3 Engine

Number	Independent	Dependent
1	ADP Mass Flow	ADP Net Thrust
2	ADP FAR	SLS T4
3	TOC FAR	TOC Net Thrust
4	SLS FAR	SLS Net Thrust

APPENDIX B

CPT TURBOSHAFT ENGINE MDP MODEL

In order to determine the operating conditions and design requirements of the CPT MDP model a cycle model of the CPT turboshaft engine was constructed in NPSS. This model was developed from the SPD model previously analyzed by of Snyder[100] with assumptions updated to better reflect current design limits. The following sections briefly describe implementation of steps 1 through 7 of the cycle MDP procedure on the CPT turboshaft engine.

Step 1: Identify performance requirements and constraints

The performance requirements and constraints for the CPT were derived from the report by Snyder.[100] Power requirements at six potentially critical operating conditions were identified. In addition, several different combustor exit temperature constraints were identified. These combustor exit temperature constraints correspond to the engine power rating levels defined in Table 2. The derived requirements and constraints are outlined in Table 20.

Step 2: Select engine architecture and create cycle model

The architecture for the turboshaft engine was also defined in the report by Snyder and a similar architecture was adopted for this study. The engine has a low pressure spool and high pressure spool forming the core, with a free power turbine providing power to the rotor. The high pressure compressor is comprised of several axial stages and a centrifugal stage. A block diagram showing the components of the turboshaft engine and how they are connected is provided in Figure 115.

Step 3: Identify cycle design variables and technology parameters

For the CPT turboshaft engine, a set of design variables were identified as given in Table 21.

Table 20: Performance Requirements for CPT Turboshaft Engine

Name	Value	Description
ADP Power	1800 hp	Minimum shaft power at cruise (ADP) condition
TOC Power	1900 hp	Minimum shaft power at top of climb (TOC) condition
HOGE Power	4150 hp	Minimum shaft power at hover out of ground effect (HOGE) condition
OEI Power	5150 hp	Minimum shaft power at one engine inoperative (OEI) condition
Climb Power	2600 hp	Minimum shaft power at climb start condition
Shift Power	3750 hp	Minimum shaft power at shift (SH) condition
MCP T4 Max	3260 °R	Maximum allowable combustor exit temperature for MCP flight conditions
IRP T4 Max	3410 °R	Maximum allowable combustor exit temperature for IRP flight conditions
MRP T4 Max	3460 °R	Maximum allowable combustor exit temperature for MRP flight conditions
CRP T4 Max	3510 °R	Maximum allowable combustor exit temperature for CRP flight conditions

Table 21: Design Variables for CPT Turboshaft Engine

Name	Description	Design Point
LPC PR	LPC Pressure Ratio	ADP
HPCa PR	Axial HPC Pressure Ratio	ADP
HPCc PR	Centrifugal HPC Pressure Ratio	All

Step 4: Establish technology rules

The establishment of technology rules for the CPT turboshaft engine primarily involved selection of performance maps for each of the engine components. The performance maps match those from the model analyzed by Snyder.[100]

Step 5: Specify design points and map scaling point

From the performance requirements and constraints determined in step 1, a set of 7 design points were identified and are listed in Table 22. These operating conditions are defined by the overall flight conditions (Mach number, altitude, and deviation in static temperature

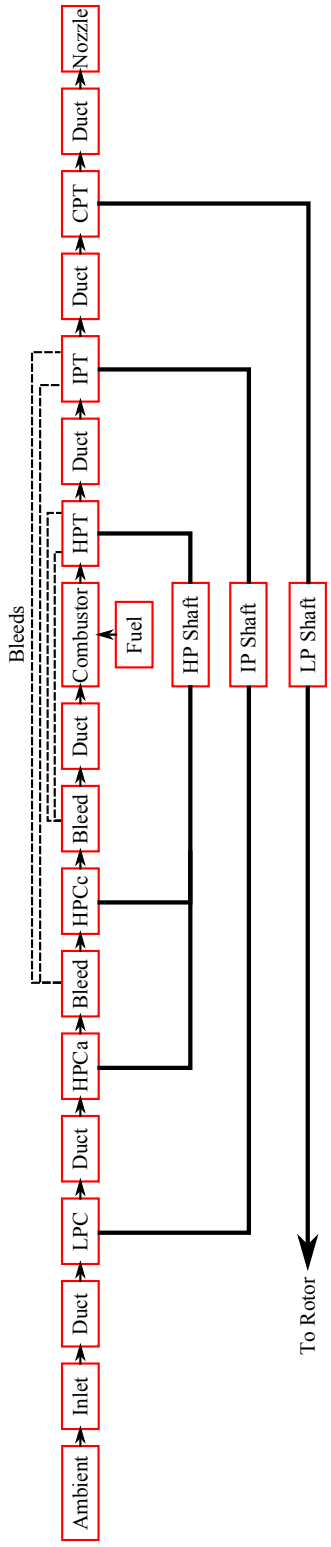

Figure 115: Block Diagram of CPT Turboshaft Engine.

from the standard day) as well as the physical shaft speed of the CPT required to match the rotor. The map scaling point is selected as the aerodynamic design point (ADP).

Table 22: Design Points for CPT Turboshaft Engine

Design Point	Label	Mach	Altitude	ΔT	%N	Rating
Aero Design Point	ADP	0.5	28000 ft	+0 °R	85.0	MCP
Top of Climb	TOC	0.5	28000 ft	+0 °R	85.0	IRP
Hover Out of Ground Effect	HOGE	0.0	5000 ft	+36 °R	100.0	MRP
One Engine Inoperative	OEI	0.0	5000 ft	+36 °R	100.0	CRP
Start of Climb	Climb	0.3	8000 ft	+36 °R	85.0	IRP
Pre-Shift	Shift1	0.25	6000 ft	+36 °R	61.5	IRP
Post-Shift	Shift2	0.25	6000 ft	+36 °R	85.0	IRP

Step 6: Create design point mapping matrix

The information gathered in the previous steps was combined to form the CPT turboshaft DPMM found in Table 23. This information was then incorporated into the turboshaft cycle model.

Step 6: Construct system of nonlinear equations

Finally, the set of design rules which are used to construct a system of nonlinear equations forming the MDP analysis. The design rules establish a set of independent values which are varied by the solver to match the performance requirements and constraints. The design rules formulated for the CPT turboshaft engine are defined in Table 24.

Table 23: Design Point Mapping Matrix for CPT Turboshaft Engine

		Design Point						
		ADP	TOC	HOGE	OEI	Climb	Shift1	Shift2
Map Scaling Point		ADP						
Design Variables	LPCPR	5.0						
	HPCaPR	3.0						
	HPCcPR	2.7						
Performance Requirements	ADP Power	1800 hp						
	TOC Power		1900 hp					
	HOGE Power			4150 hp				
	OEI Power				5150 hp			
	Climb Power					2600 hp		
	Shift Power						3750 hp	3750 hp
Component Performance Parameters	Inlet Pressure Recovery	1.0						
	LPC Adiabatic η	0.89						
	HPCa Adiabatic η	0.89						
	HPCc Adiabatic η	0.88						
	Burner η	0.999						
	HPT Adiabatic η	0.89						
	IPT Adiabatic η	0.90						
	CPT Adiabatic η	0.85						
	Nozzle Cv	0.99						
Technology Limits	MCP T4 Max	3210 °R						
	IRP T4 Max		3410 °R			3410 °R	3410 °R	3410 °R
	MRP T4 Max			3460 °R				
	CRP T4 Max				3510 °R			
	HPT Vane Temp.				2360 °R			
	HPT Rotor Temp.				2260 °R			
	IPT Vane Temp.				2360 °R			
	IPT RotorTemp.				2160 °R			

Table 24: Independent-Dependent Set for CPT Turboshaft Engine

Number	Independent	Dependent
1	ADP Mass Flow	ADP Nozzle PR
2	ADP FAR	OEI T4
3	TOC FAR	TOC Power
4	HOGE FAR	HOGE Power
5	OEI FAR	OEI Power
6	Climb FAR	Climb Power
6	Shift1 FAR	Shift1 Power
6	Shift2 FAR	Shift2 Power

APPENDIX C

VSPT TURBOSHAFT ENGINE MDP MODEL

In order to determine the operating conditions and design requirements of the VSPT MDP model a cycle model of the VSPT turboshaft engine was constructed in NPSS. This model was developed from the SPD model previously analyzed by of Snyder[100] with assumptions updated to better reflect current design limits. The following sections briefly describe implementation of steps 1 through 7 of the cycle MDP procedure on the VSPT turboshaft engine.

Step 1: Identify performance requirements and constraints

The performance requirements and constraints for the VSPT were derived from the report by Snyder.[100] Power requirements at five potentially critical operating conditions were identified. In addition, several different combustor exit temperature constraints were identified. These combustor exit temperature constraints correspond to the engine power rating levels defined in Table 2. The derived requirements and constraints are outlined in Table 25.

Step 2: Select engine architecture and create cycle model

The architecture for the VSPT engine was also defined in the report by Snyder and a similar architecture was adopted for this study. The engine has a low pressure spool and high pressure spool forming the core, with a free power turbine on its own shaft. The high pressure compressor is comprised of several axial and a centrifugal stage. A block diagram showing the components of the VSPT engine and how they are connected is provided in Figure 116.

Step 3: Identify cycle design variables and technology parameters

For the VSPT turboshaft engine, a set of design variables were identified as given in Table 21.

Step 4: Establish technology rules

Table 25: Performance Requirements for VSPT Turboshaft Engine

Name	Value	Description
ADP Power	1800 hp	Minimum shaft power at cruise (ADP) condition
TOC Power	1900 hp	Minimum shaft power at top of climb (TOC) condition
HOGE Power	4150 hp	Minimum shaft power at hover out of ground effect (HOGE) condition
OEI Power	5150 hp	Minimum shaft power at one engine inoperative (OEI) condition
Climb Power	2600 hp	Minimum shaft power at climb start condition
MCP T4 Max	3260 °R	Maximum allowable combustor exit temperature for MCP flight conditions
IRP T4 Max	3410 °R	Maximum allowable combustor exit temperature for IRP flight conditions
MRP T4 Max	3460 °R	Maximum allowable combustor exit temperature for MRP flight conditions
CRP T4 Max	3510 °R	Maximum allowable combustor exit temperature for CRP flight conditions

Table 26: Design Variables for VSPT Turboshaft Engine

Name	Description	Design Point
LPC PR	LPC Pressure Ratio	ADP
HPCa PR	Axial HPC Pressure Ratio	ADP
HPCc PR	Centrifugal HPC Pressure Ratio	ADP

The establishment of technology rules for the VSPT turboshaft engine primarily involved selection of performance maps for each of the engine components. The performance maps match those from the model analyzed by Snyder.[100]

Step 5: Specify design points and map scaling point

From the performance requirements and constraints determined in step 1, a set of 5 design points were identified and are listed in Table 27. These operating conditions are defined by the overall flight conditions (Mach number, altitude, and deviation in static temperature from the standard day) as well as the physical shaft speed of the VSPT required to match the rotor. The map scaling point is selected as the aerodynamic design point (ADP).

Step 6: Create design point mapping matrix

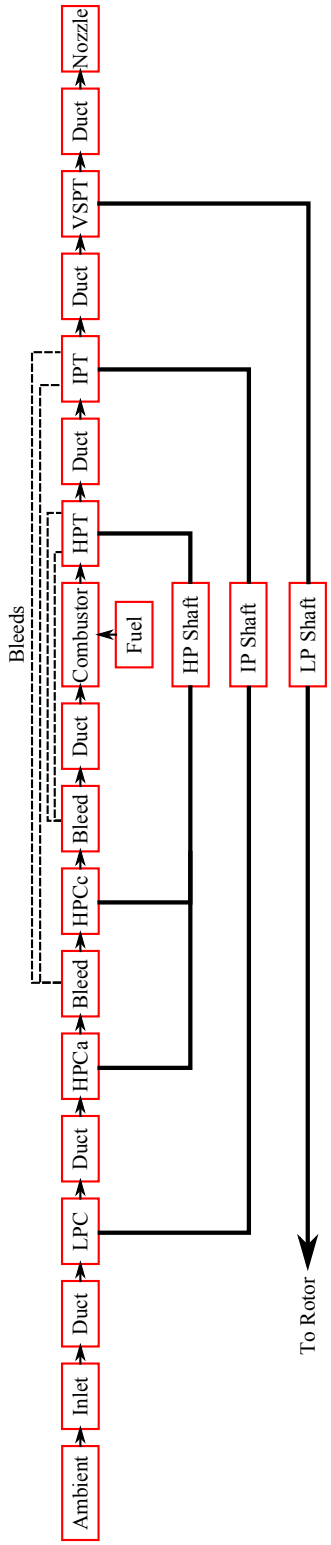

Figure 116: Block Diagram of VSPT Turboshaft Engine

Table 27: Design Points for VSPT Turboshaft Engine

Design Point	Label	Mach	Altitude	ΔT	%N	Rating
Aero Design Point	ADP	0.5	28000 ft	+0 °R	85.0	MCP
Top of Climb	TOC	0.5	28000 ft	+0 °R	85.0	IRP
Hover Out of Ground Effect	HOGE	0.0	5000 ft	+36 °R	100.0	MRP
One Engine Inoperative	OEI	0.0	5000 ft	+36 °R	100.0	CRP
Start of Climb	Climb	0.3	8000 ft	+36 °R	85.0	IRP

The information gathered in the previous steps was combined to form the VSPT turboshaft DPMM found in Table 28. This information was then incorporated into the turboshaft cycle model.

Step 6: Construct system of nonlinear equations

Finally, a the set of design rules which are used to construct a system of nonlinear equations forming the MDP analysis. The design rules establish a set of independent values which are varied by the solver to match the performance requirements and constraints. The design rules formulated for the VSPT turboshaft engine are defined in Table 29.

Table 28: Design Point Mapping Matrix for VSPT Turboshaft Engine

		Design Point				
		ADP	TOC	HOGE	OEI	Climb
Map Scaling Point		ADP				
Design Variables	LPC PR	5.0				
	HPCa PR	3.0				
	HPCc PR	2.7				
Performance Requirements	ADP Power	1800 hp				
	TOC Power		1900 hp			
	HOGE Power			4150 hp		
	OEI Power				5150 hp	
	Climb Power					2600 hp
Component Performance Parameters	Inlet Pressure Recovery	1.0				
	LPC Adiabatic η	0.89				
	HPCa Adiabatic η	0.89				
	HPCc Adiabatic η	0.88				
	Burner η	0.999				
	HPT Adiabatic η	0.89				
	IPT Adiabatic η	0.90				
	VSPT Adiabatic η	0.85				
	Nozzle Cv	0.99				
Technology Limits	MCP T4 Max	3210 °R				
	IRP T4 Max		3410 °R			3410 °R
	MRP T4 Max			3460 °R		
	CRP T4 Max				3510 °R	
	HPT Vane Temp.				2360 °R	
	HPT Rotor Temp.				2260 °R	
	IPT Vane Temp.				2360 °R	
	IPT RotorTemp.				2160 °R	

Table 29: Independent-Dependent Set for VSPT Turboshaft Engine

Number	Independent	Dependent
1	ADP Mass Flow	ADP Nozzle PR
2	ADP FAR	OEI T4
3	TOC FAR	TOC Power
4	HOGE FAR	HOGE Power
5	OEI FAR	OEI Power
6	Climb FAR	Climb Power

APPENDIX D

E^3 LPT MDP MODEL DESCRIPTION

This appendix details the implementation of the turbine MDP method on the E^3 LPT design problem which was summarized in section 5.5.1. Steps 1 through 8 of turbine MDP procedure are covered in this description.

Step 1: Identify turbine requirements and constraints

For the E^3 LPT, many of performance requirements and operating constraints were derived from an MDP model of the E^3 engine. This model was developed following the cycle MDP procedure as described in Appendix A. The performance requirements consist of the power output from the turbine at three different operating conditions. Two pressure ratio constraints were also identified from the cycle analysis model at two different operating conditions. In addition to these cycle derived constraints, an AN^2 limit was developed from the baseline turbine design and used to ensure similar blade stresses across all designs. Finally, two geometric constraints were also included for the E^3 LPT redesign. These geometric constraints set the minimum and maximum allowable flare angle for any section of the annulus. The performance requirements and constraints for the E^3 LPT are defined in Table 30.

Step 2: Select turbine architecture and create turbine model

The E^3 LPT developed by GE[18, 15] was an axial design with five stages. A cross section of the flowpath for this turbine is shown in Figure 117. It should be noted that the design presented in these references is for a subscale model which was used for experimental rig testing. This design would be resized to produce the power required in the full scale engine.

With this information, a model of the E^3 LPT was developed in OTAC based on the validation model developed by Jones[66] as shown in Figure 118. This model has five stages,

Table 30: E^3 LPT Performance Requirements and Constraints

Name	Value	Description
ADP Power	14110 hp	Minimum shaft power at cruise (ADP) condition
TOC Power	15350 hp	Minimum shaft power at top of climb (TOC) condition
SLS Power	36550 hp	Minimum shaft power at sea-level static (SLS) condition
TOC PR	4.75	Pressure ratio at top of climb (TOC) condition
SLS PR	4.34	Pressure ratio at sea level static (SLS) condition
AN^2	1.75E+10 in^2 rpm^2	Maximum AN^2
Min Flare	-5°	Minimum flare angle for any annulus section
Max Flare	30°	Maximum flare angle for any annulus section

each consisting of a vane, transition duct, rotor and second transition duct. The transition ducts are included in the model to allow for changes in mean radius and area between blade rows. In addition, a transition duct is placed upstream of the first vane to enable matching the inlet flow conditions from the design and test reports. All of the rotors are connected to a single shaft which powers the fan and LPC.

With the E^3 LPT architecture selected and the overall model structure determined, the last element of this step was to specify the design in terms of similarity parameters. The similarity parameters selected for this example problem are those defined in Section 5.3.1.

Step 3: Identify available turbine design variables

The third step of the turbine MDP procedure is to identify the turbine design variables which will be used to form the design space which will be explored in the design process. For the E^3 LPT redesign study, a relatively small set of design variables were selected which focus primarily on modifying the turbine velocity vectors. The design variables include the flow coefficient, loading coefficient, reaction and axial velocity ratio for each stage as listed in Table 31. Each of these design parameters specify the design value at the aerodynamic design point (ADP). For this redesign study, similarity parameters defining the meanline radius through the turbine and the blade geometry for the loss model were held constant

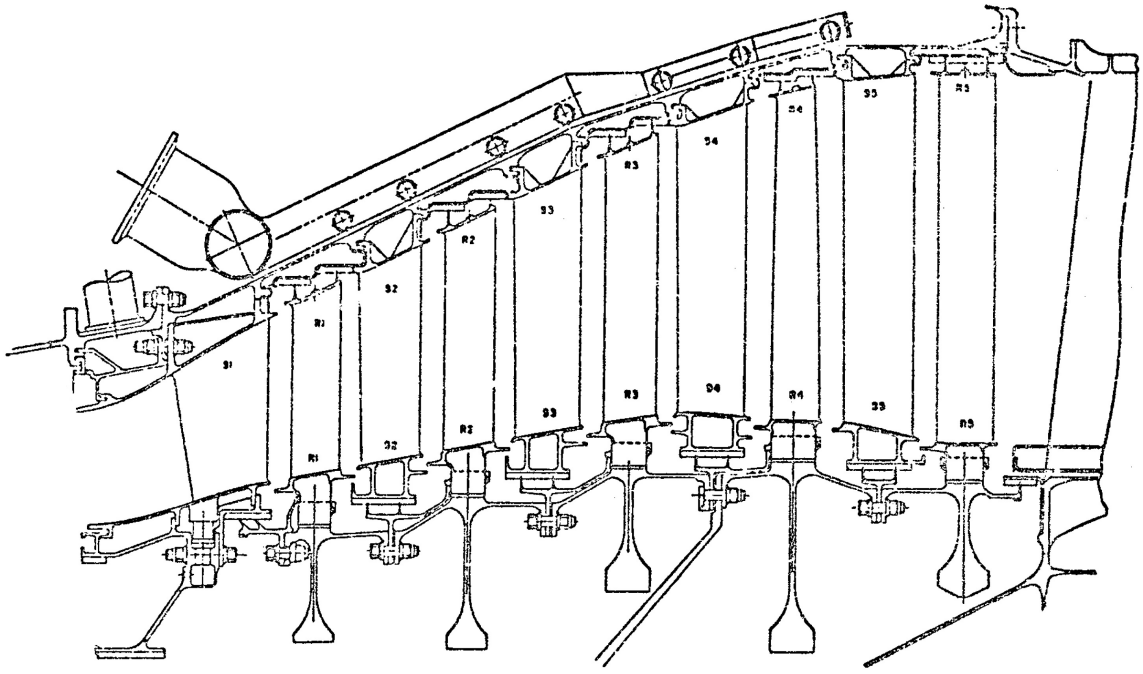

Figure 117: E^3 LPT Flowpath[15]

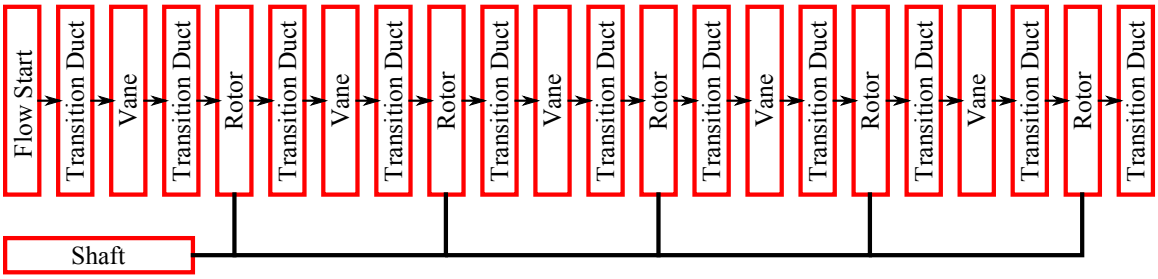

Figure 118: E^3 LPT Model Schematic

and are therefore not included in the list of design variables. For the design variables selected for this study, acceptable ranges for their values are defined in Step 8.

Step 4: Establish technology rules

An important part of the turbine MDP process is defining technology rules for the meanline analysis. These technology rules relate the performance characteristics of individual components of the turbine to the design inputs or outputs from other parts of the analysis. For the E^3 LPT redesign study, the technology rules implemented are those which define the

Table 31: E^3 LPT Design Variables

Name	Description	Stages	Design Point
ϕ	Stage Flow Coefficient	All	ADP
ψ	Stage Loading Coefficient	All	ADP
R	Stage Reaction	All	ADP
μ	Rotor Axial Velocity Ratio	All	ADP

losses in pressure produced across each blade row. These technology rules form the overall loss model implemented in analysis. In this study, the technology rules used to calculate the losses across all blade rows come from the loss model described by Kacker and Okappu.[67] The loss sources included in this model are those attributed to the blade profile, secondary flows, trailing edge thickness and tip clearance. In addition, the overall loss computations account for the Reynolds' number of the flow for each blade row.

Step 5: Specify the design points

The next step in the turbine MDP method is to identify the relevant design points which must be included in the analysis. For the E^3 LPT redesign problem, a total of three design points were identified for inclusion in the analysis. These three design points were determined from the cycle model of the engine along with the performance requirements and constraints specified in Step 1. The three design points are summarized in Table 32. The first design point is the aerodynamic design point which is representative of the cruise operating condition. It is at this point where most of the design variables for the turbine are specified. Furthermore, the turbine efficiency computed at this point is an important metric in assessing different turbine designs as the engine spends a significant portion of the flight operating at this condition. The second design point is for the top of climb flight condition which is important for the overall engine analysis as it sets the maximum corrected speed and corrected flow. The third design point is that of sea level static operation of the engine. This design point is at a lower corrected speed but corresponds to the maximum power output required for the engine.

Step 6: Create design point mapping matrix and incorporate into turbine model

Table 32: E^3 LPT Design Points

Design Point	Label	Pt	Tt	Np
Aero Design Point	ADP	39.8 psi	1915 °R	100%
Top of Climb	TOC	42.0 psi	1975 °R	101.1%
Sea-Level Static	SLS	100.3 psi	2145 °R	96.9%

The sixth step of the process to create a design point mapping matrix (DPMM). As described in the previous section, the DPMM links the design points with the design variables, performance requirements and constraints. The DPMM for the E^3 LPT is given in Table 33. For the design variables in this DPMM, a single value is listed corresponding to the baseline E^3 LPT design. Design ranges for each of these variables are specified in Step 8.

Step 7: Construct systems of equations and constraint relations that couple design points

Step 7 of the turbine MDP process is to construct the system of nonlinear equations which couple the design points. Using the information contained in the DPMM, a set of design rules for the E^3 LPT were developed based on the analysis completed in Section 5.3.2. The performance requirements identified at each design point are the power output required from the turbine at that operating condition. In addition, design rules are required to satisfy operating limits for pressure ratio and AN^2. This resulted in a total of 5 dependent equations which need to be satisfied by varying independent parameters. For the sizing independent parameter, the mean radius at the entrance to the turbine was selected. The mean radius throughout the rest of the turbine is referenced back to this value allowing the overall turbine to be sized. Consistent with the analysis completed in Section 5.3.2, the mass flow rate at ADP and the exit static pressure at TOC and SLS are used as operating parameters to match power output. Finally, the shaft speed at ADP is included as an independent to satisfy the AN^2 requirement. The shaft speed at the other design points is set based on the percent corrected speed specified in the design point definition in Step 5. The design rules formulated for the E^3 LPT are summarized in Table 34. In addition, the constraints applied within the MDP process are paired with a dependent equation in the model as described in Table 35.

Table 33: E^3 LPT Design Point Mapping Matrix

		Design Points														
			ADP					TOC					SLS			
	Stage →	1	2	3	4	5	1	2	3	4	5	1	2	3	4	5
Design Variables	Stage ϕ	1.27	1.14	1.08	1.03	1.07										
	Stage ψ	3.19	3.05	2.88	2.27	1.43										
	Stage R	0.35	0.35	0.37	0.38	0.34										
	Rotor μ	1.01	1.04	1.02	0.98	0.94										
Performance Requirements	ADP Power	14110 hp														
	TOC Power	15350 hp														
	SLS Power	36550 hp														
	SLS PR	4.34														
	SLS AN^2	1.75E10														
Design Constraints	TOC PR	4.75														
	Min Flare	-5°														
	Max Flare	30°														

Table 34: E^3 LPT Independent-Dependent Set

Number	Independent	Dependent
1	ADP Mass Flow	SLS PR
2	ADP N	SLS AN^2
3	Inlet Mean Radius	ADP Power
4	TOC Exit Static Pressure	TOC Power
5	SLS Exit Static Pressure	SLS Power

Table 35: E^3 LPT Constraint-Dependent Pairings

Constraint	Dependent	Min/Max
TOC PR	SLS PR	Max
Vane Min Flare	ADP Stage ϕ	Min
Rotor Min Flare	ADP Rotor μ	Min
Vane Max Flare	ADP Stage ϕ	Max
Rotor Max Flare	ADP Rotor μ	Max

Step 8: Assign values to turbine design variables

The next step in the process is to assign values to the turbine design variables. For this redesign study, a design space was developed by specifying a valid range of values for each of the design variables. This range is roughly centered around the baseline design variable values provided in the DPMM in Step 6. The design variable ranges selected for each variable in this study are listed in Table 36.

Table 36: E^3 LPT Design Variable Ranges

Variable	Stage1		Stage 2		Stage 3		Stage 4		Stage 5	
	Min	Max	Min	Max	Min	Max	Min	Max	Min	Max
ϕ	1.20	1.40	1.00	1.20	1.00	1.20	0.90	1.10	1.00	1.20
ψ	3.10	3.30	2.90	3.10	2.80	3.00	2.20	2.40	1.30	1.50
R	0.30	0.50	0.30	0.50	0.30	0.50	0.30	0.50	0.30	0.50
μ	0.90	1.10	0.90	1.10	1.00	1.10	0.95	1.05	0.90	1.00

APPENDIX E

CONVENTIONAL POWER TURBINE MDP MODEL DESCRIPTION

This appendix details the implementation of the turbine MDP method on the conventional power turbine design problem which was summarized in section 5.5.2. Steps 1 through 8 of turbine MDP procedure are covered in this description.

Step 1: Identify turbine requirements and constraints

Step 1 in the turbine MDP method is to identify the turbine performance requirements and constraints. The performance requirements for this turbine were primarily derived from the analysis of tiltrotor engine design requirements by Snyder[100] and are summarized in Table 37. The performance requirements include the power output from the turbine at six different operating conditions. In addition, primary operating constraints are specified for the turbine AN^2 at the one engine inoperative condition and the pressure ratio across the turbine at all operating points other than ADP. Finally, a minimum value of the stage reaction is specified for all stages at the Shift1 operating condition.

Step 2: Select turbine architecture and create turbine model

The second step of the MDP process selects the turbine architecture and creates the turbine model with an appropriate design parameterization. For the conventional power turbine, previous studies[91, 113] have identified a three stage axial architecture as the most likely turbine architecture. Therefore, this architecture was selected for the conventional power turbine design study in this research. With this three stage architecture selected, an OTAC meanline model was constructed as shown in Figure 119. In this model each stage consists of a vane, transition duct, rotor and second transition duct.

Construction of the OTAC model for the conventional power turbine also involved selecting a set of similarity parameters which specify the design. For this model, the similarity

Table 37: CPT Performance Requirements and Constraints

Name	Value	Description
ADP Power	1800 hp	Minimum shaft power at cruise (ADP) condition
TOC Power	1900 hp	Minimum shaft power at top of climb (TOC) condition
HOGE Power	4150 hp	Minimum shaft power at hover out of ground effect (HOGE) condition
OEI Power	5150 hp	Minimum shaft power at one engine inoperative (OEI) condition
Climb Power	2600 hp	Minimum shaft power at climb start condition
Shift Power	3750 hp	Minimum shaft power at shift conditions
OEI AN^2	5.0E+10 in^2 rpm^2	Maximum AN^2 at one engine inoperative (OEI) condition
TOC PR	5.1	Pressure ratio at top of climb (TOC) condition
HOGE PR	4.25	Pressure ratio at hover out of ground effect (HOGE) condition
OEI PR	4.8	Pressure ratio at one engine inoperative (OEI) condition
Climb PR	3.6	Pressure ratio at climb start condition
Shift1 PR	4.45	Maximum pressure ratio at pre-shift condition
Shift2 PR	4.25	Maximum pressure ratio at post-shift condition
Shift1 R	0.1	Minimum degree of reaction for any stage at pre-shift condition

parameters defined in Section 5.3.1 were used with one modification. The similarity parameters defining the mean radius across each blade row and transition duct were redefined such that the denominator for all μ parameters referenced the mean radius at the inlet of the turbine. This change was made to allow for better definition of the CPT meanline design through the use of a quadratic curve as discussed in the next step.

Step 3: Identify available turbine design variables

The next step for applying the turbine MDP to the conventional power turbine design problem was to identify design variables. For the design of the conventional power turbine, a larger set of design variables were selected compared to the E^3 LPT redesign problem. The available design variables are listed in Table 38 and include both velocity vector and blade row geometry similarity parameters. This list has been abbreviated by listing the velocity

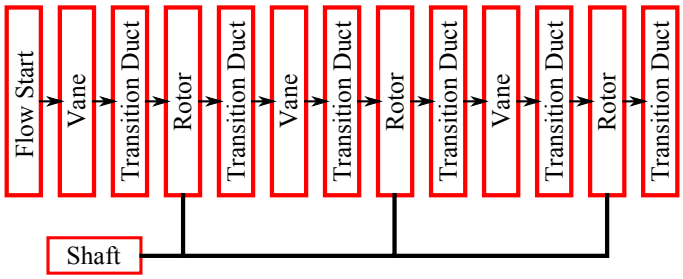

Figure 119: CPT Model Schematic

vector and blade row design variables for only a single stage with a column noting the stages to which they apply. The last three design variables listed in the table are used to define the axial and radial location of two control points which determine the meanline radius for the entire turbine. The definition of these three parameters is provided in Figure 120. Defining the meanline radius in using such a curve reduces the number of design variables which the designer must input and ensures that the meanline radius has a smooth, consistent shape.

Table 38: CPT Design Variables

Name	Description	Stages	Design Point
ϕ	Stage Flow Coefficient	All	ADP
ψ	Stage Loading Coefficient	All	ADP
R	Stage Reaction	All	ADP
μ	Rotor Axial Velocity Ratio	All	ADP
i_V	Vane Incidence Angle	All	ADP
t/c_V	Vane Thickness-to-Chord	All	-
AR_V	Vane Aspect Ratio	All	-
σ_V	Vane Solidity	All	-
i_R	Rotor Incidence Angle	All	ADP
t/c_R	Rotor Thickness-to-Chord	All	-
AR_R	Rotor Aspect Ratio	All	-
σ_R	Rotor Solidity	All	-
x_1	Meanline Curve Control Point 1 Axial Location	-	-
r_1	Meanline Curve Control Point 1 Radial Location	-	-
r_2	Meanline Curve Control Point 2 Radial Location	-	-

Step 4: Establish technology rules

The technology rules implemented for the conventional power turbine are similar to those implemented for the E^3 LPT. The technology rules defining the losses for each blade row

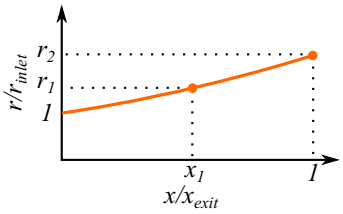

Figure 120: Meanline Radius Parameter Definition

were again those defined by Kacker and Okappu. However, these design rules were further supplemented by the use of an improved incidence loss computation published by Moustapha, Kacker and Tremblay.[77] In addition, a technology rule describing the stagger angle (Φ) of each blade row as a function of the leading edge and trailing edge blade angles was implemented as given by Equation 74. The stagger angle technology rule is based on the work of Kacker and Okapuu.[67]

$$\begin{aligned}\Phi =& 25.1587499999988 - 1.32683143939394 \times \beta_1 - 0.500886363636326 \times \beta_2 \\ &+ \beta_1^2 \times -0.0014535984848485 + \beta_1 \times \beta_2 \times 0.0156757575757576 \\ &+ \beta_2^2 \times 0.0131249999999997\end{aligned} \tag{74}$$

Step 5: Specify the design points

For the conventional power turbine design problem, a total of seven design points were identified for inclusion in the MDP process. These points were determined from the performance requirements and constraints identified in Step 1 of the process and are summarized in Table 39. The design points listed in this table are presented in the order which they are encountered during a typical flight. The first point encountered is for hover out of ground effect which requires high turbine speeds to match with the high rotor speeds needed for hover. The second operating point considers the potential for an engine to be lost during this hover phase, requiring the other three engines on the aircraft to produce excess power to allow for an emergency landing. This condition has the highest inlet flow pressure and temperature as a result of the engine being run in a contingency power state. After the aircraft transitions from a hover configuration to forward flight, the next two engine operating conditions encountered are those associated with shifting gear ratios in the multi-speed

transmission. A notional shifting procedure was developed by Snyder.[100] In this procedure, the rotor and engine speed are first reduced to near the preferred cruise rotor speeds. Next, a single engine is taken offline with cross-shafting enabling the other three engines to provide power to both rotors. The speed of the offline engine is then increased before it is brought back online at a different gear ratio. This process of pulling an engine offline and adjusting its speed is then repeated for the other three engines. From this process, pre-shift and post-shift design points were identified which have different shaft speeds and inlet flow conditions, but both requiring the same shift power to be produced as defined in Step 1. The next two design points are for the start and end of the climb segment of the flight, respectfully. Lastly, the aerodynamic design point for the turbine corresponds to a typical cruise flight condition. It is at this point where most of the design variables for the turbine are specified. The thermodynamic properties of the flow entering the turbine and shaft speed at each of these design points was determined from a cycle MDP model of the turboshaft engine with a notional conventional power turbine. This development of this cycle MDP model is described in Appendix B.

Table 39: CPT Design Points

Design Point	Label	Pt	Tt	N
Hover Out of Ground Effect	HOGE	55.7 psi	1855 °R	100%
One Engine Inoperative	OEI	64.2 psi	1990 °R	100%
Pre-Shift	Shift1	56.6 psi	1875 °R	70%
Post-Shift	Shift2	53.6 psi	1815 °R	85%
Start of Climb	Climb	41.5 psi	1645 °R	85%
Top of Climb	TOC	27.0 psi	1565 °R	85%
Aero Design Point	ADP	25.9 psi	1530 °R	85%

Step 6: Create design point mapping matrix and incorporate into turbine model

Step six of the turbine MDP method integrates the design information gathered as part of the first five steps into a summary Design Point Mapping Matrix and incorporates this information into the turbine model. The DPMM for the conventional power turbine is provided in Table 40 with the values provided for each of the design variables coming from a baseline turbine design. The information from this table was then integrated into the

OTAC MDP model of the conventional power turbine.

Table 40: CPT Design Point Mapping Matrix

		Design Points																							
		ADP			TOC			HOGE			OEI			Climb			Shift1			Shift2					
	Stage →	1	2	3	1	2	3	1	2	3	1	2	3	1	2	3	1	2	3	1	2	3			
Design Variables	Stage ϕ	1	0.95	0.977																					
	Stage ψ	2.95	3.01	2.46																					
	Stage R	0.625	0.472	0.475																					
	Vane ν	0.972	0.932	0.951																					
	Duct1 ν	1	1	1																					
	Duct1 μ	1	1	1																					
	Rotor ν	0.974	0.969	0.978																					
	Rotor μ	0.9	0.881	0.868																					
	Duct2 ν	1	1	1																					
	Duct2 μ	1	1	1																					
	Vane i, deg	0	0	0																					
	Vane t/c	0.2	0.2	0.2																					
	Vane AR	2	2	2.8																					
	Vane σ	1.11	1.67	1.43																					
	Vane e/s	0.01	0.015	0.015																					
	Rotor i, deg	0	0	0																					
	Rotor t/c	0.2	0.2	0.2																					
	Rotor AR	2	2.5	3																					
	Rotor σ	1.67	1.67	1.43																					
	Rotor e/s	0.035	0.03	0.03																					
Performance Requirements	ADP Power		1800 hp																						
	TOC Power					1900 hp																			
	HOGE Power								4150 hp																
	OEI Power											5150 hp													
	Climb Power														2600 hp										
	Shift Power																	3750 hp				3750 hp			
	OEI AN$^{\{}$2$\}$											5.0E+10 in^{2}rpm^2													
	HOGE PR								4.25																
Design Constraints	TOC PR					5.1																			
	OEI PR											4.8													
	Climb PR														3.6										
	Shift1 PR																	4.45							
	Shift2 PR																					4.25			
	Shift1 R_1																	0.1							
	Shift1 R_2																	0.1							
	Shift1 R_3																	0.1							

Step 7: Construct systems of equations and constraint relations that couple design points

Following the development of the DPMM, the next step in the turbine MDP process is to determine the design rules which couple the design points. For the conventional power turbine design problem, the performance requirements and operating constraints identified in Step 1 fit the classes identified in Section 5.3.2. These requirements and constraints therefore all become dependent equations which must be paired with unique independent parameters. The sizing parameter and operating parameters selected for the CPT are similar to those selected for the E^3 LPT. The mean radius at the entrance to the turbine is included as the sizing parameter. The operating parameters used to match the power requirements at all design point are the exit static pressure except at the aerodynamic design point where the actual mass flow is used. Finally, the shaft speed at the aerodynamic design point is added to ensure that the AN^2 constraint is satisfied. The complete set of design rules implemented for the CPT design problem are listed in Table 41. The constraints applied in the MDP solution are also paired with a dependent equation in the model as defined in Table 42.

Table 41: CPT Independent-Dependent Set

Number	Independent	Dependent
1	ADP Mass Flow	HOGE PR
2	ADP N	OEI AN^2
3	Inlet Mean Radius	ADP Power
4	TOC Exit Static Pressure	TOC Power
5	HOGE Exit Static Pressure	HOGE Power
6	OEI Exit Static Pressure	OEI Power
7	Climb Exit Static Pressure	Climb Power
8	Shift1 Exit Static Pressure	Shift1 Power
9	Shift2 Exit Static Pressure	Shift2 Power

Step 8: Assign values to turbine design variables

The eighth step of the turbine MDP method is to assign values to the design variables identified in Step 3. For the design of the CPT, a design space was formed by specifying allowable ranges for each of the design variables. These ranges are roughly centered around the baseline design values presented in the DPMM in Step 6. The minimum and maximum values for all of the design variables are provided in Table 43. The top portion of the table

Table 42: CPT Constraint-Dependent Pairings

Constraint	Dependent	Min/Max
TOC PR	HOGE PR	Max
OEI PR	HOGE PR	Max
Climb PR	HOGE PR	Max
Shift1 PR	HOGE PR	Max
Shift2 PR	HOGE PR	Max
Shift1 R_1	ADP R_1	Min
Shift1 R_2	ADP R_2	Min
Shift1 R_3	ADP R_3	Min

lists the ranges for the parameters that are specified for each stage with the bottom portion of the table list values for design variables which apply across all stages.

Table 43: CPT Design Variable Ranges

Variable	Stage 1		Stage 2		Stage 3	
	Min	Max	Min	Max	Min	Max
ϕ	0.65	0.85	0.65	0.85	0.70	0.90
ψ	2.10	2.50	2.10	2.50	1.70	2.30
R	0.40	0.60	0.40	0.60	0.40	0.60
μ	0.85	0.95	0.85	0.95	0.75	0.85
i_V	-5.00	5.00	-5.00	5.00	-5.00	5.00
t/c_V	0.15	0.25	0.15	0.25	0.15	0.25
AR_V	2.30	2.70	2.80	3.20	3.10	3.50
σ_V	1.25	2.00	1.25	2.00	1.25	2.00
i_R	-5.00	5.00	-5.00	5.00	-5.00	5.00
t/c_R	0.15	0.25	0.15	0.25	0.15	0.25
AR_R	2.30	2.70	2.90	3.30	3.20	3.60
σ_R	1.25	2.00	1.25	2.00	1.25	2.00
		Min			Max	
z_1		0.25			0.75	
r_1		1.10			1.40	
r_2		1.20			1.50	

APPENDIX F

VARIABLE SPEED POWER TURBINE MDP MODEL DESCRIPTION

This appendix details the implementation of the turbine MDP method on the variable speed power turbine design problem which was summarized in section 5.5.3. Steps 1 through 8 of turbine MDP procedure are covered in this description.

Step 1: Identify turbine requirements and constraints

The first step of the MDP method is to identify the performance requirements and operating constraints which must be satisfied by the turbine design. The requirements and constraints for the VSPT are similar to those identified for the CPT and were derived from the work of Snyder.[100] The primary difference is that the turboshaft engine with a VSPT is not required to go through the complex shifting procedure as the VSPT is designed to operate efficiently over the entire speed range. Therefore, the performance requirements and constraints at the shift operating condition is not included. The remaining performance requirements and constraints are identical to those used for the CPT and are listed in Table 44.

Table 44: VSPT Performance Requirements

Name	Value	Description
ADP Power	1800 hp	Minimum shaft power at cruise (ADP) condition
TOC Power	1900 hp	Minimum shaft power at top of climb (TOC) condition
HOGE Power	4150 hp	Minimum shaft power at hover out of ground effect (HOGE) condition
OEI Power	5150 hp	Minimum shaft power at one engine inoperative (OEI) condition
Climb Power	2600 hp	Minimum shaft power at climb start condition
OEI AN^2	5.0E+10 in^2rpm^2	Maximum AN^2 at one engine inoperative (OEI) condition
HOGE PR	4.45	Pressure ratio at hover out of ground effect (HOGE) condition

Step 2: Select turbine architecture and create turbine model

Next, the turbine architecture must be selected and the turbine model created. For the VSPT, previous research identified a four stage axial design as the architecture best suited to enabling the performance requirements to be met.[91, 113] With the architecture selected, an OTAC model of the VSPT was created as shown in Figure 121. As with the E^3 LPT and CPT, each stage consists of a vane, rotor and two transition ducts.

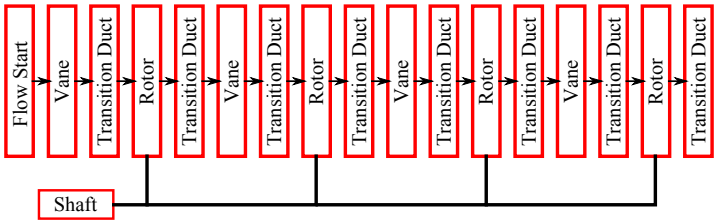

Figure 121: VSPT Model Schematic

Creation of this model also included implementation of similarity parameters to define the design. The similarity parameters used for the CPT and described in the previous section were also implemented on the VSPT. This includes the changes to the radius ratio definitions to allow for definition of the meanline radius through the turbine by a quadratic curve.

Step 3: Identify available turbine design variables

Step 3 of the turbine MDP method focuses on identifying the available design variables which will be used in the design study. For the VSPT problem, the design variables considered are identical to those used in the CPT study described previously. These design variables include similarity parameters to set both the velocity vector and blade row characteristics as listed in Table 45. The meanline radius control point parameters used in the CPT problem have also been selected as design variables for the VSPT problem.

Step 4: Establish technology rules

The fourth step of the MDP method establishes technology rules which must be incorporated into the model. These technology rules primarily are defined by the loss model

Table 45: VSPT Design Variables

Name	Description	Stages	Design Point
ϕ	Stage Flow Coefficient	All	ADP
ψ	Stage Loading Coefficient	All	ADP
R	Stage Reaction	All	ADP
μ	Rotor Axial Velocity Ratio	All	ADP
i_V	Vane Incidence Angle	All	ADP
t/c_V	Vane Thickness-to-Chord	All	-
AR_V	Vane Aspect Ratio	All	-
σ_V	Vane Solidity	All	-
i_R	Rotor Incidence Angle	All	ADP
t/c_R	Rotor Thickness-to-Chord	All	-
AR_R	Rotor Aspect Ratio	All	-
σ_R	Rotor Solidity	All	-
x_1	Meanline Curve Control Point 1 Axial Location	-	-
r_1	Meanline Curve Control Point 1 Radial Location	-	-
r_2	Meanline Curve Control Point 2 Radial Location	-	-

selected for the analysis. For the VSPT design problem, the selected loss model technology rules for all blade rows are based on the publication of Kacker and Okapuu[67] and are supplemented by the incidence loss model from Moustapha, Kacker and Tremblay.[77] Finally, the technology rule for stagger angle (Equation 74) used for the CPT was also applied to the VSPT design.

Step 5: Specify the design points

The next step in the process is to identify the design points which will eventually need to be incorporated into the MDP analysis. Based on the requirements and constraints identified in Step 1, five design points were identified for the VSPT as listed in Table 46. These design points are similar to those identified in for the CPT design problem. The flow properties and shaft speeds which define each design point were determined from an MDP cycle model of the turboshaft engine with assumed VSPT performance characteristics. The development of this turboshaft MDP model is described in Appendix C.

Step 6: Create design point mapping matrix and incorporate into turbine model

The sixth step in the MDP process gathers the information determined in the first five steps

Table 46: VSPT Design Points

Design Point	Label	Pt	Tt	N
Hover Out of Ground Effect	HOGE	57.8 psi	1885 °R	100%
One Engine Inoperative	OEI	64.8 psi	2030 °R	100%
Start of Climb	Climb	44.0 psi	1700 °R	54%
Top of Climb	TOC	28.8 psi	1620 °R	54%
Aero Design Point	ADP	27.7 psi	1580 °R	54%

and creates a design point mapping matrix (DPMM). The DPMM for the VSPT is shown in Table 47 with values for the design variables representing a baseline VSPT design. The information summarized in this table was then used to build the VSPT MDP model in OTAC.

Step 7: Construct systems of equations and constraint relations that couple design points

With the DPMM completed and an MDP model constructed, Step 7 of the MDP process is to determine the design rules which couple the design points and incorporate them into the model. The design rules for the VSPT consist of a set of dependent equations and corresponding independent parameters. The dependent equations for the VSPT are developed from the performance requirements and operating constraints identified in Step 1. Unique independent parameters are paired with these equations to form a solvable system of equations as shown in Table 48. These independents and dependents are similar to those used in both the E^3 LPT and CPT analyses previously described. For the VSPT design problem, no additional constraints were defined that need to be paired with dependent equations in the model.

Step 8: Assign values to turbine design variables

The next step in the process is to assign values to the turbine design variables. Similar to the E^3 LPT and CPT implementations, a design space was formed for the VSPT by specifying ranges on all the design variables. Table 49 provides the design ranges for the stage-by-stage variables in the top potion with the bottom portion of the table gives ranges for the variables used to define the meanline radius. The experimental results shown in the next section use this design space except where noted.

Table 47: VSPT Design Point Mapping Matrix

		Design Point																			
		ADP				TOC				HOGE				OEI				Climb			
	Stage →	1	2	3	4	1	2	3	4	1	2	3	4	1	2	3	4	1	2	3	4
Design Variables	Stage ϕ	1.0	0.95	0.977	1.134																
	Stage ψ	2.95	3.01	2.46	1.98																
	Stage R	0.625	0.472	0.475	0.543																
	Vane ν	0.972	0.932	0.951	0.977																
	Duct1 ν	1.0	1.0	1.0	1.0																
	Duct1 μ	1.0	1.0	1.0	1.0																
	Rotor ν	0.974	0.969	0.978	0.993																
	Rotor μ	0.9	0.881	0.868	0.862																
	Duct2 ν	1.0	1.0	1.0	1.0																
	Duct2 μ	1.0	1.0	1.0	1.0																
	Vane i, deg	0.0	0.0	0.0	0.0																
	Vane t/c	0.2	0.2	0.2	0.2																
	Vane AR	2.0	2.0	2.8	3.25																
	Vane σ	1.11	1.67	1.43	1.43																
	Vane e/s	0.01	0.015	0.015	0.015																
	Rotor i, deg	0.0	0.0	0.0	0.0																
	Rotor t/c	0.2	0.2	0.2	0.2																
	Rotor AR	2.0	2.5	3.0	3.5																
	Rotor σ	1.67	1.67	1.43	1.25																
	Rotor e/s	0.035	0.03	0.03	0.025																
	Rotor k/h	0.0	0.0	0.0	0.0																
Performance Requirements	ADP Power	1800 hp																			
	TOC Power					1900 hp															
	HOGE Power									4150 hp											
	OEI Power													5150 hp							
	Climb Power																	2600 hp			
	OEI AN^2													$5.0E{+}10\ \mathrm{in}^2\mathrm{rpm}^2$							
	HOGE PR									5.0											

Table 48: VSPT Independent-Dependent Set

Number	Independent	Dependent
1	ADP Mass Flow	HOGE PR
2	ADP N	OEI AN^2
3	Inlet Mean Radius	ADP Power
4	TOC Exit Static Pressure	TOC Power
5	HOGE Exit Static Pressure	HOGE Power
6	OEI Exit Static Pressure	OEI Power
7	Climb Exit Static Pressure	Climb Power

Table 49: VSPT Design Variable Ranges

Variable	Stage 1		Stage 2		Stage 3		Stage 4	
	Min	Max	Min	Max	Min	Max	Min	Max
ϕ	0.90	1.10	0.90	1.10	0.90	1.10	0.90	1.10
ψ	2.80	3.00	2.80	3.00	2.40	2.60	1.90	2.10
R	0.40	0.60	0.40	0.60	0.40	0.60	0.40	0.60
μ	0.85	0.95	0.85	0.95	0.85	0.95	0.80	0.90
i_V	-5.00	5.00	-5.00	5.00	-5.00	5.00	-5.00	5.00
t/c_V	0.15	0.25	0.15	0.25	0.15	0.25	0.15	0.25
AR_V	2.30	2.70	2.80	3.20	3.10	3.50	3.20	3.60
σ_V	1.25	2.00	1.25	2.00	1.25	2.00	1.25	2.00
i_R	-5.00	5.00	-5.00	5.00	-5.00	5.00	-5.00	5.00
t/c_R	0.15	0.25	0.15	0.25	0.15	0.25	0.15	0.25
AR_R	2.30	2.70	2.90	3.30	3.20	3.60	3.30	3.70
σ_R	1.25	2.00	1.25	2.00	1.25	2.00	1.25	2.00

	Min	Max
z_1	0.25	0.75
r_1	1.10	1.40
r_2	1.20	1.50

APPENDIX G

E^3 ENGINE AND LPT MLMDP MODEL DESCRIPTION

This appendix details the implementation of the MLMDP method for the design of the E^3 engine and its LPT which was summarized in section 6.5.1. The application of the MLMDP method to this problem draws heavily from the implementation of the cycle and turbine MDP methods to portions of this problem as described in Appendices A and D respectively. Steps 1 through 7 of MLMDP procedure are covered in this description.

Step 1: Identify turbine requirements and constraints

Performance requirements and constraints for the E^3 engine were identified based on a previous model developed by Claus.[21] The requirements capture the required engine thrust at the engine aerodynamic design point (cruise), top of climb operating condition and sea level static. Additionally, a maximum allowable combustor temperature is specified for all flight conditions. These performance requirements for the cycle are defined in Table 50

Table 50: Performance Requirements for E^3 Engine

Name	Value	Description
ADP Thrust	8500 lbf	Minimum net thrust at cruise (ADP) condition
TOC Thrust	9100 lbf	Minimum net thrust at top of climb (TOC) condition
SLS Thrust	40000 lbf	Minimum net thrust at sea-level static (SLS) condition
Maximum T4	3100 °R	Maximum allowable combustor exit temperature

For the E^3 LPT, many of performance requirements and operating constraints were derived from the corresponding cycle design. The performance requirements consist of the power output from the turbine at the three operating conditions used in the cycle analysis. Two pressure ratio constraints were also identified from the cycle analysis model at two different operating conditions. In addition to these cycle derived constraints, an AN^2

limit was developed from a baseline turbine design and used to ensure similar blade stresses across all designs. Finally, two geometric constraints were also included for the E^3 LPT redesign. These geometric constraints set the minimum and maximum allowable flare angle for any section of the annulus. The performance requirements and constraints for the E^3 LPT are defined in Table 51.

Table 51: E^3 LPT Performance Requirements and Constraints

Name	Value	Description
ADP Power	Set by cycle	Minimum shaft power at cruise (ADP) condition
TOC Power	Set by cycle	Minimum shaft power at top of climb (TOC) condition
SLS Power	Set by cycle	Minimum shaft power at sea-level static (SLS) condition
TOC PR	Set by cycle	Pressure ratio at top of climb (TOC) condition
SLS PR	Set by cycle	Pressure ratio at sea level static (SLS) condition
AN^2	1.75E+10 in^2 rpm^2	Maximum AN^2
Min Flare	-5°	Minimum flare angle for any annulus section
Max Flare	30°	Maximum flare angle for any annulus section

Step 2: Select turbine architecture and create turbine model

The architectures for the E^3 engine and LPT were not altered from the original configurations selected during the E^3 research program. The E^3 engine is a high BPR mixed flow turbofan engine with an architecture defined by the components shown in Figure 122.[30]

The E^3 LPT developed by GE[18, 15] was an axial design with five stages. With this information, a model of the E^3 LPT was developed in OTAC based on the validation model developed by Jones[66] as shown in Figure 123. This model has five stages, each consisting of a vane, transition duct, rotor and second transition duct. The transition ducts are included in the model to allow for changes in mean radius and area between blade rows. In addition, a transition duct is placed upstream of the first vane to enable matching the inlet flow conditions from the design and test reports. All of the rotors are connected to a single shaft which powers the fan and LPC. The E^3 LPT model was also defined in terms of similarity parameters as defined in Section 5.3.1.

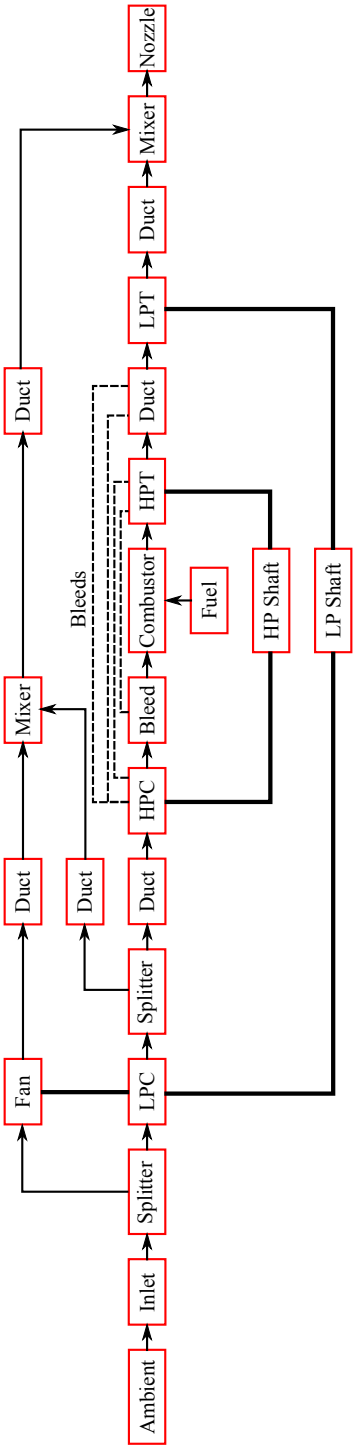

Figure 122: Block Diagram of E^3 Engine.

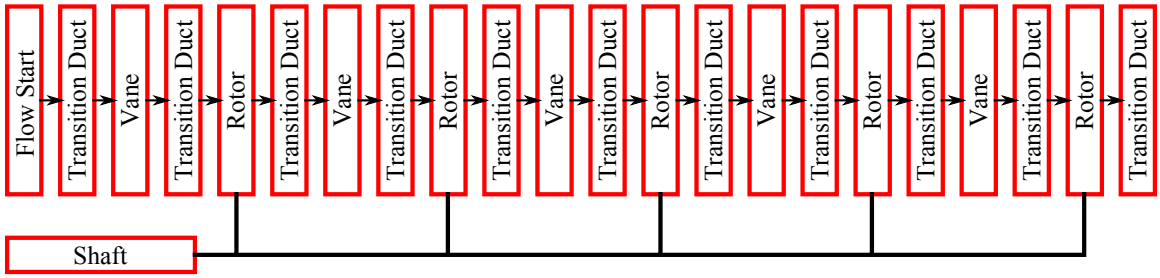

Figure 123: E^3 LPT Model Schematic

Step 3: Identify available turbine design variables

The third step of the MLMDP procedure is to identify the available engine and turbine design variables. For the E^3 engine, the three design variables identified were the fan pressure ratio (FPR), overall pressure ratio (OPR), and combustor exit temperature (T4). These design variables and the design points at which they apply are specified in Table 52.

Table 52: Design Variables for E^3 Engine

Name	Description	Design Point
FPR	Fan Pressure Ratio	ADP
OPR	Overall Pressure Ratio	ADP
T4max	Maximum Combustor Exit Temperature	All

For the E^3 LPT, a relatively small set of design variables were selected which focus primarily on modifying the turbine velocity vectors. The design variables include the flow coefficient, loading coefficient, reaction and axial velocity ratio for each stage as listed in Table 31. Each of these design parameters specify the design value at the aerodynamic design point (ADP).

Table 53: E^3 LPT Design Variables

Name	Description	Stages	Design Point
ϕ	Stage Flow Coefficient	All	ADP
ψ	Stage Loading Coefficient	All	ADP
R	Stage Reaction	All	ADP
μ	Rotor Axial Velocity Ratio	All	ADP

Step 4: Establish technology rules

The establishment of technology rules for the E^3 engine primarily involved selection of performance maps for each of the engine components. The performance maps for each component for this model were taken from a previously developed E^3 model by Denney.[1] Two additional design rules were added which altered the bypass ratio of each splitter to maintain a constant extraction ratio (ratio of the total pressures) in each mixer.

For the E^3 LPT, the technology rules implemented are those which define the losses in pressure produced across each blade row. These technology rules form the overall loss model implemented in analysis. In this study, the technology rules used to calculate the losses across all blade rows come from the loss model described by Kacker and Okappu.[67] The loss sources included in this model are those attributed to the blade profile, secondary flows, trailing edge thickness and tip clearance. In addition, the overall loss computations account for the Reynolds' number of the flow for each blade row.

Step 5: Specify the design points

The fifth step in the MLMDP method is to identify the relevant design points which must be included in the analysis. From the performance requirements and constraints identified for the cycle in step 1, three design points were identified. These included the engine aerodynamic design point, top-of-climb and sea-level static. Reviewing the E^3 LPT performance requirements and constraints also identified three design points of interest at that level. These design points correspond to the design points identified for the cycle. As a result, the complete list of design points which must be considered in the MLMDP model consists of three design points as specified in Table 54. In this table, values specifying the overall engine operating conditions are given such as the freestream Mach number, altitude and deviation in static temperature from standard day conditions. Values for the LPT inlet total pressure, total temperature and percent of corrected shaft speed needed for the turbine MDP are not included as they are derived from the cycle model.

[1] Unpublished NPSS model from Russell Denney, Research Engineer II in the Aerospace Systems Design Laboratory at the Georgia Institute of Technology, October 2015.

Table 54: Design Points for E^3 Engine

Design Point	Label	Mach	Altitude	ΔT
Aero Design Point	ADP	0.8	35000 ft	+18 °R
Top of Climb	TOC	0.8	35000 ft	+18 °R
Sea-Level Static	SLS	0.0	0 ft	+27 °R

Step 6: Create design point mapping matrix and incorporate into turbine model

The sixth step of the process is to create the design point mapping matrices (DPMM) for the cycle and turbine. These DPMMs links the design points with the design variables, performance requirements and constraints specific to that level. The DPMMs for the E^3 engine and LPT are given in Tables 55 and 56, respectively. In both of these tables, the same design points have been listed across the top to reflect the paired points that must be added to each model.

Table 55: Design Point Mapping Matrix for E^3 Engine

		Design Point		
		ADP	TOC	SLS
Map Scaling Point		ADP		
Design Variables	FPR	1.64		
	LPCPR	1.66		
	HPCPR	22.4		
	T4			3100 °R
Performance Requirements	ADP Thrust	8500 lbf		
	TOC Thrust		9100 lbf	
	SLS Thrust			40000 lbf
Component Performance	Inlet Pressure Recovery	1.0		
	Fan Adiabatic η	0.894		
	LPC Adiabatic η	0.906		
	HPC Adiabatic η	0.861		
	Burner η	0.98		
	HPT Adiabatic η	0.927		
	LPT Adiabatic η	Set by Meanline		
	Nozzle Cv	1.0		
Technology Limits	T4 Max			3100 °R

Step 7: Construct systems of equations and constraint relations that couple design points

Step 7 of the MLMDP process constructs the system of nonlinear equations which couple

Table 56: E^3 LPT Design Point Mapping Matrix

		Design Points														
		ADP					TOC					SLS				
	Stage →	1	2	3	4	5	1	2	3	4	5	1	2	3	4	5
Design Variables	Stage ϕ	1.27	1.14	1.08	1.03	1.07										
	Stage ψ	3.19	3.05	2.88	2.27	1.43										
	Stage R	0.35	0.35	0.37	0.38	0.34										
	Rotor μ	1.01	1.04	1.02	0.98	0.94										
Performance Requirements	ADP Power	Set by Cycle														
	TOC Power						Set by Cycle									
	SLS Power											Set by Cycle				
	SLS PR											Set by Cycle				
	SLS AN^2											1.75E10				
Design Constraints	TOC PR						Set by Cycle									
	Min Flare	-5°														
	Max Flare	30°														

the design points within and across the analysis levels. Using the information contained in the DPMM, a set of design rules were first developed to couple the design points at the cycle level. These design rules are summarized in Table 57. The design rules establish a set of cycle independent values which are varied by the solver to match the cycle performance requirements and constraints.

Table 57: E^3 Engine MDP Independent-Dependent Set

Number	Independent	Dependent
1	ADP Mass Flow	ADP Net Thrust
2	ADP FAR	SLS T4
3	TOC FAR	TOC Net Thrust
4	SLS FAR	SLS Net Thrust

The information in the DPMM was also used to determine the system of equations required to couple the design points at the turbine analysis level. The design rules formulated for coupling the turbine design points are summarized in Table 58. In addition, constraints identified at the turbine level were paired with a dependent equation as described in Table 59.

Table 58: E^3 LPT MDP Independent-Dependent Set

Number	Independent	Dependent
1	ADP Mass Flow	SLS PR
2	ADP N	SLS AN^2
3	Inlet Mean Radius	ADP Power
4	TOC Exit Static Pressure	TOC Power
5	SLS Exit Static Pressure	SLS Power

Table 59: E^3 LPT MDP Constraint-Dependent Pairings

Constraint	Dependent	Min/Max
TOC PR	SLS PR	Max
Vane Min Flare	ADP Stage ϕ	Min
Rotor Min Flare	ADP Rotor μ	Min
Vane Max Flare	ADP Stage ϕ	Max
Rotor Max Flare	ADP Rotor μ	Max

Finally, the cross-level coupling equations for the MLMDP analysis were developed.

These cross-level coupling equaitons assure that the design points at each level have identical turbine operating conditions and performance characteristics. Since the cycle design points will always be run prior to their associated turbine design points, the operating condition and some performance values can be directly passed between the levels. Specifically, these parameters are the turbine inlet total pressure, total temperature, fuel-to-air ratio, power output and pressure ratio. As a result, a nonlinear equation which must be solved by a Newton-Raphson solver was not required. However, nonlinear equations assure the turbine performance characteristics match across the levels were required to be converged by a Newton-Raphson solver. The independent and dependent pairs for these cross-level coupling equations are listed in Table 60.

Table 60: E^3 Cross-Level Independent-Dependent Set

Number	Independent	Dependent
1	Cycle ADP LPT Efficiency	ADP LPT Efficiency Error
2	Cycle TOC LPT Efficiency	TOC LPT Efficiency
3	Cycle TOC LPT Corrected Flow	TOC LPT Corrected Flow
4	Cycle SLS LPT Efficiency	SLS LPT Efficiency
5	Cycle SLS LPT Corrected Flow	SLS LPT Corrected Flow

APPENDIX H

TURBOSHAFT AND CONVENTIONAL POWER TURBINE MLMDP MODEL DESCRIPTION

This appendix details the implementation of the MLMDP method for the design of a turboshaft engine with a conventional power turbine which was summarized in section 6.5.2. The the application of the MLMDP method to this problem draws heavily from the implementation of the cycle and turbine MDP methods to portions of this problem as described in Appendices B and E respectively. Steps 1 through 7 of MLMDP procedure are covered in this description.

Step 1: Identify turbine requirements and constraints

Step 1 in the MLMDP method is to identify the turbine performance requirements and constraints. The performance requirements and constraints for the turboshaft engine were derived from the report by Snyder.[100] Power requirements at six potentially critical operating conditions were identified. In addition, several different combustor exit temperature constraints were identified. These combustor exit temperature constraints correspond to the engine power rating levels defined in Table 2. The derived requirements and constraints are outlined in Table 61.

The performance requirements for the conventional power turbine were primarily derived from the associated turboshaft engine and are summarized in Table 62. The performance requirements include the power output from the turbine at six different operating conditions. In addition, primary operating constraints are specified for the turbine AN^2 at the one engine inoperative condition and the pressure ratio across the turbine at all operating points other than ADP. Finally, a minimum value of the stage reaction is specified for all stages at the Shift1 operating condition.

Table 61: Performance Requirements for CPT Turboshaft Engine

Name	Value	Description
ADP Power	1800 hp	Minimum shaft power at cruise (ADP) condition
TOC Power	1900 hp	Minimum shaft power at top of climb (TOC) condition
HOGE Power	4150 hp	Minimum shaft power at hover out of ground effect (HOGE) condition
OEI Power	5150 hp	Minimum shaft power at one engine inoperative (OEI) condition
Climb Power	2600 hp	Minimum shaft power at climb start condition
Shift Power	3750 hp	Minimum shaft power at shift (SH) condition
MCP T4 Max	3260 °R	Maximum allowable combustor exit temperature for MCP flight conditions
IRP T4 Max	3410 °R	Maximum allowable combustor exit temperature for IRP flight conditions
MRP T4 Max	3460 °R	Maximum allowable combustor exit temperature for MRP flight conditions
CRP T4 Max	3510 °R	Maximum allowable combustor exit temperature for CRP flight conditions

Step 2: Select turbine architecture and create turbine model

The architecture for the turboshaft engine was also defined in the report by Snyder and a similar architecture was adopted for this study. The engine has a low pressure spool and high pressure spool forming the core, with a free power turbine providing power to the rotor. The high pressure compressor is comprised of several axial stages and a centrifugal stage. A block diagram showing the components of the VSPT engine and how they are connected is provided in Figure 124.

For the conventional power turbine, previous studies[91, 113] have identified a three stage axial architecture as the most likely turbine architecture. Therefore, this architecture was selected for the conventional power turbine design study in this research. With this three stage architecture selected, an OTAC meanline model was constructed as shown in Figure 125. In this model each stage consists of a vane, transition duct, rotor and second transition duct.

Construction of the OTAC model for the conventional power turbine also involved selecting a set of similarity parameters which specify the design. For this model, the similarity

Table 62: CPT Performance Requirements and Constraints

Name	Value	Description
ADP Power	1800 hp	Minimum shaft power at cruise (ADP) condition
TOC Power	1900 hp	Minimum shaft power at top of climb (TOC) condition
HOGE Power	4150 hp	Minimum shaft power at hover out of ground effect (HOGE) condition
OEI Power	5150 hp	Minimum shaft power at one engine inoperative (OEI) condition
Climb Power	2600 hp	Minimum shaft power at climb start condition
Shift Power	3750 hp	Minimum shaft power at shift conditions
OEI AN^2	5.0E+10 in^2 rpm^2	Maximum AN^2 at one engine inoperative (OEI) condition
TOC PR	5.1	Pressure ratio at top of climb (TOC) condition
HOGE PR	4.25	Pressure ratio at hover out of ground effect (HOGE) condition
OEI PR	4.8	Pressure ratio at one engine inoperative (OEI) condition
Climb PR	3.6	Pressure ratio at climb start condition
Shift1 PR	4.45	Maximum pressure ratio at pre-shift condition
Shift2 PR	4.25	Maximum pressure ratio at post-shift condition
Shift1 R	0.1	Minimum degree of reaction for any stage at pre-shift condition

parameters defined in Section 5.3.1 were used with one modification. The similarity parameters definiting the mean radius across each blade row and transition duct were redefined such that the denominator for all μ parameters referenced the mean radius at the inlet of the turbine. This change was made to allow for better definition of the CPT meanline design through the use of a quadratic curve as discussed in the next step.

Step 3: Identify available turbine design variables

The next step for applying the MLMDP method to the turboshaft and conventional power turbine design problem was to identify design variables. For the CPT turboshaft engine, two design variables were identified as given in Table 63.

For the design of the conventional power turbine, a larger set of design variables were selected compared to the E^3 LPT redesign problem. The available design variables are

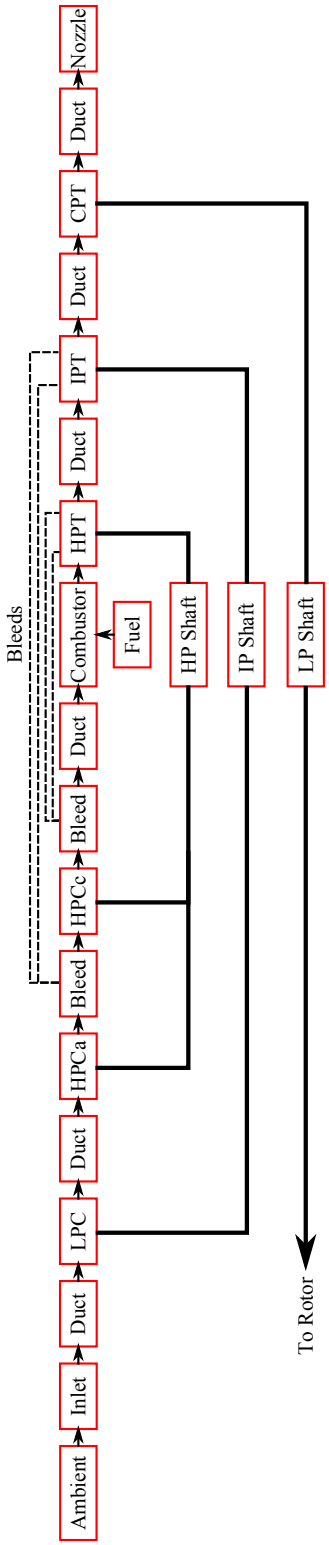

Figure 124: Block Diagram of CPT Turboshaft Engine.

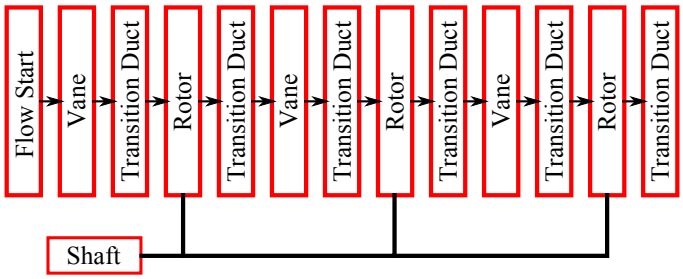

Figure 125: CPT Model Schematic

Table 63: Design Variables for CPT Turboshaft Engine

Name	Description	Design Point
OPR	Overall Pressure Ratio	ADP
NPR	Nozzle Pressure Ratio	ADP

listed in Table 64 and include both velocity vector and blade row geometry similarity parameters. This list has been abbreviated by listing the velocity vector and blade row design variables for only a single stage with a column noting the stages to which they apply. The last two design variables listed in the table are used to define a quadratic curve that sets the meanline radius through the turbine. The first variable describes the radial location at the exit of the turbine relative to the turbine radius while the second variable defines the meanline angle relative to axial at the turbine exit. The definition of these two parameters is graphically shown in Figure 126. Defining the meanline radius in using such a curve reduces the number of design variables which the designer must input and ensures that the meanline radius has a smooth, consistent shape.

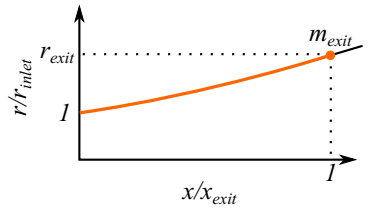

Figure 126: Meanline Radius Parameter Definition

Step 4: Establish technology rules

Table 64: CPT Design Variables

Name	Description	Stages	Design Point
ϕ	Stage Flow Coefficient	All	ADP
ψ	Stage Loading Coefficient	All	ADP
R	Stage Reaction	All	ADP
μ	Rotor Axial Velocity Ratio	All	ADP
i_V	Vane Incidence Angle	All	ADP
t/c_V	Vane Thickness-to-Chord	All	-
AR_V	Vane Aspect Ratio	All	-
σ_V	Vane Solidity	All	-
i_R	Rotor Incidence Angle	All	ADP
t/c_R	Rotor Thickness-to-Chord	All	-
AR_R	Rotor Aspect Ratio	All	-
σ_R	Rotor Solidity	All	-
r_{exit}	Meanline Curve Control Point Radial Location	-	-
m_{exit}	Meanline Curve Control Point Slope	-	-

The establishment of technology rules for the CPT turboshaft engine primarily involved selection of performance maps for each of the engine components. The performance maps match those from the model analyzed by Snyder.[100] Also, to enable use of OPR as an input to the cycle a design rule was added which varies the pressure ratio of the axial portion of the HPC.

The technology rules implemented for the conventional power turbine are similar to those implemented for the E^3 LPT. The technology rules defining the losses for each blade row were again those defined by Kacker and Okappu. However, these design rules were further supplemented by the use of an improved incidence loss computation published by Moustapha, Kacker and Tremblay.[77] In addition, a technology rule describing the stagger angle (Φ) of each blade row as a function of the leading edge and trailing edge blade angles was implemented as given by Equation 75. The stagger angle technology rule is based on the work of Kacker and Okapuu.[67]

$$\begin{aligned}\Phi =& 25.1587499999988 - 1.32683143939394 \times \beta_1 - 0.500886363636326 \times \beta_2 \\ &+ \beta_1^2 \times -0.0014535984848485 + \beta_1 \times \beta_2 \times 0.0156757575757576 \\ &+ \beta_2^2 \times 0.0131249999999997\end{aligned} \tag{75}$$

Step 5: Specify the design points

From the performance requirements and constraints determined in step 1, a set of 7 design points were identified and are listed in Table 65. These operating conditions are defined by the overall flight conditions (Mach number, altitude, and deviation in static temperature from the standard day) as well as the physical shaft speed of the VSPT required to match the rotor. The design points listed in this table are presented in the order which they are encountered during a typical flight. The first point encountered is for hover out of ground effect which requires high turbine speeds to match with the high rotor speeds needed for hover. The second operating point considers the potential for an engine to be lost during this hover phase, requiring the other three engines on the aircraft to produce excess power to allow for an emergency landing. This condition has the highest inlet flow pressure and temperature as a result of the engine being run in a contingency power state. After the aircraft transitions from a hover configuration to forward flight, the next two engine operating conditions encountered are those associated with shifting gear ratios in the multi-speed transmission. A notional shifting procedure was developed by Snyder.[100] In this procedure, the rotor and engine speed are first reduced to near the preferred cruise rotor speeds. Next, a single engine is taken offline with cross-shafting enabling the other three engines to provide power to both rotors. The speed of the offline engine is then increased before it is brought back online at a different gear ratio. This process of pulling an engine offline and adjusting its speed is then repeated for the other three engines. From this process, pre-shift and post-shift design points were identified which have different shaft speeds and inlet flow conditions, but both requiring the same shift power to be produced as defined in Step 1. The next two design points are for the start and end of the climb segment of the flight, respectfully. Lastly, the aerodynamic design point for the turbine corresponds to a typical cruise flight condition. It is at this point where most of the design variables for the turbine are specified.

Step 6: Create design point mapping matrix and incorporate into turbine model

The sixth step of the MLMDP process is to create the design point mapping matrices

Table 65: Design Points for CPT Turboshaft Engine

Design Point	Label	Mach	Altitude	ΔT	%N	Rating
Hover Out of Ground Effect	HOGE	0.0	5000 ft	+36 °R	100.0	MRP
One Engine Inoperative	OEI	0.0	5000 ft	+36 °R	100.0	CRP
Pre-Shift	Shift1	0.25	6000 ft	+36 °R	61.5	IRP
Post-Shift	Shift2	0.25	6000 ft	+36 °R	85.0	IRP
Start of Climb	Climb	0.3	8000 ft	+36 °R	85.0	IRP
Top of Climb	TOC	0.5	28000 ft	+0 °R	85.0	IRP
Aero Design Point	ADP	0.5	28000 ft	+0 °R	85.0	MCP

(DPMM) for the cycle and turbine. These DPMMs links the design points with the design variables, performance requirements and constraints specific to that level. The DPMM for the turboshaft engine is given in Table 66 with the DPMM for the CPT given in Table 67. In both of these tables, the same design points have been listed across the top to reflect the paired points that must be added to each model.

Step 7: Construct systems of equations and constraint relations that couple design points
Following the development of the DPMM, the next step in the MLMDP process is to determine the design rules which couple the design points within and across the levels. The design rules formulated to couple the cycle design points are defined in Table 24. These design rules vary the FAR at each design point along with the ADP mass flow to match the power, nozzle pressure ratio and maximum T4 requirements at various operating points.

For the conventional power turbine, the system of equations formulated to couple the turbine design points are listed in Table 69. These equations are similar to those identified in the turbine MDP implementation. They vary the exit static pressure at each design point along with the shaft speed and inlet mean radius to match the power, AN^2 and pressure ratio requirements identified in Step 1. In addition, constraints were considered as part of the turbine design and the pair of those constraints with a dependent equation in the model is defined in Table 70.

Finally, the cross-level coupling equations for the MLMDP analysis were developed in this step. These cross-level coupling equations assure that the design points at each level have identical turbine operating conditions and performance characteristics. Since the

Table 66: Design Point Mapping Matrix for CPT Turboshaft Engine

		Design Point						
		ADP	TOC	HOGE	OEI	Climb	Shift1	Shift2
Map Scaling Point		ADP						
Design Variables	LPCPR	5.0						
	HPCaPR	3.0						
	HPCcPR	2.7						
Performance Requirements	ADP Power	1800 hp						
	TOC Power		1900 hp					
	HOGE Power			4150 hp				
	OEI Power				5150 hp			
	Climb Power					2600 hp		
	Shift Power						3750 hp	3750 hp
Component Performance Parameters	Inlet Pressure Recovery	1.0						
	LPC Adiabatic η	0.89						
	HPCa Adiabatic η	0.89						
	HPCc Adiabatic η	0.88						
	Burner η	0.999						
	HPT Adiabatic η	0.89						
	IPT Adiabatic η	0.90						
	CPT Adiabatic η	Set by Meanline						
	Nozzle Cv	0.99						
Technology Limits	MCP T4 Max	3210 °R						
	IRP T4 Max		3410 °R			3410 °R	3410 °R	3410 °R
	MRP T4 Max			3460 °R				
	CRP T4 Max				3510 °R			
	HPT Vane Temp.				2360 °R			
	HPT Rotor Temp.				2260 °R			
	IPT Vane Temp.				2360 °R			
	IPT RotorTemp.				2160 °R			

Table 67: CPT Design Point Mapping Matrix

		Design Points																					
		ADP			TOC			HOGE			OEI			Climb			Shift1			Shift2		
	Stage →	1	2	3	1	2	3	1	2	3	1	2	3	1	2	3	1	2	3	1	2	3
Design Variables	Stage ϕ	1	0.95	0.977																		
	Stage ψ	2.95	3.01	2.46																		
	Stage R	0.625	0.472	0.475																		
	Vane ν	0.972	0.932	0.951																		
	Duct1 ν	1	1	1																		
	Duct1 μ	1	1	1																		
	Rotor ν	0.974	0.969	0.978																		
	Rotor μ	0.9	0.881	0.868																		
	Duct2 ν	1	1	1																		
	Duct2 μ	1	1	1																		
	Vane i, deg	0	0	0																		
	Vane t/c	0.2	0.2	0.2																		
	Vane AR	2	2	2.8																		
	Vane σ	1.11	1.67	1.43																		
	Vane e/s	0.01	0.015	0.015																		
	Rotor i, deg	0	0	0																		
	Rotor t/c	0.2	0.2	0.2																		
	Rotor AR	2	2.5	3																		
	Rotor σ	1.67	1.67	1.43																		
	Rotor e/s	0.035	0.03	0.03																		
Performance Requirements	ADP Power		1800 hp																			
	TOC Power				1900 hp																	
	HOGE Power							4150 hp														
	OEI Power										5150 hp											
	Climb Power													2600 hp								
	Shift Power																Set by Cycle			Set by Cycle		
	OEI $AN^{\dagger}2\}$										5.0E+10 $in^2 rpm^2$											
	HOGE PR							Set by Cycle														
Design Constraints	TOC PR				Set by Cycle																	
	OEI PR										Set by Cycle											
	Climb PR													Set by Cycle								
	Shift1 PR																Set by Cycle					
	Shift2 PR																			Set by Cycle		
	Shift1 R_1																0.1					
	Shift1 R_2																0.1					
	Shift1 R_3																0.1					

Table 68: Independent-Dependent Set for CPT Turboshaft Engine

Number	Independent	Dependent
1	ADP Mass Flow	ADP Nozzle PR
2	ADP FAR	OEI T4
3	TOC FAR	TOC Power
4	HOGE FAR	HOGE Power
5	OEI FAR	OEI Power
6	Climb FAR	Climb Power
7	Shift1 FAR	Shift1 Power
8	Shift2 FAR	Shift2 Power

Table 69: CPT Independent-Dependent Set

Number	Independent	Dependent
1	ADP Mass Flow	HOGE PR
2	ADP N	OEI AN^2
3	Inlet Mean Radius	ADP Power
4	TOC Exit Static Pressure	TOC Power
5	HOGE Exit Static Pressure	HOGE Power
6	OEI Exit Static Pressure	OEI Power
7	Climb Exit Static Pressure	Climb Power
8	Shift1 Exit Static Pressure	Shift1 Power
9	Shift2 Exit Static Pressure	Shift2 Power

Table 70: CPT Constraint-Dependent Pairings

Constraint	Dependent	Min/Max
TOC PR	HOGE PR	Max
OEI PR	HOGE PR	Max
Climb PR	HOGE PR	Max
Shift1 PR	HOGE PR	Max
Shift2 PR	HOGE PR	Max
Shift1 R_1	ADP R_1	Min
Shift1 R_2	ADP R_2	Min
Shift1 R_3	ADP R_3	Min

cycle design points will always be run prior to their associated turbine design points, the operating condition and some performance values can be directly passed between the levels. Specifically, these parameters are the turbine inlet total pressure, total temperature, fuel-to-air ratio, power output and pressure ratio. As a result, a nonlinear equation which must be solved by a Newton-Raphson solver was not required. However, nonlinear equations assure the turbine performance characteristics match across the levels were required to be

converged by a Newton-Raphson solver. The independent and dependent pairs for these cross-level coupling equations are listed in Table 71.

Table 71: Turboshaft and CPT Cross-Level Independent-Dependent Set

Number	Independent	Dependent
1	Cycle ADP CPT Efficiency	ADP CPT Efficiency Error
2	Cycle TOC CPT Efficiency	TOC CPT Efficiency
3	Cycle TOC CPT Corrected Flow	TOC CPT Corrected Flow
4	Cycle HOGE CPT Efficiency	HOGE CPT Efficiency
5	Cycle HOGE CPT Corrected Flow	HOGE CPT Corrected Flow
6	Cycle OEI CPT Efficiency	OEI CPT Efficiency
7	Cycle OEI CPT Corrected Flow	OEI CPT Corrected Flow
8	Cycle Climb CPT Efficiency	Climb CPT Efficiency
9	Cycle Climb CPT Corrected Flow	Climb CPT Corrected Flow
10	Cycle Shift1 CPT Efficiency	Shift1 CPT Efficiency
11	Cycle Shift1 CPT Corrected Flow	Shift1 CPT Corrected Flow
12	Cycle Shift2 CPT Efficiency	Shift2 CPT Efficiency
13	Cycle Shift2 CPT Corrected Flow	Shift2 CPT Corrected Flow

APPENDIX I

TURBOSHAFT AND VARIABLE SPEED POWER TURBINE MLMDP MODEL DESCRIPTION

This appendix details the implementation of the MLMDP method on the turboshaft and variable speed power turbine design problem which was summarized in section 6.5.3. The application of the MLMDP method to this problem draws heavily from the implementation of the cycle and turbine MDP methods to portions of this problem as described in Appendices C and F respectively. Steps 1 through 7 of MLMDP procedure are covered in this description.

Step 1: Identify turbine requirements and constraints

The first step of the MLMDP method is to identify the performance requirements and operating constraints which must be satisfied by the engine and turbine designs. The performance requirements and constraints for the turboshaft engine were derived from a report by Snyder.[100] Power requirements at five potentially critical operating conditions were identified. In addition, several different combustor exit temperature constraints were identified. These combustor exit temperature constraints correspond to the engine power rating levels defined in Table 2. The derived requirements and constraints are outlined in Table 72.

The requirements and constraints for the VSPT were derived from the engine model and are similar to those identified for the CPT. The primary difference is that the turboshaft engine with a VSPT is not required to go through the complex shifting procedure as the VSPT is designed to operate efficiently over the entire speed range. Therefore, the performance requirements and constraints at the shift operating condition is not included. The remaining performance requirements and constraints are identical to those used for the CPT and are listed in Table 73.

Table 72: Performance Requirements for VSPT Turboshaft Engine

Name	Value	Description
ADP Power	1800 hp	Minimum shaft power at cruise (ADP) condition
TOC Power	1900 hp	Minimum shaft power at top of climb (TOC) condition
HOGE Power	4150 hp	Minimum shaft power at hover out of ground effect (HOGE) condition
OEI Power	5150 hp	Minimum shaft power at one engine inoperative (OEI) condition
Climb Power	2600 hp	Minimum shaft power at climb start condition
MCP T4 Max	3260 °R	Maximum allowable combustor exit temperature for MCP flight conditions
IRP T4 Max	3410 °R	Maximum allowable combustor exit temperature for IRP flight conditions
MRP T4 Max	3460 °R	Maximum allowable combustor exit temperature for MRP flight conditions
CRP T4 Max	3510 °R	Maximum allowable combustor exit temperature for CRP flight conditions

Table 73: VSPT Performance Requirements

Name	Value	Description
ADP Power	1800 hp	Minimum shaft power at cruise (ADP) condition
TOC Power	1900 hp	Minimum shaft power at top of climb (TOC) condition
HOGE Power	4150 hp	Minimum shaft power at hover out of ground effect (HOGE) condition
OEI Power	5150 hp	Minimum shaft power at one engine inoperative (OEI) condition
Climb Power	2600 hp	Minimum shaft power at climb start condition
OEI AN^2	5.0E+10 in^2rpm^2	Maximum AN^2 at one engine inoperative (OEI) condition
HOGE PR	4.45	Pressure ratio at hover out of ground effect (HOGE) condition

Step 2: Select turbine architecture and create turbine model

The architecture for the VSPT engine was also defined in the report by Snyder and a similar architecture was adopted for this study. The engine has a low pressure spool and high pressure spool forming the core, with a free power turbine on its own shaft. The high pressure compressor is comprised of several axial and a centrifugal stage. A block diagram

showing the components of the VSPT engine and how they are connected is provided in Figure 127.

For the VSPT, previous research identified a four stage axial design as the architecture best suited to enabling the performance requirements to be met.[91, 113] With the architecture selected, an OTAC model of the VSPT was created as shown in Figure 128.

Creation of this model also included implementation of similarity parameters to define the design. The similarity parameters used for the CPT and described in Appendix H were also implemented on the VSPT. This includes the changes to the radius ratio definitions to allow for definition of the meanline radius through the turbine by a quadratic curve.

Step 3: Identify available turbine design variables

Step 3 of the MLMDP method focuses on identifying the available design variables which will be used in the design study. For the VSPT turboshaft engine, a set of design variables were identified as given in Table 74.

Table 74: Design Variables for VSPT Turboshaft Engine

Name	Description	Design Point
OPR	Overall Pressure Ratio	ADP
NPR	Nozzle Pressure Ratio	ADP

For the VSPT, the design variables considered are identical to those used in the CPT study described previously. These design variables include similarity parameters to set both the velocity vector and blade row characteristics as listed in Table 75. The meanline radius control point parameters used in the CPT problem have also been selected as design variables for the VSPT problem.

Step 4: Establish technology rules

The establishment of technology rules for the VSPT turboshaft engine primarily involved selection of performance maps for each of the engine components. The performance maps match those from the model analyzed by Snyder.[100] Also, a design rule was added which varies the pressure ratio of the axial portion of the HPC to enable use of OPR as an input

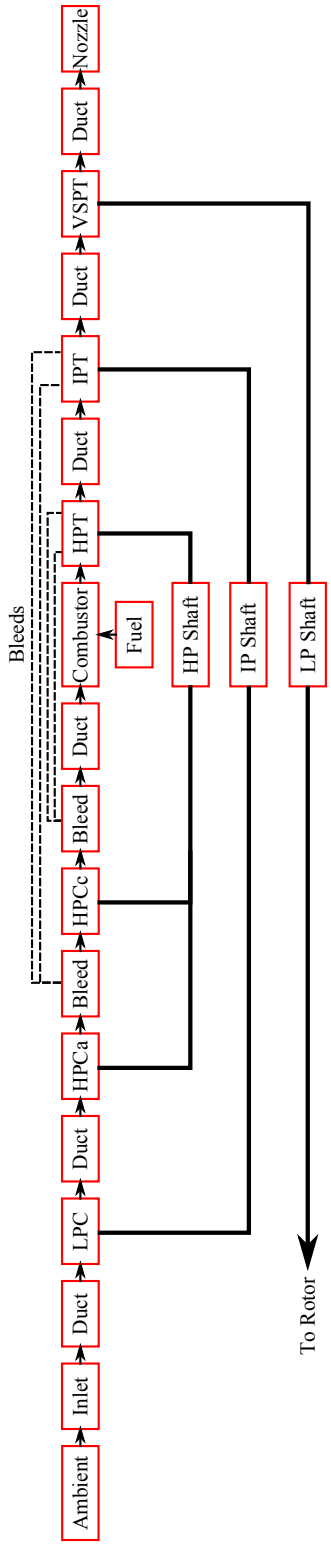

Figure 127: Block Diagram of VSPT Turboshaft Engine

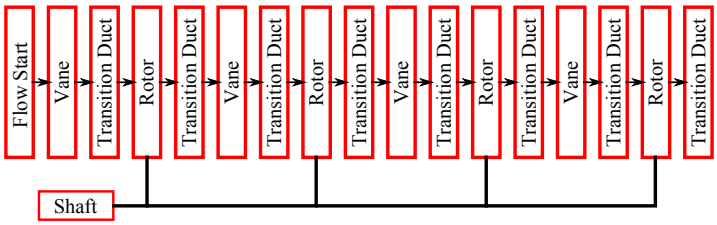

Figure 128: VSPT Model Schematic

Table 75: VSPT Design Variables

Name	Description	Stages	Design Point
ϕ	Stage Flow Coefficient	All	ADP
ψ	Stage Loading Coefficient	All	ADP
R	Stage Reaction	All	ADP
μ	Rotor Axial Velocity Ratio	All	ADP
i_V	Vane Incidence Angle	All	ADP
t/c_V	Vane Thickness-to-Chord	All	-
AR_V	Vane Aspect Ratio	All	-
σ_V	Vane Solidity	All	-
i_R	Rotor Incidence Angle	All	ADP
t/c_R	Rotor Thickness-to-Chord	All	-
AR_R	Rotor Aspect Ratio	All	-
σ_R	Rotor Solidity	All	-
r_{exit}	Meanline Curve Control Point Radial Location	-	-
m_{exit}	Meanline Curve Control Point Slope	-	-

to the cycle.

For the VSPT, this step involves the selection of the loss model as well as identification of any other geometric design correlations. The selected loss model technology rules for all blade rows are based on the publication of Kacker and Okapuu[67] and are supplemented by the incidence loss model from Moustapha, Kacker and Tremblay.[77] Additionally, the technology rule for stagger angle (Equation 74) used for the CPT was applied to the VSPT design.

Step 5: Specify the design points

The next step in the process is to identify the design points which will eventually need to be incorporated into the MLMDP analysis. Based on the requirements and constraints

identified in Step 1, five design points were identified for the turboshaft and VSPT as listed in Table 76. These design points are similar to those identified in for the CPT design problem.

Table 76: Design Points for Turboshaft and VSPT.

Design Point	Label	Mach	Altitude	ΔT	%N	Rating
Aero Design Point	ADP	0.5	28000 ft	+0 °R	85.0	MCP
Top of Climb	TOC	0.5	28000 ft	+0 °R	85.0	IRP
Hover Out of Ground Effect	HOGE	0.0	5000 ft	+36 °R	100.0	MRP
One Engine Inoperative	OEI	0.0	5000 ft	+36 °R	100.0	CRP
Start of Climb	Climb	0.3	8000 ft	+36 °R	85.0	IRP

Step 6: Create design point mapping matrix and incorporate into turbine model

The sixth step in the MLMDP process gathers the information determined in the first five steps to create the design point mapping matrices (DPMM) for the cycle and turbine. The DPMM for the turboshaft and VSPT is shown in Tables 77 and 78 respectively. In both of these tables, the same design points have been listed across the top to reflect the paired points that must be added to each model.

Step 7: Construct systems of equations and constraint relations that couple design points

With the DPMM completed and an MLMDP model constructed, Step 7 of the MLMDP process is to determine the design rules which couple the design points within and across the levels then incorporate them into the model. The design rules formulated for the turboshaft engine are defined in Table 79. These design rules vary the ADP mass flow and FAR at each design point to satisfy the cycle performance requirements.

The design rules for the VSPT are similar to those selected for the VSPT MDP analysis. The rules are summarized in Table 80 and include varying the mass flow, exit static pressure, shaft speed and inlet mean radius to satisfy the turbine performance requirements. For the VSPT design problem, no additional constraints were defined that need to be paired with dependent equations in the model.

The last part of this step was to formulate the cross-level coupling equations for the MLMDP analysis. The independent and dependent pairs for these cross-level coupling

Table 77: Design Point Mapping Matrix for VSPT Turboshaft Engine

		Design Point				
		ADP	TOC	HOGE	OEI	Climb
Map Scaling Point		ADP				
Design Variables	LPC PR	5.0				
	HPCa PR	3.0				
	HPCc PR	2.7				
Performance Requirements	ADP Power	1800 hp				
	TOC Power		1900 hp			
	HOGE Power			4150 hp		
	OEI Power				5150 hp	
	Climb Power					2600 hp
Component Performance Parameters	Inlet Pressure Recovery	1.0				
	LPC Adiabatic η	0.89				
	HPCa Adiabatic η	0.89				
	HPCc Adiabatic η	0.88				
	Burner η	0.999				
	HPT Adiabatic η	0.89				
	IPT Adiabatic η	0.90				
	VSPT Adiabatic η	Set by Meanline				
	Nozzle Cv	0.99				
Technology Limits	MCP T4 Max	3210 °R				
	IRP T4 Max		3410 °R			3410 °R
	MRP T4 Max			3460 °R		
	CRP T4 Max				3510 °R	
	HPT Vane Temp.				2360 °R	
	HPT Rotor Temp.				2260 °R	
	IPT Vane Temp.				2360 °R	
	IPT RotorTemp.				2160 °R	

equations are again similar to those used for the E^3 and CPT design problems and are listed in Table 81.

Table 78: VSPT Design Point Mapping Matrix

		Design Point																			
		ADP				TOC				HOGE				OEI				Climb			
	Stage →	1	2	3	4	1	2	3	4	1	2	3	4	1	2	3	4	1	2	3	4
Design Variables	Stage ϕ	1.0	0.95	0.977	1.134																
	Stage ψ	2.95	3.01	2.46	1.98																
	Stage R	0.625	0.472	0.475	0.543																
	Vane ν	0.972	0.932	0.951	0.977																
	Duct1 ν	1.0	1.0	1.0	1.0																
	Duct1 μ	1.0	1.0	1.0	1.0																
	Rotor ν	0.974	0.969	0.978	0.993																
	Rotor μ	0.9	0.881	0.868	0.862																
	Duct2 ν	1.0	1.0	1.0	1.0																
	Duct2 μ	1.0	1.0	1.0	1.0																
	Vane i, deg	0.0	0.0	0.0	0.0																
	Vane t/c	0.2	0.2	0.2	0.2																
	Vane AR	2.0	2.0	2.8	3.25																
	Vane σ	1.11	1.67	1.43	1.43																
	Vane e/s	0.01	0.015	0.015	0.015																
	Rotor i, deg	0.0	0.0	0.0	0.0																
	Rotor t/c	0.2	0.2	0.2	0.2																
	Rotor AR	2.0	2.5	3.0	3.5																
	Rotor σ	1.67	1.67	1.43	1.25																
	Rotor e/s	0.035	0.03	0.03	0.025																
	Rotor k/h	0.0	0.0	0.0	0.0																
Performance Requirements	ADP Power	1800 hp																			
	TOC Power					1900 hp															
	HOGE Power									4150 hp											
	OEI Power													5150 hp							
	Climb Power																	2600 hp			
	OEI AN^2													$5.0E{+}10\ \mathrm{in}^2\mathrm{rpm}^2$							
	HOGE PR									Set by Cycle											

Table 79: Independent-Dependent Set for VSPT Turboshaft Engine

Number	Independent	Dependent
1	ADP Mass Flow	ADP Nozzle PR
2	ADP FAR	OEI T4
3	TOC FAR	TOC Power
4	HOGE FAR	HOGE Power
5	OEI FAR	OEI Power
6	Climb FAR	Climb Power

Table 80: VSPT Independent-Dependent Set

Number	Independent	Dependent
1	ADP Mass Flow	HOGE PR
2	ADP N	OEI AN^2
3	Inlet Mean Radius	ADP Power
4	TOC Exit Static Pressure	TOC Power
5	HOGE Exit Static Pressure	HOGE Power
6	OEI Exit Static Pressure	OEI Power
7	Climb Exit Static Pressure	Climb Power

Table 81: Turboshaft and VSPT Cross-Level Independent-Dependent Set

Number	Independent	Dependent
1	Cycle ADP VSPT Efficiency	ADP VSPT Efficiency Error
2	Cycle TOC VSPT Efficiency	TOC VSPT Efficiency
3	Cycle TOC VSPT Corrected Flow	TOC VSPT Corrected Flow
4	Cycle HOGE VSPT Efficiency	HOGE VSPT Efficiency
5	Cycle HOGE VSPT Corrected Flow	HOGE VSPT Corrected Flow
6	Cycle OEI VSPT Efficiency	OEI VSPT Efficiency
7	Cycle OEI VSPT Corrected Flow	OEI VSPT Corrected Flow
8	Cycle Climb VSPT Efficiency	Climb VSPT Efficiency
9	Cycle Climb VSPT Corrected Flow	Climb VSPT Corrected Flow

APPENDIX J

ADDITIONAL RESULTS COMPARING THE TURBINE SPD AND MDP METHODS

This appendix provides additional results to complement those discussed in Section 5.6. The first section below provides additional comparisons of the turbine design spaces for the E^3 LPT and VSPT. The second section presents comparisons of individual designs produced by the turbine MDP and SPD methods.

J.1 Design Space Comparisons

J.1.1 E^3 LPT

Figures 129 to 132 show slices of the E^3 LPT design space for stages 1, 2, 3 and 5. The stage 4 design space slice is not included as it was shown in Section 5.6.

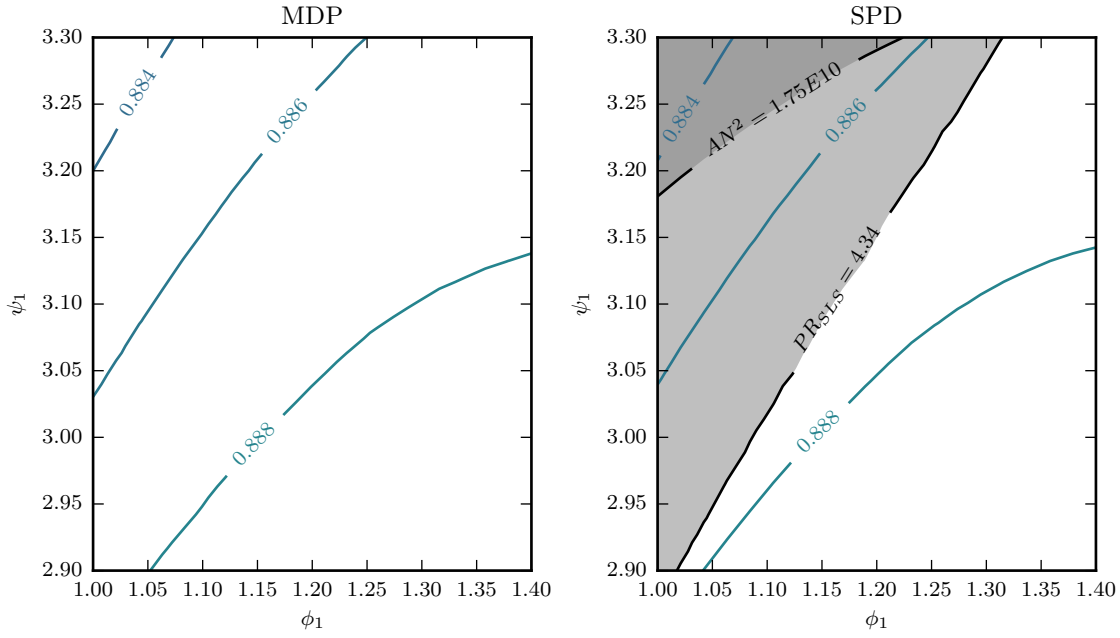

Figure 129: Comparison of the MDP and SPD Generated Design Spaces for the E^3 LPT Stage 1 Flow and Loading Coefficients

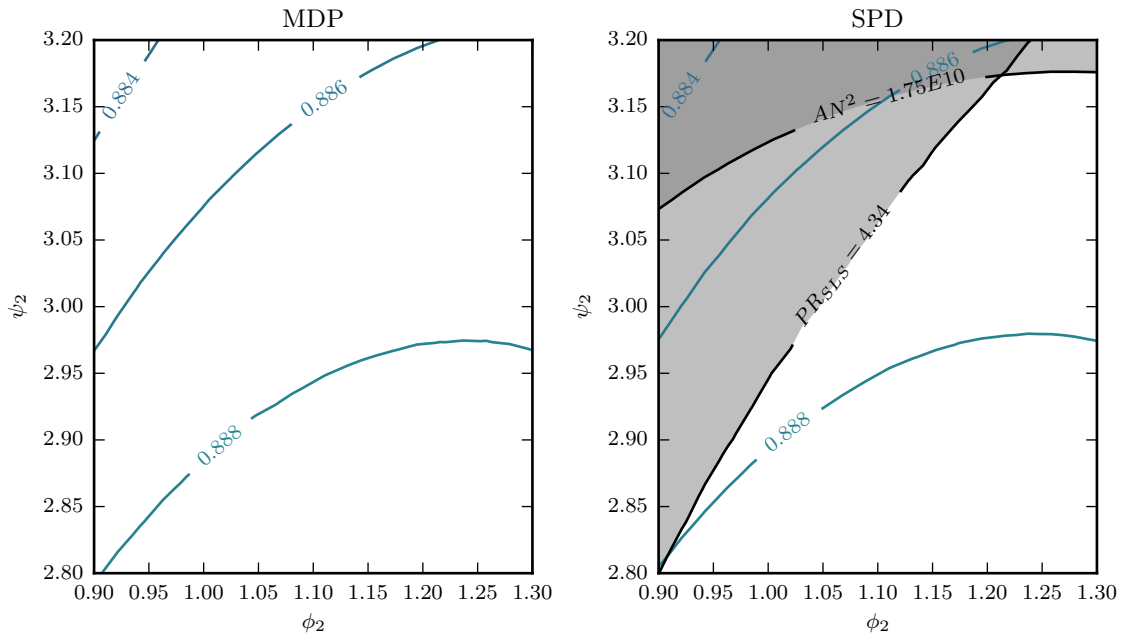

Figure 130: Comparison of the MDP and SPD Generated Design Spaces for the E^3 LPT Stage 2 Flow and Loading Coefficients

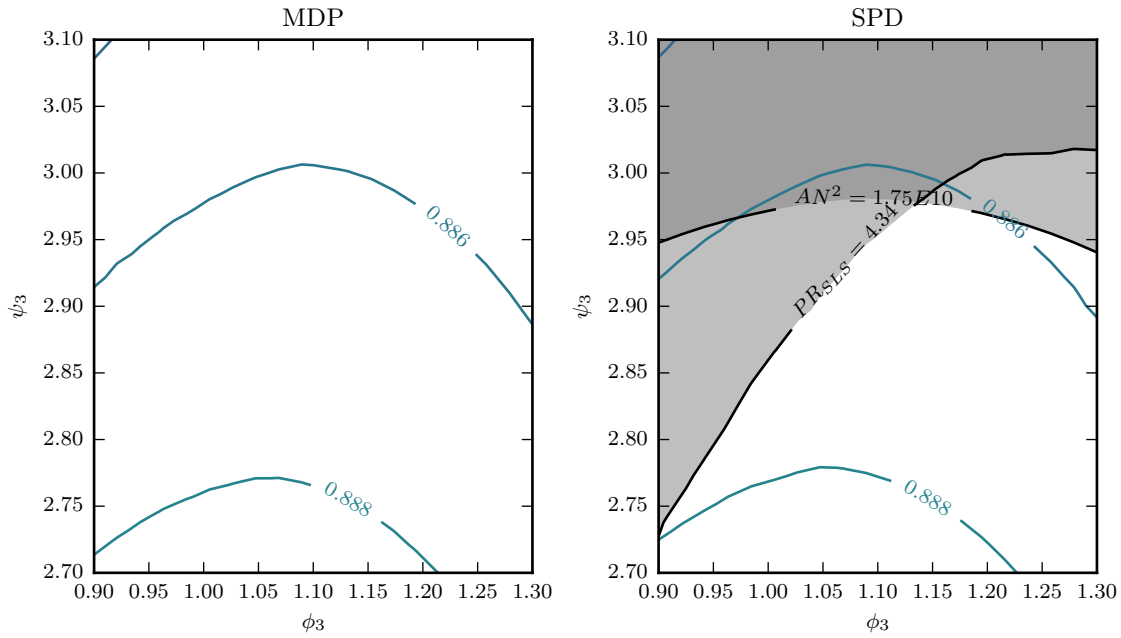

Figure 131: Comparison of the MDP and SPD Generated Design Spaces for the E^3 LPT Stage 3 Flow and Loading Coefficients

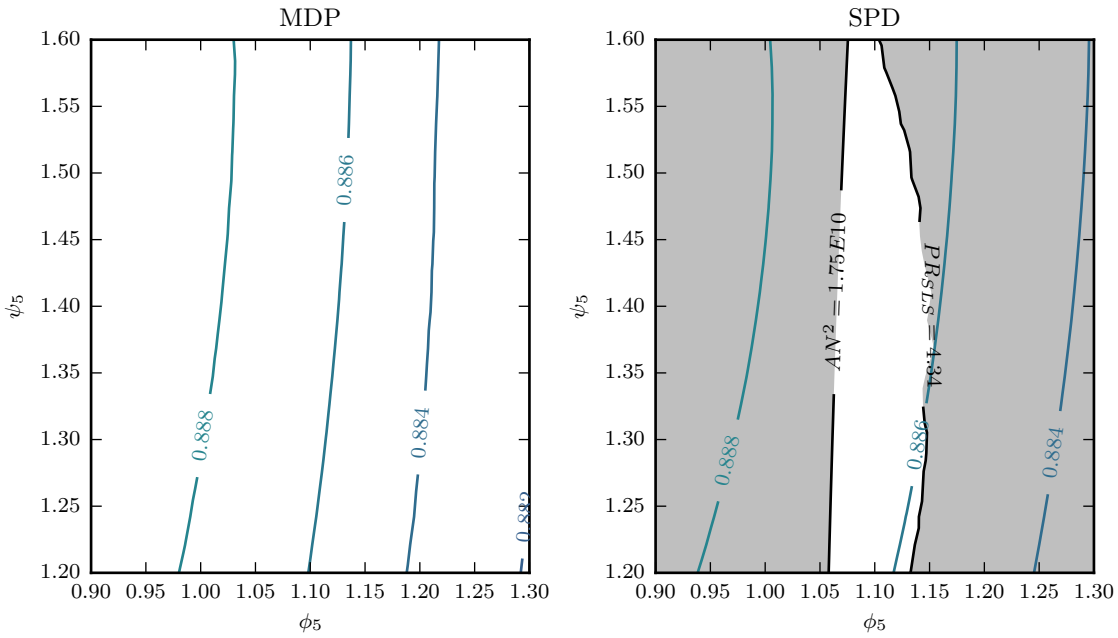

Figure 132: Comparison of the MDP and SPD Generated Design Spaces for the E^3 LPT Stage 5 Flow and Loading Coefficients

J.1.2 VSPT

Figures 133 to 135 show slices of the VSPT design space for stages 1, 2 and 4. The stage 3 design space slice is not included as it was shown in Section 5.6.

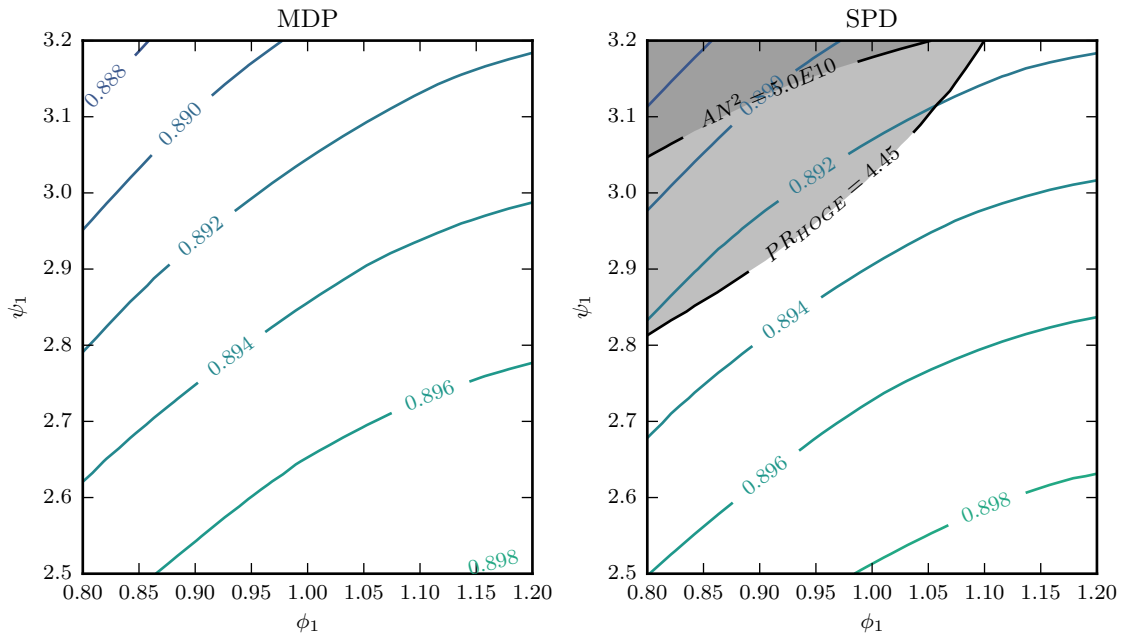

Figure 133: Comparison of the MDP and SPD Generated Design Spaces for the VSPT Stage 1 Flow and Loading Coefficients

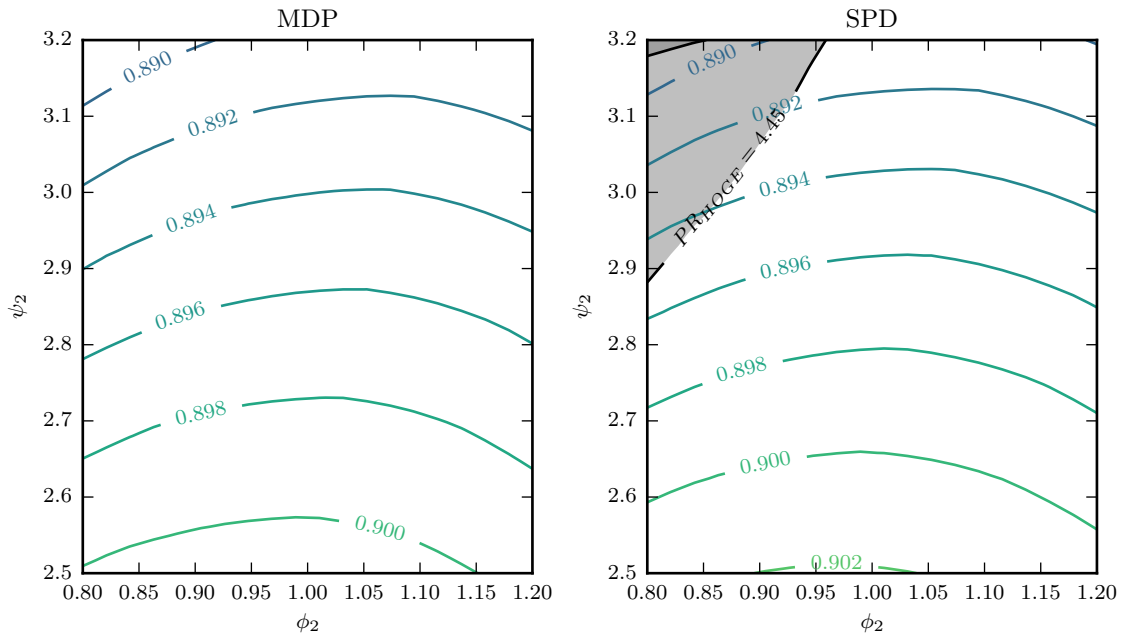

Figure 134: Comparison of the MDP and SPD Generated Design Spaces for the VSPT Stage 2 Flow and Loading Coefficients

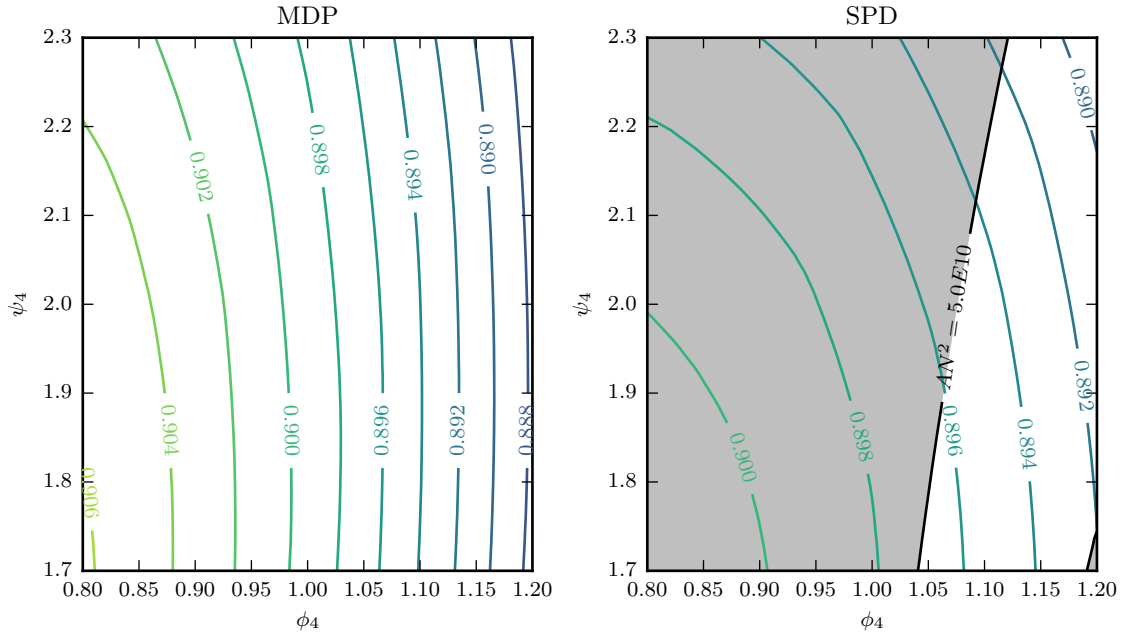

Figure 135: Comparison of the MDP and SPD Generated Design Spaces for the VSPT Stage 4 Flow and Loading Coefficients

J.2 Individual Design Comparisons

J.2.1 E^3 LPT

This section presents three additional design comparisons for the E^3 LPT to supplement those presented in the body of the thesis. The first example is shown in Figures 136 to 138, the second is shown in Figures 139 to 141, and finally the third example is shown in Figures 142 to 144.

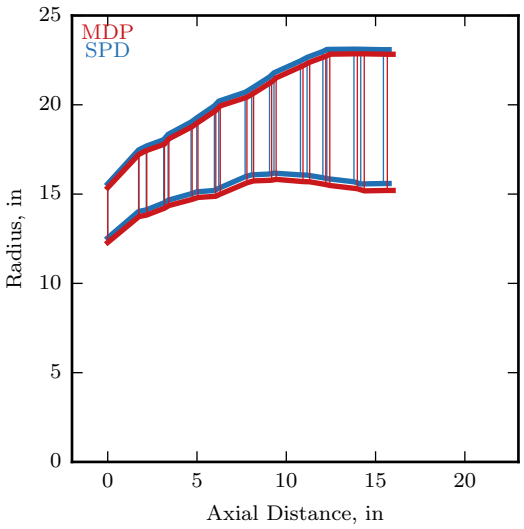

Figure 136: E^3 LPT Example 3: MDP and SPD Generated Annulus Geometry

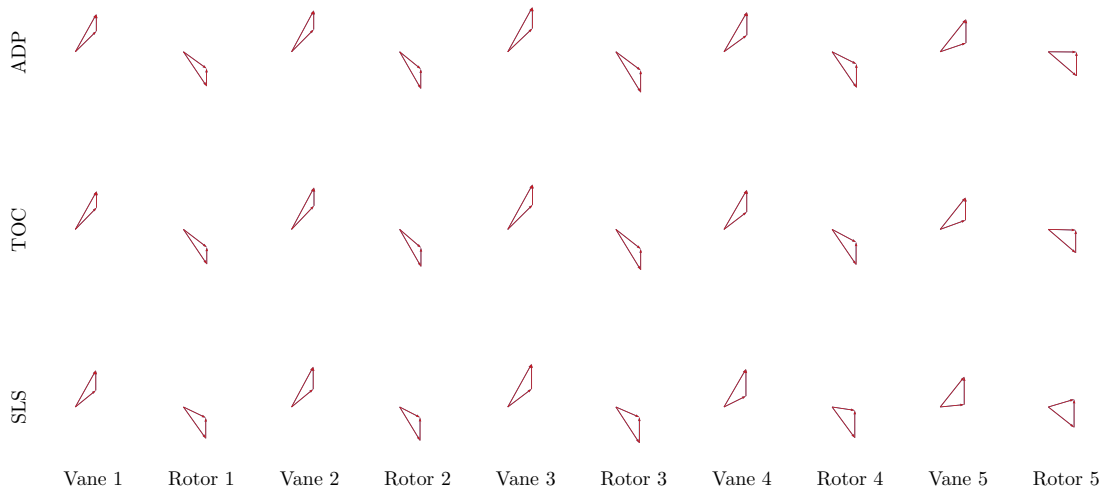

Figure 137: E^3 LPT Example 3: MDP and SPD Generated Velocity Triangles

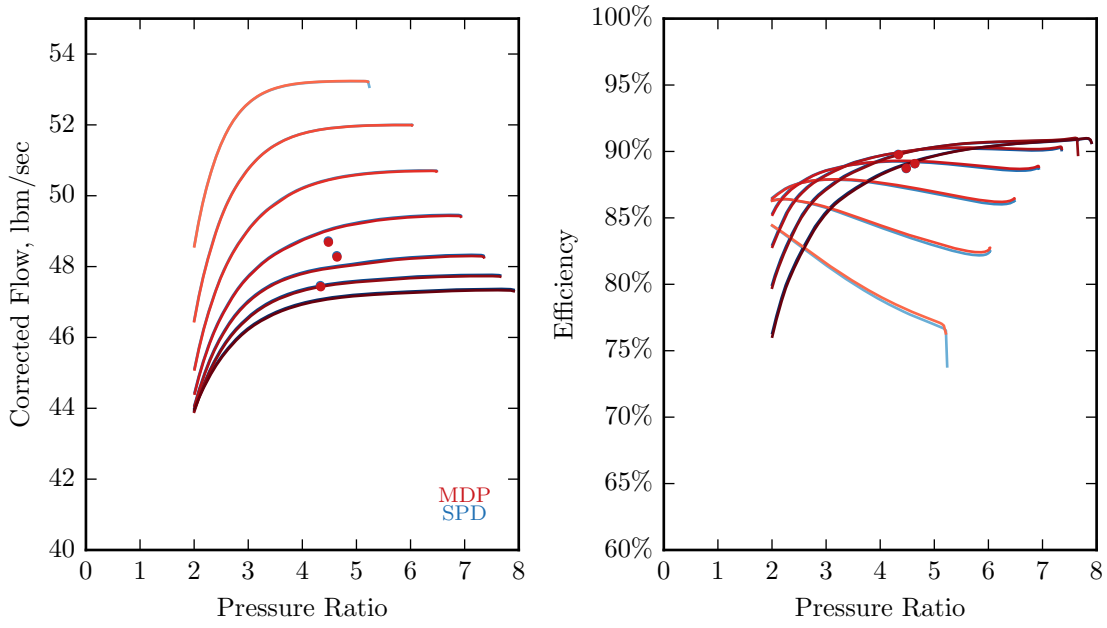

Figure 138: E^3 LPT Example 3: MDP and SPD Generated Performance Maps

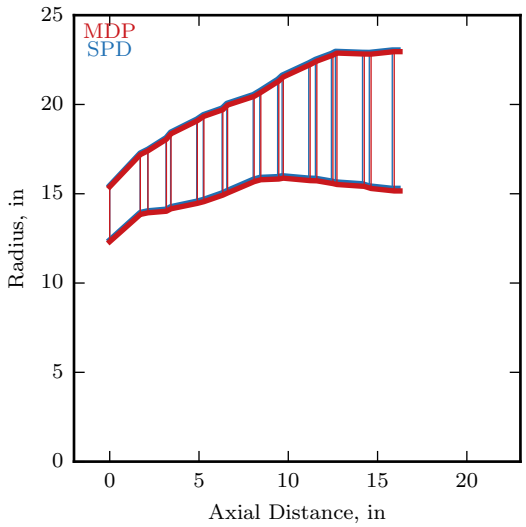

Figure 139: E^3 LPT Example 4: MDP and SPD Generated Annulus Geometry

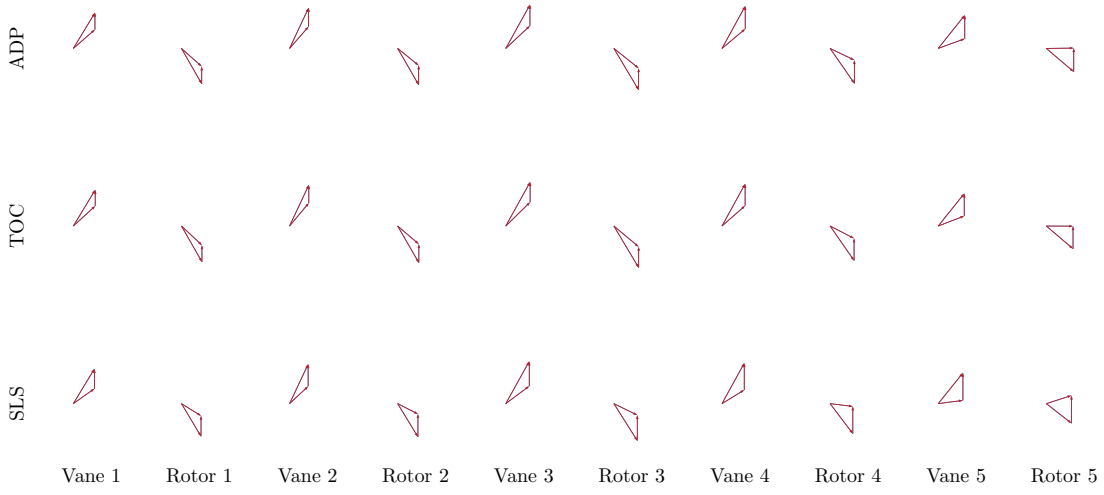

Figure 140: E^3 LPT Example 4: MDP and SPD Generated Velocity Triangles

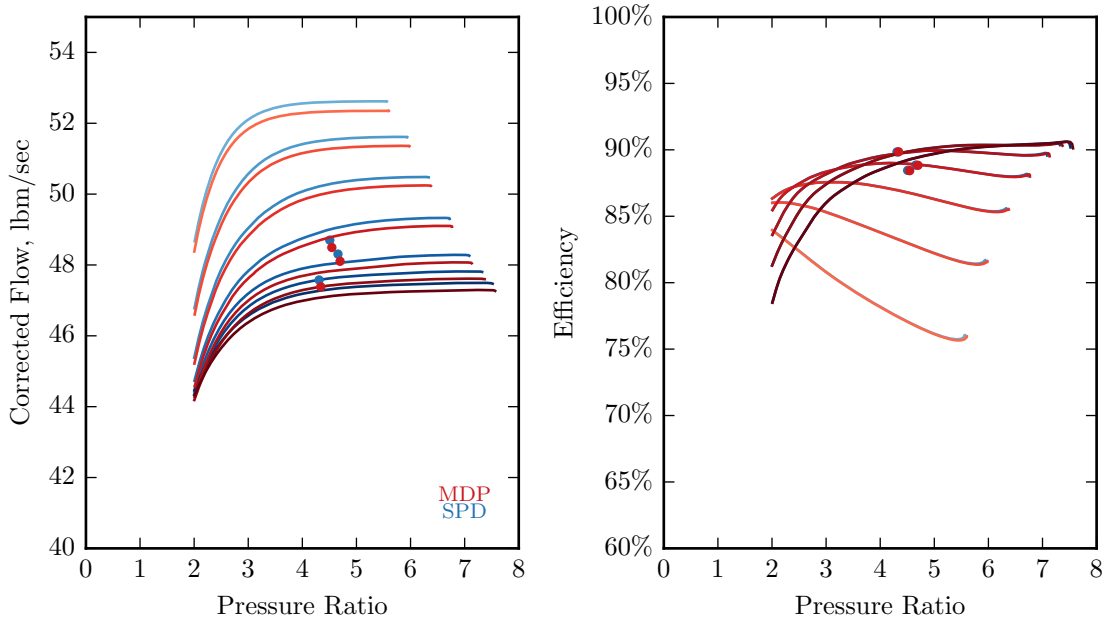

Figure 141: E^3 LPT Example 4: MDP and SPD Generated Performance Maps

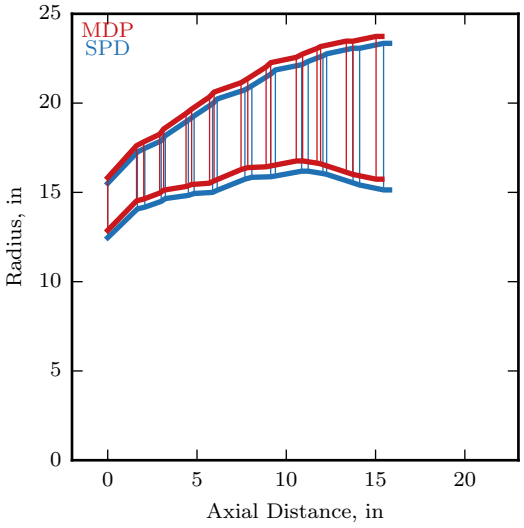

Figure 142: E^3 LPT Example 5: MDP and SPD Generated Annulus Geometry

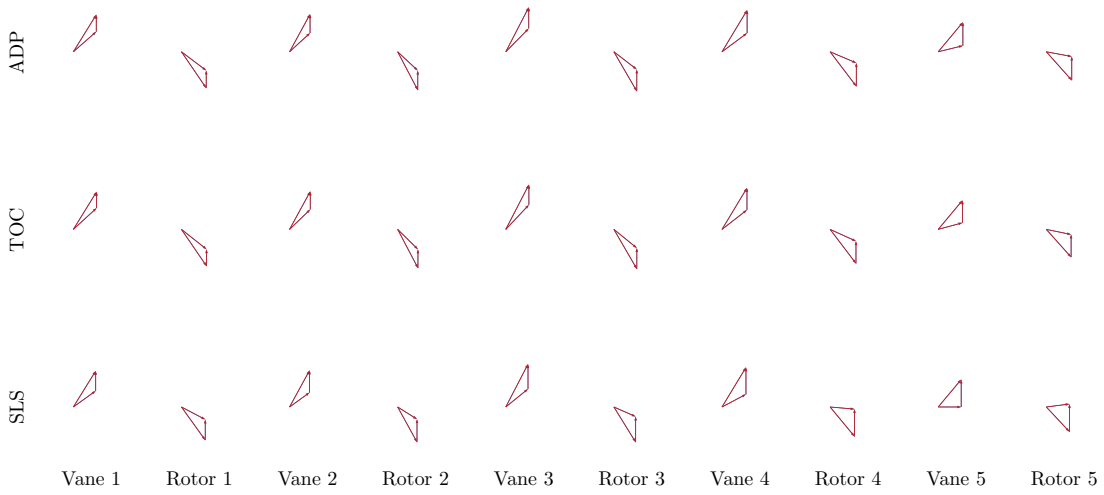

Figure 143: E^3 LPT Example 5: MDP and SPD Generated Velocity Triangles

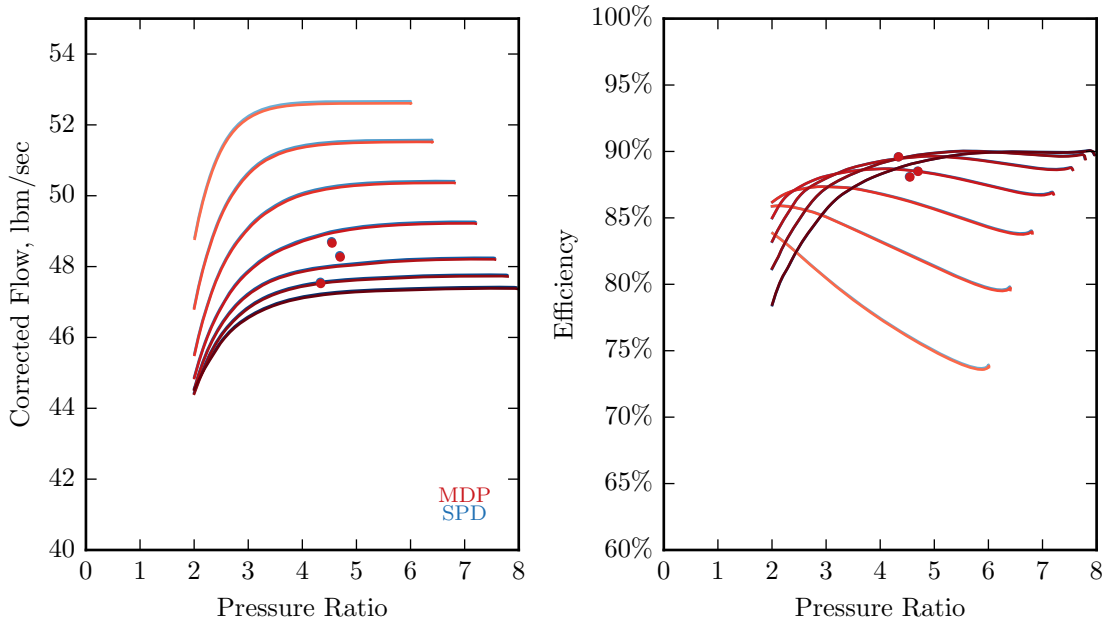

Figure 144: E^3 LPT Example 5: MDP and SPD Generated Performance Maps

J.2.2 CPT

This section presents one additional design comparisons for the CPT to supplement those presented in the body of the thesis. This example is shown in Figures 145 to 147.

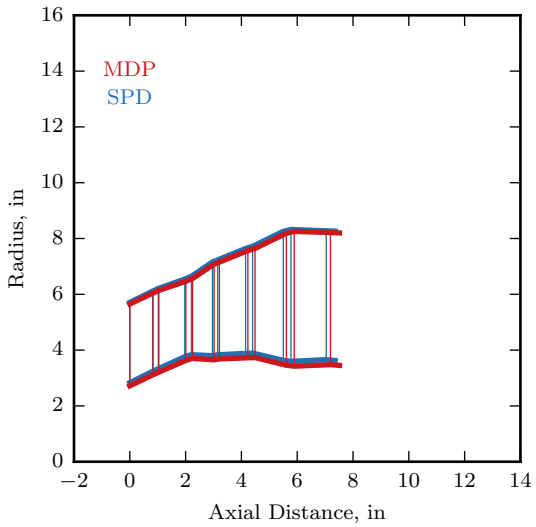

Figure 145: CPT Example 3: MDP and SPD Generated Annulus Geometry

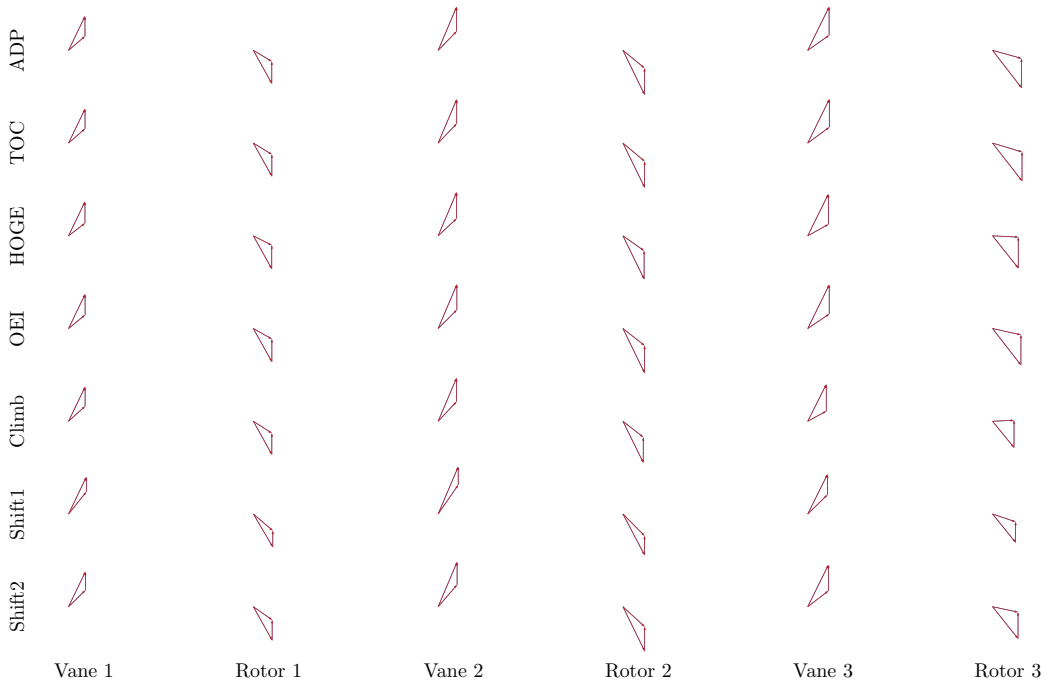

Figure 146: CPT Example 3: MDP and SPD Generated Velocity Triangles

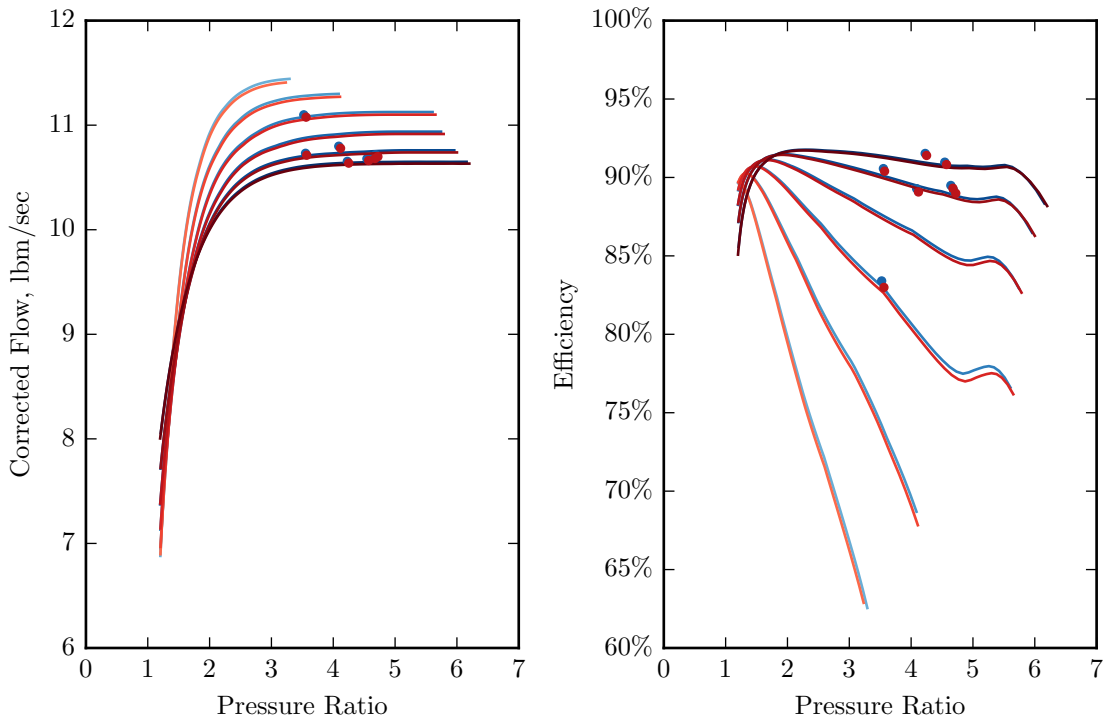

Figure 147: CPT Example 3: MDP and SPD Generated Performance Maps

J.2.3 VSPT

This section presents one additional design comparisons for the VSPT to supplement those presented in the body of the thesis. This example is shown in Figures 148 to 150.

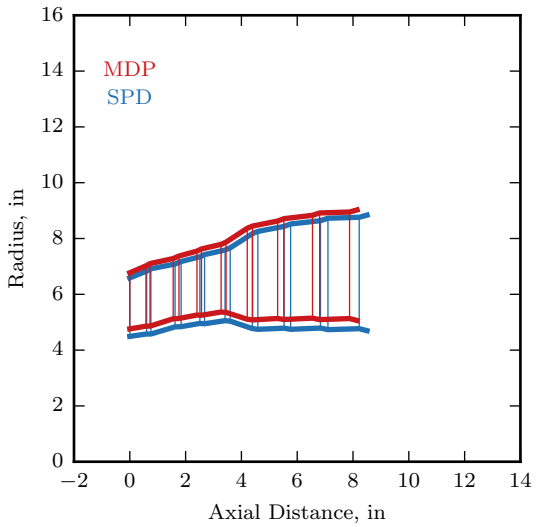

Figure 148: VSPT Example 3: MDP and SPD Generated Annulus Geometry

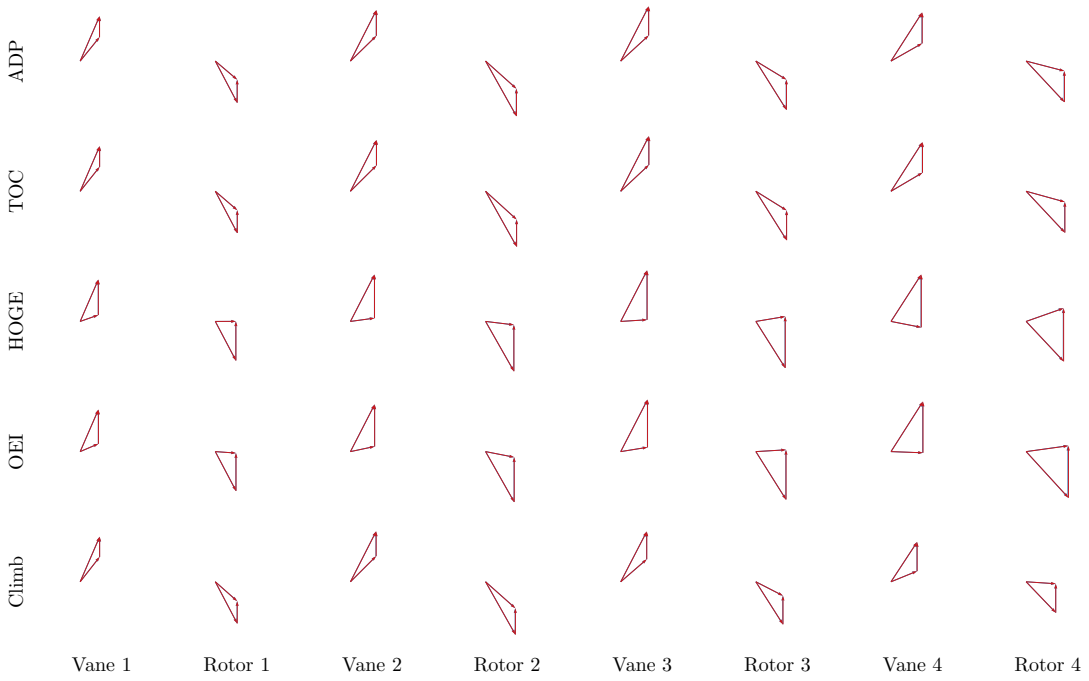

Figure 149: VSPT Example 3: MDP and SPD Generated Velocity Triangles

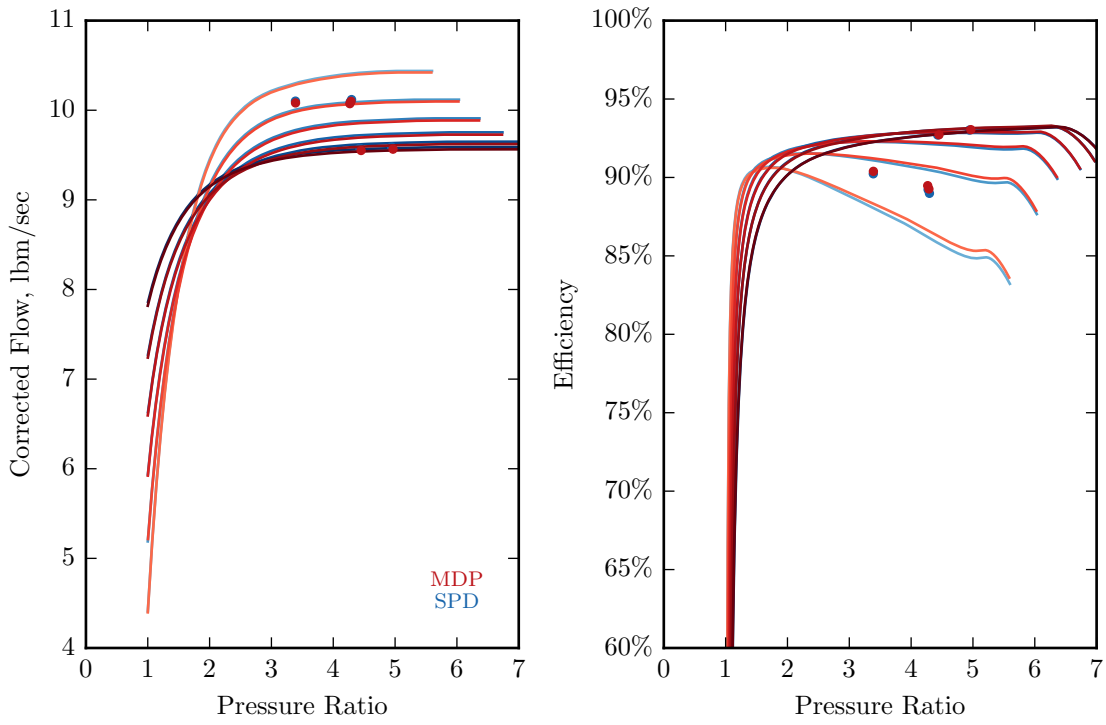

Figure 150: VSPT Example 3: MDP and SPD Generated Performance Maps

REFERENCES

[1] "NPSS Team Wins Prestigious NASA Software of the Year Award." Online: `https://mdao.grc.nasa.gov/topstories.html`. Accessed October 30, 2014.

[2] "Civil Tiltrotor Missions and Applications: A Research Study," Tech. Rep. NASA/CR-177452, July 1987.

[3] "Civil Tiltrotor Missions and Applications Phase II: The Commercial Passenger Market," Tech. Rep. NASA/CR-177576, January 1991.

[4] "Aircraft Propulsion System Performance Station Designation and Nomenclature," in *Aerospace Recommended Practice (ARP) 755B*, Society of Automotive Engineers, 1994.

[5] "Environmental Design Space Progress." Presented at the ICAO Committee on Aviation Environmental Protection 7th Meeting, 2007. Montreal, Canada.

[6] "OpenMDAO: An open-source MDAO framework written in Python." Online: `openmdao.org`, April 2016. Accessed April 1, 2016.

[7] Acree, C. W. and Snyder, C., "Influence of Alternative Engine Concepts on LCTR2 Sizing and Mission Profile," Conference Paper ARC-E-DAA-TN4635, NASA, March 2012.

[8] Acree, C. W., Yeo, H., and Sinsay, J. D., "Performance Optimization of the NASA Large Civil Tiltrotor," Technical Memorandum NASA/TM-2008-215359, NASA, June 2008.

[9] Ainley, D. and Mathieson, G., *A Method of Performance Estimation for Axial-Flow Turbines*. Defense Technical Information Center, 1951.

[10] Ameri, A., Giel, P. W., and McVetta, A. B., "Validation of a CFD Methodology for Variable Speed Power Turbine Relevant Conditions," NASA TM-2013-217860, 2013.

[11] Andrews, H., "Rolling Along - The V/STOL Wheel," *Vertilifte*, vol. 43, pp. 32–33, Spring 1997.

[12] Atkinson, K. E., *An Introduction to Numerical Analysis*. New York: Wiley, second ed., 1989.

[13] Bowles, M. D., "The Apollo of Aeronautics, NASA's Aircraft Energy Efficiency Program." NASA SP-2009-574, 2010.

[14] Brandt, D. and Wesorick, R., "GE Gas Turbine Design Philosophy," Tech. Rep. GER-3434D, General Electric, 1994.

[15] Bridgeman, M., Cherry, D., and Pedersen, J., "Energy Efficient Engine: Low Pressure Turbine Scaled Test Vehicle Performance Report," Tech. Rep. NASA/CR-168290, July 1983.

[16] Broyden, C. G., "A Class of Methods for Solving Nonlinear Simultaneous Equations," *Mathematics of Computation*, vol. 19, no. 92, pp. 577–593, 1965.

[17] Cheney, W. and Kincaid, D., *Numerical Mathematics and Computing*. Monterey, California: Brooks/Cole, 1980.

[18] Cherry, D., Gay, C., and Lenahan, D., "Energy Efficient Engine: Low Pressure Turbine Test Hardware Detailed Design Report," Tech. Rep. NASA/CR-167956, August 1982.

[19] Chung, W., Linse, D., Paris, A., Salvano, D., Trept, T., Wood, T., Gao, H., Miller, D., Wright, K., Young, R., and Cheng, V., "Modeling High-Speed Civil Tiltrotor Transports in the Next Generation Airspace," Tech. Rep. NASA/CR-2011-215960, October 2011.

[20] Chung, W., Salvano, D., Rinehart, D., Young, R., Cheng, V., and Lindsey, J., "An Assessment of Civil Tiltrotor Concept of Operations in the Next Generation Air Transportation System," Tech. Rep. NASA/CR-2012-215999, January 2012.

[21] Claus, R., Beach, T., Turner, M., Siddappaji, K., and Hendricks, E., "Geometry and Simulation Results for a Gas Turbine Representative of the Energy Efficient Engine (EEE)," Technical Memorandum NASA/TM-2015-218408, NASA, February 2015.

[22] Claus, R. W., Evans, A. L., Lytle, J. K., and Nichols, L. D., "Numerical propulsion system simulation," *Computing Sytems in Engineering*, vol. 2, no. 4, pp. 357–364, 1991.

[23] Claus, R. W., Lavelle, T., Townsend, S., Turner, M., and Reed, J., "Variable fidelity analysis of complete engine systems," in *43rd AIAA/ASME/SAE/ASEE Joint Propulsion Conference*, (Cincinnati, Ohio), AIAA, July 2007. AIAA 2007-5042.

[24] Claus, R., Evans, A., and Follen, G., "Multidisciplinary propulsion simulation using npss," in *4th AIAA Symposium on Multidisciplinary Analysis and Optimization*, AIAA, 1992. AIAA-92-4709-CP.

[25] Claus, R., Lavelle, T., Townsend, S., and Turner, M., "Challenges in the development of a multi-fidelity, coupled component simulation of complex systems," in *44th AIAA/ASME/SAE/ASEE Joint Propulsion Conference*, (Hartford, Connecticut), AIAA, July 2008. AIAA 2008-4651.

[26] Claus, R., Lavelle, T., Townsend, S., and Turner, M., "Coupled component, full engine simulation of a gas turbine engine," in *45th AIAA/ASME/SAE/ASEE Joint Propulsion Conference*, (Denver, Colorado), AIAA, August 2009. AIAA 2009-5017.

[27] Craig, H. R. M. and Cox, H. J. A., "Performance Estimation of Axial Flow Turbines," in *High Speed Computer and Algorithm Organization* (Lipcoll, D. J.,

Lawrie, D. H., and Sameh, A. H., eds.), no. 185 in Fast Computers, part 3, pp. 179–183, New York: Academic Press, third ed., Sept. 1970.

[28] Cumpsty, N., *Jet Propulsion: A Simple Guide to the Aerodynamic and Thermodynamic Design and Performance of Jet Engines*. Cambridge engine technology series, Cambridge University Press, 2003.

[29] D'Angelo, M., "Wide Speed Range Turboshaft Study," NASA CR-198380, 1995.

[30] Davis, D. and Stearns, E., "Energy Efficient Engine: Flight Propulsion System Final Design and Analysis," Tech. Rep. NASA/CR-168219, August 1985.

[31] Dring, R. P. and Heiser, W. H., "Turbine Aerodynamics," in *The Aerothermodynamics of Aircraft Gas Turbine Engines* (Oates, G. C., ed.), chapter 18, USAF Aero Propulsion Laboratory, 1978. AFAPL-TR-78-52.

[32] Dunham, J. and Came, P., "Improvements to the Ainley-Mathieson Method of Turbine Performance Prediction," *Journal of Engineering for Power*, vol. 92, p. 252, 1970.

[33] Farokhi, S., *Aircraft Propulsion*. No. v. 10 in Aircraft propulsion, Wiley, 2009.

[34] Federal Aviation Administration, "Advisory Circular No. 33.7-1." Online, June 2010.

[35] Federal Aviation Administration, "Administrator's Fact Book." Online, March 2011.

[36] Federal Aviation Administration, "Aerospace Forecast: Fiscal Years 2014 - 2034." Online, March 2014.

[37] Flegel-McVetta, A. B., Giel, P. W., and Welch, G. E., "Aerodynamic Measurements of a Variable-Speed Power-Turbine Blade Section in a Transonic Turbine Cascade at Low Inlet Turbulence," NASA TM-2013-218069, 2013.

[38] Follen, G. and AuBuchon, M., "Numerical zooming between a npss engine system simulation and a one-dimensional compressor analysis code," Technical Memorandum NASA/TM-2000-209913, NASA, Glenn Research Center, Cleveland OH 44135, USA, March 2000.

[39] Ford, A., Bloxham, M., Turner, E., Clemens, E., and Gegg, S., "Design optimization of incidence-tolerant blading relevant to large civil tilt-rotor power turbine applications," NASA-CR-2012-217016, 2012.

[40] Gentry, J., Duffy, K., and Swedish, W., "Airport Capacity Profiles," May 2014.

[41] Gerald, C. F. and Wheatley, P. O., *Applied Numerical Analysis*, vol. 2. Reading, Massachusetts: Addison-Wesley, third ed., 1984.

[42] Glassman, A. J., "Turbine Design and Application," Special Publication NASA/SP-290, NASA, Lewis Research Center, Cleveland OH 44135, USA, June 1994.

[43] Glassman, A. J., "Design Geometry and Design/Off-Design Performance Computer Codes for Compressors and Turbines," Contractor Report NASA/CR-198433, NASA, Lewis Research Center, Cleveland OH 44135, USA, December 1995.

[44] Gorton, S., Yamauchi, G., Johnson, W., and Zakrajsek, J., "Fundamental Aeronautics Subsonic - Rotary Wing Reference Document," May 2006.

[45] Gorton, S. A., López, I., and Theodore, C. R., "Subsonic Rotary Wing Project Overview," Presentation at the NASA ARMD Fundamental Aeronautics Program Technical Conference, March 13-15, 2012, Cleveland, Ohio.

[46] Gray, J. S., Moore, K. T., and Naylor, B. A., "OPENMDAO: An Open Source Framework for Multidisciplinary Analysis and Optimization," in *13th AIAA/ISSMO Multidisciplinary Analysis and Optimization Conference, Fort Worth, TX, AIAA, AIAA-2010-9101*, (Fort Worth, Texas), AIAA, August 2010.

[47] Griewank, A. and Walther, A., *Evaluating Derivatives: Principles and Techniques of Algorithmic Differentiation*. Society for Industrial and Applied Mathematics, second ed., 2008.

[48] Hall, E. J., "Modular Multi-Fidelity Simulation for Multiple Spool Turbofan Engines," February 2000. NASA High Performance Computing and Communications Computational Aerosciences Workshop, NASA Ames Research Center.

[49] Hall, E. J., Delaney, R. A., Lynn, S. R., and Veres, J. P., "Energy Efficient Engine Low Pressure Subsystem Flow Analysis," Technical Memorandum NASA/TM-1998-208402, NASA, Lewis Research Center, Cleveland OH 44135, USA, July 1998.

[50] Hall, E. J., Lynn, S. R., Heidegger, N. J., and Delaney, R. A., "Energy Efficient Engine Low Pressure Subsystem Flow Analysis," Contractor Report NASA/CR-1998-206597, NASA, Lewis Research Center, Cleveland OH 44135, USA, April 1998.

[51] Halliwell, I., "Preliminary Engine Design: An Advanced Course for Practicing Engineers at the NASA John H. Glenn Research Center." Short Course, Oct. 2001.

[52] Hearsey, R. M., "Program HT0300 Versions 2.356 & 2.357 User's Manual," 2011.

[53] Hendricks, E. S., "Development of an Open Rotor Cycle Model in NPSS Using a Multi-Design Point Approach," GT2011-46694, ASME 2011 Turbo Expo: Turbine Technical Conference and Exposition, Vancouver, British Columbia, Canada, June 6-10, 2011.

[54] Hendricks, E. S., "Meanline Analysis of Turbines with Choked Flow in the Object-Oriented Turbomachinery Analysis Code," in *54th AIAA Aerospace Sciences Meeting*, (San Diego, California), AIAA, January 2016. AIAA 2016-0119.

[55] Hesse, W. J. and Mumford Jr., N. V., *Jet Propulsion for Aerospace Applications*. New York: Pitman, 1964.

[56] Hill, P. G. and Peterson, C. R., "Mechanics and Thermodynamics of Propulsion," *Reading, MA, Addison-Wesley Publishing Co., 1992, 764 p.*, vol. 1, 1992.

[57] Horlock, J. H., *Axial Flow Turbines*. Malabar, Florida: Krieger Publishing, 1966.

[58] Hughes, M. J., Perullo, C., and Mavris, D. N., "Common Core Engine Design for Multiple Applications using a Concurrent Multi-Design Point Approach," AIAA-2014-3443, 50th AIAA/ASME/SAE/ASEE Joint Propulsion Conference, July 28-30, 2014, Cleveland, OH.

[59] Jansen, P. and Perez, R., "Constrained Structural Design Optimization Via a Parallel Augmented Lagrangian Particle Swarm Optimization Approach," *Computers and Structures*, vol. 89, no. 13-14, pp. 1352–1366, 2011.

[60] Japikse, D. and Baines, N. C., *Introduction to Turbomachinery*. White River Junction, Vermont and Oxford: Concepts ETI and Oxford University Press, 1997.

[61] Jenkinson, L. R., Simpkin, P., and Rhodes, D., *Civil Jet Aircraft Design*. AIAA Education Series, AIAA, 1999.

[62] Johnson, J., Stouffer, V., Long, D., and Gribko, J., "Evaluation of the National Throughput Benefits of the Civil Tiltrotor," Tech. Rep. NASA/CR-2001-211055, September 2001.

[63] Johnson, W., Yamauchi, G. K., and Watts, M. E., "NASA Heavy Lift Rotorcraft Systems Investigation," Technical Publication NASA/TP-2005-213467, NASA, December 2005.

[64] Jones, S. M., "An Introduction to Thermodynamic Performance Analysis of Aircraft Gas Turbine Engine Cycles Using the Numerical Propulsion System Simulation Code," Technical Memorandum NASA/TM-2007-214690, NASA, March 2007.

[65] Jones, S. M., "Development of an Object-Oriented Turbomachinery Analysis Code within the NPSS Framework," Technical Memorandum NASA/TM-2014-216621, NASA, January 2014.

[66] Jones, S. M., "Design of an Object-Oriented Turbomachinery Analysis Code: Initial Results," in *22nd International Symposium on Air Breathing Engines*, (Phoenix, AZ), October 2015. ISABE2015-20015.

[67] Kacker, S. and Okapuu, U., "Mean Line Prediction Method for Axial Flow Turbine Efficiency," *J. Eng. Power;(United States)*, vol. 104, no. 1, 1982.

[68] Kelley, C., *Iterative Methods for Linear and Nonlinear Equations*. Philadelphia: Society for Industrial and Applied Mathematics, 1995.

[69] Kelley, C., *Iterative Methods for Optimization*. Philadelphia: Society for Industrial and Applied Mathematics, 1999.

[70] Kirby, M. R. and Mavris, D. N., "The Environmental Design Space," ICAS 2008-4.7.3, 26th International Congress of the Aeronautical Sciences, Anchorage, Alaska, 2008.

[71] Lytle, J. K., "The Numerical Propulsion System Simulation: A Multidisciplinary Design System for Aerospace Vehicles," Technical Memorandum NASA/TM-1999-209194, NASA, Glenn Research Center, Cleveland OH 44135, USA, July 1999.

[72] Lytle, J. K., "The Numerical Propulsion System Simulation: An Overview," Technical Memorandum NASA/TM-2000-209215, NASA, Glenn Research Center, Cleveland OH 44135, USA, June 2000.

[73] Lytle, J. K., "Multi-fidelity Simulations of Air Breathing Propulsion Systems," in *42nd AIAA/ASME/SAE/ASEE Joint Propulsion Conference*, (Sacramento, California), AIAA, July 2006. AIAA-2006-4967.

[74] Mattingly, J. D., Heiser, W. H., and Daley, D. H., *Aircraft Engine Design*. AIAA Education Series, Washington, D.C.: American Institute of Aeronautics and Astronautics, 1987.

[75] Mattingly, J., *Elements of Propulsion: Gas Turbines And Rockets*. AIAA Education Series, American Institute of Aeronautics and Astronautics, 2006.

[76] Modern Technologies Corporation, "A Manual for Preliminary Design of Gas Turbine Engines, Volume I: Overview," September 2001. NASA Contract NAS3-00178: Task Order 3.

[77] Moustapha, S., Kacker, S., and Tremblay, B., "An Improved Incidence Losses Prediction Method for Turbine Airfoils," *J. Turbomachinery;(United States)*, vol. 112, no. 2, 1990.

[78] Numerical Propulsion System Simulation Consortium, "NPSS User Guide Reference Sheets Software Release 2.5D2," 2013.

[79] Numerical Propulsion System Simulation Consortium, "NPSS User Guide Software Release 2.7.1," 2015.

[80] Oates, G. C., "Ideal Cycle Analysis," in *The Aerothermodynamics of Aircraft Gas Turbine Engines* (Oates, G. C., ed.), chapter 5, USAF Aero Propulsion Laboratory, 1978. AFAPL-TR-78-52.

[81] Onat, E. and Klees, G., "A Method to Estimate Weight and Dimensions of Large and Small Gas Turbine Engines," NASA-CR-159481, 1979.

[82] Pachidis, V., Pilidis, P., Templalexis, I., Barbosa, J. B., and Nantua, N., "A de-coupled approach to component high-fidelity analysis using computational fluid dynamics," *Proceedings of the Institution of Mechanical Engineers, Part G: Journal of Aerospace Engineering*, vol. 221, pp. 105–113, Jan. 2007.

[83] Pachidis, V., Pilidis, P., Texeira, J., and Templalexis, I., "A comparison of component zooming simulation strategies using streamline curvature," *Proceedings of the Institution of Mechanical Engineers, Part G: Journal of Aerospace Engineering*, vol. 221, pp. 1–15, January 2007.

[84] Pachidis, V., Pilidis, P., Guindeuil, G., Kalfas, A., and Templalexis, I., "A Partially Integrated Approach to Component Zooming Using Computational Fluid Dynamics," in *ASME Turbo Expo 2005*, (Reno-Tahoe, Nevada), ASME, 2005. GT2005-68457.

[85] Pachidis, V., Pilidis, P., Talhouarn, F., Kalfas, A., and Templalexis, I., "A Fully Integrated Approach to Component Zooming Using Computational Fluid Dynamics," *Journal of Engineering for Gas Turbines and Power*, vol. 128, no. 3, pp. 579–584, 2006.

[86] Pearson, C. E., *Numerical Methods in Engineering and Science*. New York: Van Nostrand Reinhold, 1986.

[87] Perez, R. E., Jansen, P. W., and Martins, J. R. R. A., "pyOpt: A Python-based object-oriented framework for nonlinear constrained optimization," *Structures and Multidisciplinary Optimization*, vol. 45, no. 1, pp. 101–118, 2012.

[88] Perullo, C. A., Tai, J. C., and Mavris, D. N., "Effects of Advanced Engine Technology on Open Rotor Cycle Selection and Performance," *Journal of Engineering for Gas Turbines and Power*, vol. 135, no. 7, 2013.

[89] Plybon, R. C., VanDeWall, A., Sampath, R., Balasubramaniam, M., Mallina, R., and Irani, R., "High Fidelity System Simulation of Multiple Components in Support of the UEET Program," Contractor Report NASA/CR-2006-214230, NASA, Glenn Research Center, Cleveland OH 44135, USA, March 2006.

[90] Reed, J. A., Turner, M. G., Norris, A., and Veres, J. P., "Towards an Automated Full-Turbofan Engine Numerical Simulation," Technical Memorandum NASA/TM2003-212494, NASA, August 2003.

[91] Robuck, M., Wilkerson, J., Maciolek, R., and Vonderwell, D., "The Effect of Rotor Cruise Tip Speed, Engine Technology and Engine/Drive System RPM on the NASA Large Civil Tiltrotor (LCTR2) Size and Performance," Contractor Report ARC-E-DAA-TN7289, March 2012.

[92] Robuck, M., Wilkerson, J., Zhang, Y., Snyder, C., and Vonderwell, D., "Design Study of Propulsion and Drive Systems for the Large Civil TiltRotor (LCTR2) Rotorcraft," Technical Memorandum NASA/TM-2013-218102, December 2013.

[93] Sampath, R., Irani, R., Balasubramaniam, M., Plybon, R., and Meyers, C., "High Fidelity System Simulation of Aerospace Vehicles Using NPSS," in *42nd AIAA Aerospace Sciences Meeting and Exhibit*, (Reno, Nevada), AIAA, January 2004. AIAA 2004-371.

[94] Saravanamuttoo, H., Rogers, G., and Cohen, H., *Gas Turbine Theory*. Pearson Education, 2001.

[95] Schobeiri, M., *Turbomachinery Flow Physics and Dynamic Performance*. Springer, 2005.

[96] Schutte, J., Tai, J. C., and Mavris, D. N., "Multi-Design Point Cycle Design Incorporation into the Environmental Design Space," in *48th AIAA/ASME/SAE/ASEE Joint Propulsion Conference & Exhibit*, (Atlanta, Georgia), AIAA, July 2012. AIAA-2012-3812.

[97] Schutte, J. S., *Simultaneous Multi-Design Point Approach to Gas Turbine On-Design Cycle Analysis for Aircraft Engines*. PhD dissertation, Georgia Institute of Technology, School of Aerospace Engineering, 2009.

[98] Seidel, J., "Propulsion Systems Analysis Office Benchmark Peer Review of Aeropropulsion Systems Analysis Methods." Presentation, May 1998.

[99] Smith, S. F., "A Simple Correlation of Turbine Efficiency," *Journal of Royal Aeronautical Society*, vol. 69, pp. 467–470, July 1965.

[100] Snyder, C., "Defining Gas Turbine Engine Performance Requirements for the Large Civil Tiltrotor (LCTR2)," Technical Memorandum NASA/TM-2013-218101, NASA, December 2013.

[101] Snyder, C. A. and Acree, C. W., "Preliminary Assessment of Variable Speed Power Turbine Technology on Civil Tiltrotor Size and Performance," in *Presentation at AHS 68th Annual Forum and Technnology Display*, (Fort Worth, Texas), AHS, May 2012. ARC-E-DAA-TN5287.

[102] Southwest Research Institute, "SwRI to manage Numerical Propulsion System Simulation (NPSS) Consortium." Online: `http://www.swri.org/9what/releases/2013/npss.htm#.VFJqb_ldU1I`, March 2013. Accessed October 30, 2014.

[103] Steinmetz, R. and Wagner, M., "Turbofan Engine Cycle Design Selection - Year 2000," in *AlAA/AHS/ASEE Aircraft Systems Design & Technology Meeting*, (Dayton, Ohio), AIAA, October 1986. Paper No. 86-2705.

[104] Stetson, G. M., "Turbine Technology and Design." Presentation. United Technologies Pratt & Whitney.

[105] Stouffer, V., Johnson, J., and Gribko, J., "Civil Tiltrotor Feasibility Study for the New York and Washington Terminal Areas," Tech. Rep. NASA/CR-2001-210659, January 2001.

[106] Suchezky, M. and Cruzen, G. S., "Variable-Speed Power-Turbine for the Large Civil Tilt Rotor," NASA CR-2012-217424, 2012.

[107] Sullerey, R. K. and Kumar, S., "A Study of Axial Turbine Loss Models in a Streamline Curvature Computing Scheme," *Journal of Engineering for Gas Turbines and Power*, vol. 106, pp. 591–597, July 1984.

[108] Turner, M. G., "Lessons Learned from the GE90 3D Full Engine Simulations," in *48th AIAA Aerospace Sciences Meeting*, (Orlando, Florida), AIAA, January 2010. AIAA-2010-1606.

[109] Turner, M. G., Reed, J. A., Ryder, R., and Veres, J. P., "Multi-Fidelity Simulation of a Turbofan Engine With Results Zoomed Into Mini-Maps for a Zero-D Cycle Simulation," Technical Memorandum NASA/TM-2004-213076, NASA, November 2004.

[110] Walsh, P. P. and Fletcher, P., *Gas Turbine Performance*. Oxford: Blackwell Science and ASME, second ed., 2004.

[111] Wei, N., *Significance of Loss Models in Aerothermodynamic Simulation for Axial Turbines*. PhD dissertation, Royal Institute of Technology, Department of Energy Technology, 2000.

[112] Welch, G. E., "Assessment of Aerodynamic Challenges of a Variable-Speed Power Turbine for Large Civil Tilt-Rotor Application," Technical Memorandum NASA/TM-2010-216758, NASA, August 2010.

[113] Welch, G. E., McVetta, A. B., Stevens, M. A., Howard, S. A., Giel, P. W., Ameri, A. A., To, W., Skoch, G. J., and Thurman, D. R., "Variable-Speed Power-Turbine Research at Glenn Research Center," Technical Memorandum NASA/TM-2012-217605, NASA, July 2012.

[114] Wilson, D. G. and Korakianitis, T., *The Design of High-Efficiency Turbomachinery and Gas Turbines*. Upper Saddle River, New Jersey: Prentice-Hall, second ed., 1998.

[115] Young, L., Chung, W., Paris, A., Salvano, D., Young, R., Gao, H., Wright, K., and Cheng, V., "Civil Tiltrotor Operations," in *11th AIAA Aviation Technology, Integration, and Operations (ATIO) Conference*, (Virginia Beach, Virginia), AIAA, September 2011. AIAA-2011-6898.

[116] Young, L., Chung, W., Paris, A., Salvano, D., Young, R., Gao, H., Wright, K., Miller, D., and Cheng, V., "A Study of Civil Tiltrotor Aircraft in NextGen Airspace," in *10th AIAA Aviation Technology, Integration, and Operations (ATIO) Conference*, (Fort Worth, Texas), AIAA, September 2010. AIAA-2010-9106.

VITA

Eric S. Hendricks attended the Georgia Institute of Technology where he completed a Bachelors of Science in Aerospace Engineering in 2007 and a Masters of Science in Aerospace Engineering in 2009. Following the completion of his Ph.D. coursework, he accepted a position in the Multidisciplinary Design, Analysis and Optimization Branch (later renamed the Propulsion Systems Analysis Branch) at NASA Glenn Research Center in 2010 where he completed the research presented in this dissertation.